
# THE ROLE OF GABA IN PLANT SALINITY AND HYPOXIA RESPONSES

Ying Meng

School of Agriculture, Food and Wine
Faculty of Sciences, Engineering and Technology

Submitted on Feb 22, 2023 for the degree of Doctor of Philosophy

# Contents

# Abstract

My research is focused on establishing a better understanding of how $\gamma$-aminobutyric acid, GABA, contributes to the stress responses of plants, using the model plant *Arabidopsis thaliana* wild type (WT) and GABA mutants. Some mutants target decreased GABA production due to T-DNA insertion(s) in the major GABA producing gene(s) *Glutamate Decarboxylase* (*GAD*). Others target increased GABA poduction through overexpression of *GAD* or T-DNA knockout in the sole GABA catabolising gene *GABA-transaminase* (*GABA-T*). The two *GAD1* mutants were genotyped and the *GAD1* expression was examined in both the roots and shoots; while *gad1KO* was confirmed as a knock out line of *GAD1*, *gad1** had high levels of expression of *GAD1* in both shoots and roots that was comparable, if not greater than WT. Similarly, *pop2-8*, which cannot degrade GABA, had significantly higher GABA concentration in their leaves than all other lines; while the *GAD2*-overpression lines did not.

In plants, the rapid accumulation of GABA in response to abiotic and biotic stress is common, including salinity and hypoxia. During my PhD I have induced salt and hypoxia stress to the above lines, explored their differences in response to salinity and submergence (hypoxia), and found that the mutants had varied tolerance to these two types of abiotic stress. Young and mature seedlings grown in square petri dishes and hydroponic system, respectively, were used to examine the impact of salt on root elongation, biomass and shoot ion content. To examine the response of plants with altered GABA metabolism to hypoxia, plants were grown for up to 4.5 weeks in short day conditions, then submerged in water for 6 d under light/dark cycles (slightly dimmed light during the day to represent the natural floods), and recovered for 2 d. This research highlights the importance of a tightly controlled and adjusted GABA content through *GAD* and *GABA-T*, as well as the essential role of *GAD1* expression for plants in response to salinity and hypoxia. When GABA cannot be utilised (in the case of *pop2-8*), these plants had larger root growth and biomass compared to WT plants under normal and salt stress, but this appears to result in deficient recovery after submergence. After submergence, *GAD1* expression was largely up-regulated in all plants with a higher fold change than that previously reported for *GAD4*. Moreover, *GAD4* and *GABA-T* both impact the regulation of circadian rhythm, which were not significantly affected in the *GAD1* lines under normal conditions. RNAseq and metabolite data suggests GABA regulation of hypoxia responses appears to occur

through regulating circadian rhythm, amino acid metabolism, organic acid metabolism and transport, signalling transduction and photosynthesis.

GABA biosynthesis (in the cytosol) consumes protons while the final step in catabolism (in the mitochondria) produces protons, thus GABA metabolism can alter pH in a cell. The final aim of this thesis was to examine how pH regulates the activity of Aluminum-activated Malate Transporter proteins (ALMTs), which are proteins shown to catalyse the movement of carboxylate ions across membranes and are inhibited by GABA. Specifically, the impact of a histidine residue within the putative GABA binding domain of wheat (*Triticum aestivum*, Ta) TaALMT1, was examined for its role in regulating the pH sensitivity of its malate transport capacity. TaALMT1 has greater malate-activated malate transport at alkaline pH than at acidic pH. The histidine residue is completely conserved among plant species, so its impact on transport of ALMT was studied here for the first time, in terms of its role in ion transport and pH sensitivity. Histidine carries a positive charge below pH 6 but is neutral above, therefore changes in pH would influence the charge states of histidine, and potentially its role in proton sensing and regulating activity of TaALMT1 at different pHs. This study conducted a single substitution of histidine to either alanine (H224A) or arginine (H224R) in TaALMT1, expressed the cRNA in *Xenopus laevis* oocytes, and then recorded the steady state currents in solutions of different pH (with or without malate). The results showed the H224R mutation increased, while the H224A inhibited, the external malate activated currents (mediated by TaALMT1) at both acidic (pH 4.5 and 5.5) and alkaline (pH 7.5) pH. These results indicate the importance of the H224 residue in maintaining the activity of TaALMT1 protein for ion transport but could not alter pH sensitivity of the protein.

Taken together, this thesis mainly focused on the role of GABA metabolism under salinity and hypoxia, and also explored the role of histidine within the putative GABA binding motif in pH sensing for the pH sensitivity of ion transport. Knowledge from the current study has expanded our understanding of how GABA contributes to plant stress tolerance and signal transduction, and may be valuable for developing resilient crops given the fact that salinity and flooding are two of the major hazardous disasters happening not only in Australia, but also worldwide.

# Declaration

I certify that this work contains no material which has been accepted for the award of any other degree or diploma in my name, in any university or other tertiary institution and, to the best of my knowledge and belief, contains no material previously published or written by another person, except where due reference has been made in the text. In addition, I certify that no part of this work will, in the future, be used in a submission in my name, for any other degree or diploma in any university or other tertiary institution without the prior approval of the University of Adelaide and where applicable, any partner institution responsible for the joint award of this degree.

I give permission for the digital version of my thesis to be made available on the web, via the University's digital research repository, the Library Search and also through web search engines, unless permission has been granted by the University to restrict access for a period of time.

Ying Meng

Feb 22 2023

# Acknowledgements

Firstly, I would like to express my thanks to my supervisors Professor Matthew Gilliham, Dr Megan Shelden and Dr Jiaen Qiu. I am very fortunate to have been supervised by you all. Thank you for giving me great advice and valuable ideas in my experimental designs and data analysis, which helped me a lot and guided me along my path. Thanks you Matt, for taking me as your student and giving me the opportunity to conduct this exciting research. My gratitude for your excellent supervision is beyond words. Thank you for always having a sympathetic ear and reaching out to so many people to help me, for all the advice in doing academic research. I also want to thank you for the financial support during my study and the first extension. Thank you Megan, for always being there to help and so patient in reading and revising my thesis. Thank you for all the suggestions and tips on time arrangement, conducting experiments and writing. I am also immensely grateful to you, Jiaen, for the enormous help inside and outside the lab, when I required support with data analysis/interpretation or while planning or conducting experiments. Thank you for always being so patient and approachable.

I also want to thank the China Scholarship Council and the University of Adelaide for giving me the opportunity to study here, without your support, my research project would not have been possible. Moreover, I have to thank my other colleagues and lab members. Foremost, I would like to thank Dr Rebecca Vandeleur, you were like an angel to me and you made everything possible. Also, many thanks to Wendy for all the technical support and assistance. There are many others I want to thank, unfortunately, I am not able to mention all of you here. Additional thanks for Dr Xiangxiang Meng from the La Trobe University and Dr Alexander Lee from Centre of Excellence Plant Energy Biology. Thank you for your advice and help when I conducted my submergence experiment. There were a lot of discussions and suggestions on how to perform the experiment and collect data, from which I benefited a lot.

I also want to give my thanks to my friends and family. Your support and love is valuable to me. During the most emotional or stressful times, I have gained so much energy and mental support from you. Charlotte, you have become one of my great friends. Thank you for many exciting discussions around RNAseq and GABA. I am grateful for the brilliant support from your and for the knowledge and skills you shared, and especially thankful

for all the tears and laughter and food we shared/cooked. Dear mum, you are my super hero whom I admired the most, you are the best mum in the world and there are so many qualities in you that I am still learning. Mel, we have had three long years living together, with the cat. I enjoyed getting to know you and your family, and I am extremely thankful for your help in doing grocery shopping for me and sharing meals with me when I was so busy into study. You are like my Australian mother.

Last but not the least, I want to thank myself. There were hard times and difficulties, when I had to switch labs and projects, when I made mistakes in conducting experiments, or when I need to acquire new skills and knowledge. I thank myself for going through this journey and not giving up, for taking the responsibility for the love and support I have always got along the way.

Love is patient, love is kind. It does not envy, it does not boast, it is not proud. Love rejoices with the truth and never fails. Thank you all for letting me experience love so profoundly.

# Glossary

**2-OG**: 2-oxoglutarate; also named $\alpha$-ketoglutarate.
**2-OGDH**: 2-oxoglutarate dehydrogenase; EC 1.2.4.2.
**4-ABAL**: 4-aminobutanal.

**ABA**: Abscisic acid.
**ABAL**: 4-aminobutanal.
**ADC**: Arginine decarboxylase; EC 4.1.1.9.
**ADH**: Alcohol dehydrogenase; EC 1.1.1.1.
**AGT**: Alanine:glyoxylate aminotransferase; EC 2.6.1.44.
**Ala**: Alanine.
**AlaAT**: Alanine aminotransferase; EC 2.6.1.2.
**ALDH**: $NAD(P)^+$-dependent aldehyde dehydrogenase; a superfamily of oxidoreductases involved in aldehydes oxidation; EC 1.2.1.3.
**ALMT**: Aluminum-activated malate transporter.
**AMADH**: Aminoaldehyde dehydrogenase; EC 1.2.1.19.
**AMT1;2**: Ammonium transporter 1 member 2.
**Arg**: Arginine.
**ARGA**: Arginase; EC 3.5.3.1.
**ASN**: Asparagine synthase/synthetase; EC 6.3.5.4.
**Asn**: Asparagine.
**Asp**: Aspartic acid, Aspartate.
**AspAT**: Aspartate:2-oxoglutarate aminotransferase; ASP; EC 2.6.1.1.

**Boxplot**: Box show median (Q2, 50th percentile) with interquartile range (IQR, Q3 - Q1). Whiskers represent ranges from Q3 to Q3+1.5*IQR, and from Q1-1.5*IQR to Q1.
**BR**: Brassinosteroid.

**C:N**: Carbon:Nitrogen.
**CAT**: Cationic amino acid transporter.
**CuAO**: Copper-containing amine oxidase; EC 1.4.3.22.

**DAG**: Days after germination.
**DAO**: Diamine oxidases; EC 1.4.3.6.

**DIT**: Dicarboxylate transporter.
**DW**: Dry weight.

**EIN3**: ETHYLENE INSENSITIVE 3.
**ERF-VIIs**: Group VII of Ethylene Responsive transcription factors.

**Fv/Fm**: Potential quantum efficiency of Photosystem II.
**FW**: Fresh weight.

**GABA**: $\gamma$-aminobutyric acid.
**GABA-T**: GABA transaminase; gene name is POP2; EC 2.6.1.96.
**GABP**: GABA permease.
**GAD**: Glutamate decarboxylase; EC 4.1.1.15.
**GAT**: GABA transporter.
**GDH**: Glutamate dehydrogenase; EC 1.4.1.3.
**GHB**: $\gamma$-hydroxybutyric acid.
**GHBDH**: $\gamma$-hydroxybutyric acid dehydrogenase.
**GLN**: Glutamine synthetase; GS; EC 6.3.1.2.
**Gln**: Glutamine.
**GLT1**: NADH-dependent glutamate synthase 1; NADH-dependent glutamine:2-OG amidotransferase (NADH-GOGAT); EC 1.4.1.14.
**Glu**: Glutamic acid; glutamate.
**GLU1**: Ferredoxin-dependent glutamate synthase 1; Ferredoxin-dependent glutamine:2-OG amidotransferase (Fd-GOGAT); EC 1.4.7.1.
**Gly**: Glycine.
**GORK**: Guard cell outward rectifying $K^+$ channel.
**GSA**: L-glutamate 5-semialdehyde.

**HRG**: Hypoxia responsive gene.

**LHC**: Light harvesting chlorophyll protein complex.

**MAPK**: Mitogen-activated protein kinase.
**MDA**: Malondialdehyde.
**MDH**: Malate dehydrogenase; EC 1.1.1.37.
**mETC**: Mitochondrial electron transport chain.
**MRGR**: Main Root Growth Rate.

**NAD**: Nicotinamide adenine dinucleotide.
**NERP**: N-end rule signalling pathway.

**OAA**: Oxaloacetate.
**OAT**: Delta-ornithine aminotransferase; $\delta$-OAT; EC .

**ODC**: Ornithine decarboxylase; EC 4.1.1.17.
**OMT**: 2-oxoglutarate/malate translocator.
**Orn**: Ornithine.

**P5C**: Δ-1-pyrroline-5-carboxylate.
**P5CDH**: Δ-1-pyrroline-5-carboxylate dehydrogenase; ALDH12A1; EC 1.2.1.88.
**P5CR**: Δ-1-pyrroline-5-carboxylate reductase; EC 1.5.1.2.
**P5CS**: Δ-1-pyrroline-5-carboxylate synthetase; EC 2.7.2.11 1.2.1.41.
**PA**: Polyamine.
**PAO**: FAD-dependent polyamine oxidase; E.C. 1.5.3.16.
**PDC**: Pyruvate decarboxylase; EC 4.1.1.1.
**PDH**: Pyruvate dehydrogenase; EC 1.2.4.1.
**PIF**: Phytochrome interacting factor.
**Pro**: Proline.
**ProT**: Proline transporter.
**PSI**: Photosystem I.
**PSII**: Photosystem II.
**Put**: Putrescine.

**RBOHD**: NADPH oxidase; EC 1.6.3.1.
**ROS**: Reactive oxygen species.
**RWC**: Relative water content.

**SDH**: Succinate dehydrogenase; EC 1.3.5.1.
**Ser**: Serine.
**Spd**: Spermidine.
**SPDS**: Spermidine synthase; EC 2.5.1.16.
**Spm**: Spermine.
**SPMS**: Spermine synthase; EC 2.5.1.22.
**SSA**: Succinic semialdehyde.
**SSADH**: Succinic semialdehyde dehydrogenase; ALDH5F1; EC 1.2.1.16.
**SSR**: Succinic semialdehyde reductase; GLYR; EC 1.1.1.61.
**SUS**: Sucrose synthase; EC 2.4.1.13.

**TCA cycle**: Tricarboxylic acid cycle; Citric acid cycle.
**TF**: Transcription factor.
**Thr**: Threonine.
**TW**: Turgid weight.

**UCP**: Plant uncoupling mitochondrial protein; PUMP.

**Val**: Valine.

# List of Figures

# List of Tables

CHAPTER 1

# Background

Plants are exposed to various environmental conditions, many of which are unfavourable and are defined as stresses that are abiotic (e.g. salinity, drought, heat and cold) or biotic (e.g. herbivore pests attacks, anecrotrophic fungi and pathogen infection). As they are unable to move, plants have developed complicated mechanisms to cope with different stresses, including physiological, transcriptomic and metabolic adaptations. Cytosolic $Ca^{2+}$ concentration is often rapidly elevated in response to many abiotic stresses, e.g. cold/heat, salt, drought, mechanical stimuli (touch and wind), ozone, hypoxia, osmotic and oxidative stresses (Reddy et al., 2011). Cross-talk between plant hormones, i.e. abscisic acid (ABA), ethylene, cytokinins, brassinosteroids and auxins, plays a crucial role in plants' tolerance to abiotic stresses through either synergistic or antagonistic interactions (Peleg and Blumwald, 2011). The concentration of $\gamma$-aminobutyric acid, GABA, a four carbon nonproteinogenic amino acid, is in fact accumulated in response to a variety of biotic and abiotic stresses, and the induced GABA fold-change in some of the stresses is shown in Table 1.1.

GABA has been hypothesized to be involved in cytosolic pH regulation, carbon and nitrogen metabolism and protection against biotic and abiotic stress (Fait et al., 2005; Al-Quraan and Al-Omari, 2017). Its concentration increases in plant tissue has been shown to restrict the spread of fungi and against pathogen/insect attacks on plants such as *Botrytis*, larvae of *Spodoptera littoralis* and *Choristoneura rosaceana* (Seifi et al., 2013; Bown et al., 2006). GABA is thought to mitigate stress via up-regulating antioxidant defense systems to scavenge reactive oxygen species (ROS), which includes free radicals (superoxide anion $O_2^{\bullet -}$, hydroxyl radical $^{\bullet}OH$) and non-radical molecules (hydrogen peroxide $H_2O_2$, single oxygen $O_2$) (Ramos-Ruiz et al., 2019). In addition to its metabolic role relating to Carbon:Nitrogen (C:N) reconfiguration, GABA is also hypothesized to act as an endogenous signalling molecule regulating plant growth and development under normal and stress conditions (Bouché and Fromm, 2004; Shelp and Zarei, 2017; Ramesh et al., 2015). Using available

*Arabidopsis* RNA-seq data, Biniaz et al. (2022) reported that most transcriptomic changes induced by the two classes of stress (abiotic and biotic) do not overlap; they found only 21 differentially expressed genes were shared between abiotic (drought, heat, salt) and biotic stress and the majority were transcription factors (TFs), which are sequence-specific DNA-binding proteins that contain one or more specific DNA-binding domains and regulate gene transcription (Latchman, 1997). However, one of the most common natural hazards, floods, were not included in their analysis. Plants face multiple biotic and abiotic stresses during flooding and afterwards (during the recovery period), e.g. lower oxygen and light, higher risk of insect and pathogen attack (Tamang and Fukao, 2015). There have been many studies examining transcriptomic, metabolomic responses during flooding (Mustroph et al., 2009; Wang et al., 2021b; Meng et al., 2020), and one of the major responses of the plant is an increase in GABA concentration, however the significance of this is not fully understood. In this study the transcriptomic changes in a collection of GABA mutants that were exposed under flooding stress were specifically examined. In order to illustrate how GABA might contribute to plants coping with abiotic stress, GABA metabolism in plants is reviewed in the following section.

**Table 1.1:** Stress-related GABA accumulation in plants

| Stress | Plant | | GABA | Age (Time stressed) | Reference |
|---|---|---|---|---|---|
| | Species | Tissue | fold-change | | |
| Salinity | *Arabidopsis* | plantlets | 1.5-4 | 10d (2-8d) | Renault et al. (2010) |
| | *Arabidopsis* | Roots | 1.5 | 10d (4d) | Renault et al. (2010) |
| | *Arabidopsis* | Leaves | 2.0 | 5w (2d) | Zarei et al. (2016) |
| | Tomato | Leaves | 1.5-1.3 | 4 true leaf (2-4d) | Wu et al. (2020) |
| | Soybean | Roots | 11-17 | 2w (6d) | Xing et al. (2007) |
| | Wheat | Leaves | 3-7 | 2w (10d) | Al-Quraan and Al-Omari (2017) |
| Hypoxia | *Arabidopsis* | Leaves | 1-12 | 3-4w (2, 4, 6h) | Allan et al. (2012) |
| | | Leaves | 2.5-6 | 4w (0-4h) | Breitkreuz et al. (2003) |
| Anoxia | Tea | Leaves | 20 | 14d (11h) | Liao et al. (2017) |
| | Fava bean | Sprouts | 2.21 | 5d | Yang et al. (2013) |
| | | Cotyledons | 1.57 | 5d | Yang et al. (2013) |
| | | Embryo | 8.26 | 5d | Yang et al. (2013) |
| Hypoxia + Cold | Soybean | Seeds | 7.2 | 24h (0-18h) | Yang et al. (2015) |
| Cadmium | Tomato | Leaves | 1.2-1.9 | 10d (7d) | Chaffei et al. (2004) |
| | Tomato | Leaves | 1.5 | 116d (90d) | Hediji et al. (2010) |

## 1.1 GABA metabolism in plants

GABA biosynthesis mainly occurs via two pathways using either glutamate or polyamines as the precursor, being converted to GABA via glutamate decarboxylase (GAD) in the cytosol and diamine oxidases (DAO) in the peroxisome in the GABA-shunt and polyamine pathway, respectively (Fig 1.1) (Podlešáková et al., 2019; Shelp et al., 2021).

### 1.1.1 The GABA-shunt pathway

The GABA-shunt was first reported in potato (*Solanum tuberosum*) by Dent et al. (1947), and it is the major GABA producing pathway in plants (Shelp et al., 2017). It is composed of three enzymes (Fig 1.1): glutamate decarboxylase (GAD), GABA transaminase (GABA-T) and succinic semialdehyde dehydrogenase (SSADH). It is called the GABA-shunt because it bypasses two steps of the mitochondrial-based citric acid cycle / tricarboxcylic acid cycle (TCA cycle), catalysed by two enzymes sensitive to oxidative stress. They are 2-oxoglutarate dehydrogenase (2-OGDH) that converts $\alpha$-ketoglutarate/2-OG to succinyl-CoA, and succinyl-CoA synthetase which converts succinyl-CoA to succinate (Bouché and Fromm, 2004). During $H_2O_2$-induced oxidative stress, the inhibition of 2-OGDH is critical for limiting NADH production, a major respiratory energy substrate. Therefore, the GABA-shunt can partially restore the impaired respiratory processes under stress conditions and help alleviate oxidative injury in plants (Song et al., 2010).

The TCA cycle intermediate 2-oxoglutarate (2-OG) is a precursor for the GABA-shunt. 2-OG is converted to glutamate (Glu) by glutamate dehydrogenase (GDH), and Glu can be transported from the mitochondria to cytosol directly by the uncoupling protein (UCP) where it enters the GABA shunt pathway (Fig 1.1). Alternatively, 2-OG/malate translocator (OMT) can transport mitochondrial 2-OG to the cytoplasm, where alanine/aspartate aminotransferase (AspAT/AlaAT) catalyses 2-OG into Glu, which enters the GABA shunt pathway (Fig 1.1).

**Glutamate decarboxylase**. As the first step of the GABA shunt, GABA is synthesized from the irreversible cytosolic decarboxylation of Glu - catalysed by glutamate decarboxylase (GAD), which also produces $CO_2$. This is a proton consuming reaction, and it reduces the weak acid content and increases pH (Gibbs and Greenway, 2003). Plant GADs contain a calmodulin (CaM) binding domain (CaM-BD) which is comprised of 22-25 amino acids at the C-terminal end; $Ca^{2+}$ ions can complex with CaM to activate the enzyme at neutral pH and maximally activate GADs at pH 5.8 (Shelp et al., 2012). Under abiotic or biotic stress, plant cytosolic $H^+$ and/or $Ca^{2+}$ concentrations usually increase, and both mechanisms can stimulate GAD activity and thus result in GABA accumulation (Snedden et al., 1995, 1996; Shelp et al., 2017). *Arabidopsis* has five genes encoding GADs, among which only GAD1, GAD2 and GAD4 has a C-terminal CaM-BD while *in silico* analysis suggests that GAD3 and GAD5 proteins are CaM independent (Shelp and Zarei, 2017). *GAD1* is predominantly expressed in roots, *GAD2* is constitutively expressed in all organs, while expression of *GAD3, GAD4, GAD5* is generally weak in all organs (Bouché and Fromm, 2004; Zik et al., 1998).

**GABA transaminase**. GABA is transported back from the cytosol to mitochondria

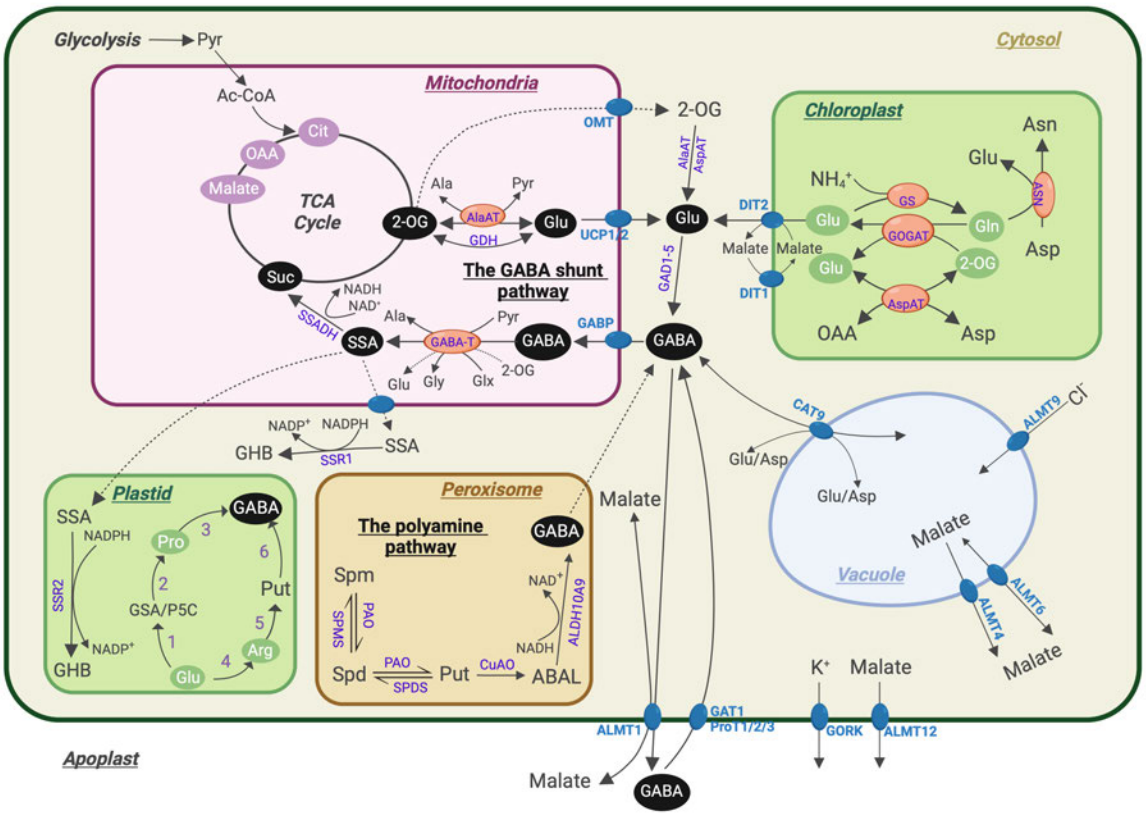


**Figure 1.1:** GABA metabolism and signalling model in *Arabidopsis*. The black ovals represent important GABA shunt metabolites. The blue ovals represent transporters either in the GABA shunt, or linked to the GABA shunt through other pathways/organelles, or potentially link the TCA cycle back to the GABA shunt. The other important metabolites in TCA cycle metabolites and GS-GOGAT cycle were pink or green ovals, respectively. All enzymes are in purple and those with orange ovals are involved in amino acid metabolism. Dashed lines refer to processes lacking convincing experimental support. Abbreviations: ABAL, 4-aminobutanal; Ac-CoA, acetyle-CoA; Ala, alanine; AlaAT, alanine aminotransferase; ALDH10A9, aldehyde dehydrogenase family 10; ALMT, aluminum-activated malate transporter; ASN, asparagine synthase/synthetase; Asp, aspartate; AspAT: aspartate:2-oxoglutarate aminotransferase; CAT, catonic amino acid transporter; Cit, citrate; CuAO, copper amino oxidase; DIT, dicarboxylate transporter; GABA, $\gamma$-aminobutyric acid; GABA-T, GABA-transaminase; GABP, GABA permease; GAD, glutamate decarboxylase; GAT, GABA transporter; GDH, glutamate dehydrogenase; GHB, $\gamma$-hydroxybutyric acid; Gln, glutamine; Glu, glutamate; Glx, gloxylate; Gly, glycine; GOGAT, glutamate synthase; GORK, guard cell outward rectifying $K^+$ channel; GS, glutamine synthetase (GLN); GSA, L-glutamate 5-semialdehyde; OAA, oxaloacetate; 2-OG, 2-oxoglutarate; OMT, 2-oxoglutarate/malate translocator; P5C, $\Delta$-1-pyrroline-5-carboxylate; PAO, polyamine oxidase; Pro, proline; ProT, proline transporter; Put, putrescine; Pyr, pyruvate; Spd, spermidine; SPDS, spermidine synthase; Spm, spermine; SPMS, spermine synthase; Suc, succinate; SSA, succinic semialdehyde; SSADH, succinic semialdehyde dehydrogenase; SSR, succinic semialdehyde reductase; UCP, uncoupling protein; 1, P5C synthetase (P5CS); 2, P5C reductase (P5CR); 3, spontaneous decarboxylation of proline to pyrrolidin$^{-1}$-yl, which is easily converted $\Delta$-1-pyrroline/ABAL and then GABA via aldehyde dehydrogenase (ALDH10A8); 4, urea cycle; 5, arginine decarboxylase (ADC); 6, CuAO and ALDH10A8. Model generated through Biorender (`https://biorender.com`). Own work based on Podlešáková et al. (2019) and Shelp et al. (2021).

by a mitochondrial-located GABA permease (GABP), linking the TCA cycle and GABA shunt (Michaeli et al., 2011). This is an important process to ensure proper GABA-mediated respiration and carbon metabolism, especially for plant growth upon limited carbon availability (Michaeli et al., 2011). In mitochondria, GABA is converted to succinic semialdehyde (SSA) by the mitochondrial GABA transaminase (GABA-T) using 2-OG (GABA-TK) or pyruvate (GABA-TP) as an amino acid acceptor, producing Glu and alanine (Ala), respectively (Bouché and Fromm, 2004). This last step of the GABA shunt provides both succinate and NADH to the respiratory chain. Since part of the Glu recycled by GABA-TK would subsequently feed back into the GABA shunt, the former seems to provide a futile cycle. However, this might contribute to maintain GABA/Glutamate balance in mitochondria. Assays of *Arabidopsis* wildtype and knockout mutants by Clark et al. (2009) confirmed that GABA-TP can also utilize glyoxylate but not 2-OG as amino acceptors, to produce glycine, therefore its activity is not dependent upon 2-OG. However, the pyruvate-dependent reaction is reversible, but the glyoxylate-dependent reaction is irreversible. Unlike other plants, *Arabidopsis* genome contains only one *GABA-T* gene (AT3G22200).

**Succinic semialdehyde dehydrogenase**. As the ultimate enzyme of the GABA-shunt pathway, succinic semialdehyde dehydrogenase (SSADH) oxidises SSA to succinate, generating NADH and a hydrogen. Both succinate and NADH are electron donors to the mitochondrial electron transport chain (mETC) which finally produces ATP. There is only one SSADH in *Arabidopsis* and tomato, whose activity can be inhibited by ATP and NADH (Shelp et al., 2017). Alternatively, SSA can be reduced to $\gamma$-hydroxybutyrate (GHB) via SSA reductase (SSR). SSR is also known as glyoxylate reductase (GLYR) as it catalyses the reduction of glyoxylate to glycolate via NADPH-dependent reactions. There are two isoforms of GLYR proteins in *Arabidopsis*, GLYR1 and GLYR2, present in cytosol and chloroplast, respectively (Simpson et al., 2008; Hoover et al., 2007). Under stress, accumulated GABA is not necessarily converted into succinate by SSADH, as the enzyme has restricted activity due to stress-induced increase of redox potential, this means the accumulation of SSA can result in feedback inhibition of GABA-T (Podlešáková et al., 2019). Allan et al. (2008) found stress-induced GHB co-occurred with higher NADPH/NADP($^+$) ratio, increased GABA and alanine levels, and decreased glutamate levels. They also observed enhanced expression of *SSR1* under salt, drought, submergence, cold and heat stress, and *SSR2* under cold and heat stress.

### 1.1.2 The Polyamine pathway

The other pathway for GABA production is through polyamine catabolism which also contributes to stress-induced GABA accumulation. FAD-dependent polyamine oxidase (PAO) catalyses spermidine (Spd) and spermine (Spm) production which finally produces

putrescine (Put) (Rossi et al., 2021). Put can be degraded into 4-aminobutanal (4-ABAL) by copper-containing diamine oxidase (DAO) named CuAO, which can also catalyse the conversion of 1,3-diaminopropane to 3-aminopropanal (3-APAL) (Shelp and Zarei, 2017). A further oxidation of 3-APAL and 4-ABAL by $NAD^+$-dependent aminoaldehyde dehydrogenases (AMADHs) lead to the biosynthesis of $\beta$-alanine and GABA, respectively (Zarei et al., 2016). *Arabidopsis* has two cytoplasmic located PAOs (AtPAO1 and AtPAO5) and three peroxisome located PAOs (AtPAO2, AtPAO3, and AtPAO4). Several studies showed that salinity-, hypoxia- and anoxia-induced accumulation of GABA is reduced by 39%, 32% and 25% by aminoguanidine, a diamine oxidase inhibitor that represses the production of Put (Xing et al., 2007; Yang et al., 2013; Liao et al., 2017). The PAO protein is localised in the nucleus, cytoplasm, and cell wall of the guard cells, it is a source of $H_2O_2$ generation in *Arabidopsis* guard cells and plays crucial roles in regulating stomatal movement (HOU et al., 2013).

The synthesis of polyamines (PAs) in plants starts from the decarboxylation of either ornithine (Orn) by Orn decarboxylase (ODC), or arginine (Arg) by Arg decarboxylase (ADC), respectively. As summarised by Patel et al. (2017), ODC directly converts Orn to Put, while ADC converts Arg to agmatine, and Put is finally produced with two additional enzymes, agmatine iminohydrolase (AIH) and N-carbamoyl putrescine aminohydrolase (NLP1). Based on the correlation of between increased *ADC2* expression and increased *ARGAH2* expression in response to various stresses (drought, oxidative stress, wounding, and external application of methyl jasmonate), Patel et al. (2017) also proposed a third plastid pathway for Put biosynthesis. Instead of being exported to the cytoplasm for conversion to Put by AIH and NLP1, agmatine was produced by ADC2 in the plastid and converted to Put by ARGA in the chloroplast. *Arabidopsis* is the only plant lacking ODC activity and therefore restricts PAs biosynthesis to the ADC pathway, and it has two genes encoding ADCs, i.e. *ADC1* and *ADC2* (Hanfrey et al., 2001). The proper function of ADC is important as double mutants of both *AtADC* genes shows a defect in seed development (Urano et al., 2005). Rossi et al. (2021) showed that salicylic acid (SA) could modulate PA metabolism during plant-pathogen interactions and induce Put accumulation by increased biosynthesis (ADC pathway which uses Arg) and decreased catabolism (oxidased by CuAO).

## 1.2 The role of GABA under abiotic stress

GABA is proposed to function as a metabolite and as a component of signalling pathways in the process of plants coping with different environmental conditions (Gilliham and Tyerman, 2016). For example, GABA is proposed to act as an effective osmolyte and scavenger of ROS under water stress (Liu et al., 2011). From the previous section, it

is clearly shown that GABA metabolism is closely related to amino acid and carbon metabolism. GABA may also play a key role in plants' acclimation to combined stresses e.g. high light and heat, potentially by promoting autophagy; GABA, together with another six metabolites (rhamnose, glycerol, succinate, gluconic acid, arginine and tyrosine), only accumulated in plants subjected to both types of stress but not when individual stresses were applied (Balfagón et al., 2022).

### 1.2.1 Exogenous GABA alleviates abiotic stresses

Exogenous application of GABA had been reported to enhance the tolerance to various abiotic stresses in plants, likely through affecting GABA metabolism, plant hormones biosynthesis, reactive oxygen species detoxification, and carbon and nitrogen metabolism (Barbosa et al., 2010; Hijaz and Killiny, 2019). For example, GABA-treated creeping bentgrass showed a significantly better recovery from 9 d drought stress than non-treated plants (Li et al., 2016b); exogenous GABA alleviated alkaline stress in *Malus hupehensis* by regulating the accumulation of organic acids (Li et al., 2020); exogenous GABA has been proposed to alleviate stress-induced oxidative damage (due to $H^+$, $Al^{3+}$ accumulation) by promoting activities of antioxidant enzymes and reducing carbonylated proteins caused by ROS (Song et al., 2010). In addition, Garg et al. (2017) found exogenous application of GABA to stressed plants increased levels of endogenous GABA and several other amino acids: glutamate (Glu), aspartate (Asp), threonine (Thr), serine (Ser), alanine (Ala), and valine (Val). GABA's impact on physiology can occur through multiple routes including: (i) regulation of stomata movement (Xu et al., 2021) and maintenance of photosynthesis (Li et al., 2016a); (ii) modulation of polyamine biosynthesis and degradation (Wang et al., 2014); (iii) enhanced redox balance and capacity of antioxidant and ROS scavenging (Ma et al., 2018; Jin et al., 2019); (iv) regulatory roles for $H_2O_2$ and ethylene (Shi et al., 2010), and (v) promotion of the activity of GABA-shunt pathway which results in an increased endogenous GABA, succinate and fumarate (Carillo, 2018; Hijaz and Killiny, 2019), providing ATP and energy for plants through the TCA cycle.

Exogenous GABA treatment also affects metabolism of plants under non-stressed conditions. Compared to non-treated citrus leaves, exogenously applied GABA induced higher expression of *GABA-T*, *SSADH*, and mitochondrial TCA cycle regulatory genes malate dehydrogenase (*MDH*) and succinic dehydrogenase (*SDH*), indicating increased GABA shunt capability and conversion of GABA to succinate as well as an induction of respiration in these plants (Hijaz et al., 2018). At the same time, exogenously applied GABA also increased concentrations of endogenous GABA, plant hormones (salicylic acid, jasmonic acid, indole acetic acid and ABA), amino acids (Gly, Ala, Pro, Asn and Gln) and organic acids (benzoic acid, cinnamic acid, indole propionic acid), suggesting a significant metabolism change in GABA-treated plants (Hijaz et al., 2018). Similarly, immersing

citrus petioles in 10 mM GABA for 2 weeks resulted in elevated levels of endogenous GABA, succinic acid and fumaric acid in leaf blades, supporting the idea that exogenous GABA was metabolized to succinate and fed back into the TCA cycle (Hijaz and Killiny, 2019). However, 10 mM is a relatively high GABA concentration, which could potentially induce osmotic stress, and 2 weeks is a rather long time, so the increased metabolites could be a response to both osmotic stress acclimation and GABA application in combination.

GABA treatment increases the content of free PAs and improves stress tolerance of plants. Ferreira et al. (2019) showed PAs were involved in GABA-regulated salinity-alkalinity stress tolerance in muskmelon plants. Their pre-application of GABA reduced the $Na^+/K^+$ ratio in stressed plants compared to control plants, resulting in decreased membrane lipid peroxidation and stress tolerance. Higher expression of PA-related genes and elevated levels of Arg, Met and free PA content were also observed in GABA-treated plants under stress conditions.

### 1.2.2 Carbon cycle and nitrogen balance related to GABA metabolism

GABA accumulation is part of the stress-responsive C:N network and various signalling pathways, and stress-induced GABA may help plants conserve cellular carbon (Shelp et al., 2012; Gilliham and Tyerman, 2016). This section will focus on metabolic processes that are closely related to GABA, as in this thesis some genes and metabolites involved in these pathways will be examined to elucidate how *Arabidopsis* GABA mutants with an altered GABA shunt efficiency cope with submergence.

#### 1.2.2.1 Glutamate metabolism

Glutamate, the precursor of GABA biosynthesis, plays a central role in plant C:N metabolism. Glu is not only a substrate for the synthesis of GABA, but also Gln, Arg, Pro, Orn and 2-OG (Forde and Lea, 2007). Glutamate (Glu) is produced from glutamine (Gln), 2-OG, Δ-1-pyrroline-5-carboxylate dehydrogenase (P5C) by glutamine-dependent glutamate synthase 1, alanine or aspartate aminotransferase (AspAT, AlaAT), and P5C dehydrogenase P5CDH, respectively. Glutamate synthase 1 is also known as glutamine:2-oxoglutarate aminotransferase (GOGAT). The reaction requires 2-OG and is reductant-driven, eventually transferring the amide amino group of Gln to 2-OG to yield two molecules of Glu. Two forms of GOGAT exists in plants, one is ferredoxin-dependent (GLU1; Fe-GOGAT) and the other is NADH-dependent (GLT1; NADH-GOGAT) (Fontaine et al., 2012). GLU1/Fe-GOGAT is able to utilise light directly as a supply of reductant and is normally present in high activities in the chloroplast of photosynthetic tissues, while GLT1/NADH-GOGAT is also present in plastids but mostly in non-photosynthetic cells (Forde and Lea, 2007).

Gln is synthesised from Glu and ammonia by ATP-dependent glutamine synthetase (GLN; GS), while GDH catalizes Glu to 2-OG and ammonia. *GDH* and *GLN1* are both nitrogen (N) mobilisation- and senescence-associated genes, with Pro and Glu being the main inducers of their expression, respectively. *Arabidopsis* has five cytosolic GS1 isoenzymes designated as GLN1.1 to GLN1.5, and one chloroplastic/mitochondrial GS2 (i.e. GLN2). Three GLN1 encoding genes, i.e. *GLN1.1* to *GLN1.3*, mainly contribute to nitrogen re-mobilisation and seed yield (Moison et al., 2018). Although the *Arabidopsis GLN2* encodes dual-targeted GLN, the net ammonia assimilation occurs mainly in the chloroplast, where GLU1 activity requires 2-OG (Hirel and Lea, 2002).

As shown in Fig 1.1 Glutamine synthetase (GS) and glutamate synthase (GOGAT) are the two enzymes in the GS/GOGAT cycle (Hodges, 2002). Serine produced in mitochondria during photorespiration catalysed by the glycine decarboxylase (GDC) is a major source of ammonium, which is rapidly assimilated into non-toxic organic compounds almost exclusively through the plastidal GS/GOGAT pathway/cycle and further into amino acids and proteins (Hodges, 2002). After 7 d dark treatment, *gdh1-2-3* triple mutant had significantly lower leaf 2-OG and ammonium and root organic acids (2-OG, malate, citrate, nitrate) than WT plants, but largely accumulated Ala, Asp and GABA in both tissues (Fontaine et al., 2012). Gln was reduced in the triple mutant, but Glu increased at 3d and eventually dropped. Therefore, the NADH-dependent GDH functions mainly in providing 2-OG for the TCA cycle, and the *gdh1-2-3* mutant activated GABA shunt in the roots to compensate for its lack of GDH.

#### 1.2.2.2 Arginine and proline metabolism

Two enzymes, arginine decarboxylase (ADC) and arginase (ARGA), can both catalyse arginine degradation. ADC converts Arg into $CO_2$ and agmatine in the cytosol and chloroplast, and is also a rate-limiting enzyme, as the first enzyme, in PAs synthesis (see previous section Polyamine pathway 1.1.2 ) (Hanfrey et al., 2001). *ADC2* is stress inducible and is required for accumulation of putrescine in salt tolerance (Urano et al., 2004). ARGAH1 and ARGAH2 converts Arg into Orn and urea, which takes place in mitochondrion, cytosol, peroxisome and chloroplast. The mitochondrial $\delta$-ornithine aminotransferase (OAT) converts Orn to L-glutamate 5-semialdehyde (GSA), which spontaneously cyclizes to $\delta$-1-pyrroline-5-carboxylate (P5C), and P5C is either further reduced to Pro by P5C reductase (P5CR) or oxidased to Glu (Krasensky and Jonak, 2012).

Proline (Pro) also accumulates under stresses and its biosynthesis takes place in cytosol (and potentially in plastids of stressed plants) while its degradation is a mitochondrial oxidative process (Kovács et al., 2019). As mentioned above, Orn pathway contributes to osmotic stress-induced Pro accumulation (Funck et al., 2008). Glutamate (Glu), a

common precursor for the synthesis of GABA and Pro, is the main biosynthetic pathway of Pro which consists of two consecutive steps: (i) the rate-limiting enzyme $\delta$-1-pyrroline-5-carboxylate synthetase (P5CS) catalyses Glu to glutamate-5-semialdehyde (GSA), which spontaneously cyclizes to P5C; (ii) P5C is then reduced to Pro by P5C reductace (P5CR) in a NADPH dependent reaction (Delauney and Verma, 1993). The two *Arabidopsis* P5CS enzymes perform non-redundant functions: P5CS1 plays a role in responses to hyperosmotic stress and is regulated by ABA signals, whereas P5CS2 is considered to be a housekeeping gene and is induced by pathogens via salicylic acid-dependent signals (Kovács et al., 2019). For *Arabidopsis* plants under salinity, both Orn and Glu pathways collectively play important roles in Pro accumulation in young plantlets (12 d), but in older plants (28 d) the increased Pro was mainly due to enzymes in Glu pathway (Roosens et al., 1998). Although Glu can produce both Pro and GABA, Liu et al. (2011) studied excised tobacco leaves during a 16-hour dehydration and reported that Glu metabolic flux to produce GABA is dominant with a significantly higher scavenging ability for $O_2^{\bullet -}$, $H_2O_2$, and $^1O_2$ than that of Pro.

### 1.2.3 Disturbed GABA metabolism affects plants' acclimation to stresses

Plants with disturbed GABA metabolism, e.g. knockout of one or more genes in the GABA shunt (Section 1.1.1) or polyamine pathway (Section 1.1.2), showed different stress responses in various studies.

GABA-T is involved in C:N metabolism during the plant development process, and lack of its function affects GABA catabolism and stress tolerance. Jalil et al. (2017) suggested GABA-T participated in controlling the onset of leaf senescence of plants during stress conditions. They studied two GABA-T lines of *Arabidopsis* Landsberg (Ler) ecotype, i.e. *pop2-1* and *pop2-3* under various stresses by inducing dark, cold, wounding, dehydration, osmotic and oxidative stresses to detached leaves, and both mutants showed early leaf senescence during various these conditions. The two GABA-T mutants had decreased photosynthesis efficiency, GABA and chlorophyll content, and GABA-T and GAD activity, but increased membrane ion leakage and malondialdehyde (MDA) content than wild type.

As the final enzyme in the GABA shunt pathway (Fig 1.1), SSADH plays an important role in preventing ROS accumulation and cell death, both of which appears to be essential for plants under stress conditions. The *Arabidopsis ssadh* (T-DNA knockout) mutants had a higher accumulation of ROS which was associated with dwarfism and hypersensitivity to light (especially UV-B) and heat stress, and contain five times higher GHB, whose level in *Arabidopsis* is light dependent; however, when mutants were treated with a specific GABA-T inhibitor, $\gamma$-vinyl-$\gamma$-aminobutyrate, ROS and GHB accumulation as well as cell

death were inhibited, and plant growth was improved (Bouché et al., 2003; Fait et al., 2005). This could be when GABA production through GABA-T is blocked, the *ssadh* mutants accumulated less toxic SSA. Therefore, under adverse conditions which inhibit the TCA cycle, impair respiration, and enhance the accumulation of ROS, maintaining the ability of the GABA shunt to supply NADH and/or succinate to the TCA cycle is critical to decrease aldehydes. Another study using *Arabidopsis ssadh*, *pop2* and *ssadh pop2* double mutants, confirmed that the second GABA-T mutation was able to suppress the severe phenotypes of *ssadh* plants, and only *ssadh* accumulated peroxides; compared to wild type, the double mutant also showed higher sensitivity to exogenous SSA or GHB treatment, suggesting the oxidative stress and retardated growth of *ssadh* plants is not due to lack of succinate and NADH supply to the TCA cycle, but rather due to elevated levels of toxic GABA-T downstream product SSA and/or GHB (Ludewig et al., 2008).

Mutants with impaired polyamine pathway also showed altered stress responses. The *Arabidopsis* ALDH10A8 and ALDH10A9 are two isoforms of ALDH enzymes, and they are located in the plastid and peroxisome, respectively. A recent study on aldehyde dehydrogenase (ALDH) genes *aldh10a8* and *aldh10a9* knockout mutants showed that GABA concentration in *Arabidopsis* was not changed under control conditions, however, all the mutants accumulated significantly less GABA (only 50% of the GABA content induced in WT) in response to 2d salt treatment; interestingly, $\beta$-alanine accumulation under salinity was not severely inhibited in the mutants (Zarei et al., 2016). Sagor et al. (2016) studied *Arabidopsis* single and double *pao* mutants under salinity and drought. They found that all five single mutants and *pao2 pao4* double mutant exhibit WT-like responses to high salinity (14 d on media contains 100 mM NaCl), but *pao1 pao5* which lost cytoplasmic PAO activity was less sensitive than WT. This salt tolerance phenotype was further confirmed when they used a range of NaCl concentrations, as *pao1 pao5* had significantly longer main roots than WT when grown on 50 to 100 mM NaCl. It was concluded that *pao1 pao5* had increased tolerance to both abiotic stresses due to reducing ROS production and activating subsets of defense-related genes.

### 1.2.4 GABA plays a signalling role

GABA may not just act as a stress-related metabolite, it may regulate gene expression in *Arabidopsis*. For example, GABA down-regulates the expression of 14-3-3 gene family members in a $Ca^{2+}$, ethylene- and ABA-dependent manner (Lancien and Roberts, 2006). GABA is also proposed to play a signalling role in long-distance nitrate transport, supported by the evidence that exogenous GABA regulates nitrate uptake and utilisation in the roots of *Arabidopsis* (Barbosa et al., 2010) and canola (Beuve et al., 2004). Therefore, GABA could possibly function beyond the role as a nitrogen source, modulating enzymes activity as a signalling molecule. During changing environmental conditions, the regulation

of intracellular pH and ion concentration through membrane transport systems is crucial for plants to maintain pH and ion homeostasis as well as to form an electrochemical potential across the plasma membrane. The Aluminum-activated Malate Transporters (ALMTs), which contains a 12 amino acid residue putative GABA biding motif, were proposed to be a plant GABA receptor (Ramesh et al., 2015). This is the first evidence that GABA directly acts as a plant GABA signalling with ion channel modulation, suggesting GABA's role beyond its effects on C:N metabolism in modulating plant growth and stress adaptation in plants. As shown in Fig 1.1, transporters likely involved in GABA metabolism are ALMTs, guard cell outward rectifying $K^+$ (GORK), GABA transporter (GAT), and dicarboxylate transporter (DITs).

Accumulated GABA can improve aluminum, drought and hypoxia tolerance of plants by regulating the activity of ALMTs and the GORK channel, respectively (Shelp et al., 2021). GABA acts as an inhibitory neurotransmitter in mammalian nerve terminals, via its activation of two GABA receptors: ionotropic $GABA_A$ and metabotropic $GABA_B$, respectively (Bloom and Iversen, 1971). However, in plants, GABA inhibits ALMT activity. Nonetheless in both animal and plant kingdoms, GABA-regulated anion flux leads to a relative hyperpolarised state of the cells (Žárskỳ, 2015). Ramesh et al. (2015) found that low pH and increased aluminum ($Al^{3+}$) concentration reduced root GABA but increased malate efflux in wheat via ALMT1, which is plasma membrane located; however, root GABA concentration is high and malate efflux is low in the absence of $Al^{3+}$, and exogenous GABA application to roots also reduced malate efflux and root tolerance to $Al^{3+}$. Batushansky et al. (2015) exposed *Arabidopsis* ecotype *Wassilewskija* wild type (WS) and *gat1* seedlings to exogenous GABA (0.5 and 1 mM), and measured the growth and metabolic profiles in different media (low C, low N). Their results suggested that GABA possibly mediated C:N metabolism through the ALMT.

As the focus of this thesis is understanding the role of GABA in salinity and hypoxia response, as well as the role of the histidine residue in the putative GABA-binding motif in ion transport and pH sensitivity, more detailed review regarding these subjects are explored in the following sections.

## 1.3 Salinity and GABA

Salinity is a common abiotic stress that plants can face, which inhibits their growth and reduces yield through osmotic stress (short-term) and toxic effects of ions (long-term) (Munns and Termaat, 1986). In saline soils, lowered osmotic potential due to sodium ($Na^+$) and chloride ($Cl^-$) accumulation results in decreased water and nutrient availability, increased lipid peroxidation, altered metabolic and photosynthetic activity in plants (Munns

et al., 2006; Deinlein et al., 2014). At mild to moderate stress levels, salt mainly limits photosynthesis by affecting $CO_2$ diffusion (due to a decrease in mesophyll and stomatal conductance) rather than directly impacting $CO_2$ assimilation machinery (Flexas et al., 2004). Turgor generation and cell-wall properties can also be affected by salinity, restricting cell expansion, root and leaf development (Taleisnik et al., 2009). In order to maintain growth and avoid toxicity, plants generally cope with salinity through increased osmotic adjustment and tolerance, $Na^+$ and $Cl^-$ exclusion, $Na^+$ and $Cl^-$ compartmentalisation at cellular and intracellular level (Munns and Tester, 2008).

In addition, oxidative stress, which is mediated by reactive oxygen species (ROS), accompanies salinity as a secondary stress. Although highly reactive and can cause damage to plant cells, ROS are also signalling molecules at low concentrations and are involved in regulating germination, transpiration, defense response, cell death and plant growth (Lindermayr and Durner, 2015). They also have a pivotal role for root growth and development (Yamada et al., 2018; Zeng et al., 2017; Yu et al., 2016), including lateral root formation (Biswas et al., 2019). ROS scavenging enzymes includes catalase (CAT), superoxide dismutase (SOD), peroxidase (POD), ascorbate peroxidase (APX). These ROS scavengers accumulate under multiple stresses including salinity and help plants cope with adverse environments.

$Ca^{2+}$ signalling is reported to be the predominant response in plant cells, and plants under salinity also experience metabolic reprogramming (e.g. amino acids metabolism) and phytohormone regulation, in order to survive (Köster et al., 2018). For example, cytokinins and auxins act antagonistically to control lateral root initiation, with cytokinins inhibiting and auxins stimulating cell division (Coenen and Lomax, 1997). Light-grown garden pea double mutants (*phyA phyB*) produce more ethylene than WT, and have many severe defects (distorted short thick internodes, reduced leaf expansion, and decreased chlorophyll content and CAB gene transcription), which can be rescued by treating the mutant with an ethylene biosynthesis inhibitor "aminoethoxy vinylglycine" (Foo et al., 2006). This suggests the role of phytochromes in regulating ethylene concentrations under light to prevent ethylene's inhibitory effects on vegetative growth. This elevated ethylene is not related to the other hormones (IAA, BR), unlike in other studies, but due to an interaction with GA.

### 1.3.1 GABA alleviates salt stress

As GAD activity can be stimulated by increased $Ca^{2+}$ concentration, GABA accumulates rapidly in stressed plants and an increasing amount of research has shown that GABA plays a role in plant stress tolerance, linking the GABA shunt to mitochondrial respiration. Salt stress inhibits mitochondrial respiration and promotes GABA shunt activity, which provides an alternative carbon source for mitochondrial respiration as it bypasses some of

the salt-sensitive enzymes of the TCA cycle. For more details on GABA metabolism and signalling, see the previous Section 1.1 of this chapter.

GABA alleviates salt-induced harmful effects as an osmolyte on its own, and it also enhances antioxidant system and scavenges ROS. For example, Che-Othman et al. (2020) and Bao et al. (2015) studied salt stressed wheat and tomato, respectively, and reported that both species accumulated GABA (one fold increase) and had increased GAD activity. In addition, tomato plants exposed to 200 mM NaCl for 5 d also had 25% decrease in succinate content. The salt treated wheat leaves experienced higher respiration rate and extensive metabolite changes, with elevated concentration of succinate, 2-OG, Glu and Gln, but reduced activity and abundance of pyruvate dehydrogenase (PDH) and 2-oxoglutarate dehydrogenase (2-OGDH) as well as TCA cycle organic acids (citrate, aconitate, fumarate and malate). Therefore, the researchers concluded that: (i) salinity promoted a shift of wheat mitochondrial respiration from the TCA cycle to the GABA shunt, with the latter accounting for an approximate 20% increase in the transpiration rate of stressed leaves, despite of lower PDH and PDC oxidation; and (ii) the glutamate synthase, i.e. either Ferredoxin-dependent or NADH-dependent glutamine:2-OG amidotransferase (Fe-GOGAT or NADH-GOGAT), and glutamate dehydrogenase (GDH), are likely to be indicating N assimilation into Glu under salinity.

GABA could also contribute to a plants' ability to cope with salinity through regulating other metabolic pathways (ABA, ethylene, flavonoid) and transcription factors TFs. Shi et al. (2010) found that $H_2O_2$, putrescine and ethylene producing genes, e.g. *NADPH oxidase*, *amine oxidase*, *ACC oxidase*, were up-regulated at the mRNA level by 10 mM GABA within 24 hours under 300 mM NaCl, although $H_2O_2$ accumulation in both roots and leaves were inhibited. The reason could be that as a second messenger, $H_2O_2$ actively participates in signal transduction pathways, e.g. ABA signalling (Kwak et al., 2003). *Arabidopsis* salt-stressed plantlets had elevated GABA concentrations, which are associated with inducible co-expression of TFs (*WRKY28, WRKY30, WRKY40, MYB2, MYB25, MYB108*), *CaM37*, *ALMT2* and *GAD4* (Zarei et al., 2017). A soybean WRKY (*GmWRKY16*) enhances salt and drought tolerance of transgenic *Arabidopsis* plants through an ABA-mediated pathway (Ma et al., 2019). Under salinity, salt-related MYB1(SRM1) negatively affects *Arabidopsis* seed germination and seedling survival through regulating the content of the stress hormone abscisic acid (ABA) (Wang et al., 2015). SRM1 can directly activate the expression of *NCED3/STO1* (key ABA biosynthetic gene) and two prominent stress integrators (*RD26* and *ANAC019*). Xie et al. (2019) studied salt-stressed poplar with either inhibition of 2-OGDH) activity or exogenous GABA application, and found that the expression of flavonoid biosynthetic genes as well as GABA-shunt activity were changed in both cases. Flavonoid is a secondary metabolite derived from the phenylpropanoid pathway and is closely related to C:N metabolism.

Therefore GABA probably plays a role in allocating carbon and nitrogen under control or salinity through regulating the flavonoids biosynthesis pathway.

Akçay et al. (2012) studied salt stressed (up to three weeks) *Nicotiana sylvestris* wild type and the cytoplasmic male sterile (CMS) II mutant, which had impaired mitochondrial function due to the deletion of NAD7 subnit of complex I. The TCA cycle activity of CMSII mutant is maintained by complex II and alternative dehydrogenases that bypasses complex I. Under short term stress (within 24 hours), both lines had induced GAD activity as well as elevated GABA concentration, but the activities of glutamate dehydrogenase (GDH) and GAD as well as GABA content was significantly higher in wild type than in CMSII. However, in the long term, unlike wild type, salt induced GABA accumulation in CMSII didn't correlate to GAD activity, which was much lower than in non-stressed CMSII plants. This suggests that the GABA shunt pathway is not the only source of GABA in plants. Interestingly, GAD activity in non-stressed CMSII mutants also increased weakly without accumulating GABA, suggesting the efficient and fast catabolism of GABA. This provided more evidence of improved GABA-shunt activity due to impaired TCA cycle, and again indicates a non-direct correlation between GAD activity and GABA concentrations.

### 1.3.2 Modified GABA metabolism alters salt tolerance

Plants with altered GABA metabolism display altered tolerance. Bao et al. (2015) studied the tomato *GAD*, *GABA-T* and *SSADH* genes through virus-induced gene silencing. They found that silencing of *SlGADs* and *SlGABA-Ts* both increased ROS accumulation and sensitivity to 200 mm NaCl stress, but *SSADH*-silenced plants were less sensitive to salinity than WT, although they cannot degrade GABA and had a dwarf phenotype and elevated ROS levels under normal conditions. This suggests the catabolism of SSA to GHB as reported previously in *Arabidopsis* may play a role in salt stressed plants. Su et al. (2019) studied a GABA deficient double mutant *gad1,2* and a GABA accumulation line *pop2-5* under normal and salt conditions and found the latter more tolerant to salinity. After growing on medium containing NaCl for one week, young seedlings of the double mutant had minimal GABA content which could not be induced by salinity. In contrast, *pop2-5* which cannot catabolise GABA through GABA-T, had the highest GABA content among all three lines even under control conditions, with additional salinity-promoted GABA accumulation. After a longer period of salt stress (up to 3 weeks in the medium) and higher NaCl concentration (up to 150 mM), *pop2-5* also showed higher survival rates and larger biomass than *gad1,2*. They concluded that GABA improves salinity tolerance by conferring better membrane potential maintenance and optimal $Na^+/K^+$ ratio mainly through more negative regulating ion transporters. The plasma membrane $Na^+/K^+$ antiporter *SOS1* transports $Na^+$ from cytoplasm to the apoplast, functioning in $Na^+$ exclusion upon salinity. *SOS1* is regulated by the $P_{3A}$ type of $H^+$-ATPase encoded by *AHA* genes (Kim

et al., 2013). The vacuolar $Na^+/K^+$ exchanger NHX1 mediates $Na^+$ compartmentalisation, with constitutive overexpression in *Arabidopsis* leading to increased salt tolerance (Amin et al., 2020; Apse et al., 1999). Salt-stressed *pop2-5* roots had up-regulated expression of *SOS1*, *AHA2* and *NHX1*, while in *gad1,2* their transcription levels barely changed. The outward-rectifying $K^+$ efflux channels (*GORK*) gene expression was much higher in *gad1,2* than in *pop2-8*. This suggests the reduced $Na^+$ concentration in the cytoplasm, lowered ROS-inducible $K^+$ efflux from root epidermis, and better $K^+$ retention due to lower GORK channel activity, all contribute to the salt-resistant phenotype of *pop2-8* (Su et al., 2019).

On the contrary, Renault et al. (2010) found that GABA transaminase (GABA-T), was a sensitive step of GABA metabolism responding to salt stress, as *pop2-1* mutant was oversensitive to ionic stress but not to osmotic stress. They also observed decreased content of shoot succinate, 2-OG, Gln and root Gln but accumulated Glu in salt stressed mutant. Additionally, they reported *pop2-1* under salinity had altered cell wall composition and hypocotyl development, reduced expression of sucrose-related genes, and reduced starch metabolism, accompanied by decreased sugars. This observation could be due to: (i) a different ecotype Lansberg, instead of Columbia was used in Renault et al. (2010) study, and natural variation in salt tolerance does exist between *Arabidopsis* accessions (Katori et al., 2010; Julkowska et al., 2016); (ii) GABA may efficiently operate only within a range of concentrations, as the content of GABA in salt stressed *pop2-1* is twice as high than that of *pop2-5* (Su et al., 2019), this could be beyond its optimal functioning range.

Stress-induced ROS leads to excessive accumulation of aldehydes, which are intermediates in several fundamental metabolic processes and are produced under normal and various stresses. The detoxification of over accumulated ALDHs are through the activity of 'aldehyde scavengers', $NAD(P)^+$-dependent aldehyde dehydrogenase (ALDHs), by catalysing the oxidation of aldehydes into the corresponding carboxylic acids, eventually reducing lipid preoxidation (Kirch et al., 2004). *Arabidopsis* ALDHs belong to nine different families, some of the stress-related proteins are: (i) family 3, 5 and 7, such as ALDH3I1, ALDH3H1, ALDH3F1, ALDH7B4, and ALDH5F1 which is also named SSADH and is involved in the GABA shunt; (ii) the betaine aldehyde dehydrogenase (BADH) homologues ALDH10A8 and ALDH10A9 which are involved in PA metabolism (Kirch et al., 2004). Significant amounts of toxic aldehydes are produced during dehydration, salt, heat, and oxidative stresses, followed by increased expression of *ALDH* genes, and plants with over-expressed and knock-out *ALDHs* are more tolerant and more sensitive to these stresses compared to wild type, respectively (Tagnon and Simeon, 2017). Zarei et al. (2016) reported that during an up to 2 d salt stress, two *ssadh* mutants showed reduced shoot GABA concentration and inhibited root growth compared to wild type. Although *ssadh* mutants cannot convert SSA to succinate, their shoot GABA concentration was not altered under control conditions,

and the mutants accumulated significantly less GABA under salt stress (only 50% of the GABA content induced in WT). This suggested the importance of GABA shunt activity under salinity and the other pathways could not compensate for the loss of SSADH.

### 1.3.3 Exogenous GABA application increases salinity tolerance

Multiple researchers have shown that exogenous GABA, either applied before stress (plant priming) or during stress, usually stimulate endogenous GABA concentration, reduce ROS accumulation, thus help plants cope with stresses including salinity.

Exogenous GABA alleviates salt damage to tomato seedlings through induced endogenous GABA to reduce $Na^+$ uptake, promotion of amino acid synthesis and osmotic and antioxidant accumulation (Wu et al., 2020). Exogenous GABA also improved photosynthesis and enhanced activities of antioxidant enzymes under salinity, and increased salt tolerance of wheat (Li et al., 2016a). Çekiç (2018) found endogenous GABA increased more under NaCl+GABA treatment than either salt or GABA treatment alone, and they proposed that exogenous GABA could enhance the stress tolerance through the production of some phenolic acids as well as endogenous GABA in plant under salinity. Furthermore, exogenous GABA has regulatory roles for $H_2O_2$ and ethylene production on gene expression of *Caragana intermedia* roots under NaCl stress. A study on Maize (*Zea mays*) under NaCl stress also showed that exogenous GABA promoted ROS scavenger enzymes activities (SOD, CAT and POD), and inhibited $H_2O_2$ accumulation (Tian et al., 2005).

Salt stress reduces mETC efficiency which eventually results in reduced photosynthetic performance. In accordance to this, exogenous GABA has been reported to have positive effects on salt stressed muskmelon (Xiang et al., 2016) and lettuce seedlings (Kalhor et al., 2018), through functioning as osmotic substrates which potentially alleviates damages to mesophyll cell walls, and indirectly affecting photochemical efficiency by regulating C:N ratio, respectively.

### 1.3.4 Polyamines contribute to salt-induced GABA production

It has been reported that for multiple species polyamine biosynthesis contributes to plants' adaptation to salinity, mainly through modulating antioxidant system, osmolytes and secondary metabolism, and salinity induces alteration of PA concentrations in plants (Hu et al., 2015). Salinity induces altered PA concentrations in plants. Studies have shown that Spm accumulates under salt stressed rice, and it is not a salt tolerance trait (Maiale et al., 2004). When subjected to long-term salinity (7d, 14d and 21d), two rice cultivars with different levels of salt tolerance both had decreased ADC and S-adenosyl-L-methionine decarboxylase (SAMDC) activities compared with control plants. Salt stress also reduced

putrescine and spermidine concentration, although more dramatically in the sensitive cultivars. However, spermidine synthase (SPDS) activity was only reduced in the tolerant but not the sensitive cultivar during salt stress (Maiale et al., 2004).

The polyamine pathway also contributes to plant adaptation to salt stress. Studies on *Arabidopsis* leaves (Zarei et al., 2016), soybean roots (Xing et al., 2007) confirmed over one third of greater GABA accumulated under salt stress could be occur via PA degradation due to strongly promoted diamine oxidases (DAO) activity. Xing et al. (2007) proposed that higher concentrations of GABA could be accumulated under salt stress in soybean roots, and the reason could also be through increased diamine oxidases (DAO) activity. They found that the PA pathway could contribute to about 39% of salt-induced GABA. Yamaguchi et al. (2006) showed that a double knockout mutant *acl5 spms* (which cannot produce spermine) was hypersensitive to high salt, and this could be ameliorated by exogenous application of spermine. A study by Hu et al. (2015) on muskmelon leaves and roots under $Ca(NO)_3$ also suggested that exogenous applied GABA improved plants stress tolerance through promoting PAs and GABA biosynthesis.

In this thesis, the GABA mutants with altered GABA shunt capacity will be studied under salinity, in order to examine their tolerance and explore the role of GABA under salinity in detail.

## 1.4 Hypoxia and GABA

Flooding is a natural hazard that inhibits worldwide agricultural productivity (Voesenek and Bailey-Serres, 2015). Due to climate change a recent climate model predicts that approximately by 2050 there will be approximately 450 million people exposed to increased flooding, an additional 1.3 billion people influenced by coastal floods due to Antarctic ice and glaciers melting, with more than 1.7 billion hectares of land being affected (Arnell et al., 2016). Submergence describes a type of flooding stress where the entire plant is completely immersed in water, while "partial submergence" means part of the shoot system stays above the water surface (Sasidharan et al., 2017). The term "waterlogging" or "soil flooding" is also used when excessive water presents in the soil or other rooting media and can be regarded as a special case of "partial submergence" when only the root-zone is flooded. Similarly, "partial waterlogging" or "partial soil flooding" means only part of the root-zone is flooded (Sasidharan et al., 2017). GABA rapidly accumulates to the greatest extent in plant tissues under low oxygen compared to other abiotic stresses such as drought, salt, heat and cold (Ham et al., 2012). In this thesis, I am going to explore GABA metabolism on flooding response using wild type and GABA shunt mutants subjected to complete submergence. Prior to that, general responses of plants under

flooding/submergence conditions are introduced here.

The prevailing proportion of $O_2$ in air at sea level is currently 20.95%. Decreased oxygen availability, i.e. hypoxia stress, always accompanies the (partial) flooding or submergence of plants, mainly due to slow $O_2$ diffusion in water and the roots' competition with respiring microorganisms. Anoxia means the complete absence of $O_2$ in a system and studies usually induce anoxia by replacing the natural atmosphere with inert gas such as argon/nitrogen (Branco-Price et al., 2008; Loreti et al., 2005), or submerging plants using degassed water (Baud et al., 2004). As the photosynthetic light reaction generates molecular $O_2$, many anoxic stresses are conducted in the dark.

Moreover, dark on its own induces senescence and disturbs the expression of thousands of genes, as Lin and Wu (2004) reported nearly 2000 genes were over threefold up-regulated upon darkness (up to 6 d). Buchanan-Wollaston et al. (2005) compared developmental senescence and dark-induced senescence, and they confirmed that 66% (550) of the 827 natural senescence-enhanced genes were also at least two-fold up-regulated in the leaves of dark-treated plants, meaning that about 1500 dark-induced genes were not due to natural aging. The remaining 34% (277) genes were not up-regulated at all under dark, and most of these genes were found to be involved in the salicylic acid (SA) signalling pathway which only appeared in developmental senescence. With respect to GABA metabolism, during dark treatment they also observed that there was 10.82-fold and 21.43-fold increase of *GAD1* and *GAD4* expression in mid-senescent stage leaves compared to before flowering mature and green leaves, respectively. This is consistent with the review of Bouché and Fromm (2004) that proposed that GABA may play a signalling role in coordinating C:N balance in limited nutrient environments as occurring during leaf aging. Therefore, dark submergence, as a combined stress, may not properly represent natural floods, under which plants still maintain day-light cycles as well as partial photosynthesis (either under or above water). Underwater photosynthesis can increase internal oxygen concentration and carbohydrates contents compared to plants under dark submergence, thereby alleviating some of the adverse effects of flooding (Mommer and Visser, 2005). As a consequence I will conduct my research by subjecting all stressed plants to light during submergence in order to mimic plants under natural floods.

### 1.4.1 Oxygen sensing in plants

Oxygen sensing and signalling of plants is reviewed by van Dongen and Licausi (2015) in detail; specifically, plants mainly sense low oxygen in a cell via the N-end rule signalling pathway (NERP) targeted proteolysis and regulation of key hypoxia-responsive transcription factors (TFs). Even plants grown under non-stressed conditions can encounter some degree of hypoxia in certain organs, such as tubers, fruit, vascular bundles,

developing seeds, roots and leaves, due to increased respiratory demand or endogenous barriers to oxygen diffusion (Bailey-Serres et al., 2012). As a result, hypoxic niches are established in these developing tissues, and oxygen gradients can act as a regulatory cue. Recent studies have shown that hypoxic conditions and apical hypoxic niches are required to regulate the production of new leaves (Weits et al., 2019) and lateral roots (Shukla et al., 2019) when plants were under aerobic conditions, via inhibiting the proteolysis of NERP enzymes, therefore linking oxygen sensing to developmental regulation and hormones such as auxin. Moreover, de Marchi et al. (2016) showed that the NERP positively regulates the biosynthesis of plant-defense metabolites (e.g. glucosinolates), and the biosynthesis and response to jasmonic acid which plays a key role in plant immunity.

The hypoxia-associated group VII ethylene-responsive factors (ERF-VIIs) in *Arabidopsis thaliana* were identified as substrates of the NERP, through a characteristic conserved motif initiating with Methionine-Cysteine (Met-Cys) at the amino terminus (Gibbs et al., 2011). This pathway efficiently induces oxygen-dependent cellular molecular responses: decreased oxygen availability attenuates the oxidation of the Cysteine 2 (Cys2) residue, ubiquitin ligation, and proteasomal degradation, eventually leading to nucleus accumulation of ERF-VIIs (van Dongen and Licausi, 2015). Classified as members of the ERF/AP2 superfamily that contain a single APETALA 2 (AP2), ERF-VIIs are able to sense molecular oxygen, translate oxygen availability into the transcriptional reprogramming, and cellular ATP decline which contributes to at least one *Arabidopsis* ERF nuclear localisation (Schmidt et al., 2018). *Arabidopsis* ERF-VIIs are regulated via the attenuation of their first step during the conversion into a Proteolysis 6 (PRT6)-dependent N-degron, which is catalysed by oxygen-dependent Plant Cysteine Oxidases (PCOs) (van Dongen and Licausi, 2015; Gibbs et al., 2015). There are five members in the *Arabidopsis* ERF-VII protein family: RELATED TO AP2 12 (RAP2.12), RAP2.2, RAP2.3, hypoxia-responsive ERF1 (HRE1) and HRE2 (Papdi et al., 2015). Enhanced stability of HRE2 under oxygen deprivation improves hypoxia survival of *Arabidopsis*, but a major rice submergence tolerance determinant SUB1A-1 was not a substrate of the N-end rule pathway, suggesting difference between wetland and terrestrial plants (Gibbs et al., 2011).

Changes in $O_2$ and nitric oxide (NO) can both regulate the stability of *Arabidopsis* ERF-VIIs, whose proteolysis mediates plants' adaptation under flooding-induced hypoxia (Abbas et al., 2015). The nonsymbiotic hemoglobins (Hbs) are also proposed to restrict the oxidation of the N-terminal Cys of RAP2.12, thus promoting the anaerobic response (Igamberdiev et al., 2014). A recent study of Hartman et al. (2019) found plants were able to rapidly sense submergence via ethylene entrapment, and this signal can be used to pre-adapt plants to the upcoming flooding. Ethylene can enhance the stability of ERF-VII proteins prior to hypoxia by increasing the NO-scavenger PHYTOGLOBIN1. Therefore, this ethylene mediated NO depletion in their study, together with consequent accumulation

of ERF-VIIs contribute to plants' survival of subsequent hypoxia.

The other indirect pathways for hypoxia sensing involves: (i) the sucrose nonfermenting kinase SnRK1, which senses energy and control multiple processes including transcription; and (ii) the precise and dynamic mRNA translation regulation which involves SnRK1 and SnRK1 phosphorylated translation initiation factor eIFiso4G (Lee and Bailey-Serres, 2020). *Arabidopsis* WRKY33 and WRKY12 are recently unveiled by Tang et al. (2020) to be acting upstream of ERF-VII-dependent gene expression during hypoxia. Their study suggested WRKY33 can interact with WRKY12 protein to up-regulate RAP2.2 during submergence. Membrane depolarisation (Zeng et al., 2014), changes in transporter activity (Shabala et al., 2014) as well as ROS and NO production (Pucciariello and Perata, 2016) were reported to occur immediately in plant tissues exposed to hypoxia. Thus, although the ERF-VIIs are indeed essential for mediating plant responses to hypoxia, the fact that it could take hours for them to function after the stress onset indicates that they may appear after above changes or their function requires these changes.

As oxygen sensing plays a role in normal growth and hypoxia tolerance, and the gene expression and protein stability of ERFs can be regulated by other TFs and signals, in this research, the expression of ERFs in GABA mutants will be checked, in order to better understand how disturbed GABA metabolism affect the plant response under control and submerged conditions.

### 1.4.2 Plants under hypoxia and recovery

#### 1.4.2.1 Energy crisis and co-occurring stress

Flooding tolerance is strongly dependent not only on viability during submergence but also postflooding (i.e. de-submergence/recovery). Yeung et al. (2018) showed that different rates of recovery between two *Arabidopsis* accessions correlate with submergence tolerance and fecundity. As shown in Fig 1.2, flooded plants encounter not only low oxygen, but also lower light and nutrient availability, and higher risk of pathogen and insect attack (Tamang and Fukao, 2015). The water around the plants has an effect on the quantity and quality of light and $CO_2$ availability, both of which are required for photosynthesis, therefore affecting subsequent carbohydrate (substrate for respiration) and $O_2$ production (van Dongen and Licausi, 2015). Nitrogen availability is also affected during flooding (León et al., 2020).

During the following recovery period of de-submergence (reoxygenation and increased illumination), plants are exposed to higher oxygen and light and higher risk of pathogen and insect attack, as well as leaf dehydration (although sufficient soil water) and other

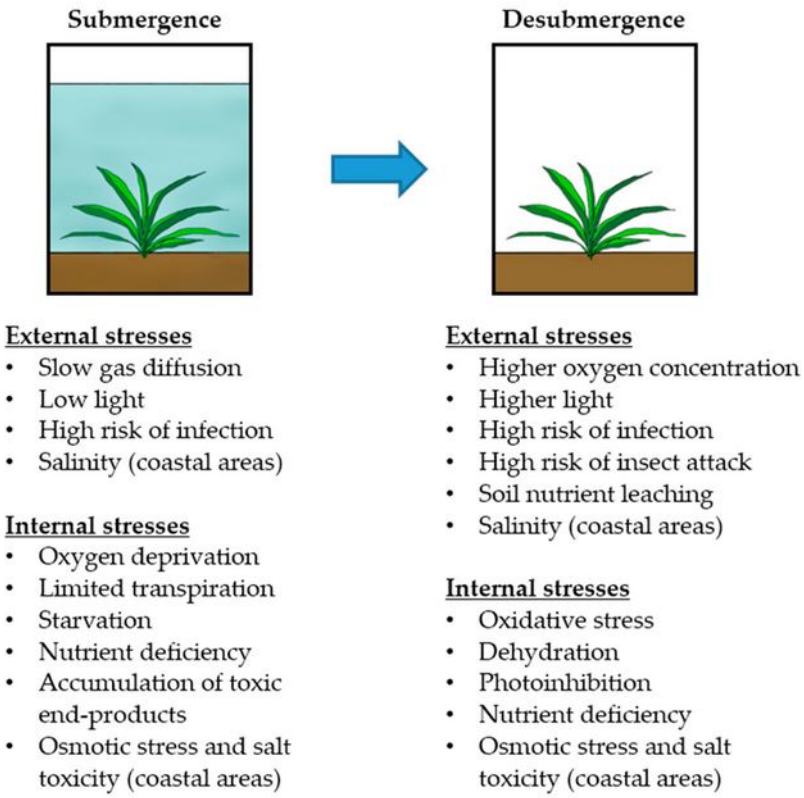


**Figure 1.2:** Co-occurring stresses during submergence and recovery (Tamang and Fukao, 2015). Multiple external and internal stresses co-occurred in addition to low oxygen that plants have to cope with during submergence and the following recovery period.

stresses (Tamang and Fukao, 2015). The primary cause of post-hypoxic injuries in plants are bursts of reactive oxygen species (ROS) and acetaldehyde, which is oxidized from anaerobically accumulated ethanol. Aldehyde detoxification is through the activity of aldehyde dehydrogenase enzymes (ALDHs), which catalyse the oxidation of a broad range of aliphatic and aromatic aldehydes (e.g. acetaldehyde) into their corresponding much less toxic carboxylic acid (e.g. acetate) using $NAD^+$ or $NADP^+$ as cofactors. Acetaldehyde accumulation in rice and maize during re-aeration following submergence have been reported, and the lower submergence tolerance of maize than rice is partially due to the weaker ALDH activity during recovery (Tsuji et al., 2003; Meguro et al., 2006). There are a few ALDH enzymes related to GABA metabolism: SSADH converts SSA into succinate in the GABA shunt pathway, while ALDH10A8, ALDH10A9, ALDH2B7 and ALDH7B4 converts 4-aminobutanal to GABA in the polyamine pathway. Therefore, the differences between GABA mutants under submergence and recovery may be correlated to their altered aldehyde scavenging ability, which contributes to stress tolerance and post-hypoxic recovery.

A reduction in the available $O_2$ in atmosphere contradictorily can result the accumulation of ROS in submerged plants. For example, $H_2O_2$ formation in plants during and after low oxygen stress were reported in rice roots and wheat seedlings, increased ROS-responsive transcripts were observed, and the activities of ROS-scavenging enzymes were also detected

in barley leaves and roots and *Arabidopsis* seedlings (Chang et al., 2011; Pucciariello and Perata, 2016). This is probably due to the fact that complete submergence prevents direct $O_2$ and $CO_2$ exchange between plants and the air, but underwater photosynthesis remains active in some way (at least partially) and can alleviate internal $O_2$ shortage to a small degree, therefore residual $O_2$ which cannot diffuse into the air can provoke ROS production in these plants (Mommer and Visser, 2005). ROS produced in response to oxygen deprivation via either the mitochondrial electron transport chain (mETC) or the plasma membrane localised NADPH oxidase (Pucciariello and Perata, 2016). Inhibition of the terminal step of mETC is a universal consequence upon low oxygen in eukaryotes, while the up-regulated ROS-responsive transcripts could prevent this inhibition, with ROS concentration being actually elevated (Chang et al., 2011). Wu et al. (2021) reported that the increased GABA content under hypoxia is essential for preventing ROS-induced disturbance to ion homeostasis. In current study, the genes related to detoxification of ROS will also be checked to find out how altered GABA metabolism affects plants' detoxification capability.

#### 1.4.2.2 Differential tolerance and metabolic adjustment

Flooding creates an energy crisis and activates adaptive energy management in plants. The main metabolic acclimations include the following as reviewed in detail by van Dongen and Licausi (2015); Bailey-Serres and Voesenek (2008, 2010); Huang et al. (2008); Mustroph et al. (2010): (1) The activity of energy consuming processes is repressed as the oxygen availability decreases, such as ribosome biogenesis, cell wall formation, lipid and protein synthesis, which are particularly affected due to their higher ATP need; (ii) The activity of pathways that don't need oxidative phosphorylation to generate ATP is promoted, such as glycolysis and fermentation, sucrose catabolism, sucrose synthesis preferentially by sucrose synthase (SUS) rather than invertase under low oxygen; (iii) The bifurcation of the TCA cycle, which can partly split into an oxidative and a reductive branch, thus finely regulating the $NAD(P)^+$/NAD(P)H ratio in mitochondria as well as controlling the respiratory oxygen consumption by mETC, whose activity also changes with the concentration of available oxygen; and, (iv) The induction of protective processes, such as ROS scavenging, chaperone catabolism, production of alanine, GABA and succinate under hypoxia, which could also contribute to ATP production.

Plants have evolved a variety of physiological, tissue specific morphological and metabolic adaptations to survive oxygen deprivation, and plant species have varied tolerance to low oxygen as well as differed strategies to cope with short/long term stress. As a representative of wetland plants, rice (*Oryza sativa*) can survive complete submergence while terrestrial plants such as maize (*Zea mays*) and *Arabidopsis* seedlings can only endure short periods of hypoxia/anoxia (Winkel et al., 2013; Meguro et al., 2006). Long-term tolerance is

usually related to developmental changes, e.g. forming root aerenchyma, enhancing shoot elongation, developing adventitious root as well as altering root porosity and morphology (Fukao and Bailey-Serres, 2004). Adventitious roots and aerenchyma formation upon flooding both require ROS and ethylene as second messengers, and in addition $Ca^{2+}$ is also involved for the latter (Fukao and Bailey-Serres, 2004). As the activity of the GABA biosynthesis enzyme GAD is regulated by pH and $Ca^{2+}$, a disturbed GABA metabolism could potentially have effects on aerenchyma formation and flooding tolerance.

Promoted anaerobic pyruvate metabolism is among the most common initial cellular metabolic responses in both hypoxia-tolerant and -sensitive plants. Decreased oxygen availability limits the production of ATP from mitochondrial respiration and induces the glycolytic and fermentative pathway in plants that produces ethanol. Pyruvate decarboxylase (PDC) and alcohol dehydrogenase (ADH) are two of the main enzymes during these processes, with PDC catalyzing pyruvate into acetaldehyde, which is then reduced to ethanol by ADH. The importance of these enzymes was confirmed by the fact that maize, rice and *Arabidopsis* PDC and ADH loss-of-function mutants cannot cope with oxygen deprivation (Fukao and Bailey-Serres, 2004), while overexpression of either *PDC* gene in *Arabidopsis* could improve tolerance to low oxygen (Ismond et al., 2003). Overexpression of *ADH1* didn't promote hypoxia tolerance, probably due to unaffected carbon flow and ethanol content in the mutant, which suggests that ADH content are already in excess in wild-type and are above a threshold so do not correlate with the survival (Ismond et al., 2003). On the other hand, uncontrolled or constitutive fermentation can also be detrimental to plant survival as it results in rapid loss of carbohydrate resources which are needed for basic cellular homeostasis (Licausi et al., 2011).

Other metabolic process such as trehalose metabolism, ABA biosynthesis and catabolism, signal transduction including mitogen-activated protein kinases (MAPKs) signalling, and nitrogen metabolism, also mediates plants' tolerance to abiotic stresses including hypoxia and can also be activated in response to hypoxia (Wang et al., 2021b).

Sucrose can be cleaved either into glucose and fructose by invertase, or into uridine diphosphate glucose (UDP-glucose, UDPG) and fructose by sucrose synthase (SUS), preserving energy as UDPG, whose ready and continuous supply is essential in plants for cell wall synthesis (Paul et al., 2008). Trehalose is synthesised by two steps in plants: UDPG and glucose-6-phosphate (G6P) were converted to trehalose-6-phosphate (T6P) and UDP by trehalose-6-phosphate synthase (TPS); then T6P was dephosphorylated into trehalose and inorganic phosphate (Pi) by T6P-phosphatase (TPP) (Schluepmann and Paul, 2009). *Arabidopsis* has 11 and 10 genes encoding TPS and TPP, respectively. Trehalose is hydrolyzed into two molecules of glucose by trehalase. T6P plays an important role in sugar signalling, plant growth and development, and regulation of sucrose use and stomatamal movement

(Paul et al., 2008). T6P inhibits SNF1-related kinase 1, SnRK1, thereby altering gene expression and promoting growth processes; the T6P/SnRK1 signalling pathway enables growth recovery following relief of a sink limitation such as low temperature (Nunes et al., 2013). A study has shown that submergence-tolerant rice induced greater amount of three TPS mRNAs than intolerant rice, therefore T6P is related to the regulation of growth under submergence (Mustroph et al., 2010). Moreover, a homolog of *TPP* in rice, *OsTPP7* was found to be important for anaerobic germination tolerance (Kretzschmar et al., 2015). An earlier study of wild type and submergence-tolerance transgenic *Arabidopsis* also suggested altered trehalose metabolism and T6P concentration might facilitate the increased sugar flux to anaerobic respiration (Liu et al., 2005). It would be interesting to study GABA mutants, to examine whether they display different degrees of energy crisis under submergence, and therefore distinguishable trehalose metabolism.

Chang et al. (2011) showed that mitochondrial ROS production upon oxygen deprivation transiently activates MAPK6, and this activation functions in retrograde signalling which can contribute to stress tolerance. Pucciariello et al. (2012) re-analysed publicly available *Arabidopsis* microarray data and found that although a common core of genes related to the anaerobic metabolism were shared between anoxia and hypoxia, differences occurred in terms of their response to ROS-related genes. They proposed: (i) oxygen deprivation induced $H_2O_2$ production appeared to be a trait present in very early stage of anoxia; (ii) the regulation of a set of genes belonging to the heat shock proteins and ROS-mediated groups requires ROS; and, (iii) this mechanism, which is involved in plant stress tolerance, is not likely to be regulated by thy N-end rule oxygen sensing pathway, but rather mediated by the NADPH oxidase.

#### 1.4.2.3 Transcription acclimation

At the transcriptional level, plants under low oxygen accumulate transcripts coding enzymes that are involved in metabolic reprogramming upon hypoxia. This involves a core group of 49 ubiquitously hypoxia-responsive genes that are rapidly activated for transcription and prioritised for translation across cell types (both shoots and roots), while most other transcripts are sequestered from translation complexes until reaeration, as reported by Mustroph et al. (2009) when they subjected young *Arabidopsis* seedlings to 2 h dark submergence. They also compared transcriptomic adjustments to various low oxygen treatments in a later study, i.e. short term hypoxia/anoxia, root waterlogging and complete submergence in 21 organisms across several kingdoms (Plantae, Animalia, Fungi, and Bacteria), and highlighted conserved and plant-specific response genes (Mustroph et al., 2010). Induction of these hypoxia responsive genes (HRGs) is thought to contribute to survive prolonged hypoxia. These genes encode proteins associated with metabolism reconfiguration, e.g. ATP production and energy maintenance, NO and ROS scavenging, $O_2$

sensing, fermentation, and perception and biosynthesis of ethylene. Some of the core HRGs are sucrose synthase (*SUS4*), ATP-dependent-phosphofructokinase (*PFK*), *PDC1* and *PDC2*, alanine aminotransferase (*AlaAT*), ROS-responsive genes, and the putative lactate transporter Nodulin 26-like Intrinsic Protein *NIP2;1* which belongs to a subgroup of the aquaporin superfamily of membrane channel proteins. Up-regulation of hormone-related genes and transcripts encoding enzymes that contribute to ROS-mediated signalling and amelioration are also observed upon hypoxia. For example genes involved in ethylene biosynthesis (*ACC synthase*,*ACS*; *ACC oxidase*, *ACO*) and jasmonic acid signalling repression *JASMONATE ZIM DOMAIN PROTEIN 3* (*JAZ3*) were up-regulated, providing a link between hypoxia and hormone directed growth (Mustroph et al., 2010).

Some low-oxygen experiments using the mutants confirmed the role of the above HRGs, e.g. *nip2;1* plants experience poorer survival during argon-induced hypoxia stress (Beamer et al., 2021). In *Arabidopsis*, there are 4 *PDC* genes and 1 *ADH* gene. Kürsteiner et al. (2003) showed that *AtPDC1* was the only gene induced by oxygen limitation but it was not required during other environmental stresses, and the *pdc1* null mutant was more susceptible to anoxia but no other stresses. A later study by Mithran et al. (2014), however, showed that both *PDC1* (mainly expressed in roots) and *PDC2* (leaf-specific) contributed to anoxia tolerance, as both genes were up-regulated in response to various low-oxygen conditions, and mutation of either gene resulted in a lower tolerance to submergence. They also observed a high expression of *PDCs* at both transcript and protein level, even under control conditions when ADH is almost absent, suggesting PDC has a role under aerobic conditions that is not coupled to fermentative metabolism. Recent research by Ventura et al. (2020) also highlighted the importance of PDC, ADH and fermentative metabolism for aerobic plant growth. They studied wild type, *adh1* and *pdc1 pdc2* single or double mutants and reported that compared to wild type plants, all mutants had greater growth penalty under aerobic normal aerobic conditions rather than under hypoxia, regardless of long-term waterlogging (19 d) or short-term dark submergence (35 h). They also found that submergence to be more detrimental to all plants than waterlogging.

Table A.1 shows the full list of 52 core HRGs in response to low oxygen, including the 49 core hypoxia-responsive genes reported by Mustroph et al. (2009) as well as three more genes, i.e. *HRE1*, *ALAAT2* and *NIP2;1*. The latter two were listed with the other 49 core genes in their study and were displayed separately in Table A.1 due to an improved understanding of their function. In this research these 52 core HRGs will be checked before and after submergence in order to: (i) validate that they could be induced in pre-submerged GABA mutants and/or in submerged lines under the current experiment conditions; and (ii) how the differences in submergence tolerance among genotypes could be correlated to HRGs expression, linking disturbed GABA metabolism to hypoxia tolerance.

In addition to the 52 core HRGs, there are other genes involved in hypoxia and recovery. For example, genes related to heat and oxidative stresses were progressively activated during hypoxia, and nuclear-regulated stress-responsive genes were highly translated during reaeration (Lee and Bailey-Serres, 2019). Preventing $K^+$ leak via knocking out guard cell outward rectifying $K^+$ channel (GORK) is proposed to promote hypoxia tolerance, while reduced NADPH oxidase (RBOHD) activity has a hypoxia-sensitive phenotype and RBOHD is crucial in hypoxia-induced $Ca^{2+}$ signalling for stress sensing and acclimation mechanism, as reported by Wang et al. (2017). Mitochondrial retrograde signals, facilitated by endoplasmic reticulum (ER)-located NAC TFs, are also capable of inducing nuclear gene expression under hypoxia. Recently Meng et al. (2020) reported that ANAC017 increased hypoxia tolerance by assisting retrograde signalling-coordinated chloroplast function, probably via transcriptional reprogramming and including other TF genes (*WRKY40* and *WRKY45*). They showed the *anac017* knock-out mutants had lower photosynthetic rate and chlorophyll content but higher ROS production than wildtype during submergence and the following reaeration. Although specific roles of the two WRKY TFs under hypoxia are largely unknown, WRKY40 or WRKY45 overexpression and their knockout improved and repressed submergence tolerance in *Arabidopsis*, respectively (Meng et al., 2020). The SENSITIVE TO PROTON RHIZOTOXICITY 1 (STOP1) transcription factor can also promote *Arabidopsis* root tolerance to waterlogging through up-regulating the expression of both *GDH* genes and a *HEAT SHOCK FACTOR A2 (HsfA2)* gene (Enomoto et al., 2019). Moreover, STOP1 induces *AtALMT1* expression in *Arabidopsis* (Balzergue et al., 2017).

One of the plant hormones involved in hypoxia and reoxygenation responses is ethylene, whose early signalling regulates hypoxia acclimation and anaerobic metabolism. Ethylene is also proposed to inhibit $Al^{3+}$-induced malate efflux by targeting TaALMT1 (Tian et al., 2014). Recently Hartman et al. (2019) showed that ethylene pre-treatment enhanced the hypoxia tolerance of *Arabidopsis* plants, by stablising ERF-VII transcription factors. They reported rapid nuclear accumulation (<1 h after submergence) of Ethylene Insensitive 3 (EIN3) protein, a key TF of ethylene signalling, in *Arabidopsis* root tips. Tsai et al. (2016) reported ethylene-regulated glutamate dehydrogenase (GDH) via EIN3 fine-tunes plant metabolism during anoxia and recovery. EIN3 helps plants to better adjust metabolism by regulating the induction of GDHs, *GDH1* and *GDH2*, both of which are involved in low oxygen tolerance and reoxygenation. This also confirmed that the double mutant *gdh1 gdh2*, which loses GDH activity, was more sensitive and had more wilted leaves than WT after 7 d recovery from 36 h dark submergence. As illustrated in Chapter 1 Section 1.1.1, GDH can catalise glutamate into 2-OG. Thus the metabolic results of Tsai et al. (2016) suggested that 2-OG is a co-substrate that facilitates the breakdown of alanine by AlaAT when plants are relieved from hypoxia (Fig 1.1).

Diab and Limami (2016) proposed the reconfiguration of nitrogen metabolism during hypoxia and recovery, and highlighted the importance of AlaAT and GDH. Their model showed that under hypoxia, pyruvate derived from glycolysis pathway is competitively used by the AlaAT/GDH cycle and leads to Ala accumulation and $NAD^+$ regeneration. Therefore carbon, instead of being lost through fermentation pathway in the form of ethanol during hypoxia, is saved in a nitrogen store and can be used during the post-hypoxia recovery period through the reverse reaction of the AlaAT/GDH cycle. In the meantime, pyruvate produced in this reverse cycle can be funneled back to the TCA cycle. Two aminotransferases in GABA shunt, AlaAT and GABA-T, are both involved in alanine and pyruvate transformation (Fig 1.1). It will be worthwhile to check their expression levels in GABA mutants and testify whether the above proposed AlaAT/GDH cycle contributes to hypoxia tolerance.

### 1.4.3 GABA plays a role under hypoxia and recovery

Flooding induces a dramatic increase in plant GABA content, which is one of the most prominent metabolic alterations and has been reported for a long time (Michaeli and Fromm, 2015; Shelp et al., 2017). The GABA-shunt, the main GABA metabolism pathway, bypasses two steps of the TCA cycle, and increased activity of GABA-shunt can compensate for the decreased activity of the TCA cycle, providing NADH and succinate to the cycle (Section 1.1 and Fig 1.1).

Several studies have found that exogenous GABA and induced expression of some *GAD* genes are beneficial to plants under oxygen deficiency. Shabala et al. (2014) described that GABA pretreated barley roots showed alleviated cell death, increased $Ca^{2+}$ extrusion which is ROS-induced, and reduced the magnitude of $H_2O_2$-induced $K^+$ leak under hypoxia. Salvatierra et al. (2016) reported that exogenous applied GABA to *Prunus* rootstocks transiently improved root hypoxia tolerance of the sensitive ecotype but not the tolerant one. They found one of the early differentially expressed genes had high homology to the root-specific *Arabidopsis* glutamate decarboxylase, *AtGAD1*. Hypoxia-induced injury on muskmelon roots can also be alleviated by application of exogenous GABA, and Lü et al. (2019) proved that the mitochondrial malate dehydrogenase (mMDH) was involved during the alleviation process, via increasing some TCA cycle intermediates content. Miyashita and Good (2008) observed that during 24-hour dark hypoxia, *GAD2* expression gradually decreased, *GAD1* maintained similar levels as non-stressed plants, while *GAD4* was highly inducible (up to 20-fold than control at 8h) in *Arabidopsis* roots. In addition, they showed GABA shunt plays a role in the inhibition of hypoxia-induced alanine accumulation in flooded roots.

To further understand the role of GABA under hypoxia, Wu et al. (2021) subjected

several *Arabidopsis* mutants that was impaired in GABA shunt (*pop2*, *gad1* and *gad2*) to hypoxic treatment, and found that elevated GABA content and GABA-shunt activity under hypoxia is essential for restoring membrane potential, alleviating ROS-disturbed cytosolic $K^+$ homeostasis and $Ca^{2+}$ signalling. The GABA accumulating line, *pop2-5* showed lower concentration of $H_2O_2$ and higher hypoxia tolerance, in contrast, *gad1/2*, the GABA deficient line, showed increased sensitivity to hypoxia than wild type.

Under hypoxia, $\gamma$-hydroxybutyrate (GHB) accumulation has been reported in the leaves of several plant species, including *Arabidopsis*, tobacco, green tea and soybean (Breitkreuz et al., 2003; Allan et al., 2003, 2008, 2012). After 4h dark flooding, Breitkreuz et al. (2003) found increased GABA, alanine and GHB content but decreased *GABA-T* and *GHB dehydrogenase* (*GHBDH*) expression of in *Arabidopsis* leaves. As SSADH activity is limited during flooding-induced oxygen deficiency, their results suggested that a large portion of SSA derived from GABA under stress and SSA was converted to GHB instead of succinate, and the supply of SSA or redox balance could potentially regulate GHBDH activity. Therefore, in this thesis the genes and pathways involved in these processes will be studied to reveal how disturbed GABA shunt may transcriptionally regulate the expression of these genes.

## 1.5 The role of the putative GABA binding motif in regulating pH-dependent anion transport

In acidic soil, aluminum ions ($Al^{3+}$) have increased mobility and they tend to form highly stable complexes with phosphorus. In these conditions, plants can face not only $Al^{3+}$-rhizotoxicity but also a poor phosphate bio-availability, thus root growth and function are inhibited, especially in acidic soils (pH less than 5.5) (Barceló and Poschenrieder, 2002; Kochian, 1995). Direct exclusion of $Al^{3+}$ from root tips plays a fundamental role in preventing the accumulation of phytotoxic Al in apoplastic and symplastic compartments (Barceló and Poschenrieder, 2002). The above problems can also be solved by releasing organic acids, which chelate $Al^{3+}$ and set phosphates free (Sharma et al., 2016). Oxalate exudation can be detected in response to $Al^{3+}$ in very Al-tolerant species, citrate and malate exudation have also been found and the latter more thoroughly investigated (Barceló and Poschenrieder, 2002). As a result of incomplete oxidation of photosynthetic products, organic acids represent the stored pool of fixed carbon through various metabolic pathways and play essential roles in plant primary metabolism (e.g. carbon fixation and temporary storage), forming precursors for amino-acid biosynthesis, pH and redox regulation, stomatal function and stress adaptation, including aluminum tolerance (Igamberdiev and Eprintsev, 2016; Meyer et al., 2010a). The Aluminum-activated Malate Transporters (ALMTs), which belong to a protein family of anion channels, are found in many plant species and

contribute to plants' tolerance towards toxic aluminum ions in the soil (Meyer et al., 2011; Luu et al., 2019).

### 1.5.1 The role of ALMTs in plants

Many plant ALMTs function in both roots and leaves and are mostly plasma membrane localized (Sharma et al., 2016). Beyond $Al^{3+}$-detoxification, ALMTs can also transport other ions (e.g. $Cl^-$) and play various roles in many other physiological process across plant species, including guard cell and turgor regulation, mineral nutrition, ion homeostasis, seed development, fruit quality, microbe interactions and putatively as a GABA receptor (Sharma et al., 2016). For example, the maize ZmALMT1 (leaves) and ZmALMT2 (roots) are both involved in maintaining anion homeostasis beside $Al^{3+}$-tolerance, while ZmALMT2 also plays a role in mineral nutrition acquisition and transport (Piñeros et al., 2007; Ligaba et al., 2012). ALMTs also regulate stomatal opening and closure and play important roles in guard cell movement and gas exchange, e.g. *Arabidopsis* tonoplast AtALMT6 (Meyer et al., 2011) and AtALMT9 (Angeli et al., 2013), plasma membrane AtALMT12 (Meyer et al., 2010b) in Arabidopsis. The barley HvALMT1 regulates cell turgor and cell expansion while apple (MdMA1) and grapevine (VvALMT9) ALMTs mainly contribute to fruit flavour (Sharma et al., 2016). The focus of this chapter is malate transport ability of the wheat TaALMT1.

Wheat (*Triticum aestivum*, Ta) *TaALMT1* (formerly named *ALMT1*) was first identified by Sasaki et al. (2004) and was constitutively expressed at higher levels in the growing root apices of the Al-tolerant line (ET8) compared to Al-sensitive line (ES8). The authors expressed *TaALMT1* in *Xenopus laevis* oocytes, rice and cultured tobacco cells, and found $Al^{3+}$-activated malate efflux as well as increased tolerance of tobacco cells to $AlCl_3$ treatment. Later Yamaguchi et al. (2005) confirmed the localisation of TaALMT1 protein is on the plasma membrane. Ramesh et al. (2015) also found ET8 had a greater transcriptional level of *TaALMT1* than ES8, which coincided with greater malate efflux to chelate $Al^{3+}$ ions. Piñeros et al. (2008) expressed *TaALMT1* in *X. laevis* oocytes, confirming that adding $Al^{3+}$ to the bath solutions resulted in activating significantly larger inward (e.g. malate efflux) and outward (e.g. malate influx) TaALMT1-mediated currents. Zhang et al. (2008) studied the electrophysiological function of the TaALMT1 protein in transformed tobacco cells, and confirmed the observed currents activated by $Al^{3+}$ were identical to those in the root cells of wheat, indicating TaALMT1 on its own is likely to be responsible for those endogenous currents. Transgenic plants such as barley and rice expressing *TaALMT1* had enhanced root malate exudation, and this provided additional evidence that as a major Al-tolerance gene *ALMT1*, has the ability to confer acidic soil/$Al^{3+}$ resistance in plants (Delhaize et al., 2004; Gruber et al., 2011). Overexpression of *AtALMT1* in Arabidopsis wild type (Columbia-0 ecotype) enhanced malate excretion

from the root to the rhizosphere and the recruitment of beneficial bacterium, both of which could increase plants tolerance to stresses (Kobayashi et al., 2013). Though highly dependent on the presence of extracellular $Al^{3+}$ at acidic pH, the TaALMT1 protein is still functionally active and can regulate ion transport in the absence of $Al^{3+}$ (Piñeros et al., 2008) and is increasingly active at alkaline pH (Ramesh et al., 2015).

### 1.5.2 GABA and ALMTs

GABA has long been studied for its important roles in plants as a metabolite. Recently, several reports also suggested its potential role in signalling in plants as well as in animals, may be related to interactions with ALMT (Ramesh et al., 2015; Long et al., 2019). Cytosolic GABA concentration increases in plant tissues in response to stress, as a bypass of several reactions of the mitochondrial based TCA cycle to allow the cycle to complete (Shelp et al., 2017). It was shown that low concentrations of GABA (micromolar) regulate anion currents through ALMT proteins from various plant species. For example, in wheat, exogenous GABA application inhibits TaALMT1 activity to prevent malate efflux from roots to soil under acidic conditions, and this may also occur under other stresses, e.g. cold, heat, salinity as GABA accumulation is induced and ALMT1 is active at neutral/alkaline pH (Ramesh et al., 2015). In the meantime, a negative correlation between root malate efflux and endogenous (i.e. cytosolic) GABA concentration in the root cells was observed (Ramesh et al., 2015). Also, both GABA and muscimol (a mammalian $GABA_A$ agonist) were found to negatively regulate TaALMT1-mediated currents in *X.laevis* oocytes in the presence of $Al^{3+}$ (Ramesh et al., 2015). Cytosolic GABA efflux into the apoplast is mediated by interacting with plasma membrane-located ALMT and negatively regulating malate efflux; while high concentrations of extracellular GABA can also enter the cytosol via ALMT, inhibiting ALMT-mediated malate efflux (Ramesh et al., 2018; Long et al., 2019). Under stressful conditions it appears that GABA regulates TaALMT1 electrogenic activity and alters electrical potential across the plasma membrane (Ramesh et al., 2015). GABA modulation of ALMT activity results in altered root growth and tolerance to alkaline and acid pH and aluminum ions. Thus it was hypothesised that GABA could be an indicator of metabolic status sensed and signalled by ALMT, which alters membrane voltage and allows the signal to be transduces into physiological responses (Gilliham and Tyerman, 2016).

As mentioned above, although not all ALMTs are activated by $Al^{3+}$ or have a role in $Al^{3+}$ tolerance, by examining eight ALMTs from five plant species including Arabidopsis AtALMT1, AtALMT13 and AtALMT14, wheat TaALMT1, barley HvALMT1, rice OsALMT5 and OsALMT9, and grapevine VvALMT9, Ramesh et al. (2015) suggested that it appears to be a general feature of this family to regulate anion-activated anion currents. After comparing sequences of mammalian $GABA_A$ receptors and plant ALMTs using using Multiple Em for Motif Elicitation (MEME) analysis, the authors

discovered a predicted GABA-binding motif consisting of 12 amino acids exists in all known plant ALMTs (Fig 1.3). The first residue of this motif for five species is an aromatic and hydrophobic amino acid residue Phenylalanine (F), except that of VvALMT9 (hydrophilic Cysteine, C) and AtALMT13 and AtALMT14 (hydrophobic Leucine, L). The last residue in the motif is a positively charged Histidine (neutral, H) for all eight ALMTs, so for AtALMT1 the motif is from F182 to H193 and for TaALMT1 F213 to H224 (Fig 1.3, D.2), and the motif resides in TM6 (F182 and F213) and H1 of the CTD (H193 and H224) for both species (Wang et al., 2021a; Motoda et al., 2007). When the first amino acid residue in the TaALMT1 motif is replaced by cysteine ($TaALMT1^{F213C}$), GABA sensitivity of TaALMT1-mediated anion currents decreased, although the F213C mutation still retained the strong activation by external anions (Ramesh et al., 2015, 2018).


**Figure 1.3:** A putative GABA-binding motif for plant ALMTs. (a) Half-maximal effective concentration ($EC_{50}$) and efficacy ($E_{max}$) of GABA in regulating rat $GABA_A$ receptors or selected plant ALMTs using cRNA-injected *X. laevis* oocytes. Assayed by two-electrode voltage-clamp electrophysiology (Os=rice; At= Arabidopsis; Hv=barley; Ta= wheat; Vv= grapevine). (b) Sequence logo of the predicted GABA-binding motif. (c) Residues corresponding to logo in proteins from a. Identical residues (black), >80% similar (grey) and <60% similar (unshaded). Figure taken from Ramesh et al. (2015).

Anion transport activity of plasma membrane localised ALMT proteins is not only negatively regulated by GABA, but also affected by pH. At alkaline pH without $Al^{3+}$, a variety of anions could activate ALMT1, thus facilitate malate efflux and resulted in larger currents (Ramesh et al., 2015), and at acidic pH, TaALMT1 activity is minimal unless $Al^{3+}$ is present. External malate induced malate flux through TaALMT1 was much greater in both *X.laevis* oocytes and tobacco BY2 cells expressing *TaALMT1*, and this was again negatively regulated by GABA and muscimol (Ramesh et al., 2015). This evidence suggests ALMT is able to sense the pH, however the mechanisms are still unknown and need to be tested. Giving the fact that GABA can regulate ALMT channel activity, and its rapid accumulation under stress conditions (due to increased $H^+$- and $Ca^{2+}$-stimulated GAD activity) utilises proton ($Glu + H^+ = GABA + CO_2$), stress-induced GABA synthesis could be involved in regulating ALMT in a pH-dependent manner by targeting specific sites within the putative GABA receptor motif.

### 1.5.3 Histidine protonation and phosphorylation and its interaction with other amino acids

In the above putative GABA binding motif (Fig 1.3), the last residue Histidine (H224) is also highly conserved across these plant species in ALMT family members. Histidine is titratable at pH 6–7 and it carries a positive charge below pH 6. Biochemically, the pKa ($\approx 6.0$) of histidine side chain - the imidazole group - is the closest among all amino acids to the physiological pH, and small environmental pH change would influence the charge states of histidine (Li and Hong, 2011). Although aromatic at all pH conditions, the nonprotonated form (above pH 6) of imidazole side chain has essentially a non-charged and hydrophobic character, whereas the protonated form (below pH 6) is positively charged and hydrophilic (Rötzschke et al., 2002). Therefore, a pair of amino acids that consist of histidine and another hydrophobic residue could function as a pH-sensitive "His button": "closing" tightly at pH 7.0 but "opening" at pH 5.0, due to the fact that hydrophobic amino acids are repelled by the protonated form of histidine.

Histidine residues have been found to be involved in proton sensing in several plant channel proteins, such as mung bean vacuolar proton pumping pyrophosphatase ($H^+$-PPase), spinach aquaporin SoPIP2;1 and Arabidopsis S-type anion channel AtSLAH3 (Hsiao et al., 2004; Törnroth-Horsefield et al., 2006; Lehmann et al., 2021). When several histidine residues in mung bean $H^+$-PPase was singly replaced by alanine, the H716A mutation significantly decreased the proton transport, the enzymatic activity, and the coupling ratio of $H^+$-PPase; while the single substitution of H704A, H716A and H758A indicated possible location of $K^+$ binding in the vicinity of domains surrounding these histidine residues, as partially released effect of $K^+$ stimulation were observed (Hsiao et al., 2004).

Histidine phosphorylation (pHis) is crucial for signal transduction and as an intermediate for some metabolic enzymes; pHis is reversible and heat and acid labile but stable under alkaline conditions (Fuhs and Hunter, 2017). Histidine is mainly involved in four interactions with other amino acids, and according to the energy needed from high to low, they are: coordinate, cation-(pi)$\pi$, hydrogen-$\pi$, and $\pi$-$\pi$ interactions (Liao et al., 2013a). The cation-$\pi$ interactions are attractive when the histidine is in neutral form but turn to repulsive histidine is protonated ($His^+$). The attractive and repulsive cation-$\pi$ interactions can switch the two protonation forms (and $pK_a$ values) of histidine. In proteins, the $\pi$-$\pi$ interaction between neutral histidine and aromatic amino acids such as Phe, Tyr, Trp are in the range between -3.0 to -4.0 kcal/mol, which is significantly larger than the van der Waals energies (Liao et al., 2013a).

### 1.5.4 The structure of AtALMT1

Despite substantial physiological functions of ALMT1 already being revealed in wheat, barley, Arabidopsis and other plant species, the molecular mechanisms of $Al^{3+}$ activation, GABA binding and the sensitivity of pH-dependency have remained unresolved. The putative topology of TaALMT1 has been predicted in several studies, however, has been long debated ((Motoda et al., 2007; Ligaba et al., 2013; Dreyer et al., 2012). Among all the differences, the cellular location of C-terminal domain (CTD) that includes the GABA receptor motif is the most controversial. Motoda et al. (2007) predicts that the CTD is localised at extracellular side, whereas other studies suggest an intracellular location (Ligaba et al., 2013) A rapid malate efflux inhibition by external GABA was discovered in *TaALMT1* expressing *X. laevis* oocytes suggested that the GABA binding site is located at the extracellular side or very close to the accessible intracellular area (Ramesh et al., 2015). Later, GABA was found also be able to inhibit the anion transport of TaALMT1 from the cytosolic face reducing the ion channel opening frequency (Long et al., 2019). In addition, as previously reviewed in Chapter 1 Section 1.5.3, a histidine site is highly conserved within the GABA binding motif and might play a role in manipulating pH-dependent malate transport. To fully understand the pH-dependency of TaALMT1 anion transport activity and whether this pH regulation is correlated to GABA, it will be crucial to understand the structural information of TaALMT1.

Recently the cryo-electron microscopy (cryo-EM) structure of AtALMT1 in the apo (inactive, unbound and ligand-free), malate-bound, and Al-bound states at neutral and/or acidic pH were resolved and shed new light on the mechanism of $Al^{3+}$-activated malate transport (Wang et al., 2021a). The authors confirmed that as a functional anion channel, $ALMT1_{apo/pH5}$ is a homodimer with two subunits A and B. Each subunit contains a short amphipathic N-terminal $\alpha$-helix (N-terminal 0, N0), six transmembrane $\alpha$-helices (TM1-TM6) forming the trans-membrane domain (TMD, TM1–TM3 and TM4–TM6 constructed into an internal pseudo-two-fold symmetry), and six cytoplasmic $\alpha$-helices (H1-H6) creating a large intracellular localised C-terminal domain (CTD). The twelve transmembrane $\alpha$-helices from the each TMD assemble into an ion-conducting pore, with TM2 and TM5 forming the pore-lining helices at the centre and the other TMDs on the periphery. Two pairs of Arginines resudues (Arg80 from the two TM3 domains and Arg165 from the two TM6 domains) locate in the pore centre are essential for malate recognition and binding in the presence of $Al^{3+}$ (Wang et al., 2021a). This was further supported by the significantly decreased channel conductance of two mutants (R80A and R165A) compared to WT at -180 mV when examined in HEK239 cells. Upon Al treatment, significantly inhibited root growth of Arabidopsis lacking ALMT1 or R80A and R165A mutant lines were observed, which also coincided with substantially decreased malate secretion (Wang et al., 2021a), further validating the importance of R80 and R165 in

gating $Al^{3+}$- dependent malate conductance. TaALMT1 shares 63% sequence similarity with the structure resolved AtALMT1 (Gilliham and Hrmova, 2021), naturally providing a good opportunity to optimize the prediction of cellular location of putative GABA binding motif and examine its roles in regulating pH-dependent malate transport.

To investigate the role of the histidine residue in the putative plant GABA-binding motif in terms of pH sensitivity and ion transport, mutagenesis of histidine to alanine ($TaALMT1^{H224A}$) and arginine ($TaALMT1^{H224R}$) were used in this study. Alanine is hydrophobic and non-changed while arginine is positively charged and hydrophilic. Arginine is chemically the closest homologue of the charged form of histidine, and its codon usage differs from histidine only in one base, which may suggest a close functional relation of these two amino acids during the evolution of proteins. In contrast to histidine, its side chains remain unchanged at pH between 5.0 and 7.0 (Rötzschke et al., 2002). Therefore, replacements by alanine (Ala) alters both the affinity for water, the charge and molecular weight of the residue, which may result in a structure less susceptible to pH changes as the histidine presents at the C- terminal of TaALMT1. On the contrary, the replacement of histidine (His) by arginine (Arg) should stabilise the pH-sensitivity of the TaALMT1 protein. TaALMT1 and $TaALMT1^{F213C}$ were also included in this study as controls to compare the response of them with the H224 mutants. TaALMT1 was also structurally aligned to the resolved AtALMT1 to predict the location of the putative GABA binding site and the biochemical properties of Histidine residue under various pH conditions.

## 1.6 Research gaps

Much of the previous research was conducted using single/double *GAD* mutants and/or GABA-T knockout mutants, yet how plants cope with abiotic stress when GABA production through the GABA shunt is totally blocked remains to be further elucidated. When plants are not able to catabolise GABA at all through the GABA shunt (the *GABA-T* knockout), how they cope with salinity and hypoxia also remains to be fully understood.

Many of the previous hypoxia/anoxia experiments were short-term dark submergence/flooding (e.g. a few hours or up to one or two days), or inert gases induced stresses on young seedlings (e.g. one week old), or root flooding instead of the whole plant complete submergence. However, plants in nature could be experiencing a longer period of flooding, either partial or whole plant submerged, with the underwater photosynthesis still going on (although lower light availability than normal conditions). Therefore, how plants cope with prolonged and complete submergence under normal day-night cycles when photosynthesis is partially maintained, still need to be further examined.

Although GABA accumulation has been reported when plants face low oxygen or flooding, the detailed roles it plays during the process are still not very clear. Therefore studying how GABA mutants that have disturbed GABA shunt ability under prolonged complete light submergence, will contribute to the understanding of the above questions.

The research presented in my thesis focuses on gaining a better understanding of how GABA contributes to the stress responses of plants, using the model plant *Arabidopsis* (*At*). Salt and hypoxia stresses were induced on wild type and mutants. The mutants include GABA-deficient lines through GAD knockout, GABA-accumulating lines by *GAD2* over expression, and GABA-accumulating lines through *GABA-T* knockout. Under non-stressed conditions, plant GAD activity can be restrained by the auto-inhibitory domain in the C-terminal segment of GADs. See Table 1.2 for details of accessions used in this thesis. The mutants are all T-DNA insertion homozygous lines, same as thosed used in Feng (2021) and Piechatzek (2022).

**Table 1.2:** Information of *Arabidopsis* plants used in the research

| **Name** | **Ecotype** | **Accession info** |
|---|---|---|
| WT-Col | Columbia (Col-0) | wild type |
| *gad1** | Columbia (Col-0) | CS860068 [1] |
| *gad1KO* | Columbia (Col-0) | *GAD1* knockout (SALK_017810) [2] |
| *gad2-1* | Columbia (Col-0) | *GAD2* knockout (GABI_474_E05) |
| *gad1245* | Columbia (Col-0) | *GAD1, GAD2, GAD4, GAD5* knockout [3] |
| *gad2OE* | Columbia (Col-0) | *GAD2* over-expression by the 35S CaMV promoter [4] |
| *pop2-8* | Columbia (Col-0) | *GABA-T* knockout (SALK_007661) [5] |
| WT-Ler | Landsberg (Ler-1) | wild type |
| *pop2-1* | Landsberg (Ler-1) | *GABA-T* knockout |

[1] T-DNA insertion (51bp) was at the second intron (1323 bp) of the *GAD1* gene, same position as its parent line *gad1-4* (SALK_047648) used by Miyashita and Good (2008). However, unlike *gad1-4*, *gad1** was not a knockout because I found that *GAD1* does express in this line (Fig A.1).
[2] Previously named *gad1-1* in literature (Bouché et al., 2004).
[3] Two parent lines of *gad1245* were used in this study: *gad1KO* and *gad2-1*.
[4] Two lines (*gad2OE_B33* and *gad2OE_B97*) were used in Chapter 2, and only the former was included in Chapter 3.
[5] Previously named *gaba-t1-1* in literature (Miyashita and Good, 2008).

Anion transport by TaALMT1 is pH sensitive (Ramesh et al., 2015). As GABA accumulation is common for plants under stress, and GABA production by GAD is a proton consumption process which contributes to pH changes in cytosol, the GABA-mediated malate currents through ALMT could be related to the protein pH sensitivity, however, this needs to be examined.

## 1.7 Aims and objectives of the research

There were two major aims and a minor aim in this research. The two major aims of the current study are focused on how *Arabidopsis* plants with a disturbed GABA shunt ability cope with salinity and flooding, in order to better understand the role of GABA under normal and stress conditions. The growth of both young and mature wild type and GABA mutants and their physiological responses were investigated under different salinity treatments with the aim to elucidate the role of GABA under salt stress, specifically the role of genes encoding GAD and GABA-T enzymes. The physiological, transcriptional and metabolic responses of these GABA mutants were also studied in detail under normal, submerged and recovered conditions, to illustrate the role of GABA metabolism during these processes. Taken together, this work aims to reveal the common and unique responses of GABA mutants challenged by these two types of stress: salinity or submergence, how energy crisis is transduced to re-programmed gene expression which leads to metabolic adaptation upon stress, and how GABA participate in these processes. This could be beneficial for developing salt- and/or flooding-tolerant plants in the future.

A minor aim of this thesis is to investigate interaction of pH with ALMT, especially, the role of histidine in pH sensitivity and ion transport, using a heterozygous expression system. The pH sensitivity and ion transport capacity of ALMT1 was examined when the last residue (histidine) of ALMT1 was replaced by arginine and alanine, in order to better understand the role of histidine reside in ALMT1. By conducting site-directed mutations of the proposed plant GABA binding motif and examining their transporter activity and sensitivity to low or high pH solutions with or without malate, a better understanding of GABA's role as a signalling molecule will be achieved.

CHAPTER 2

# The role of GABA under salinity

Salinity is a major agricultural issue affecting crop yield worldwide (Munns and Tester, 2008) by leading to decreased photosynthesis and plant growth (Deinlein et al., 2014). Both mitochondrial respiration and tricarboxylic acid (TCA) cycle activity in plants are inhibited during salt stress, which impinge upon providing sufficient ATP and reductants for adaptive processes such as ion exclusion and reactive oxygen species (ROS) detoxification (Tyerman et al., 2019).

GABA accumulates in plants in response to salt stress, and it is proposed that the GABA shunt activity promoted by salt stress could provide an alternative carbon source for mitochondrial respiration (as it bypasses some stress-sensitive enzymes of the TCA cycle) (Bao et al., 2015; Ma et al., 2019). GABA could also alleviate salt stress through enhancing ROS scavenging and antioxidant capacity, and modulating amino acid synthesis (Ma et al., 2018; Che-Othman et al., 2020). Exogenously applied GABA was found to increase plant salinity tolerance through decreased $Na^+$ uptake, improved photosynthesis, and promotion of antioxidant systems (Wu et al., 2020; Li et al., 2016a; Çekiç, 2018). However, the exact role of GABA under salinity, especially on root growth, is not fully understood. Therefore, in this chapter *Arabidopsis* wild type (WT) and GABA mutants (Table 1.2, multiple *GAD* and *GABA-T* mutation lines which had putative disturbed GABA metabolism) were used to investigate the role of the GABA shunt pathway under salinity. The GABA concentration has been reported to be significantly decreased in *gad2-1* and *gad1245* but greatly increased in *pop2-8*, due knockout of the GABA biosynthesis gene *glutamate decarboxylase* (*GAD(s)*) and catabolic gene *GABA-transaminase* (*GABA-T*; *pop2*) (Xu et al., 2021; Feng, 2021; Piechatzek, 2022).

Young seedlings grown in square petri dishes and mature plants grown in a hydroponic system, with or without additional NaCl, to examine the impact of salt root elongation, biomass, and shoot ion content. Hydroponic experiments using mature plants (4 to 5 weeks

old) were also carried out for these two lines with the most disturbed GABA metabolism, and biomass, water content, ion content ($Na^+$, $K^+$, $Na^+/K^+$) of leaves were measured.

Under non-saline conditions, *gad1**, *gad1245* and *pop2-8* main root grew faster and longer than WT. Their total root length was also significantly larger than WT after 10 d, which was mainly due to their lateral roots developing faster, but was reduced to that of WT by salt treatment. Non-saline *gad1245* had a greater biomass than WT, which was also brought down to the same as WT under salinity. Although *gad1KO* and *gad1245* always had shorter roots at 4 d, after transfer to new media they maintained the same and greater main root growth rate than that of WT, respectively. *gad2OE* had a faster growth rate than WT under control, but this advantage was abolished under salt treatment. Both *pop2-8* and *gad1245* had a reduced capacity to feed GABA into the Tricarboxylic acid cycle (TCA cycle), which was advantageous for root growth under control conditions, but this advantage was reduced upon salt stress. Root growth of plate-grown young seedlings (less than 3 weeks old) showed that both *pop2* and WT from the Ler background were more sensitive to salt stress (50 mM and 100 mM NaCl) than those from the Col background. Hydroponic grown *pop2-8* and *gad1245* did not show significant altered ion contents compared to WT in the same solution, although *gad1245* had a slightly smaller $K^+$ decrease in response to 75 mM NaCl. However, *gad1245* had lower water content than WT and *pop2-8* under salt solutions. Consistent with the root growth on plates, *gad1245* had greater biomass than WT only under control conditions but not 75 mM NaCl solutions.

## 2.1 Results

Root performance is largely dependent on Root System Architecture (RSA), which is responsible for water and nutrient acquisition, and the replacement rate of plant water loss (Passioura, 1988). A total of over 1000 *Arabidopsis* seedlings (>10 per condition) were used in the root assays. All seeds were harvested from parental plants at a similar time and stored in identical conditions. *Arabidopsis* seedlings were sown and grown in square petri dishes, i.e. plates containing 1/2 MS media (with 1% sucrose unless stated otherwise). The plates were scanned after germination and the RSA parameters measured were based on Kellermeier et al. (2014) and are listed in Table 2.1.

### 2.1.1 Main root length of WT and GABA mutants

To dissect the link between a disturbed GABA shunt and early stage root growth, the main root length of WT and all mutants ($\leq$ 7 d) were measured. As shown in Fig 2.1, after germinating on 1/2 MS for 5 days, the main root length of *gad1KO* and *gad1245* were the shortest among all eight lines, while only *gad1** main roots were longer than WT.

**Table 2.1:** RSA Parameters

| Abbreviation | Unit | Description |
|---|---|---|
| MRL | mm | main root (MR) path length |
| MRGR | mm/d | Main root growth rate calculated by linear regression |
| LRL | mm | Total path length of 1st order lateral roots (LRs) |
| TRL | mm | Total root length: path length sum of MR and LRs (MRL + LRL) |
| LRN | - | Total number of 1st order LRs as |
| AvgLR | mm | Average path length of 1st order LRs (LRL/LRN) |
| LRS | % | LR size: proportion of first order LRs in TRL (LRL/TRL*100) |
| LRDen | $cm^{-1}$ | LR density: No. of LRs per cm MR (LRN/0.1MRL) |

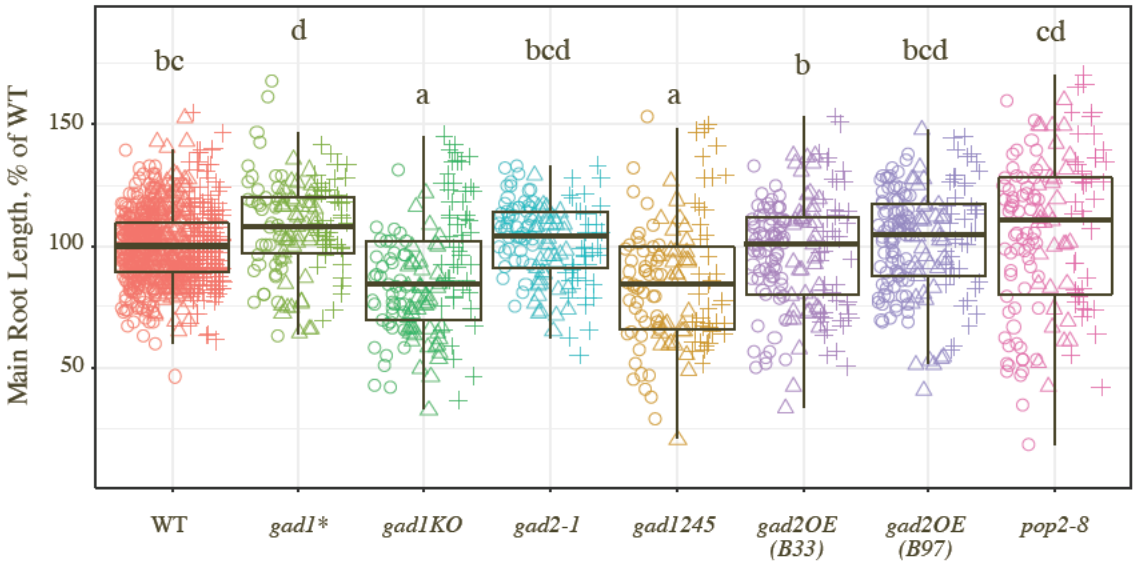


**Figure 2.1:** Normalised main root length of GABA mutants (compared to WT) at DAG5 in short day growth room (Boxplot). The media was MS (+ 1% sucrose) without presence of NaCl. ○ , △ and + indicate three repeated experiments. Number of plants (n) used in each experiments: mutants ∈ [34 ∼ 88] and WT ∈ [316, 188, 213], respectively. Letters represent significant difference between genotypes using one-way ANOVA ($P < 0.05$).

GAD2-KO (*gad2-1*) and the three GABA accumulating lines including the two GAD2-OE lines and *pop2-8*, did not show significantly altered MRL compared to WT, although *gad2OE_B33* had a shorter main root than *gad1** and *pop2-8* (Fig 2.1). However, when germinated on 1/2 MS media that doesn't contain sucrose for 4 days, *gad2-1*, *gad1245* and *pop2-8* all had significantly shorter main roots than WT, only *gad2OE_B33* maintained the same MRL as WT did (Fig B.2). *gad1245* and *pop2-8* had the shortest main roots, and the MRL of *gad2-1* were larger than *gad1245* but smaller than *gad2OE* (Fig B.2). These differences could be due to uneven germination timing, or due to altered root elongation caused by disturbed GABA metabolism during the first few days after germination, or due to the variance of randomly selected seeds. When seeds were directly germinated on salt media without sucrose, *gad1245* and its one parent line *gad1KO* still both had shorter main roots than its another parent line *gad2-1* (Fig B.3), the same pattern as in Fig B.2. *GAD1* in *Arabidopsis* was reported to be mainly expressed in the roots and

essential for maintaining root GABA level (Bouché and Fromm, 2004). So it is possible that the inhibited root elongation in *gad1KO* and *gad1245* was due to disturbed GABA metabolism in these two lines. Moreover, no obvious germination delay or defects could be observed by eyes, and it is common for seeds harvested from the same plants to be unevenly developed. As the focus of the current study is root growth, so healthy and similar length seedlings (Fig B.1a) from a plate were transferred to new plates to examine their RSA parameters during the following days on the new media B.1.

### 2.1.2 Main root growth rate of WT and GABA mutants

Main roots are initiated during embryogenesis and their development is predetermined. To minimise this impact as much as possible and further investigate the direct effect of disturbed GABA concentrations on main root elongation, i.e. main root growth rate (MRGR), germinated seedlings with similar length of main roots were transferred to new media plates (with or without NaCl).

The MRGR differences between WT and the four GAD lines (*gad1*, gad1KO, gad2-1* and *gad1245*) were explored. To directly compare between the four *GAD* mutants, MRGR was normalised as a proportion of WT in the same treatment for each mutant. First though, the main root length of these plants on transfer day (Day 0 of stress) were measured to record any existing pre-treatment differences between accessions. To directly compare between the four GAD mutants, MRGR was normalised to the proportion of WT in the same treatment for each mutant. Although pre-selected, *gad1** and *gad1KO* still had longer and shorter main roots respectively, than that of WT on transfer day (Fig 2.2). This trend was in accordance with main root length (Fig 2.1). Meanwhile, main roots of transferred *gad2-1* plants were the same length as transferred WT plants (Fig 2.2). However, as for *gad1245*, those transferred to control media had the same mean MRL as WT plants, but those transferred to 75 mM NaCl had a smaller mean MRL (10.01±0.25 mm) than that of WT (10.72±0.21 mm).

For control plants, MRGR showed no big differences between WT and *gad2-1* or *gad1KO*, but *gad1245* and *gad1** main roots grew faster than WT (Fig 2.3a). Especially after normalisation to WT level of the same conditions, non-stressed *gad1245* also had greater MRGR than its two parent lines *gad2-1* and *gad1KO* (Fig 2.3b), even though *gad1245* started with shorter main roots on transfer day than *gad2-1* (Fig 2.2).

Not surprisingly, main root growth of all salt-stressed plants was significantly decreased compared to control plants. No matter if they grew faster than WT or not on control media, 75 mM NaCl treatment decreased mutant MRGR to the same as WT (Fig 2.3a). Thus, among the 4 *GAD* lines, main root growth of *gad1** and *gad1245* were more inhibited by

75 mM NaCl than the other two lines. Except for *gad2-1*, MRGR variations in the two *GAD1* lines and *gad1245* were larger compared to WT.

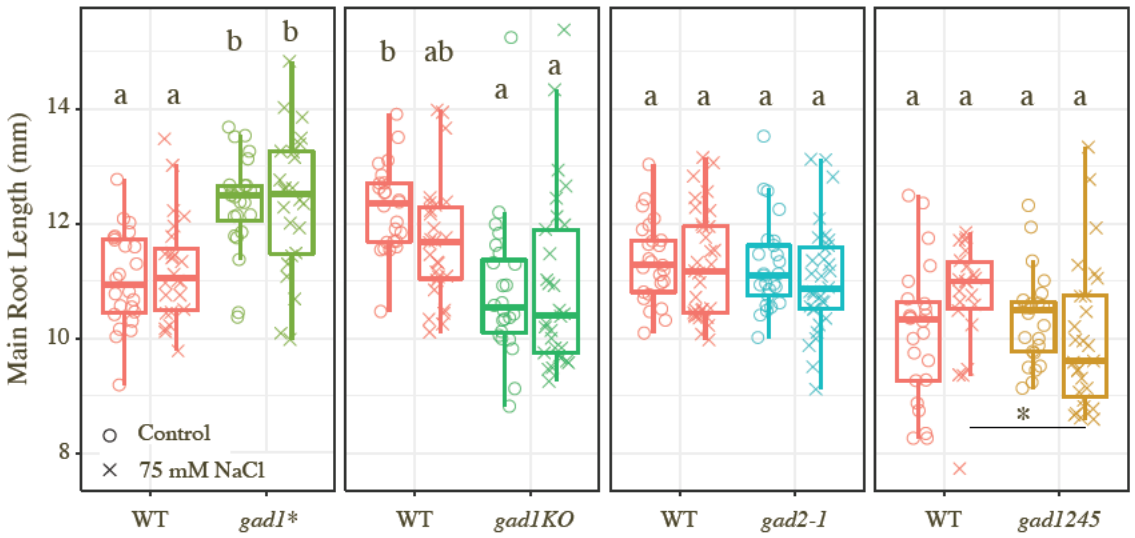


**Figure 2.2:** Main root length of WT and GAD lines on DAG4 (Transfer Day, Day 0 of stress). × and ○ represent seedlings transferred to 1/2 MS ± 75 mM NaCl, respectively. Panels represent 4 repeated experiments on a weekly basis using WT and four GAD lines, and number of biological replicates ∈ [24 ∼ 32]. Letters and star show two-way ANOVA and Welch's t-test significance, respectively ($P < 0.05$).

As Fig 2.2 showes, on Day 0 of stress, i.e. transfer day, the two *GAD1* lines started with different length of main root than WT (*gad1** longer roots than WT while *gad1KO* shorter roots than WT). After transferred on DAG4, *gad1** maintained its higher MRGR than WT only on control media but not salt media. *gad1KO*, although started with shorter roots than WT on transfer day (Fig 2.2), had the same MRGR as WT whether transferred to control or salt media (Fig 2.3b). Therefore, the two *GAD1* lines had the same MRGR as WT did during the salinity treatment (Fig 2.3).

Next main root growth rate of WT and GABA mutants including GABA-accumulating lines *gad2OE_B33*, *gad2OE_B97* and *pop2-8* were explored under different salinity treatments. After germination on 1/2 MS media for 5 days, plants with similar length of main roots were transferred to new media with or without NaCl. Three concentrations of NaCl were used (0, 50, 100 mM) and MRGR were calculated.

As shown in Fig 2.4a, under normal conditions main roots of *gad1245*, *GAD2* over-expression lines (*gad2OE_B33* and *gad2OE_B97*) and *pop2-8* grew faster than WT. Main roots of all other mutants except for *gad2OE_B97* grew faster than *gad2-1* if not stressed. MRGR didn't show significant differences between WT and mutants under 50 mM NaCl stress, although *gad2OE_B97* and *pop2-8* main roots grew faster than *gad2-1*. While under 100 mM NaCl stress, only *pop2-8* had the larger MRGR than WT, other mutants were

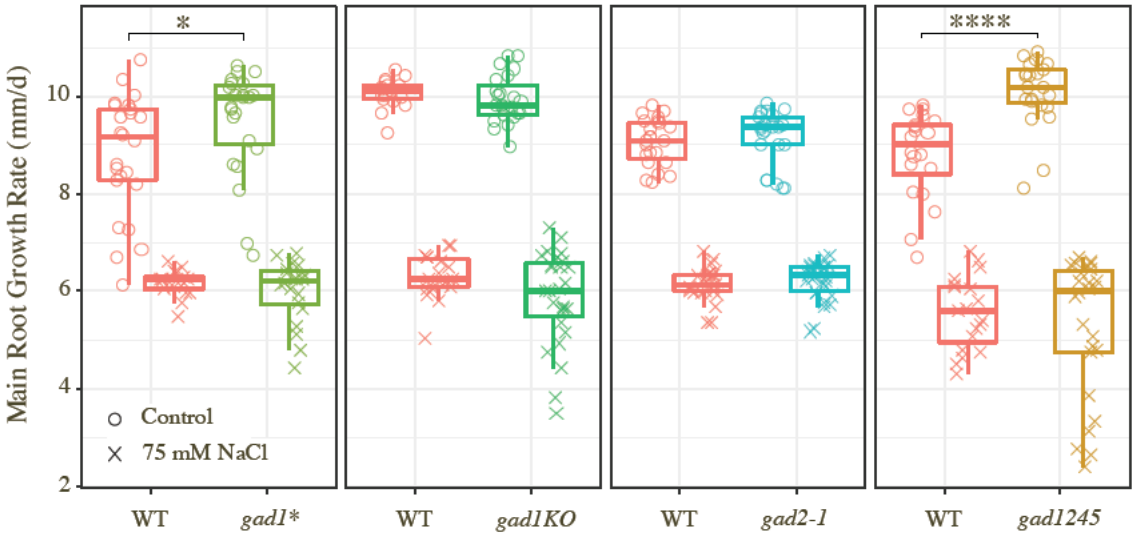


(a) Main root growth rate

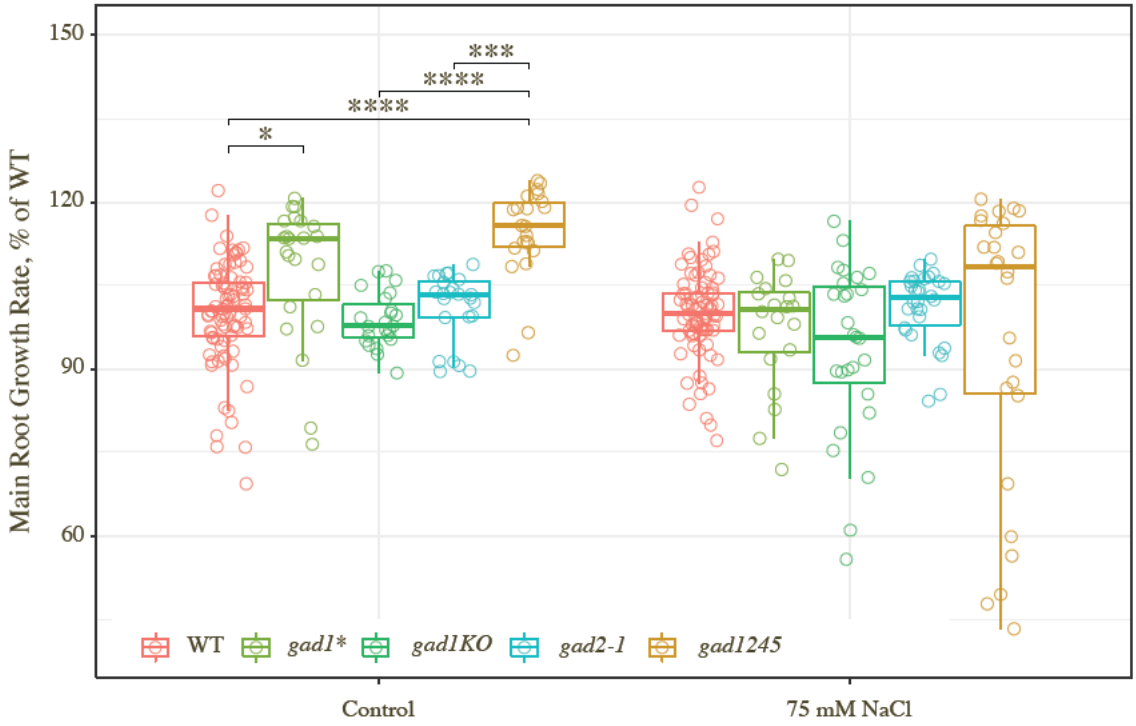


(b) Normalised main root growth rate (to WT level)

**Figure 2.3:** Main root growth rate of WT and GAD lines on different media. Seeds were sown on 1/2 MS and transferred to 1/2 MS ± 75 mM NaCl on DAG4. Plants corresponding to those in Fig 2.2 and main root growth rate was calculated during the following 11 d after transfer. Number of plants used n ∈ [22 ∼ 25]. ○ and × in (a) represent plants transferred to control and salt media, respectively. Stars showed ANOVA significance results between genotypes within each treatment. * $P < 0.05$, *** $P < 0.001$, **** $P < 0.0001$.

the same as WT.

After normalisation, Fig 2.4b showed that *gad1245*, *gad20E_B33* and *pop2-8* had a higher MRGR compared to WT under control, but not *gad20E_B97*. These results indicate that

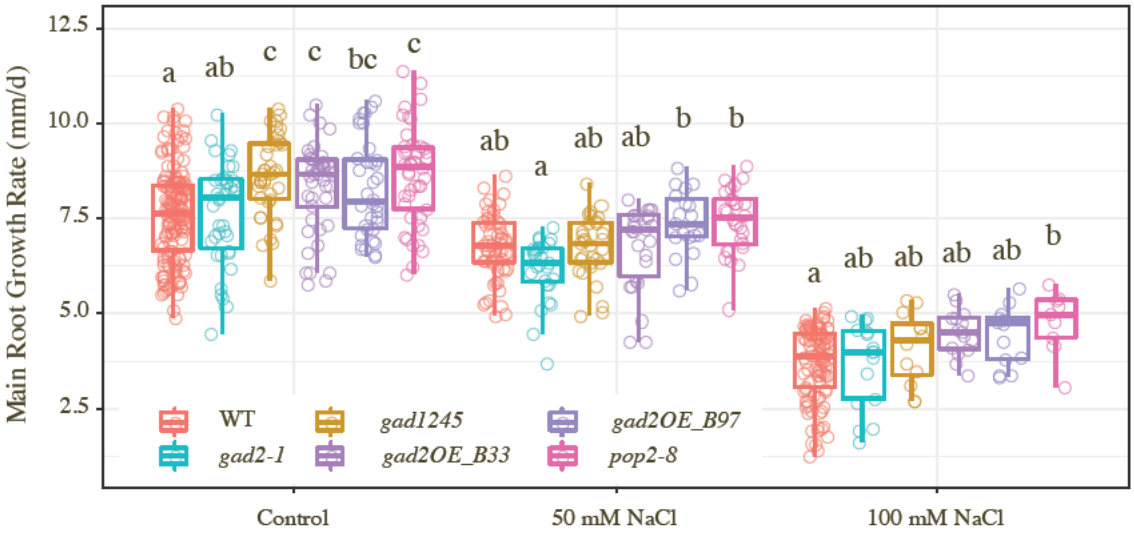


(a) Main root growth rate

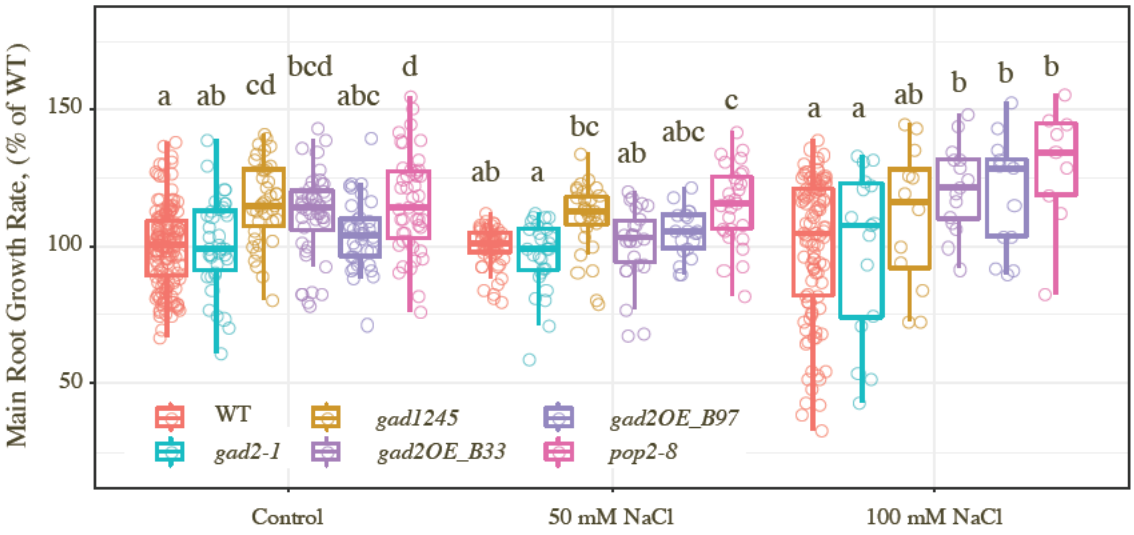


(b) Normalised main root growth rate (compared to WT under the same condition)

**Figure 2.4:** Main root growth rate of WT and GABA mutants on different media. Seeds were sown on 1/2 MS and on DAG5 seedlings were transferred to new media that contained 0 or 50 NaCl (repeated 3 times) and 0 or 100 mM NaCl (repeated three times). Letters show ANOVA significance results ($P < 0.05$).

the two *GAD2*-OE lines had some discrepancy in terms of promoting main root growth under non-stressed conditions. Under 50 mM NaCl *pop2-8* kept the highest MRGR (Fig 2.4b). Compared to *pop2-8* and *gad1245*, *gad2-1* had a lower MRGR both under control and 50 mM NaCl. Under 100 mM NaCl, the GABA-accumulating lines including *GAD2*-OE lines(*gad20E_B33*, *gad20E_B97*) and *pop2-8* had a greater MRGR than WT and *gad2-1*.

Taken together, both *gad1245* and *pop2-8* main roots grew faster than that of WT and *gad2-1* under control conditions. *pop2-8* maintained this advantage of faster main root growth under salt stresses as well, suggesting the ability to accumulate GABA (Su et al., 2019) contributed to the higher ability to attenuate salinity stress effects. It was interesting

that *gad1245* plants, in which the GABA-shunt was blocked and could not produce GABA through this pathway at all, main roots grew faster than not only WT but also its parent line *gad2-1* under control and slight salinity.

### 2.1.3 Root system architecture of WT and *GAD* mutants

As a major determinant of RSA, the formation and development of lateral roots (LRs) impacts water uptake efficiency, nutrients acquisition and plants anchorage, and thus the regulation of LRs is of great agronomic importance (Péret et al., 2009). After 6 d from transferring to control or salt media plates, parameters of RSA in addition to MRGR were examined for DAG10 WT and the four *GAD* mutants (*gad1*, gad1KO, gad2-1* and *gad1245*) in addition to MRGR. The total root length (MRL + LRL), total lateral root length (LRL) and lateral root size (proportion of lateral roots, LRS) were shown in Fig 2.5. The average length (AvgLR), number (LRN) and density (LRden) of lateral roots were shown in Fig 2.6. Salinity significantly inhibited all these RSA parameters.

In agreement with the main root growth rate results (Fig 2.3), all six RSA parameters of *gad1** were larger than that of WT if not stressed and there were no differences between *gad1** and WT under salinity (Fig 2.5, 2.6). Similarly, *gad1245* control plants had larger TRL, LRL, LRS, AvgLR and LRN than WT if not stressed, and the only exception was lateral root density. These results suggested that *gad1245* main root, which grew faster than WT on control media (Fig 2.3), was accompanied with more quantity and faster-grown lateral roots (Fig 2.5, 2.6), but the distribution of LRs on MR is the same as WT due to unaffected LRden.

In contrast to *gad1** and *gad1245*, the TRL, LRL and LRS of *gad2-1* was smaller than WT when grown on control media, but these differences could not be observed when grown on salt media (Fig 2.5). The decreased TRL of *gad2-1* plants under control media could be mainly due to decreased LRL, as the main root length of *gad2-1* and WT were not significantly different to WT on transfer day (Fig 2.2), as was the case of main root growth rate (Fig 2.3).

Although *gad1KO* plants started with a shorter main root on transfer day (Fig 2.2), they could maintain the same MRGR as WT did (Fig 2.3). This held true for the RSA parameters, and surprisingly, later root number, size and density of salt stressed *gad1KO* plants were significantly higher than that of stressed WT plants (Fig 2.5, 2.6). These observations indicate that under salinity, although *gad1KO* tend to form more lateral roots than WT, as the average length of individual lateral root was the similar to WT, the larger number of LRs was not sufficient enough to significantly increase of the LRL and TRL for *gad1KO*.

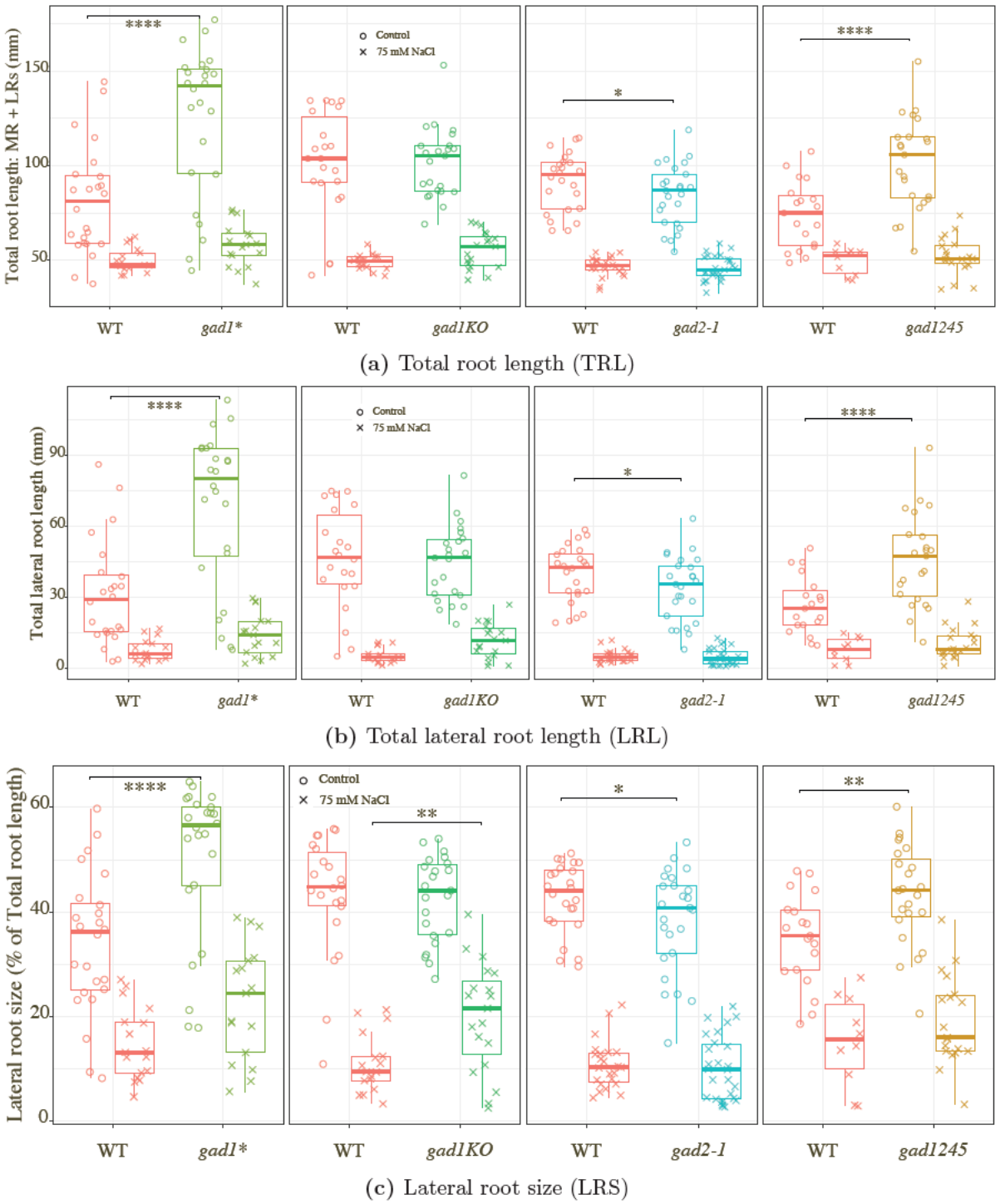


(a) Total root length (TRL)

(b) Total lateral root length (LRL)

(c) Lateral root size (LRS)

**Figure 2.5:** Total root length, lateral root length and lateral root size of WT and *GAD* mutants on control and salt media (DAG10). Seeds were sown on 1/2 MS and transferred to 1/2 MS ± 75 mM NaCl on DAG4. Plants corresponding to those in Fig 2.2. Number of plants used n ∈ [22 ∼ 25]. ○ and × represent plants transferred to control and salt media, respectively. Stars showed ANOVA significance results between genotypes within each treatment. * $P < 0.05$, ** $P < 0.01$, **** $P < 0.0001$.

### 2.1.4 Main root growth of WT and *pop2* from different ecotypes

The findings in the MRGR section 2.1.2 showed that the GABA-T knockout plants were more resistant to salinity than the other lines including WT, which was not in accordance

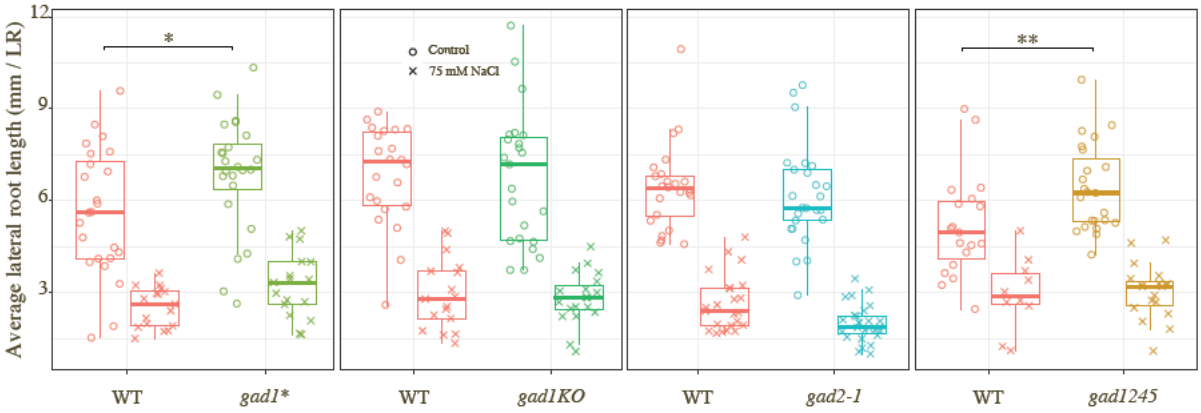


(a) Average length of lateral roots (AvgLR)

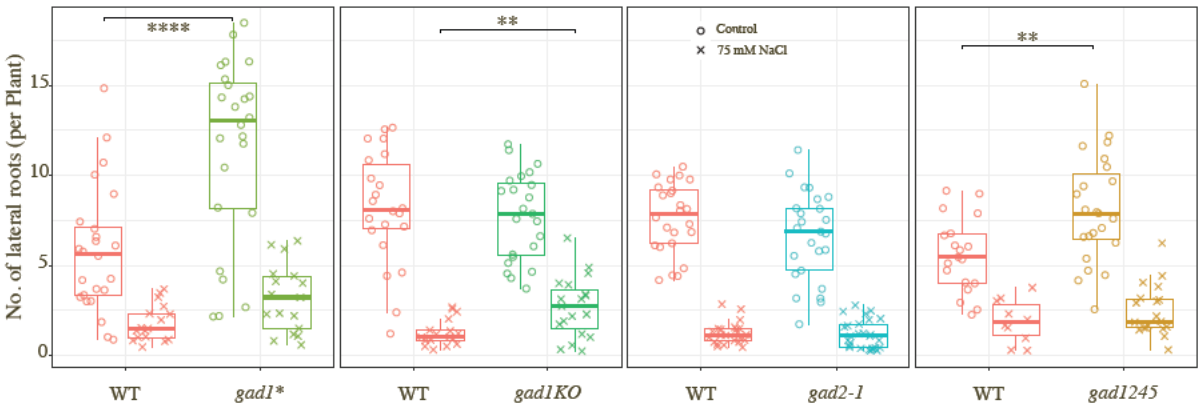


(b) Lateral root number (LRN)

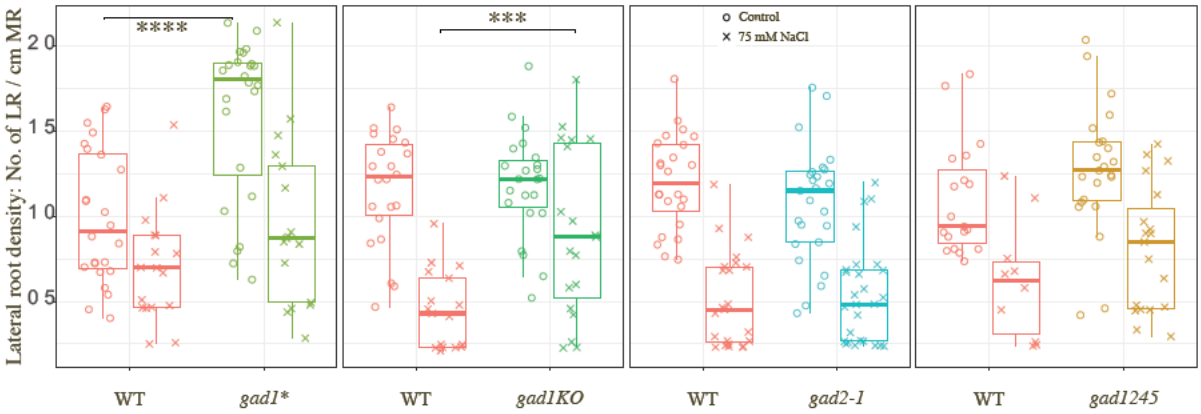


(c) Lateral root density (LRDen)

**Figure 2.6:** Average length, number and density of lateral roots in WT and *GAD* mutants transferred to control and salt media (DAG10). Seeds were sown on 1/2 MS and transferred to 1/2 MS ± 75 mM NaCl on DAG4. Plants corresponding to those in Fig 2.2. Number of plants used n ∈ [22 ∼ 25]. ○ and × represent plants transferred to control and salt media, respectively. Stars showed ANOVA significance results between genotypes within each treatment. * $P < 0.05$, ** $P < 0.01$, *** $P < 0.001$, **** $P < 0.0001$.

with some previous studies (Renault et al., 2010). Thus an assay of WT and *pop2* MRGR from Columbia and Landsberg ecotypes were used to further investigate the effects of GABA accumulation on root growth. On DAG5, seedlings with similar lengths of roots were transferred to new media with 0, 50 and 100 mM NaCl and MRL were plotted for eight days.

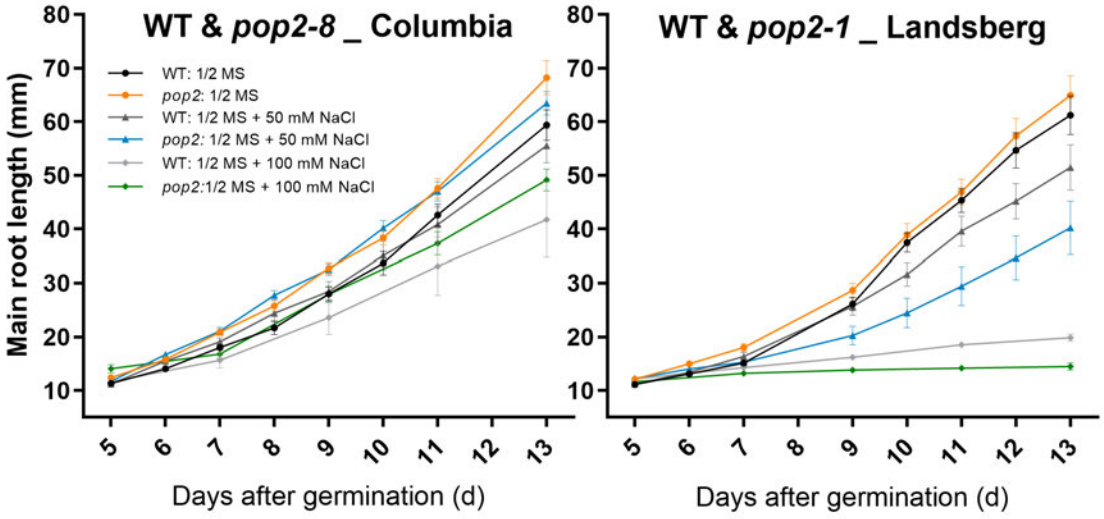


**Figure 2.7:** Main root length of WT and *pop2* from -Col and -Ler background. Seeds were sown on 1/2 MS and transferred to new media on DAG5. Number of plants used n $\in$ [10 $\sim$ 30].

Fig 2.7 showed that in general plants from Landsberg background were more sensitive to salinity than those from Columbia. Especially when stressed with 100 mM NaCl, main root growth of Landsberg lines (both WT and *pop2-1*) were greatly inhibited while the Columbia lines kept growing over 40 mm. Under normal conditions, *pop2* lines of the two ecotypes both had longer main roots than their corresponding WT on DAG13, although only the Columbia background (*pop2-8*) had significantly longer main roots than WT. *pop2-8* maintained this faster main root growth than WT under 50 mM and 100 mM NaCl as well. However, the Landsberg *pop2-1* was much more sensitive than its WT under both 50 mM and 100 mM NaCl. These results suggested that the Landsberg ecotype was in general more sensitive to salt stress, and this sensitivity was enhanced when GABA catabolism is totally blocked through the GABA shunt pathway.

### 2.1.5 Biomass and water content of WT and GABA mutants

To investigate the physiological response of disturbed GABA production through altered *GAD* and *GABA-T*, the biomass and water content of WT, *gad1**, *gad1KO*, *gad1245* and *pop2-8* were measured.

As shown in Fig 2.8a, plants of *gad1** and *gad1245* had a larger fresh weight than WT and *gad2-1* under control conditions, while under salinity there were no significant differences between the any of the *GAD* mutant and WT. After normalisation, between the non-stressed mutants, *gad1** and *gad1245* both had a larger fresh weight than that of WT, *gad1KO gad2-1* (Fig 2.8b). However, when grown on media containing 75 mM NaCl,

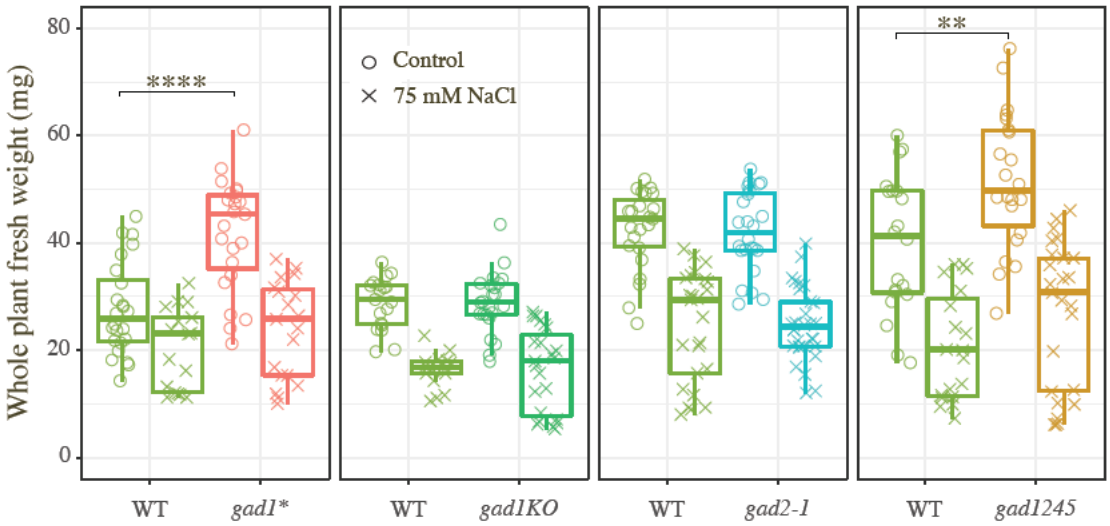


(a) Whole plant fresh weight

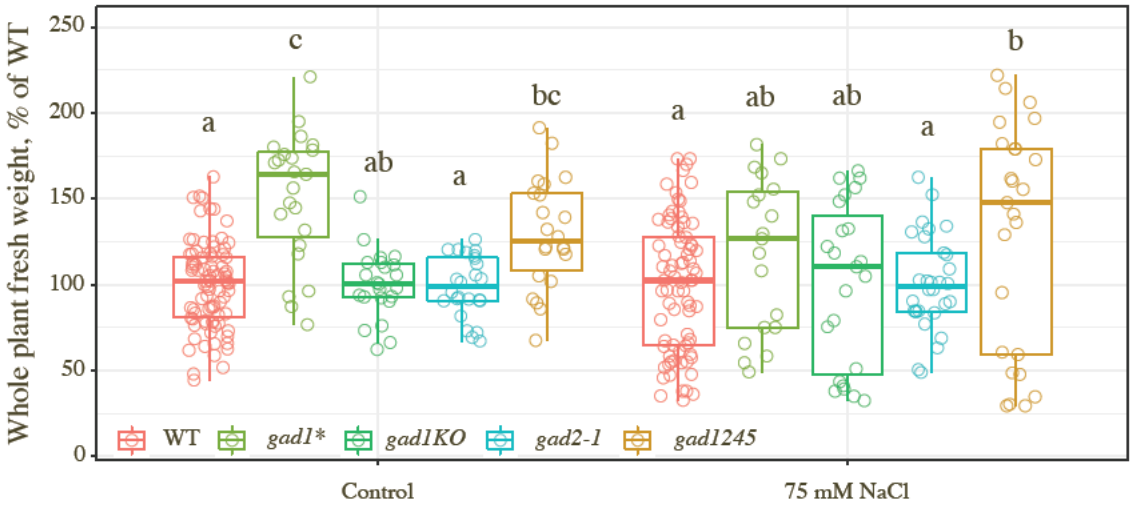


(b) Normalised whole plant fresh weight (to WT level)

**Figure 2.8:** Whole plant fresh weight of GAD lines on different 1/2 MS media. Seeds were sown on 1/2 MS and transferred to new media ± 75 mM NaCl on DAG4. Number of plants used n ∈ [22 ∼ 25]. Letters and stars show significance between genotypes within each treatment. Stars show two way ANOVA significance results. ** $P < 0.01$, **** $P < 0.0001$.

only *gad1245* maintained a higher fresh weight than that of WT, while *gad1** didn't show significance compared with the other lines (Fig 2.8b).

Two of the GABA mutants with the most disturbed GABA shunt pathway were further investigated using a hydroponic system, and these plants were older than those in the previous section (>5 weeks old). Fig 2.9 showed that under normal growth conditions there were no differences between all three lines at DAG40 and DAG46 in terms of shoot fresh weight, dry weight and water content, although *gad1245* shoots had higher fresh weight and dry weight when compared to WT at DAG46. The root dry weight of *gad1245* was also higher than WT at DAG46 under control media (Fig B.5). Under salt stress, fresh and

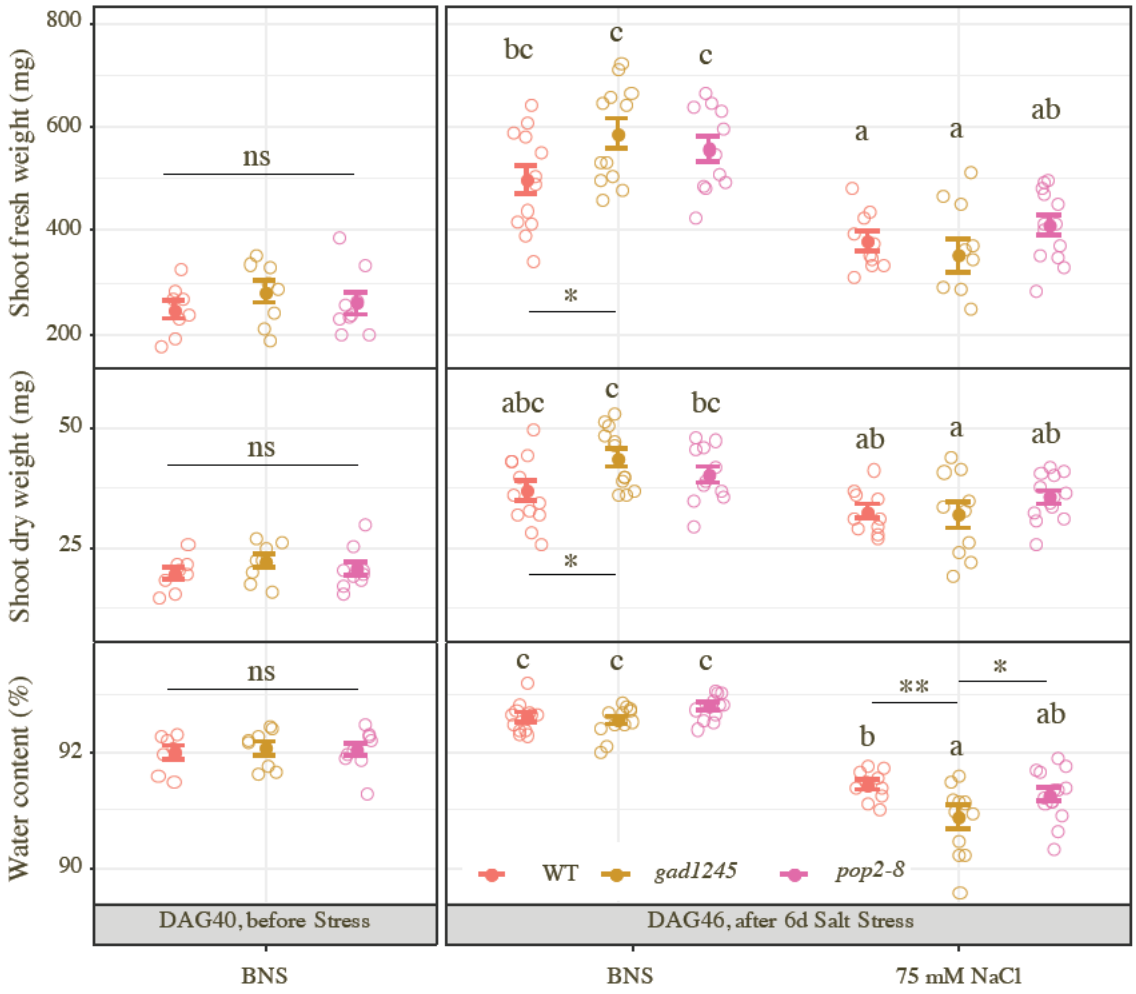


**Figure 2.9:** Biomass of hydroponically grown WT and GABA mutants before and after 6 d salt stress (BNS and BNS ± 75 mM NaCl). Data show mean ± SE. Number of biological replicates n ∈ [8 ∼ 13]. Letters show two-way ANOVA results. Stars show genotype effects within control or salt treatment (student's t-test). * $P < 0.05$, ** $P < 0.01$.

dry weight showed no significant differences between these three lines, but *gad1245* had the lowest water content. Compared to their own non-stressed plants at DAG46, 6 d salt stress inhibited shoot dry weight of *gad1245* the most (27.0%). The inhibition on shoot fresh weight and water content by salt stress was also the most in *gad1245* (40.1% and 1.81%, respectively), compared to WT (23.7% and 1.26%, respectively) and *pop2-8* (26.7% and 1.64%, respectively). Salt stress also greatly inhibited root dry weight of *gad1245* while WT and *pop2-8* were not significantly affected (Fig B.5). These observations suggested that *gad1245* was the most affected by the 6-d 75 mM NaCl treatment due to the fact that its fast growth under control conditions (higher shoot fresh and dry weight and higher root dry weight than WT) was greatly inhibited by salinity, and its ability to lose more water during salinity (lowest water content after salt stress).

### 2.1.6 Leaf ion content of WT and GABA mutants

Ion exclusion (e.g. $Na^+$ exclusion from leaves) is one of the physiological strategies plants can deploy to cope with salt stress (Munns and Tester, 2008). To investigate if the sensitivity to salt stress is correlated to the ion exclusion in GABA mutants, the content of $Na^+$, $K^+$ and $Na^+/K^+$ ratio in the hydroponically grown WT, *gad1245* and *pop2-8* shoots were measured.

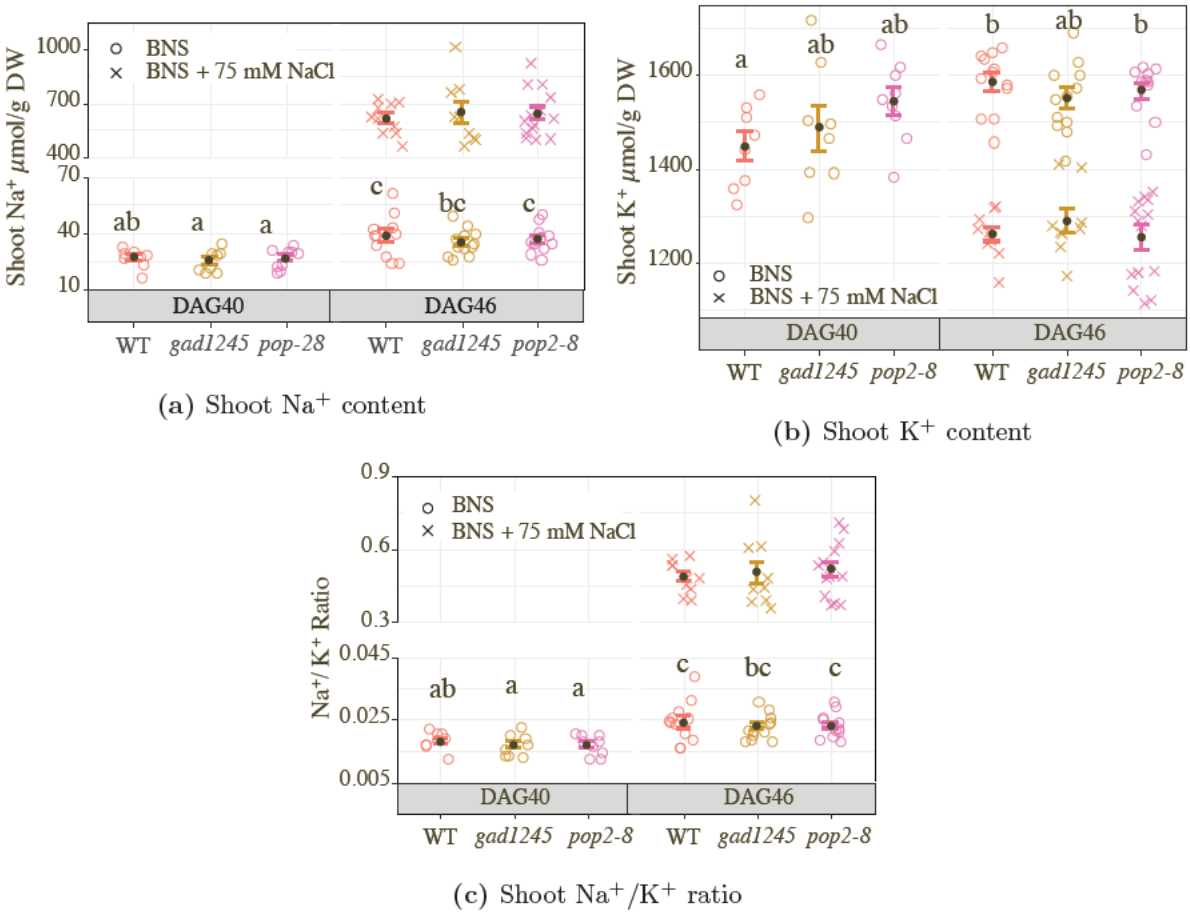


(a) Shoot $Na^+$ content

(b) Shoot $K^+$ content

(c) Shoot $Na^+/K^+$ ratio

**Figure 2.10:** Shoot $Na^+$, $K^+$ content and $Na^+/K^+$ ratio of hydroponically grown WT and GABA mutants before and after 6d Salt Stress (BNS and BNS ± 75 mM NaCl). Data show mean ± SE. ○ and × represent seedlings grown in BNS and BNS + 75 mM NaCl, respectively. Number of biological replicates n ∈ [8 ∼ 13]. Letters show two-way ANOVA results of control plants on DAG40 and DAG46.

Fig 2.10 showed that salinity increased shoot $Na^+$ content and $Na^+/K^+$ ratio of all three lines compared to control plants while decreased shoot $K^+$ content on DAG46. Compared to WT, under salinity, *gad1245* and *pop2-8* did not have significant differences in ion content. Compared to their own non-stressed plants on DAG46, however, salt stressed *gad1245* leaves had a larger increase of $Na^+$ content but smaller decrease of $K^+$ content than that of WT and *pop2-8*. For non-stressed plants during 6 days (from DAG40 to DAG46), WT shoot $K^+$ content increased but the two mutants did not, however, all three

lines shoot $Na^+$ content and $Na^+/K^+$ ratio was higher on DAG46 than on DAG40 (Fig 2.10). These results suggested that *gad1245* was more affected than WT and *pop2-8* by salinity, in line with its more severely impacted biomass and water content (Fig 2.9, B.5).

## 2.2 Discussion

Studies on salt-treated wheat leaves have shown that the GABA shunt is invoked to bypass elements of the TCA cycle under salt stress in order to provide energy to stressed plants (Che-Othman et al., 2020). There is also evidence that salinity induced GABA accumulation in *Arabidopsis* could involve *GAD1* and *GAD2* post-translational activation through cytosolic calmodulin and *GAD4* expression (Zarei et al., 2017). The balance between cell proliferation and differentiation of root-tip greatly affects root system growth (Petricka et al., 2012). Cells in the meristematic zone (MZ) exhibit higher rates of division but they do not elongate, while cells in the elongation zone (EZ) are the opposite and they start to differentiate. Lateral roots, as well as root hairs, are developed in the differentiation/maturation zone (DZ) of the main root, where the cells are fully elongated and undergo differentiation to acquire specific characteristics and functions (Menand et al., 2007). Salinity inhibits root growth through both cell division and cell elongation. In this study, under control and salinity conditions, root growth of *Arabidopsis* was affected when the GABA-shunt pathway was disturbed.

Among the five glutamate decarboxylase genes (*GADs*) in *Arabidopsis* genome, *GAD2* is constitutively expressed in all organs (most abundant transcripts in leaves), *GAD1* is mainly expressed in roots while the expression of *GAD3, GAD4, GAD5* is generally weak in all organs (Bouché and Fromm, 2004; Zik et al., 1998) with some exceptions. For example, salinity could induce *GAD4* expression in WT seedlings (Renault et al., 2010; Zarei et al., 2017) and *gad1/2* roots (Mekonnen et al., 2016). WT roots contained seven- and eight-fold higher GABA than the roots of *GAD1* knockout mutants under control and heat stress conditions, respectively (Bouché et al., 2004), indicating *GAD1* is essential for sustaining root GABA content. The *Arabidopsis gad2-1* and *gad1/2* both have been reported to have remarkably reduced GABA concentration, larger stomata aperture and defective stomata closure than WT plants (Mekonnen et al., 2016; Xu et al., 2021). Also, in *pop2-8* lines, the consumption of GABA to SSA and the following feeding into the TCA cycle is blocked. The *pop2* plants have much higher GABA content than WT plants under both control and stressed conditions (Renault et al., 2010). Therefore, all of the above scenarios significantly affect the efficiency of the GABA shunt pathway and the GABA concentration in plants.

**Lack of GABA in roots inhibited *Arabidopsis* root growth**. In this study, *gad1245*

and *gad1KO* seedlings (less than one week old) had shortest main roots among all lines when grown on 1/2 MS (Fig 2.1). Interestingly, when germinated for 4 days on 1/2 MS media that did not contain sucrose, *gad2-1*, *gad1245* and *pop2-8* all had significantly shorter main roots than WT, only *gad2OE_ B33* maintained the same MRL as WT (Fig B.2). *gad1245* and *pop2-8* had the shortest main roots, and the MRL of *gad2-1* were larger than *gad1245* but smaller than *gad2OE* (Fig B.2). These results suggested that adding a minimal amount sucrose into the media could compensate the root elongation inhibition of *gad2-1* and *pop2-8*, but not the inhibition of *gad1245*.
When directly grown on 100 mM NaCl media (- sucrose) for a week, although the majority GABA mutants had shorter main roots than WT, *gad1KO* and *gad1245* root elongation was still the most inhibited while *gad2-1* not affected (Fig B.3). On the contrary, the loss of *GAD2* did not impact the root elongation within the first week for plants either grown 5 d on control media with sucrose (Fig B.2) or grown 7 d on salt media without sucrose (B.3). The reason *gadKO* and *gad1245* plants which obtained an initial root growth inhibition in the first week after germination could be likely due to a lower availability of GABA in their roots. This study showed that blocking GABA production of either the whole plant (*gad1245*) or only roots (*gad1KO*) greatly inhibited root growth, highlighting the regulation of earlier stage root elongation by *GAD1* in *Arabidopsis* seedlings.

When WT and GABA-deficient lines (*gad1KO*, *gad2-1* and *gad1245*) plants with similar root length were transferred to new media (Fig 2.2), *gad1245* had the a significantly greater main root growth rate over the other lines only on control but no salt media (Fig 2.3a, Fig 2.3b). As there was no significant difference in MRGR between them on salt media, it seems at a later stage when plants were bigger, these three GABA-deficient lines could cope with the stress better. Different metabolism could be involved between in these GABA-deficient lines and the other mutants to achieve the same goal. Exogenous GABA improved $Ca(NO)_3$ tolerance of muskmelon pants through promoting both polyamine and GABA biosynthesis (Hu et al., 2015). Polyamine pathway was proposed to contribute to GABA accumulation in *Arabidopsis* leaves and soybean roots under salinity (Zarei et al., 2016; Xing et al., 2007) as well as in tea (Zhang et al., 2022). So, it is possible that the GABA-deficient lines could have GABA produced through the PA pathway that could be used. However, the larger MRGR reduction in *gad1245* induced by salt stress still means that *gad1245* was relative sensitive to salt stress than the other lines, and suggests the importance of GABA production through the GABA shunt pathway. As mentioned earlier, induced *GAD4* expression under salinity was observed (Renault et al., 2010; Zarei et al., 2017), while this cannot happen in *gad1245*.

The MRGR of *gad1** was higher than WT only when transferred to control but not to saline media, this is the same as *gad1245*. However, *gad1** did not result in the change of *GAD1* expression (Table 1.2, Fig A.1), and the GABA shunt pathway may be much less

affected than the other mutants. For *gad1245*, as very little of GABA can be produced through the GABA shunt pathway, the other alternative pathways could be potentially contributing to plants coping with salt stress. For example, polyamine was reported to regulate plant stress responses (Podlešáková et al., 2019). Salinity-induced accumulation of GABA is reduced by 39% by aminoguanidine, a diamine oxidase inhibitor that represses the production of Put (in the polyamine pathway) (Xing et al., 2007). Apart from the polyamine metabolism mentioned above, the amino acid metabolism such as arginine, proline, alanine and glutamate are all closely related to the GABA shun pathway (Section 1.2.2.2, 1.2.2.1), and they may play a role in the adaptation to salt stress, especially for *gad1245*. GABA regulation of photosynthesis system and activities of antioxidant enzymes has been reported to confer salt tolerance (Li et al., 2016a). In addition, when hydroponically grown for 7 d with the addition of 50 mM NaCl, *gad1** also had greener leaves than WT (Fig B.4), suggesting *GAD1* expression and sufficient GABA could contribute to the photosynthesis processes in this line.

**Disturbed GABA shunt pathway affected biomass**. Greater MRGR could contribute to the greater fresh weight of *gad1** and *gad1245* found under control conditions. Studies have shown that *GAD2* generated cytosolic GABA regulates stomatal opening and water use efficiency, and *gad2-1* and *gad2-2* has larger stomata aperture and stomata conductance than WT under drought (Xu et al., 2021). This could result in a higher rates of gas exchange rate in the *gad2-1* mutants, that contribute to maintaining the same vegetative growth as WT. *gad1245* and *pop2-8*, which had the most affected GABA shunt, were both able to exclude shoot sodium and keep similar amount of shoot potassium as WT did. Further explorations of specific pathways and/or prior-stress priming due to the mutation are needed to identify their greater growth under control condition and relative salt sensitive/tolerant phenotypes.

**MRGR of *GAD2* over-expression lines promotes main root growth after transferred to control but not saline media**. Among the two GABA-accumulating lines, *gad2OE_B33* grew faster than *pop2-8* if not stressed if the media contained sucrose (Fig B.2), but when directly grown on 1/2 MS + 100 mM NaCl that didn't contain sucrose, the two lines had similar root growth (Fig B.3). This may be due to the constantly driving by a 35S promoter in *gad2OE_B33* could be an energy-consuming process, when plants are under stress (e.g. salinity) or during energy crisis (e.g. no sucrose in the media), this could affect root growth.

***pop2* sensitivity to salinity showed ecotype differences**. In this study, two GABA-T knock out mutants and their wildtype from different ecotypes were used. We found that the *pop2-1* to be salt-sensitive while the *pop2-8* to be salt-tolerant, this is in accordance with some of the previous studies (Renault et al., 2010; Su et al., 2019). The ecotype-dependent

responses could be explained by that the fact that *pop2-1* was sensitive to ionic stress but not osmotic stress Renault et al. (2010), and in my case, the plants were grown on salt media for over a week, which is quite a long period of time for the young seedlings. The other possible reason may be in *pop2-1* the over accumulated GABA to an excessive amount beyond a particular threshold that is harmful to plants (Su et al., 2019). Thus, the *pop2-1* plants were probably not able to exclude the stress-induced accumulation of $Na^+$ and $Cl^+$ stress from root to shoot.

While for the Columbia *pop2-8* it was another story. GABA could improve plants salinity tolerance through regulating $Na^+/K^+$ ratio and $K^+$ content, as well as ROS pathway. It was found that hydroponically grown 4 weeks old *pop2-5* leaves accumulated lower $H_2O_2$ after 12 h of 100 mM NaCl stress, they also had the lowest $Na^+/K^+$ ratio, compared with WT and *gad1/2* double mutant Su et al. (2019). In my experiments, only plate-grown *pop2-8* seedlings showed salt-tolerance but not the hydroponically grown plants. This could be due to on the plates it was medium salt stress (50 mM, 75 mM) and the media contains sucrose. While my hydroponic plants were stressed with 75 mM NaCl, they were much older and maybe not the most sensitive growing stage. Also my solutions for hydroponics is BNS which is not as rich in nitrogen as 1/2 MS media, and plants were stressed for 6 days so a shorter period of time, so they may have reached an adaptive balanced state. Interestingly, when*pop2-8* plants were grown on 1/2 media without sucrose they lost any growth advantage under saline conditions compared to the other genotypes (Fig B.3). In fact, *pop2-8* had significantly shorter main roots than *gad1** and *gad2-1*, which suggests that carbon balance is important for determining how altered GABA metabolism impacts stress tolerance.

Overall, this study showed that lacking of GABA in the roots in the short term affected root growth whether under salinity or not, especially when grown on media without sucrose, with the *gad1KO* and *gad1245* being the most sensitive to salinity. However, GABA mutants were able to keep or exceed the same root growth in the long term compared to WT, especially in the case of *gad1** and *gad1245* if not stressed. The mutants also maintained similar or even higher biomass compared to WT plants, suggesting the compensatory effects due to disturbed GABA shunt, possibly through regulating polyamines and other amino acid metabolism. The different sensitivity WT and *pop2* plants to salt stress from two ecotypes suggests that there is natural variance in stress tolerance.

## 2.3 Materials and methods

***GAD1* expression of *Arabidopsis* T-DNA mutants**. *Arabidopsis gad1KO*, *gad1** T-DNA insertion homozyous mutants in the Col-0 background were obtained from The

Arabidopsis Information Resource (TAIR). Primers designed for confirming homozygous lines were gene specific left primer (LP, 5'-GTGGACTGACTTACCTCGTGG-3' and 5'-ACAAAAACGGTGCAATGAATC-3' for *gad1** and *gad1KO*, respectively), right primer (RP, 5'-GGAGCCAATGTTCAAGTAACG-3' and 5'-TTATTTCCGCAAATACCATCC-3' for *gad1** and *gad1KO*, respectively), and left T-DNA border primer LBb1.3 (5'-ATTTTGCCGATTTCGGAAC-3'). *GAD1* expression in the roots and shoots of the two GAD1 lines were examined as using real time quantitative PCR. Both tissue from 2 weeks old plants were snap-frozen and ground to fine powder in liquid nitrogen, then transferred to a 2-mL microcentriguge tube with 1 mL TRIZOL-like reagent (TRIzol RNA Isolation Reagents, Invitrogen). 200 $\mu$L acidic chloroform was added to the mixture, which was centrifuged at maximum speed for 15 min at 4 °C. The supernatant was transferred to tubes containing 500 µL 100% Isopropanol, mixed and incubated at 4°C for 10 min, then centrifuged at 11,400 rpm at 4 °C. The isolated RNA pellet was washed in 1 mL 75% ethanol and air-dried, then resuspended in 20 $\mu$L nuclease-free $H_2O$. The RNA eluate was treated with DNase using a TURBO DNA-free kit (Ambion) according to the manufacturer's instructions to remove any of genomic DNA contamination. RNA integrity was evaluated using gel electrophoresis as well as spectrophotometry (ND-1000; NanoDrop Technologies), and RNA quantity was measured using fluorometrically (Invitrogen Qubit® fluorometer).

For cDNA synthesis, 5 $\mu$g of total RNA was used in combination with SuperScript III Reverse Transcriptase (Invitrogen) and oligo(dT) primers (Promega) in a 20 $\mu$L reaction system accordance with the manufacturer's instructions. Primers used in qPCR for identifying the *GAD1* gene expression were GAD1-Fwd (5'-TCTCAAAGGACGAGGGAGTG-3') and GAD1-Rev (5'-AACCACACGAAGAACAGTGATG-3'). The PCR results confirmed that *gad1KO* is a knockout line while *gad1** still maintained the expression of *GAD1* in both leaves (Fig A.1a) and roots (Fig A.1b).

**Growth conditions, root growth and hydroponics assays**. The plants were grown at the same time and seeds were harvested before the experiment, so that the seeds were of similar age. Seeds were surface sterilised in 70% (v/v) ethanol for 3 min, rinsed with sterile distilled water three times, and then dried in the fume hood. After cold stratification in the dark for 2-3 days, the petri dishes (vertically placed unless stated horizontally) were kept in a growth chamber at average day/night temperature of 23/19 °C, 60-75% relative humidity, and 120-150 $\mu$mol $\cdot m^{-2} \cdot s^{-1}$ photosynthetic photon flux density (PPFD) with a day/night cycle of 10/14 h (short day) or 16/8 h (long day) for up to 3 weeks. Three days after germination (DAG3), the square petri dishes (referred to as plates) were scanned every day or every other day. Seedlings were harvested at the end of experiments to measure fresh weight (FW), dry weight (DW), leaf sodium, potassium and chloride contents.

For root growth assays, young seedlings (<3 weeks old) were used. Seeds were sown and grown on 1/2 MS plates, and 0.1% sucrose was added to the media unless stated otherwise. Four or five days after germination (DAG), plants with similar root length were transferred to new media with or without the addition of NaCl (50, 75 or 100 mM). These plants were referred to as "Control plants" (without NaCl) and "Salt stressed plants" (with NaCl). The RSA parameters and main root growth rate were discussed in more details using transferred plants. Alternatively, plants were grown on same plates (without transferring), and these results were mainly shown in Section 2.1.1. Multiple repeats of each experiment were performed (n > 3).

For the hydroponics salt assay, mature seedlings (>3 weeks old) were used following a protocol developed previously (Conn et al., 2013; Qiu et al., 2016). Salt stress was induced by adding 75 mM NaCl (supplemented with 3 mM $CaCl_2$) when changing the solution from Germination Buffer (GB) to Basal Nutrient Solutions (BNS). Dried shoots and roots were ground, digested in concentrated 1% $HNO_3$ at 100 °C for 3h and then analysed on a flame photometer to determine $Na^+$ and $K^+$ content. The shoot water content was determined as following: the entire shoot of control and salt stressed plants were harvested and immediately weighed for shoot fresh weight (FW), then wrapped in an envelop and oven dried at 80°C for two days to measure dry weight (DW). Water content (WC, %) was calculated using equation 2.1 (Mekonnen et al., 2016).

$$WC(100\%) = \frac{FW - DW}{FW} \times 100 \tag{2.1}$$

**Data analysis**. Root System Architecture (RSA) parameters, i.e. Main Root Length (MRL), Lateral Root length (LRL), Total Root length (TRL) and Lateral Root Number (LRN) were measured using ImageJ software with the plug-in SmartRoot(Lobet et al., 2011). Main root growth rate (MRGR) was calculated as the slope (MRL ~ DAG) of line plots of individual plants during the linear growing phase. See Fig 2.11 as an example. Lines plots for 6 seedlings from a plate were generated in order to further calculate MRGR. Data was analysed and presented using R (version 4.0) and GraphPad Prism (version 9.0.0) software. One-way ANOVA, two-way ANOVA, Student's t-test (equal population variances) and Welch's t-test (unequal population variances) were conducted.

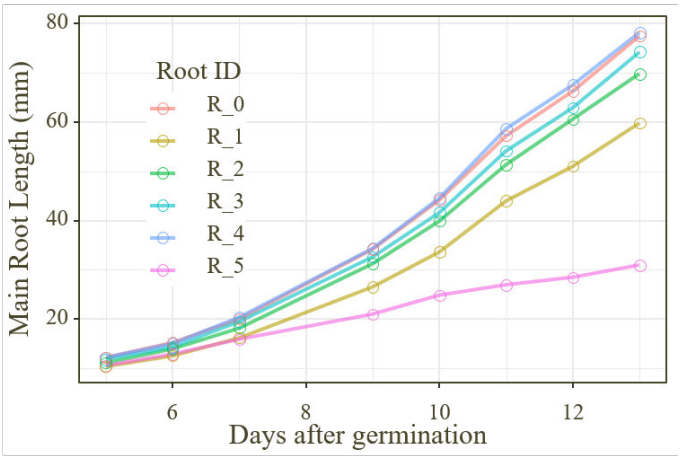


**Figure 2.11:** Line plots of main root length for 6 seedlings after transfer to new 1/2 MS media. Half WT and half GABA mutants were grown on each plate.

# CHAPTER 3

# The role of GABA under hypoxia

Floods are among the most common natural hazards, and plant GABA content is reported to be dramatically increased under flooding (Michaeli and Fromm, 2015; Shelp et al., 2017). Flooded plants encounter an energy crisis, low oxygen, and low light as well as other co-occurring stresses such as higher risks of pathogen and insect attack. Different flooding tolerance in plants also can result in varied survival rates during the following post-flooding recovery, when challenges such as high light, dehydration, oxidative stress occur, and senescence is induced. Post-hypoxic injuries due to excessive generation of reactive oxygen species (ROS) and aldehydes are common (Yeung et al., 2018). For a detailed review see Chapter 1 Section 1.4. There are still some gaps in the exact role that GABA plays in hypoxia under mid to long term natural floods (day/light cycles), as many previous studies induced dark and/or short term submergence which is often only to the rootzone, and their focus was not on how GABA contributes to hypoxia acclimation. The GABA shunt is the primary GABA metabolism pathway: glutamate decarboxylase (GAD) catalyses glutamate into GABA, which is converted to succinic semialdehyde (SSA) by GABA transaminase (GABA-T) (Chapter 1 Section 1.1 for GABA metabolism). The *Arabidopsis* genome contains five *GAD* genes and one *GABA-T* gene. In this research, multiple *GAD* mutation lines and one *GABA-T* mutation line which had disturbed GABA metabolism were used, and are referred to as 'mutant(s)' or 'GABA mutants' (described comprehensively in Chapter 1 Table 1.2). The *gad2OE* line in this chapter is the same as the *gad2OE_B33* in the last chapter 2. Whole plant submergence took place over a period of 6 d under day/light cycles (dimmed light) followed by 2 d recovery (de-submergence/re-oxygenation under standard light), and rosette leaves were collected. By investigating the acclimation responses of GABA mutants with a disturbed GABA-shunt pathway at physiological and molecular levels, as well as their metabolic profiles, a better mechanistic understanding on the role of GABA during submergence and recovery will be achieved. The goal of the present study is to decipher the contribution of GABA in the regulatory networks governing plants tolerance and/or adaptation to flooding.

Potential quantum efficiency of Photosystem II (Fv/Fm was the highest at the end of experiment in the two *GAD1* lines and *gad2-1*, while *pop2-8* had the lowest Fv/Fm and relative water content (RWC) after recovery indicating less and more damage to photosynthetic capacity, respectively. GABA concentration was consistently highest in *pop2-8*, suggesting that not being able to use GABA seemed to be doing more harm than very low levels of GABA in the *gad* knockout plants. RNAseq analysis showed that all GABA mutants already had significantly affected gene expression prior to hypoxia treatment involved in various metabolic processes such as amino acid and organic metabolism, as well as signal transduction, which was accordance with the altered amino acid and organic acid content measured with the metabolomic analysis. In addition, genes involved in oxygen-sensing, ion transport and stomatal function were also affected differently in GABA mutants under both control conditions and in response to submergence. Among them, *gad2-1* up-regulated genes were enriched in four oxygen-response GO terms under control conditions while all other mutants were not, suggesting the disturbed GABA shunt pathway influenced oxygen sensing in these mutants. Up-regulation of such pathways may be beneficial (in the case of *gad2-1*) for the subsequent submergence. After submergence, *pop2-8*, *gad2OE* and *gad1KO* down-regulated genes encoding light-harvesting chlorophyll protein complex (LHC), chloroplast protein localisation and photosythesis but up-regulated genes positively regulate senescence. These observations were in accordance with the Fv/Fm changes among these mutants.

## 3.1 Results and discussion

### 3.1.1 An impaired GABA shunt pathway increases sensitivity to submergence and recovery

Photosynthesis and aerobic respiration in submerged plants are dramatically restricted due to limited oxygen and light availability under water. Therefore, they encounter major challenges that greatly affect plant growth and survival during submergence are carbohydrate starvation and an energy crisis, which typically affects biosynthetic processes, plant growth and survival (Fukao et al., 2019). To investigate the physiological and photosynthetic responses of WT and GABA mutants under normal and hypoxia, biomass, relative water content and Fv/Fv were collected (Fig 3.1, 3.2, 3.3).

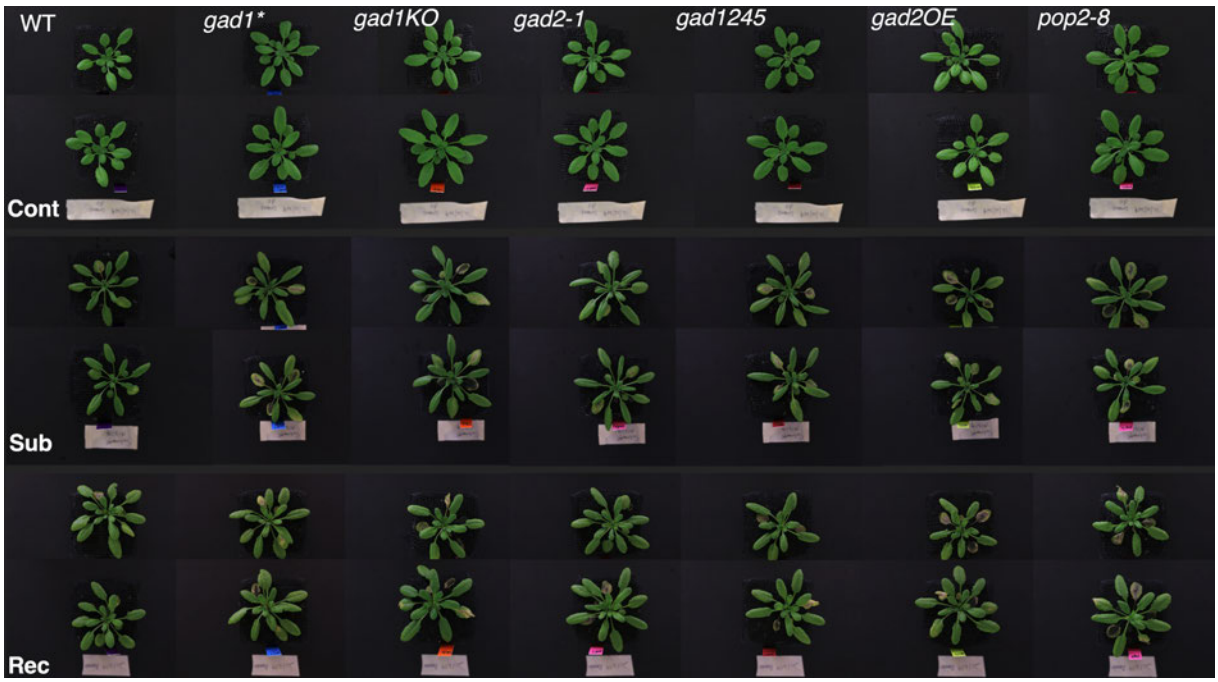


**Figure 3.1:** Representative phenotypes of WT and GABA mutants under control, submergence and recovery. Photos were taken before sampling and measuring Fv/Fm.

The phenotype of WT and the GABA mutants under control, submergence and recovery is shown in Fig 3.1. On visual inspection, the WT rosettes appeared to be a little smaller than GABA mutant lines, and *gad2-1* had the most green leaves after 2 d recovery, in contrast to *gad2OE* and *pop2-8*, but no other apparent differences could be visually observed. In general, the two mutants with the most disturbed GABA shunt pathway, *pop2-8* and *gad1245*, unlike the rest of the accessions, were affected the most by submergence and seemed to recover the least. A detailed quantified account of these experiments follows.

**Fresh weight**. Under control conditions, shoot fresh weight between all lines did not show significant differences (Fig 3.2a) although WT rosettes were visually a little smaller (Fig 3.1). Compared to control plants, after 6 d submergence, *gad1**, *gad1KO* and *gad2-1* shoot fresh biomass showed a greater increase (95%, 51% and 102%, respectively) than that of the WT, *gad1245* and GABA over-accumulating lines (*gad2OE* and *pop2-8*). At the end of submergence, these three lines maintained a significantly higher shoot fresh weight than that of the WT; *gad1** also had much greater shoot fresh weight than *gad2OE*. Compared to submerged plants, the following 2 d recovery did not alter vegetative growth significantly; less than 50 mg increased/decreased mean fresh weight was observed for all six GABA mutants, while WT gained 87 mg fresh weight. At the end of recovery, only two lines, *gad1245* and *gad2OE*, did not show a significant gain of shoot fresh weight (only approximately 24% increase) compared to their pre-submergence control plants, while *gad1** and *gad2-1* had the greatest fresh weight gain (over 83%).

**Dry weight**. The general response and pattern of shoot dry weight to control, submer-

gence and recovery was similar to that of fresh weight. Under control conditions, there was no significant difference in the shoot dry weight between any of the lines, except WT dry weight was significantly lower than *gad1245* (Fig 3.2b). Compared to control plants, after 6 d submergence, *gad1** mean dry weight increased by 83%, while no significant increase in mean dry weight was observed in WT (49%), *gad1KO* (34%), *gad2-1* (67%) and *pop2-8* (42%), with mean dry weight of *gad1245* and *gad2OE* also unchanged. Compared to the other lines under submergence, WT and *gad2OE* had the lowest dry weight while *gad1** and *gad2-1* had relative highest dry weight. Compared to the submerged plants, after 2 d recovery, no significant changes in all lines were seen using two-way ANOVA; mean dry weight of WT increased by 75%, with most GABA mutants (20∼40%) and *pop2-8* had no mean weight increase. At the end of recovery, compared to pre-submergence control plants, the two *GAD1* lines (*gad1**, *gad1KO*) and *gad2-1* showed significant shoot dry weight increase (120%, 89% and 105%, respectively) than that of *gad1245* or GABA over-accumulating lines such as and *gad2OE* and *pop2-8* (35∼38%).

The above results likely indicate that GABA accumulation has a key role in regulating shoot biomass under hypoxia conditions. Overall, among all GABA mutants, the lesser vegetative growth of *gad1245* and *gad2OE* occurred mostly during submergence, while *pop2-8* did not grow during recovery. *gad1** also showed greater biomass increase than WT, which could possibly be correlated to the *GAD1* expression in this line (Fig A.1).

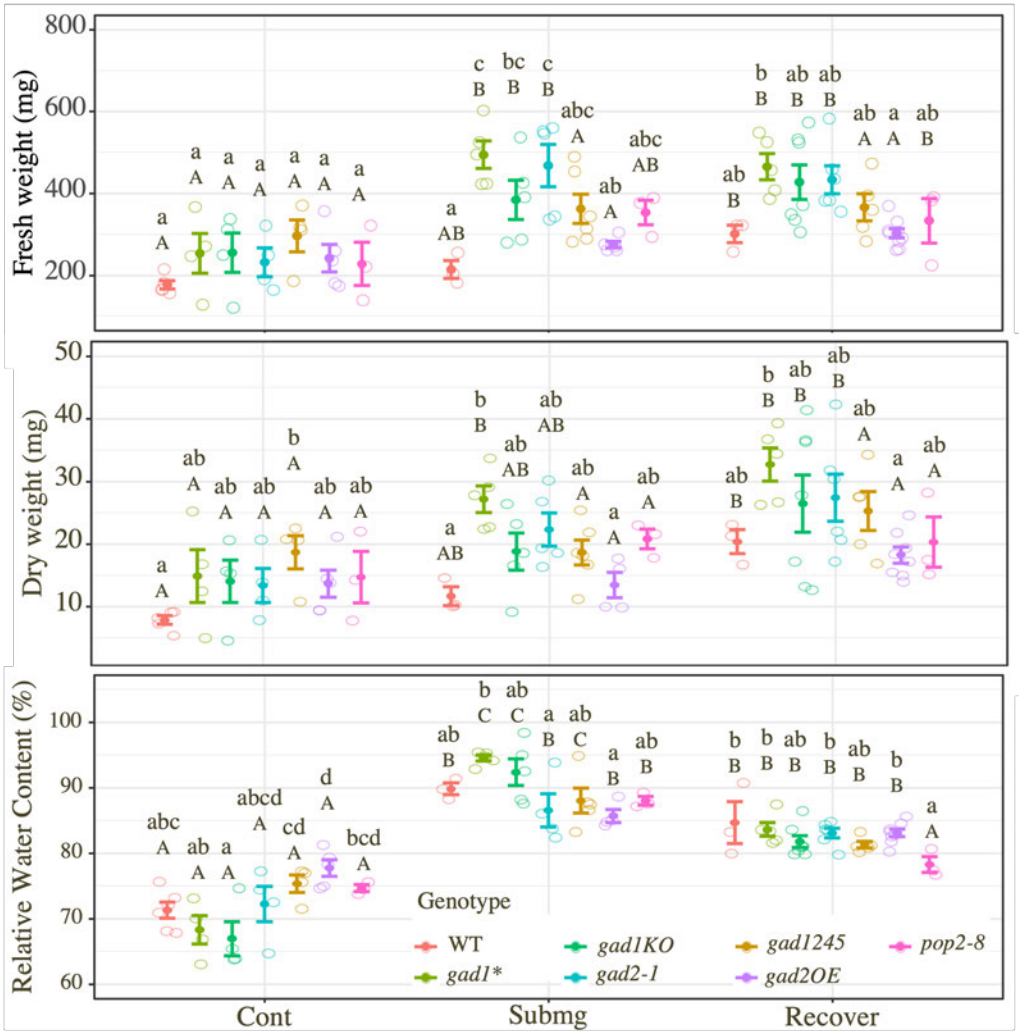


**Figure 3.2:** Rosette biomass and relative water content changes under control, submergence and recovery in WT and GABA mutants. Rosette fresh weight (a), dry weight (b) and relative water content (c) are the mean ± SE of at least 3 biological replicates. Different uppercase and lowercase letters represent statistically significant difference within treatments and genotypes, respectively (two-way ANOVA, *post hoc* Tukey, $p < 0.05$). For example, A, B and C indicates significance between treatments within one line, while a, b and c indicates significance between different lines in one treatment.

**Relative water content**. In terms of leaf water management, relative water content (RWC) reflects the balance between transpiration rate and water supply to the leaf tissue. Significant differences of RWC were observed between multiple lines under control conditions (Fig 3.2c); among them, the two *GAD1* lines shoot RWC (<69%) were significantly lower than *gad1245*, *gad2OE*. Although no dehydration or senescence symptoms were visible (Fig 3.1), the various RWC among GABA mutants suggested that a disturbed GABA shunt pathway already altered water loss under non-stressed conditions. Not surprisingly, subjecting to 6 d submergence greatly increased shoot RWC in all lines compared to there own control plants; in terms of percentage increase, the two *GAD1* lines, especially *gad1**, increased the most (38%) while *gad2OE* increased the least (10%). At the end of submergence, the *gad1** shoots had higher RWC (95%) than WT, *gad1245*

and *gad2OE* shoots (88%), which for the mutants was an opposite trend. Compared to submerged plants, 2 d recovery resulted in a significantly decreased mean shoot RWC in the two *GAD1* lines (12%), *gad1245* (8%) and *pop2-8* (11%). Among all recovered plants, *pop2-8* shoots had the lowest RWC (being significantly lower than *gad2OE*, *gad2-1*, *gad1** and WT, with all other lines maintained above 80% RWC in the leaves. At the end of recovery, all lines had increased shoot RWC compared to their pre-submergence control plants, except for *pop2-8* whose shoot RWC dropped to pre-submergence levels. In another independent experiment using the same hydroponic system as in Chapter 2 with no aeration of the growth solutions (thus imposing root submergence only), *pop2-8* RWC decreased the most after 9 d root submergence (Fig C.1). Note that the root submergence experiment was conducted in a different lab and under different growth conditions (10/14 rather than 14/10 day/night circles) underlining the robustness a higher water loss in *pop2-8* plants with the most disturbed GABA shunt efficiency due to lacking the activity of GABA-T.

**Fv/Fm**. Biomass gain and water management may be related to photosynthetic capacity, as reflected by Fv/Fm. Fig 3.3 showed that Fv/Fm across all lines were significantly decreased after submergence. Under submergence, compared to WT, *gad1** and *gad2-1* and *gad1245* had higher Fv/Fm, while Fv/Fm values in *gad1KO* the two GABA-accumulating lines *gad2OE* and *pop2-8* was the same as WT, indicated the former threee lines had the less photosystem II damage as WT. This observation indicates the involvement other GABA metabolism pathways in submerged plants in addition to the primary GABA-shunt pathway, as biosynthesis of GABA through the GABA-shunt is totally blocked in *gad1245*, yet photosystem II damage in this line was not as severe as in the two GABA-accumulating lines. Following returning to normal growth conditions for 2 d, only *gad1** showed a full recovery. On the contrary, *gad1245* Fv/Fm did not increase at all and *pop2-8* Fv/Fm significantly decreased compared to their own pre-recovery submerged plants. The rest of the lines were able to recover to some extent though could not maintain their before-stress Fv/Fm levels. These results revealed the importance of GABA metabolism (especially GABA catabolism) not only under submergence but also during recovery, and suggests it is catabolism rather than biosynthesis that seems to be playing an essential role for plants to cope with post-hypoxic stresses. Constitutive promoters, unlike native promoters, drive gene expression under all conditions and thus will lead to diversion of energy. This could partially explain why Fv/Fm of *gad2OE* decreased more than GABA-deficient lines upon submergence (energy already very limited), yet increased upon 2 recovery, while *gad1245* and *pop2-8* did not (blocked GABA biosynthesis and catabolism of GABA being more detrimental than constitutive promoter during post-hypoxic recovery).

Varied tolerance to submergence may be due to the submergence phase and/or the recovery phrase. It could be clearly seen that GABA mutants and WT had different rates of

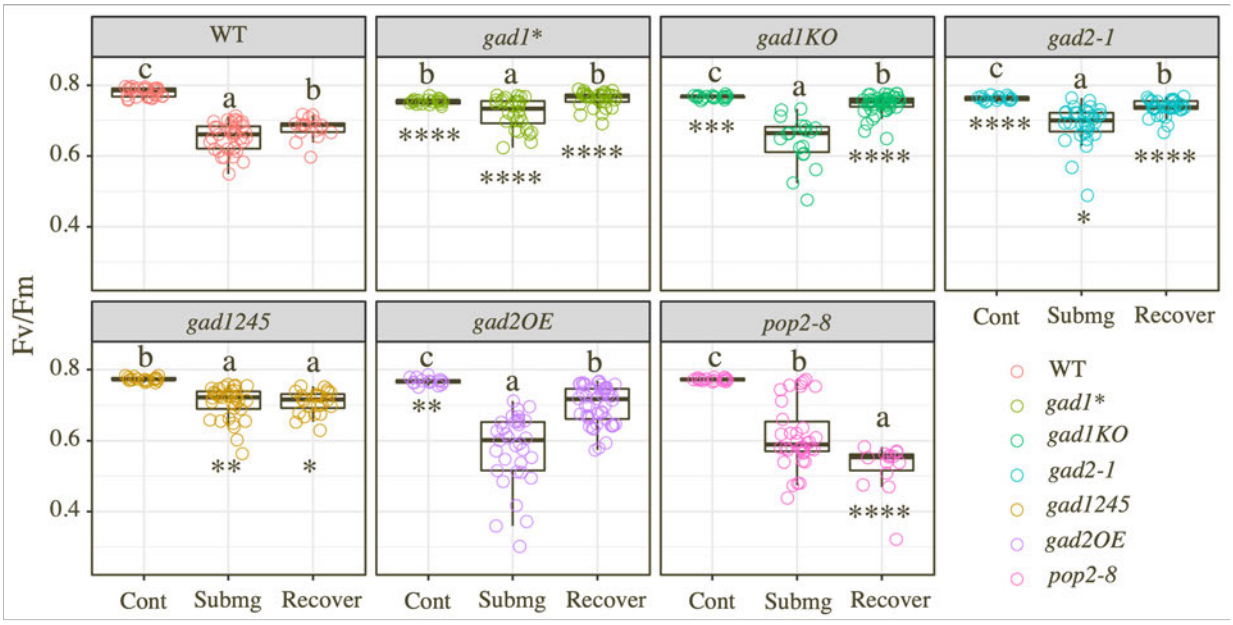


**Figure 3.3:** Quantum yield (Fv/Fm) changes under control, submergence and recover (2 §d desubmergence) in WT and GABA mutants. Fv/Fm are means ± SE of leaves from at least 3 biological replicates, specifically, WT (6,4,3), *gad1** (4,4,5), *gad1KO* (3,4,7), *gad2-1* (3,6,6), *gad1245* (4,6,5), *gad2OE* (3,6,9) and *pop2-8* (3,8,3) under control, submergence and recover. Letters indicate statistically significant differences between treatment in genotype and stars indicate statistically significant differences between WT and mutants in the same treatment (Brown-Forsythe and Welch one-way ANOVA tests, *Dunnett T3* adjusted $p < 0.05$). * $P < 0.05$. ** $P < 0.01$ *** $P < 0.001$. **** $P < 0.0001$.

vegetative growth and relative water content under control conditions and in response to submergence and recovery (Fig 3.2). The distinct pattern that *gad1** and *gad2-1* maintained i.e. relative higher biomass and greater vegetative growth under submergence and recovery period than *gad1245* and the GABA accumulating lines (*gad2OE* and *pop2-8*), suggests the latter were less tolerant to hypoxia and post-hypoxic stress, and experienced more severe energy crisis and oxidative stresses. This could be at least partially due to their more severely impaired photosynthetic capacity in *gad2OE* and *pop2-8* after 6 d submergence, as they both had the more reduced Fv/Fm than the other lines (Fig 3.3). On the contrary, Wu et al. (2021) recently reported otherwise that *pop2-5* maintained higher shoot fresh weight, chlorophyll content and Fv/Fmcompared to the *gad1,2* double mutant, therefore it was more tolerant to waterlogging (for 2 weeks). The inconsistent observation compared to what was observed here maybe due to using a different GABA-T line *pop2-5* (GABI_157D10) and/or the leaves were not submerged, both of which potentially could affect the phenotypes and underlying mechanisms.

Yeung et al. (2018) evaluated *Arabidopsis* wild type lines that were tolerant (Lp2-6) and sensitive (Bay-0) to submergence and reported that the difference in tolerance was mainly due to differences in the recovery phrase. After 5 d dark submergence, the two lines had similar shoot dry weight, relative water content and chlorophyll content; but after 5 d

recovery, Lp2-6 was able to maintain more chlorophyll and higher water than Bay-0 as well as to increase dry weight while Bay-0 could not. To eliminate the effects of darkness, they subjected both lines to dark treatment only, and saw leaf senescence without clear phenotypic differences, confirming the difference in survival was mainly determined by reaeration rather than submergence. In my research all plants were subjected to light submergence and therefore they had increased biomass (Fig 3.2) due to a partially functioning photosynthesis system (Fig 3.3). The shift from submergence (lower light) to recovery (higher light) leads to phototoxic damage to PSII. In rice, Fv/Fm can rapidly recover to their pre-submergence level after 2 h recovery, while during early recovery, a considerably decline of Fv/Fm was observed in rice, *Arabidopsis*, and three grass species (Alpuerto et al., 2015).

In another independent experiment I conducted, soil-grown plants were subjected to 5 d stress (either darkness or light submergence) and then returned to normal growth conditions for another 5 d. Darkness on its own did greater harm to GABA mutants than to WT plants, as some mutants displayed more leaf senescence than WT (Fig C.2a), with *gad2OE* being the most visible and therefore, more sensitive to energy crisis than other mutants (possible due to the constitutive promoter). Moreover, after 5 d recovery from darkness, *pop2-8* had significantly greater shoot fresh weight, and a higher but not significant shoot dry weight and RWC than *gad2OE*, meaning it could adapt better during post-darkness phrase (Fig C.2b, C.2c, C.2d). This suggests similar conditions may have been imposed by Wu et al. (2021).

Stomata are key regulators of gas exchange, e.g. $CO_2$ uptake and water loss during photosynthesis and transpiration, respectively; stomatal pores formed by pairs of guard cells in epidermis of plant shoots, and their movements can be regulated by abscisic acid and light (ichiro Shimazaki et al., 2007; Munemasa et al., 2015). Previously *gad2-1* has been reported to exhibit greater stomatal conductance and wider stomatal pores than wild-type plants (Xu et al., 2021) under non-stressed conditions. This could probably explain why *gad2-1* had a lower RWC than both WT and *pop2-8* after recovering from darkness (Fig C.2d), possibly due to a higher water loss. In the meantime, all dark-recovered plants were able to maintain higher fresh weight than submergence-recovered plants, but no differences could be seen in terms of dry weight or relative water content (Fig C.2), suggesting a higher water loss and a decreased turgid weight during post-submergence phase as common responses. Taken together, darkness effects could not be eliminated if the GABA mutants were submerged under dark conditions, and submergence under light in the current research makes perfect sense.

### 3.1.2 Transcriptomic differences between WT and GABA mutants

Prior to investigating the underlying molecular changes in GABA mutants that can be associated with responses to submergence, transcriptome analyses for all lines under control conditions were carried out first using RNA-seq to examine the main differences in their transcriptome profiles. So, in the following sub-section only control plants will be analysed and the submerged plants will not be included, starting with the multi-dimensional scaling (MDS) principal coordinate plot and identifying differential expressed genes (DEGs) in each of the GABA mutants compared to WT.

#### 3.1.2.1 Identification of differentially expressed genes in GABA mutants under control conditions

Biological replicated samples from the same genotype clustered together in the MDS principal coordinate plot (Fig C.3), although there was a large variation in one of the WT samples. Dimension 1 separates WT from GABA mutants, while dimension 2 roughly corresponds to different GABA mutants, so next the gene profiles of each GABA line compared to WT were analysed. After filtering the lowly expressed genes (i.e. genes with less than five counts in a quarter of all samples), there were in total 18,805 genes left across the 21 libraries, and their distribution were shown in Fig C.4. Compared to WT, in general there were more genes down-regulated in the mutants than up-regulated, and the up-regulated genes also had a smaller fold-change range than down-regulated genes (Fig C.4). Only genes that were up- or down- regulated with $|log2FC| > 1$ and Bonferroni adjusted $P$ value $adj.P < 0.05$ by pairwise comparisons in at least one mutant were regarded as differentially expressed genes (DEGs), and these genes were highlighted (Fig C.4).

Overall 3494 genes showed a significant changes in transcript abundance across all six mutant lines. Specifically, *gad1** had the least (915) while *pop2-8* had the greatest (2133) number of DEGs compared to WT. UpSet plotting (Fig 3.4) and hierarchical clustering (Fig 3.5) were performed to visualise the expression profiles/patterns of these DEGs in GABA mutants. 753, 282 and 260 DEGs uniquely showed up in *pop2-8*, *gad1245* and *gad2-1*, respectively, while the other three *GAD* lines had less than 100 exclusive DEGs (Fig 3.4). Collectively, nearly half (43.1%, 1506 genes) of the total 3494 DEGs were uniquely regulated in GABA mutants. In correspondence with Fig 3.4, *pop2-8*, *gad1245* and *gad2-1* had the largest number of exclusively up-/down- regulated genes as well (Fig 3.5a). There were also 469 DEGs (13.4%) shared across all six GABA mutants, leaving the rest 1519 DEGs (43.5%) shared between 2 $\sim$ 5 mutants (Fig 3.4). Most shared DEGs were in the same regulated direction (Fig 3.5a), and only 67 genes had opposite expression patterns (Fig 3.5b): up-regulated in one or more lines but down-regulated in the other

line(s). Among them, 42, 32 and 59 appeared in *gad2-1*, *gad1245* and *pop2-8*, while only 5, 14, and 5 appeared in *gad1**, *gad1KO* and *gad2OE*, respectively (Fig 3.6). In most cases it was *pop2-8* DEGs that had an opposite expression pattern compared to GABA-deficient lines (mainly *gad2-1* and *gad1245*), so these genes can be divided into three classes: Class I (21 down-regulated), Class II (38 up-regulated) and Class III (8 not-affected) in *pop2-8*, respectively. A further investigation showed that only 42 out of these 67 genes directly relate to one or more GO terms (shortest path > 4), and a full list of these terms was shown in Table C.2.

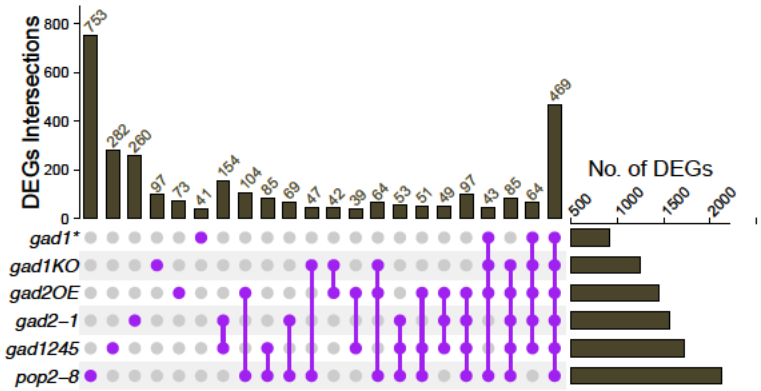


**Figure 3.4:** UpSet plot of intersected differentially expressed genes (DEGs) in GABA mutants compared to WT under control conditions. The number of DEGs in each mutant and overlapping DEGs across different mutants are shown in the bottom right bar chart and top bar chart, respectively. The dot matrix at the bottom left indicates the respective overlaps by connected purple circles. For example, *pop2-8* had the highest number of uniquely-regulated genes (753 DEGs), while 469 DEGs were shared among all six GABA mutants. Only overlaps with more than 30 DEGs were presented here.

**Class I oppositely regulated DEGs in non-stressed GABA mutants**. These are mainly light-, stress- and hormone-related genes which are repressed in *pop2-8* but induced mostly in *gad2-1* and *gad1245*. Proteins encoded by these genes are as follows. Response to auxin, light stimulus and osmotic/oxidative stress: auxin-responsive protein (IAA5), long hypocotyl in far-red 1 (HFR1). Hormone signalling and metabolism such as abscisic acid (ABA) and brassinosteroid (BR) signalling: B-box zinc finger protein 29 (BBX29). Auxin homeostasis/methylation: Indole-3-acetate O-methyltransferase 1 (IAMT1). Ammonium transmembrane transport, transcription regulation and lipid hydrolysis: ammonium transporter 1 member 2 (AMT1;2), dehydration-responsive element-binding protein 1A (DREB1A).

HFR1, a light-inducible nuclear basic helix-loop-helix (bHLH) protein, and LONG AFTER FAR-RED LIGHT1 (LAF1) are the two well-characterised transcriptional activators of the phytochrome A (phyA) signalling network; FAR-RED ELONGATED HYPOCOTYL 1 (FHY1) and FHY1-LIKE (FHL) are required to assemble photoreceptor/transcription fac-

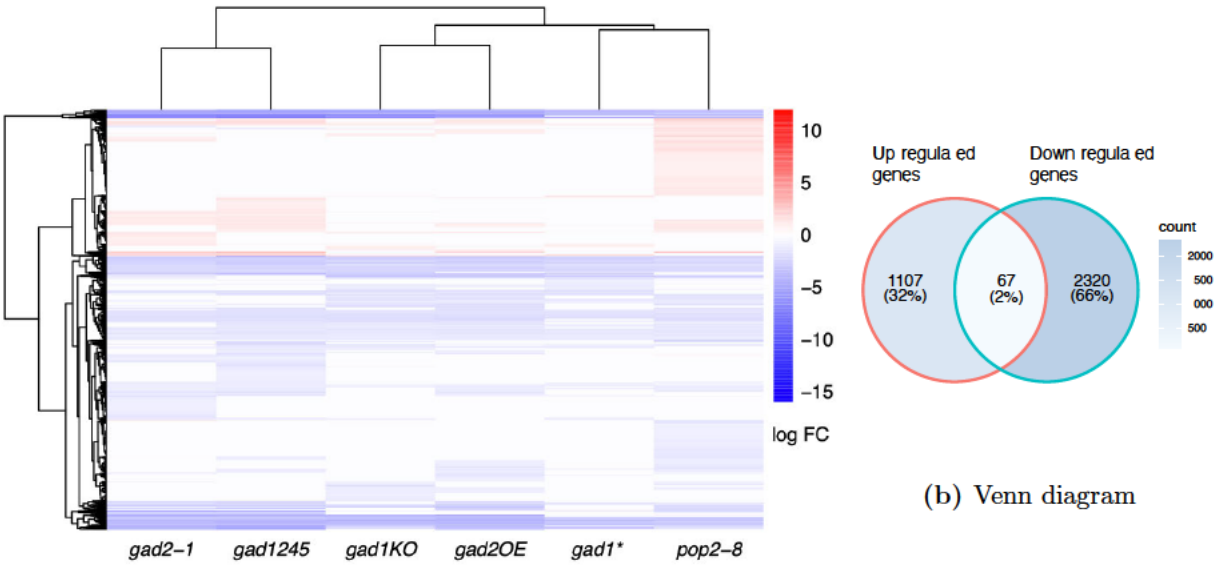


(a) Expression pattern of DEGs

(b) Venn diagram

**Figure 3.5:** Differentially expressed genes (DEGs) in GABA mutants compared to WT under control conditions. (a): Hierarchical clustering of log2 fold change. The fold change in each mutant was normalised against WT. (b): Venn diagram of DEGs number/proportion.

tor complexes for phyA signalling, and their downstream phyA signals were independently transmitted by HFR1 and LAF1 (Chen et al., 2012). In addition, HFR1 competitively participates in the regulation of light- and high temperature-promoted cell elongation with other transcription activators such as phytochrome interacting factor 4 (PIF4) and Phytochrome Rapidly Regulated 1 (PAR1), and *Arabidopsis* HFR1 also bridges circadian rhythm and flower development (Ikeda et al., 2021; Duren et al., 2019). B-box zinc finger proteins (BBXs) are photomorphogenic repressors which integrate light and hormonal signals to regulate plant growth and development, and both BBX28 and BBX29 play pivotal roles in ensuring normal development by positively regulating BR signalling in *Arabidopsis* seedlings (Cao et al., 2022). DREB1A directly interacts with the promoter of *Arabidopsis* trehalose-6-phosphate phosphatase (TPP) family genes and activate TPP transcription under drought stress (Lin et al., 2019).

**Class II oppositely regulated DEGs in non-stressed GABA mutants.** In addition to *pop2-8*, four of the Class II genes were also induced in *gad1245* (even *gad2-1* in the case of dormancy-associated protein 2, DRM2), but repressed in *gad1KO*. DRM1 is often used as a genetic marker (Rae et al., 2013) in dormant meristematic tissues, and DRMs gene family play a wider role beyond dormancy maintenance in these tissues. AtDRM1 has six splice isoforms while AtDRM2 has two, most of which are dark, stress (high/low temperature, wounding, salinity), hormone (GA, ABA, SA) and sugars (fructose, glucose and sucrose) induced or repressed (Rae et al., 2014; Gonzali et al., 2006). Rare cold inducible 2 (RCI2s) are induced by low temperatures, drought, salinity and ABA in plants and are involved in defense against major abiotic stresses (Kim et al., 2021).

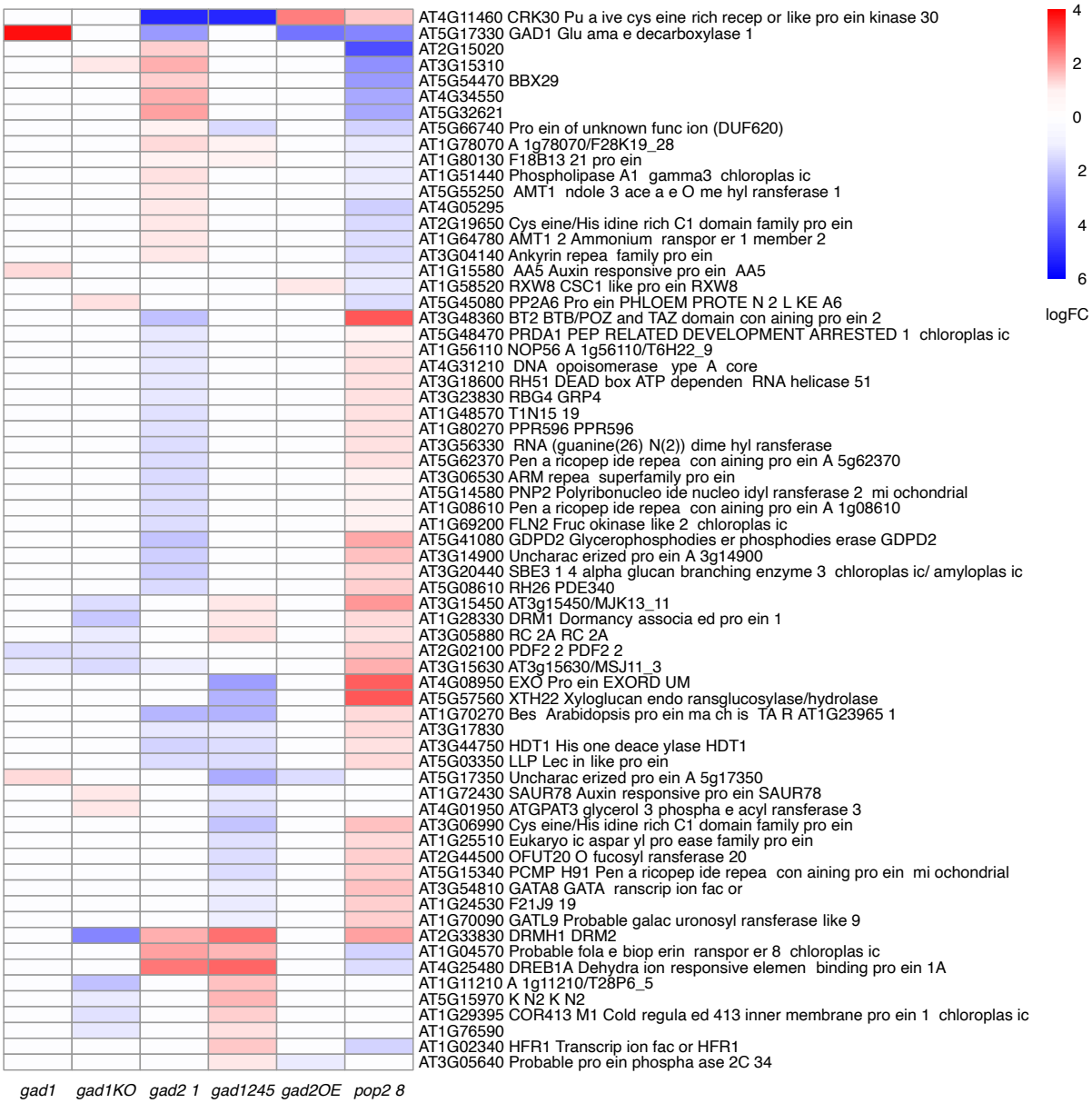


**Figure 3.6:** Log2 fold change of oppositely regulated DEGs in GABA mutants under control conditions. The fold change in mutants was normalised against WT.

The other Class II genes (induced in *pop2-8* and mainly repressed in *gad2-1* and/or *gad1245*) encode proteins that are mainly involved in the following processes. Chloroplast development: Fructokinase-like 2 (FLN2) and PEP-related development arrested 1 PRDA1). Response to stress, nitrogen, hormone (e.g. BR), pathogen attack and plant cell death: Cysteine-rich Receptor-like protein Kinase 30 (CRK30), EXORDIUM (EXO), BTB and TAZ domain protein 2 (BT2). Transcriptionally active chromosomes (TACs) are plastid-encoded RNA polymerases (PEP) associated proteins/DNA-complex (Pfalz et al., 2005). Thioredoxin z (TRX z) interacts with FLN1 and FLN2, two of the TAC components, to regulate the PEP-dependent genes transcription and chloroplast development (Arsova et al., 2010). *fln2-4* mutant had albino phenotype which can be alleviated by adding sucrose to the media (Huang et al., 2015). CPK30 belongs to a family of

plant Receptor-like protein kinases (RLKs) that contains cycterine-rich repeats at their extracellular domains, thus called Cysteine-rich Receptor-like Kinases (CRKs); RLKs regulate developmental processes and biotic/abiotic responses, and CRKs are suggested to be important in regulating pathogen defense and programmed cell death (Wrzaczek et al., 2010). BT2 regulates responses to various hormones, stress and metabolic conditions in *Arabidopsis thaliana*, and loss of BT2 causes hypersensitivity and decreased germination rate in response to sugar, ABA and $H_2O_2$; BT2-mediated responses to sugars and hormones were regulated by Global Transcription factor Group E proteins (GTE), GTE9 and GTE11 (Misra et al., 2018). The direct transcriptional activation of *BT2* by nodule inception-like protein (NLP) TFs also plays a key role in *Arabidopsis* nitrate response (Sato et al., 2017). EXO is localised to the cell wall and identified as a potential mediator of BR-promoted growth though cell expansion. In *Arabidopsis* this gene family has eight members, and over-expression of EXO promotes plant growth (shoot and root), presumably due to BR-responsive environmental or developmental signalling network (Schröder et al., 2009).

**Class III oppositely regulated DEGs in non-stressed GABA mutants**. These genes were mainly oppositely regulated between *gad1245* and the two *GAD1* lines and they are stress/hormone inducible. For example, the expression of Cold-regulated 413 inner membrane protein 1 (COR413IM1) and cold-responsive 6.6 (COR6.6/KIN2) are both induced by cold and ABA treatment, and they are also involved in salt tolerance.

Taken together, the inconsistently altered abundance of the above transcripts in *pop2-8*, *gad1245*, *gad2-1* and two GAD1 lines probably suggested that, under normal growth conditions, these GABA mutants had different transcriptional changes which would potentially be more/less beneficial to the upcoming submergence.

**Expression of core HRGs in GABA mutants under control conditions**. Core hypoxia-responsive genes (Table A.1) have been reported to be ubiquitously and rapidly activated and translated upon hypoxia stress (Mustroph et al., 2009). Surprisingly 15 HRGs showed up as differentially expressed in the GABA mutants even when non-stressed: seven down-regulated in one or more mutants and eight up-regulated uniquely in only one mutant (Fig 3.7). ADH and PDC are the two main enzymes involved in fermentative pathway. Compared to WT, *ADH1* had a lower expression in all mutants while *PDC1* was only down-regulated in *gad2-1*. Using the enzyme sucrose synthase (SUS) to breakdown sucrose usually happened during hypoxia as a target to save ATP usage, however, one of the *SUS* genes, *SUS4* is already up-regulated in *gad2-1* under normoxic condition. The phyA signalling related FHL (mentioned above) was also up-regulated in *gad1245*. LOB domain-containing protein 41 (LBD41) is a transcription repressor, and hypoxia dramatically induces its transcript level (Mustroph et al., 2009). *LBD41* transcripts were lower in the two *GAD1* mutants. For genes encoding Hypoixa Unkown Proteins (HUPs),

*HUP54* had lower expression in *gad1KO*, *gad2OE* and *pop2-8*, but *HUP39* expression was induced in *gad2-1*.

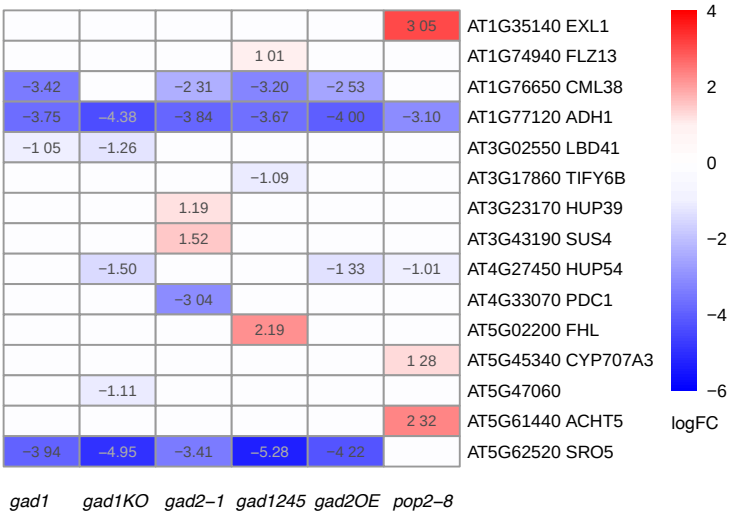


**Figure 3.7:** Log2 fold change of core hypoxia-responsive genes in GABA mutants under control conditions. The fold change in mutants was normalised against WT.

Calmodulin-like 38 (CML38), a calcium sensor in plants, had lower transcripts in four mutants (not *gad1KO* and *pop2-8*). Recent studies have shown that *Arabidopsis* CML38 is involved in root growth inhibition (Campos et al., 2018) and hypoxia-induced autophagy (Field et al., 2021). *Arabidopsis* rapid alkalinization factor 1 (AtRALF1) is a small secreted peptide hormone which inhibits root growth; CML38 (also a secreted protein) can physically bind and interact with AtRALF1 in a $Ca^{2+}$- and pH-dependent manner; CML38 has no role in AtRALF1 alkalinization, but it is essential for the AtRALF1 overexpression induced semi-dwarf phenotype (Campos et al., 2018). To deal with energy crisis during submergence, mRNA translation was restricted by plants and stress granules were rapidly accumulated, acting as storage hubs for the arrested mRNA complexes; identified as one of the proteins associated with hypoxia-induced granules, CML38 uses them as its direct regulatory targets, and CML38 associated- regulation of autophagy was suggested to be part of the RNA regulatory program during hypoxia (Field et al., 2021).

*SRO5* encodes a protein with similarity to RCD1, thus called similar to RCD5 (SRO5), and its mRNA was lower in five mutants (not *pop2-8*). Radical-induced cell death 1 (RCD1) belongs to WWE protein-protein interaction domain protein family and the (ADP-ribosyl)transferase domain-containing subfamily; RCD1 could act as an integrative node between hormonal signalling (modulating ABA, ET and JA responses) and the regulation of several stress-responsive genes (*RAB18, DREB2A*), therefore it functions in drought response; the WWE domain presents in SRO1 but was missing in SRO2 and SRO5 proteins (Ahlfors et al., 2004). An intermediate in proline biosynthesis and catabolism, Δ-1-pyrroline-5-carboxylate (P5C), together with proline metabolism, plays a key role in

stress response and ROS accumulation, and it can be reduced to glutamate (the precursor of GABA) by P5C dehydrogenase P5CDH. *SRO5* and *P5CDH* are natural *cis*-antisense gene pairs that generate both 24-nt and 21-nt siRNAs, which are named nat-siRNAs as they are derived from natural transcripts (Borsani et al., 2005). Salinity induced *SRO5* expression initiates the formation of *SRO5-P5CDH* na-siRNAs; the na-siRNAs down-regulates *P5CDH* expression through mRNA cleavage, thus leading to not only proline accumulation which is important to salt tolerance, but also increased ROS production which is normally counteracted by the SRO protein; therefore, the *SRO5-P5CDH* nat-siRNAs together with their proteins formed key components of a regulatory loop that controls ROS production and stress response (Borsani et al., 2005). The changes of *SRO5* expression in GABA mutants may be a result of altered ROS-scavenging capacity.

*Exodium-Like 1* (*EXL1*) is a brassinosteroid-regulated gene whose expression is induced under carbon- and energy-limiting conditions, e.g. sugar starvation, extended night and anoxia stress, and EXL1 protein is also required for adaptation to energy crisis and the loss (Schröder et al., 2011). Only *pop2-8* showed a strongly induced *EXL1* expression in this study, possibly because blocked GABA catabolism greatly disturbed the carbon pool 3.7. Moreover, *gad1245* showed induced and repressed expression of two genes encoding light and jasmonate (JA) related proteins, FHL as mentioned above and TIFY6B which is also known as Jasmonate ZIM-domain 3 (JAZ3), respectively. JA plays important roles in regulating plant defence and development: JA promotes JAZ proteins degradation to relieve their repression on diverse TFs that regulate early JA-responsive genes, and the JAZ-MYC transcriptional module regulates growth-defence balance in plants (Major et al., 2017).

All together, the altered expression of HRGs in mutants suggested that disturbed GABA shunt already affected hormone- and stress/stimuli-responsive genes under normal growth conditions. This could possibly be beneficial for plants during the following submergence if these mRNAs play a role in pre-priming in the mutants.

#### 3.1.2.2 GO enrichment analysis of GABA mutants under control conditions

To gain insight into the biological processes affected in GABA mutants under non-stressed conditions, DEGs in each mutant were split into up- and down- regulated genes, went through separate Gene Ontology (GO) enrichment analyses, and over-represented functional categories (GO terms) were identified (Fig 3.8). Hereafter in this chapter, 'GO-Up' and 'GO-Down' referred to enriched GO terms of up- and down-regulated genes, respectively. The total 160 GO terms could be divided into six groups based on their enrichment patterns between different mutants, as summarised in Table C.3. Group I: appeared in both GO-Up and GO-Down. Group II: partially shared among mutants in GO-Up. Group

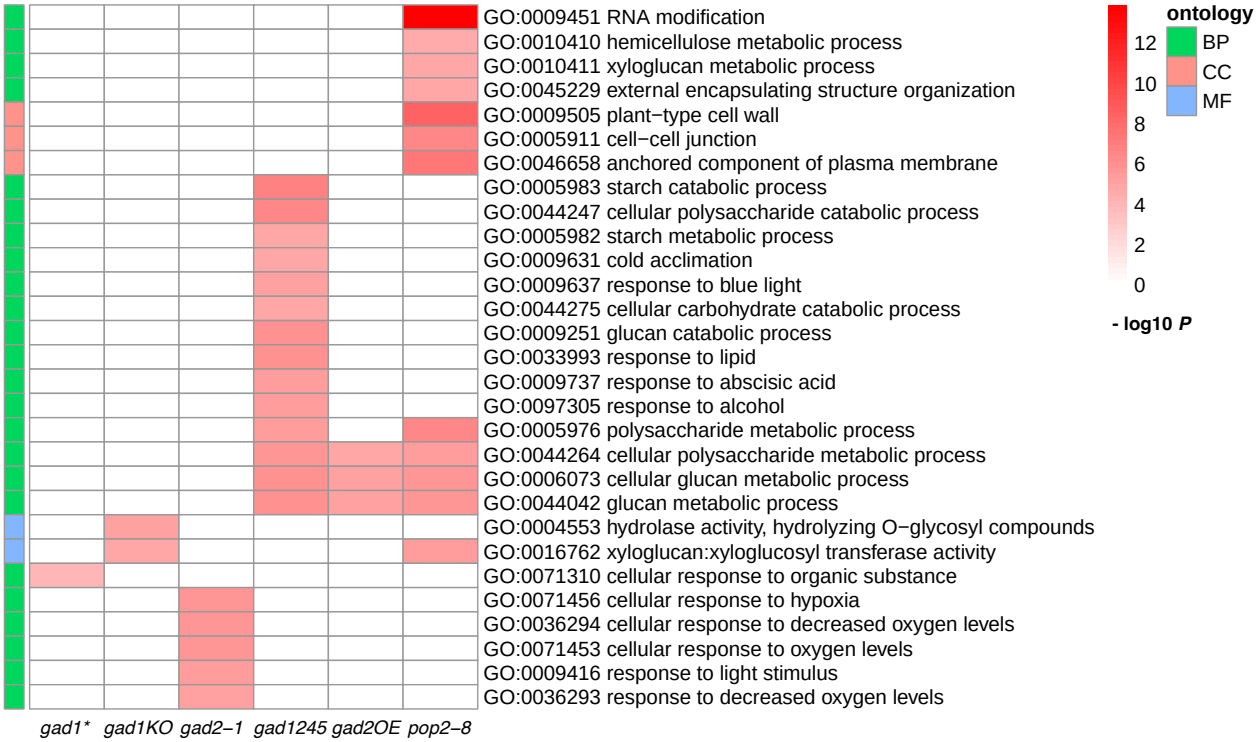


**(a)** Up-regulated genes enriched 29 GO terms

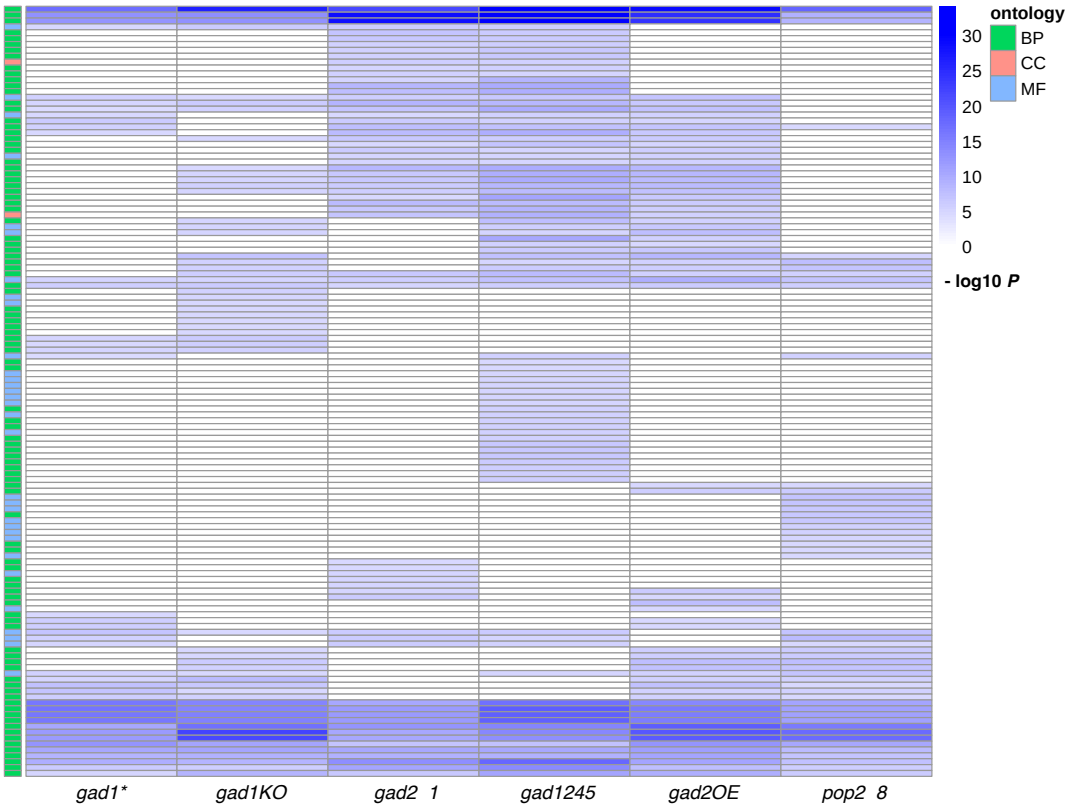


**(b)** Down-regulated genes enriched 131 GO terms

**Figure 3.8:** GO enrichment analysis of up- and down-regulated DEGs in GABA mutants under control conditions. The clustered enrichment pattern displayed the -log 10 $P$ value. All coloured cells were significantly enriched ($adj.P < 0.05$). (a) 29 terms enriched by up-regulated genes. (b) 131 terms enriched by down-regulated genes.

III: exclusive in GO-Up (except those in Group I). Group IV: shared across all mutants in GO-Down (except those in Group I). Group V: partially shared among mutants in GO-Down. Group VI: exclusive in GO-Down.

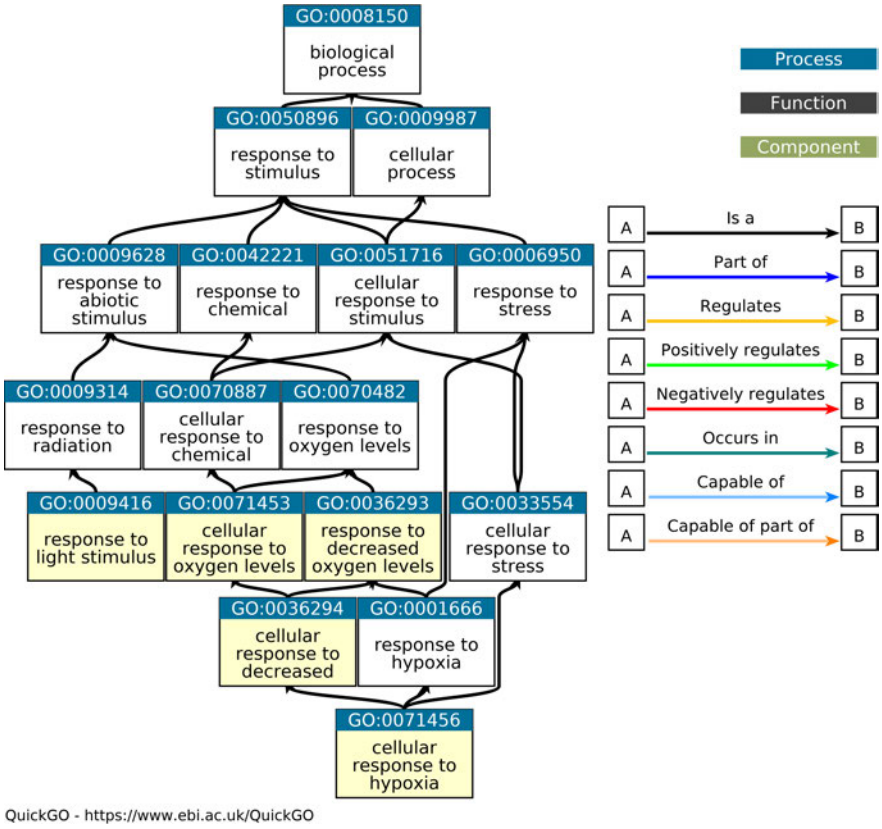


**Figure 3.9:** GO terms exclusive enriched in *gad2-1* up-regulated genes under control conditions, including the four oxygen/hypoxia-related processes in Group I category 'A', i.e. response to decreased oxygen levels (GO:0036293), cellular response to oxygen levels (GO:0071453) and decreased oxygen levels (GO:0036294), cellular response to hypoxia (GO:0071456).

**Group I: Nine terms in both GO-Up and GO-down but with distinctive patterns among GABA mutants**. These terms can be divided into 4 categories ('A', 'B', 'C', and 'D'), and DEGs involved in each category were also examined (Fig 3.10). Seven terms were shared across all mutants in GO-Down. Among them, in GO-Up, the four terms related to (cellular) response to (decreased) oxygen levels and hypoxia ('A') were specific to *gad2-1*, while the other three (response to alcohol, ABA and lipid, 'B') specific to *gad1245* (Fig 3.8a, 3.9, C.8a), indicating a more profound response in *gad2-1* and *gad1245* than the other mutants. *gad1245* up-regulated and *gad1KO* down-regulated genes both significantly affected cold acclimation ('C'), while *gad1** up-regulated and all the other mutants' (except for *gad1KO*) down-regulated genes had significant cellular response to organic substance ('D'). Overall, 487 DEGs were involved and nearly one third (159) belong to two or three categories, e.g. 134 overlapped genes between 'B' and 'D' but none between 'C' and 'D' (Fig 3.10a, Table C.1). Twenty-five shared DEGs were listed in Fig 3.10b, including transcription factors (TFs) that regulate osmotic, heat and drought response (*WRKY46*, *HSFA2*, *NAC002*), genes involved in cell wall modification (*XYH22*),

(a) Venn diagram

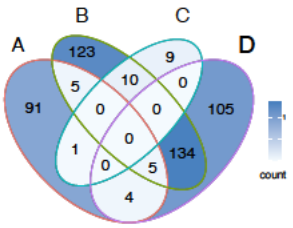


(b) 25 shared DEGs

| Gene Info | Venn |
|---|---|
| AT1G27730: ZAT10: Zinc finger protein ZAT10<br>AT1G77120: ADH1: Alcohol dehydrogenase class-P<br>AT2G33590: CRL1<br>AT4G20860: FAD-OXR: Berberine bridge enzyme-like 22<br>AT5G57560: XTH22: Xyloglucan endotransglucosylase/hydrolase | A, B |
| AT5G59820: ZAT12: Zinc finger protein ZAT12 | A, C |
| AT1G53910: RAP2-12: Ethylene-responsive transcription factor<br>AT1G72430: SAUR78: Auxin-responsive protein SAUR78<br>AT2G26150: HSFA2: Heat stress transcription factor A-2<br>AT5G13320: PBS3: Auxin-responsive GH3 family protein | A, D |
| AT1G20440: COR47: RD17<br>AT1G20450: ERD10: Dehydrin ERD10<br>AT1G29395: COR413IM1: Cold-regulated 413 inner membrane protein 1<br>AT2G42530: COR15B: Protein COLD-REGULATED 15B, chloroplastic<br>AT2G42540: COR15A: Protein COLD-REGULATED 15A, chloroplastic<br>AT3G50970: XERO2: Dehydrin Xero 2<br>AT3G50980: XERO1: Dehydrin Xero 1<br>AT4G15910: ATDI21: DI21<br>AT5G15960: KIN1: Stress-induced protein KIN1<br>AT5G66400: RAB18: RAB18 | B, C |
| AT1G01720: NAC002: NAC domain-containing protein 2<br>AT2G01150: RHA2B: RING-H2 finger protein 2B<br>AT2G46400: WRKY46: Probable WRKY transcription factor 46<br>AT3G15210: ERF4: Ethylene-responsive transcription factor 4<br>AT3G24500: MBF1C: MBF1C | A, B, D |

**Figure 3.10:** Group I GO terms related DEGs in GABA mutants under control conditions. (a) Venn diagram of DEGs involved in each category. Four GO terms in response to oxygen and hypoxia ('A'). Three GO terms in response to ABA, lipid and alcohol ('B'). Cold acclimation (GO:0009631, 'C'). Cellular response to organic substance (GO:0071310, 'D'). (b) List of 25 shared DEGs.

hormones (auxin, ABA, ethylene and gibberellin) and abiotic stress (osmotic, salinity, cold, dehydration) . For example, WRKY46 modulates *Arabidopsis* lateral root development under osmotic/salt stress, via regulating ABA signalling and auxin homeostasis (Ding et al., 2015). *WRKY 46* also functions as a transcriptional repressor of *aluminum-activated malate transporter 1 (ALMT1)* and confers higher Al resistance, as mutation of *WRKY46* increased malate secretion and reduced Al accumulation in *Arabidopsis* root apices (Ding et al., 2013). The expression of the 106 category 'A' genes in control mutants were shown in Fig C.10, including most of the 15 core HRGs (Fig 3.7), genes involved in oxygen sensing and regulation such as Group VII of Ethylene Responsive TFs (*RAP2.12*) and *LBD41*, heat-inducible TFs heat shock factor A2 (*HSFA2*). Heat and anoxia tolerance share considerable molecular mechanisms, in which HSFA2 is an important player and enhances anoxia tolerance in *Arabidopsis* (Banti et al., 2010). In this study, *HSFA2* expression was repressed in all non-stressed GABA mutants except for the two *GAD1* lines, in contrast to *RAP2.12* and *LBD41* was repressed in the two *GAD1* lines, respectively (Fig C.10). These largely induced/repressed oxygen- and stress-related genes could potentially mean that, in response to GABA deficiency/over-accumulating in plants, the mutants had already

experienced some stresses (likely low oxygen and co-occurred stresses), or had primed themselves to cope with stresses yet to come.

**Group II: Five partially shared terms in GO-Up**. These terms were shared between *pop2-8* and one or two other lines (Fig 3.8a, Table C.3) and can be divided into two categories: XTH activity (Fig C.9a, '2A'); polysaccharide metabolic, starch metabolic/catabolic and glucan/carbohydrate catabolic processes (Fig C.9c, '2B'). Xyloglucan is a hemicellulose that occurs in the primary cell wall of vascular plants and plays an important structural role. *XTH22* encodes a cell wall-modifying enzyme that is rapidly up-regulated in response to environmental stimuli and light (Sasidharan et al., 2010), and possibly contributes to petiole elongation during shade avoidance under flooding.

**Group III: Fifteen exclusive terms in GO-Up**. Among the 22 GO terms uniquely enriched in the mutants by up-regulated genes (Fig 3.8a), seven has been previously discussed in Group I, leaving the other 15 terms in this group and can be divided into seven categories (Table C.3). For example, hydrolase activity (GO:0004553) in *gad1KO*, response to light stimulus (GO:0009416) in *gad2-1* (Fig 3.9), and response to blue light (GO:0009637) in *gad1245* (Fig C.8a). In addition, *gad1245* up-regulated genes were also enriched in processes such as cellular carbohydrate/polysaccharide catabolic, starch metabolic, and glucan/starch catabolic (Fig C.8b). In *pop2-8*, however, processes such as RNA modification, hemicellulose and xyloglucan metabolism (Fig C.9c, C.11) were promoted and they mainly they mainly correspond to cell wall-related processes (Fig C.9b).

**Group IV, V and VI: Common or partially shared or exclusively terms in GO-Down**. Despite of the seven terms relating to oxygen, lipid, ABA and alcohol in Group I, another 11 down-regulated genes enriched processes were also shared among all six GABA mutants (Table C.3, Group IV). They mainly included: responses to salt stress, jasmonic acid, fatty acid and oxygen-containing compound ('4A'); leaf senescence ('4B'); monocarboxylic and organic acid catabolic, oxoacid and carboxylic acid metabolic ('4C'); lavin adenine dinucleotide binding ('4D'). Another 65 GO terms in GO-Down were shared between two to five mutants and all the rest of the terms were enriched uniquely in each mutant (Table C.3, Group V and VI). Although leaf senescence (GO:1900055) were significantly affected in all GABA mutants, its two child terms, regulation (GO:1900055) and positive regulation (GO:1900057) of leaf senescence were not enriched in *gad2-1* and *gad1245*. In addition, response to nutrient levels (GO:0031667) and chlorophyll catabolic process (GO:0015996) were also impacted in all mutants except for *gad2-1* and *gad1245* in which they were not enriched. This may suggest these two lines were less likely experiencing energy crisis under normal growth conditions than the other mutants. As for the uniquely enriched GO terms, *gad1245* and *pop2-8*, the two lines most disturbed in GABA shunt, i.e. had the greatest number (21 and 11, respectively).

### 3.1.2.3 KEGG pathway analysis of WT and GABA mutants under control conditions

The Kyoto Encyclopaedia of Genes and Genomes (KEGG) database can be used to detect whether a set of genes are over-represented (i.e. enriched) in pre-defined pathways. DEGs in each mutant went through KEGG pathway analyses, resulting in 39 enriched pathways (Fig 3.11) with distinct patterns as summarised in Table C.4. These pathways can be explored in more detail and DEGs related in each of the GABA mutant can be highlighted in the corresponding pathway maps, in order to visualise affected biological processes and illustrate the differences between these mutants under non-stressed conditions.

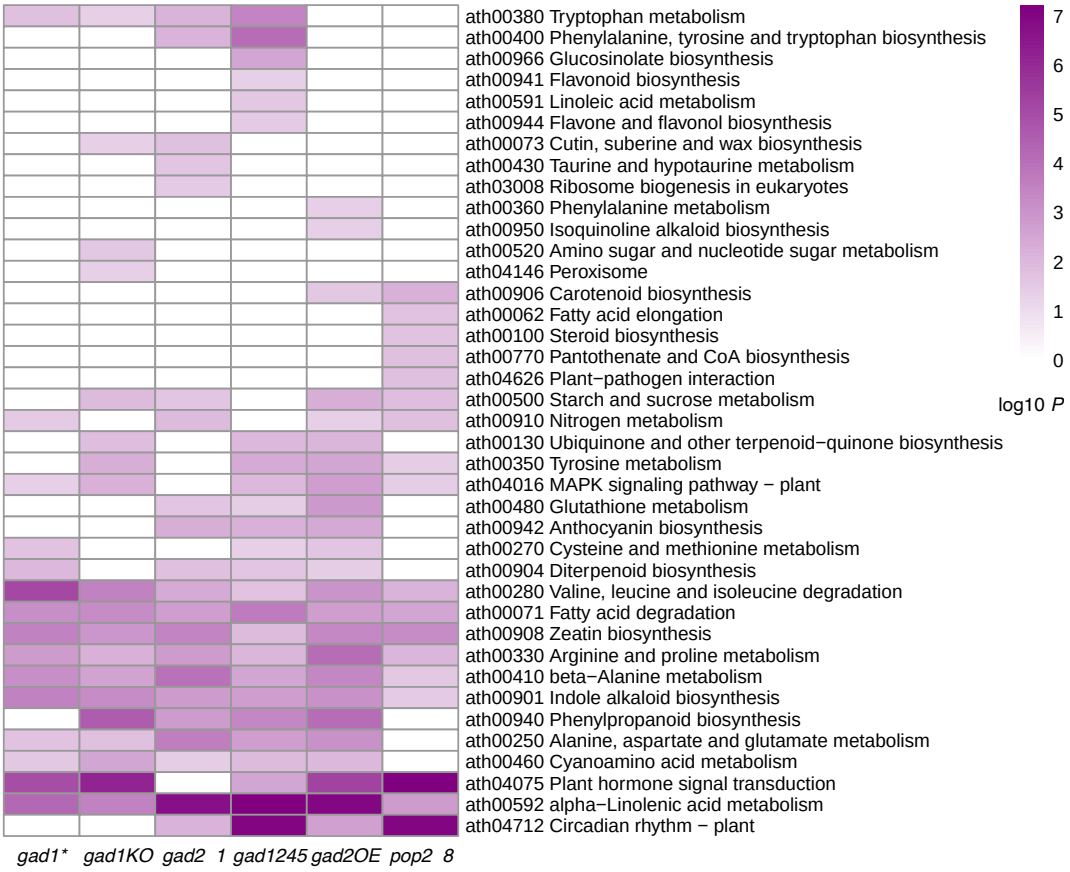


**Figure 3.11:** KEGG pathway analysis of WT and GABA mutants under control conditions. The clustered enrichment pattern displayed the -log 10 $P$ value. All coloured cells represented significantly enriched pathways with bonferroni adjusted $P < 0.05$.

Although the GABA-shunt efficiency was affected in different ways, there are some pathways that all or some of the mutants has as significantly affected, mainly metabolic processes. Seven enriched pathways were shared across all six mutants: metabolism of lipid (fatty acid degradation), amino acids (valine, leucine and isoleucine degradation), terpenoids and polyketides (alpha-linolenic acid metabolism) as well as biosynthesis of secondary metabolites such as zeatin. Another eighteen (15 were metabolic) pathways were partially enriched in two to five GABA mutants (Fig 3.11), and *pop2-8* contained only four metabolic pathways: tyrosine metabolism, carotenoid biosynthesis, nitrogen metabolism,

and starch and sucrose metabolism. Neither 'Cutin, suberine and wax biosynthesis' nor 'Starch and sucrose metabolism' was enriched in *gad1245* but both pathways were enriched in its two parent lines *gad1KO* and *gad2-1*. On the contrary, 'Cysteine and methionine metabolism' was significantly affected in *gad1245* but neither of its parent lines. Except for *gad1**, all other GABA mutants also had uniquely over-represented pathways. *gad1245* and *pop2-8* each contained four and the other three mutants each contained six pathways (Fig 3.11, Tab C.4), suggesting differences between GABA mutants due to different mutation(s).

**MAPK signalling pathway and hormone signal transduction**. Interestingly, these two signalling pathways were not enriched in *gad2-1* but all other GABA mutants, and *pop2-8* contained the largest number of DEGs (50). This suggested significant differences between *gad2-1* and the rest of the GABA mutants in these two signal transduction processes under control conditions, so pathway maps were generated (Fig C.12, C.13). Most DEGs related to MAPK and hormone signalling were repressed in GABA mutants, and some of the DEGs appeared in both pathways. There were only four exceptions in terms of MAPK signalling: genes encoding *mitogen-activated protein kinase 10 (MAPK10)* and three ABA receptors *(PYL4/5/6)* were induced in *pop2-8* leaves. *PYL4* and *PYL6* were also induced in *gad2OE*, but *PYL2* was repressed in *gad1245* leaves. In terms of hormone signalling transduction, in addition to the above genes, there were additional induced genes, e.g. those involved in ABA and auxin responses: ABA element-binding factor (ABF) and Auxin-responsive proteins (IAAs). *ABF1* was up-regulated in *gad2-1* and *gad245*, but *ABF3* was down-regulated in *gad2OE* and *pop2-8*. *IAA5* was mentioned earlier in this chapter as oppositely regulated genes (induced in *gad1** and repressed in *pop2-8*, Fig 3.6). Moreover, *IAA6* and *IAA19* were also induced in *gad1**, and the latter was also induced in *gad2-1*. Glucosinolates (GLSs) are secondary metabolites which protect plants from herbivory and pathogen attack. IAA5, IAA6 and IAA19 mediate *Arabidopsis* drought tolerance by regulating GLSs levels, probably signalling through ROS; in contrast, loss of IAA5/6/19 results in reduced GLSs levels and drought sensitivity which is associated with a defect in stomatal regulation (Salehin et al., 2019). Taken together, the altered hormone and MAPK signalling and sensitivity under control conditions maybe related to their response to submergence and recovery.

A recent whole genome sequencing revealed the existence of a second mutation in the *gad2-1* line used in this study (Piechatzek, 2022), as confirmed here there is no *MPK12* transcripts in its leaves (Fig C.14), while all other lines had significantly higher expression. The *Arabidopsis* MPK12 is not only a physiological substrate of indole-3-butric acid-response 5 (IBR5) but also a novel negative regulator of auxin signalling (Lee et al., 2009). MPK12 also plays an important role in guard cell $CO_2$ signalling, it regulates ABA-independent $CO_2$-induced stomatal closure, and controls plant water management (Hõrak et al., 2016; Tõldsepp et al., 2018). The loss-of-function *mpk12* single mutant had higher stomatal

conductance than wild type leaves under control conditions as well as under high $CO_2$ when stomatal closure was induced by $CO_2$ in wild type leaves (Tõldsepp et al., 2018). Therefore, the lower sensitivity of *gad2-1* in hormone and MAPK signalling compared to the other GABA mutants GABA mutants maybe related to the loss of *GAD2* and *MPK12* genes.

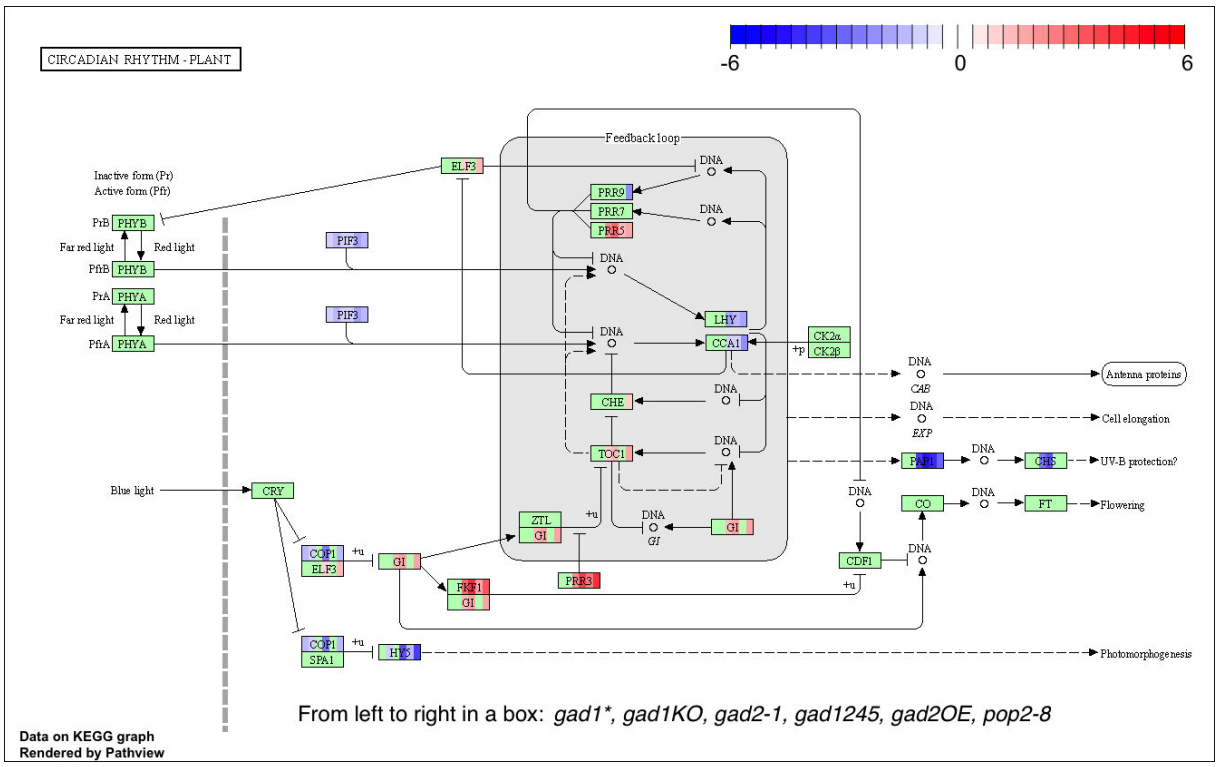


**Figure 3.12:** Differentially expressed genes of GABA mutants related to circadian rhythms (ath04712) under control conditions. From left to right in a box: *gad1*, gad1KO, gad2-1, gad1245, gad2OE, pop2-8.*

**Circadian rhythm**. Except for *gad1** and *gad1KO*, circadian rhythm related genes in all other GABA mutants were significantly affected, with *gad1245* and *pop2-8* containing the largest number of DEGs (15). This is not surprising as *GAD1* is primarily expressed in the roots instead of shoots. Light is one of the most essential environmental factors that affects plant growth and development, and light signal transduction can be mediated by COP1 and BBXs-HY5 in plants (Xu, 2019). As the pathway map showed, many genes were up-regulated in the four non-*GAD1* mutants (Fig 3.12). For example, *Early Flowering 3* (*ELF3*) had an increased expression in *gad1245* and *pop2-8*, and Pseudo-Response Regulator 3 (PRR3) were induced in all non-GAD1 mutants. Among the down-regulated genes, *Long Hypocotyls 5* (*HY5*), which is important for photomorphogenesis, was greatly repressed expression in *gad1245* and *pop2-8* (Fig 3.12). In *Arabidopsis HY5* regulates *Nitrite Reductase 1* (*NIR1*) and *Ammonium transporter 1* (*AMT1;2*), it also mediates salinity-induced proline accumulation which is light controlled (Kovács et al., 2019). Taken together, these greatly altered circadian genes in non-stressed mutants suggests significant changes in these processes, which could be beneficial or not in the upcoming submergence.

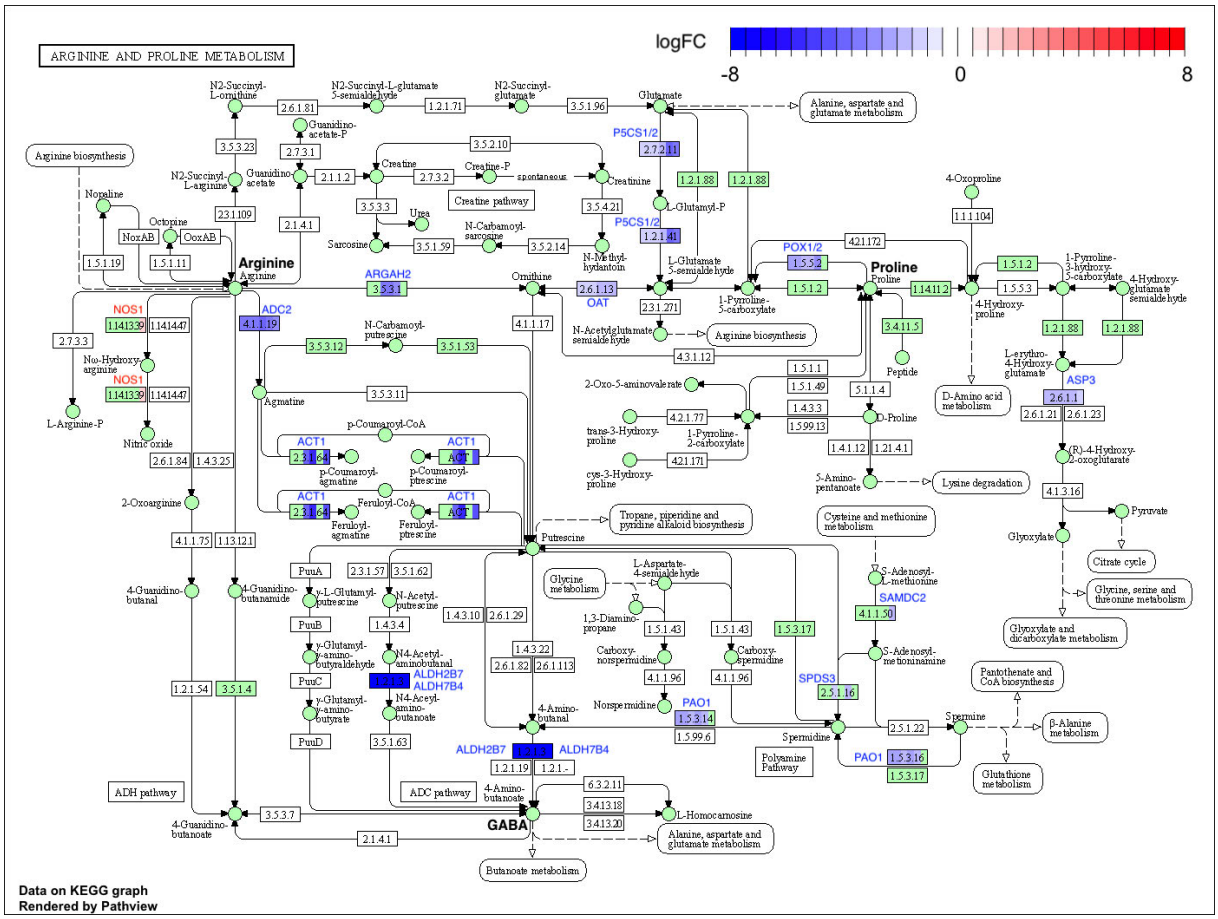


**Figure 3.13:** Differentially expressed genes of GABA mutants in arginine and proline metabolism (ath00330) under control conditions. From left to right in a box: *gad1*, gad1KO, gad2-1, gad1245, gad2OE, pop2-8.*

**Arginine and proline metabolism**. This pathway (illustrated in Chapter 1 Section 1.2.2.2) was enriched in all six GABA mutants under control conditions. Transcript levels of most DEGs were down-regulated in one or more mutants, with the only exception of mitochondrial-localised *Nitric Oxide Synthase 1* (*NOS1*) which was up-regulated. The *Arabidopsis* genome has two *ADC* genes encoding arginine decarboxylase (ADC), an enzyme catalyzes the synthesis of putrescine Put. In addition to *ADC2*, the mRNA of five genes were detected as having decreased expression in all mutants: *ALDH7B4* and *ALDH2B7*, *OAT*, *P5CS1* and *P5CS2*, and *ASP3*. Cytoplastic (*PAO1*) is one of the five genes encoding the polyamine oxidase (PAO) family members, and it was down-regulated in all the five *GAD* mutants but not in *pop2-8*. Two genes encoding proline dehydrogenases (ProDH, also known as POX), *POX1/2* were also down-regulated in all *GAD* mutants not *pop2-8*. *ADC* and *PAO* genes are both critical for PA metabolism, and PAs were reported to regulate stress response in plants by altering the GABA shunt pathway (Urano et al., 2005). S-adenosylmethionine decarboxylase (SAMDC), a key enzyme involved in the biosynthesis of the polyamines (spermidine and spermine), also influences the rate of ethylene biosynthesis (Podlešáková et al., 2019). *SAMDC2* had decreased expression in

non-stressed *pop2-8*. Collectively, these results means that when the GABA shunt pathway is disturbed, the polyamine pathway genes were also impacted, even under non-stressed conditions, linking arginine, proline and PA metabolism together.

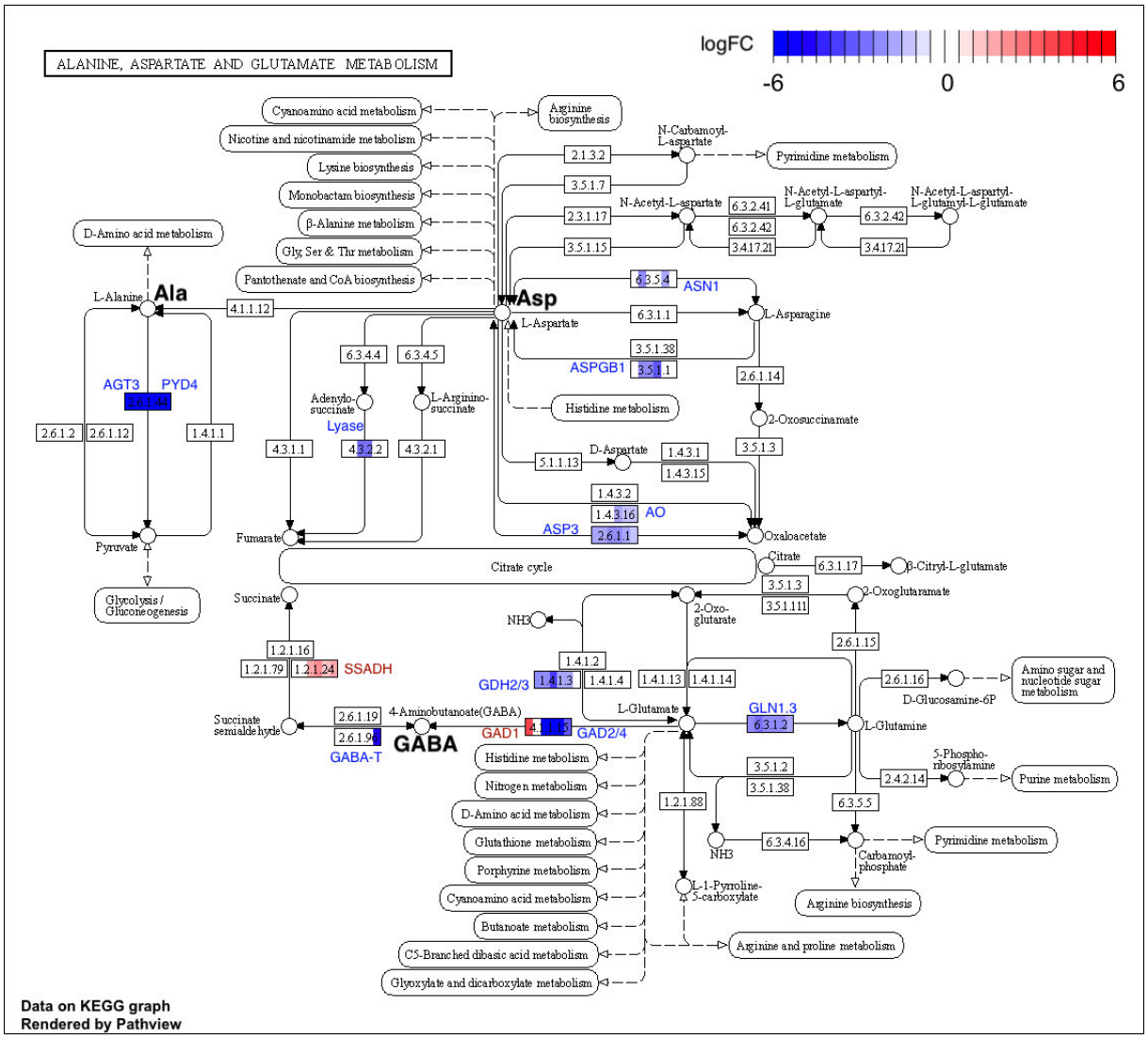


**Figure 3.14:** Differentially expressed genes of GABA mutants in alanine, aspartate and glutamate metabolism (ath00250) under control conditions.

**Alanine, aspartate and glutamate metabolism**. This is another amino acid metabolism pathway that directly interacts with GABA, and all mutants but not *pop2-8* were significantly enriched in this pathway (Fig 3.11) under non-stressed conditions, with different expression patterns of genes related to Ala, Asp and Glu metabolism. Apart from the higher *GAD1* expression in *gad1** leaves, the two *GAD1* lines displayed no differences in terms of *GABA-T* or *SSADH* expression compared to WT. *GABA-T* was down-regulated in *pop2-8* as expected, and not changed in other mutants, while *SSADH* was up-regulated in all mutants except for the two *GAD1* lines. Three *GAD* genes were all down-regulated in non-*GAD1* lines but turned out to be more complex. Compared to WT leaves, *GAD1* was increased in expression in *gad2-1*, *gad2OE* and *pop2-8* leaves, *GAD2* and *GAD4*

were both repressed in *gad2-1* and *gad1245* leaves, and *gad2OE* also had lower *GAD4* expression (Fig 3.14, 3.20).

GDH and GLN are the two enzymes utilising glutamate (Glu) as a substrate, and in almost all GABA mutants their gene expression was down-regulated, with the exception of unaffected *GDH* expression in *pop2-8*. Glutamine-dependent *asparagine synthase1* (*ASN1*) gene was down-regulated in *gad1KO* and *gad2OE*. *ASN1* is one of the dark-inducible carbon (C) starvation-responsive genes (within 3h, therefore the enzyme also named DIN6) and light has a negative effect on its mRNA accumulation, and it is also induced in senescing leaves or by exogenous photosynthesis inhibitor treatment. As a decrease of the C/N ratio in plants can also be recognized as C starvation (Yoshitake et al., 2021), the reduced expression of *ASN1* in the above two lines could potentially mean a higher C/N ratio than WT.

### 3.1.3 WT and GABA mutants' transcriptional response to submergence

The previous section reported some common and distinguishable transcriptional changes in GABA mutants included only plants that were not submerged. Next, the transcriptional response to submergence for WT and GABA mutants was explored by comparing to their own non-submerged plants, starting with the multi-dimensional scaling (MDS) principal coordinate plot and identifying differential expressed genes (DEGs). Biological replicated samples from the same genotype clustered together in the MDS principal coordinate plot (Fig C.5), although there was a large variation in one WT sample. Dimension 1 separates control and submerged plants, while dimension 2 roughly corresponds to different GABA mutants. As the MDS principal coordinate plot (Fig C.5) nicely separated the submerged plants from their controls, next the gene profiles of each line before and after submergence were evaluated in order to uncover the submergence responsive genes. After filtering lowly expressed genes (less than five counts in a quarter of all samples) there were in total 19889 genes remained across the 42 libraries. These genes were used to compare the submergence response between WT and GABA mutants. They were also used in the next Section 3.1.4 of this chapter to explore mutation-specific submergence responses.

#### 3.1.3.1 Identification of differentially expressed genes in WT and GABA mutants after submergence

After 6 d submergence, only genes that were up- or down- regulated with $|log2FC| > 1$ and Bonferroni adjusted $P$ value $adj.P < 0.05$ by pairwise comparisons were regarded as differentially expressed genes (DEGs). A large number of genes had significantly altered expression in response to submergence in all seven lines. Overall there were

10874 differentially regulated genes, resulting in 25-50% of the transcriptome in the submerged plants being altered (Fig C.6). In WT, *gad1** and *gad2-1* there were more genes down-regulated than up-regulated, however in the other four lines the number of up- or down-regulated genes was similar. *pop2-8* had the largest number of genes had the largest number of genes that changed in response to submergence (8579). Submergence also changed the expression of 6653, 7172 and 7773 genes in *gad1245*, *gad1KO* and *gad2OE*, respectively. Only 17.7% DEGs uniquely showed up in one specific line, and nearly half of them belonged to *pop2-8*. There other DEGs (82.3%) were shared between different lines: 25.6% across all seven lines while 8.5% across all six GABA mutants but not WT, and the remaining genes were shared between two to six lines (Fig 3.15).

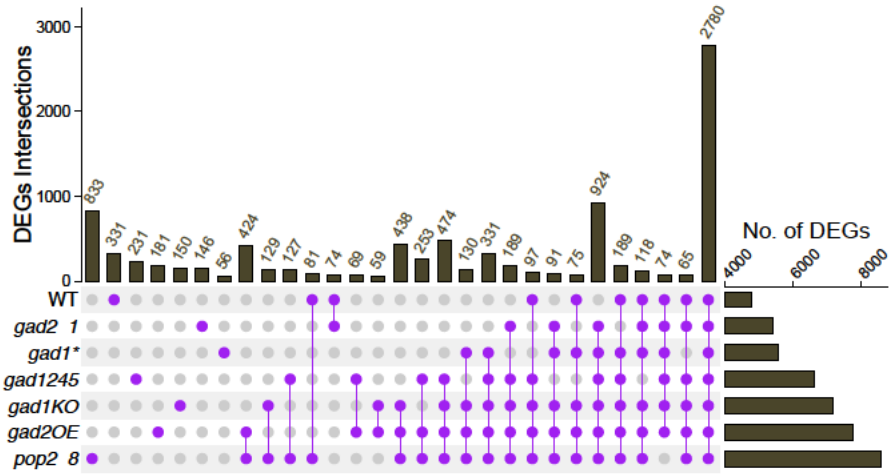


**Figure 3.15:** UpSet plot of intersected differentially expressed genes (DEGs) in WT and GABA mutants after submergence. The number of DEGs in each line and overlapping DEGs across different lines are shown in the bottom right bar chart and top bar chart, respectively. For example, *pop2-8* had the highest number of uniquely-regulated genes (833 DEGs), while 2780 DEGs were shared in all seven lines (both WT and GABA mutants) and 924 were shared in all mutants. The dot matrix at the bottom left indicates the respective overlaps by connected purple circles.

The total 10874 submergence-responsive DEGs which appeared in at least one of the seven accessions were applied to the analysis of hierarchical clustering. Most of the DEGs, if shared, were regulated in the same direction between different lines (Fig 3.16), with only 352 genes oppositely-regulated (Fig 3.16b). WT had a relatively distinct expression pattern compared to GABA mutants (Fig 3.16a, 3.17). Table 3.17b listed 25 genes that were down-regulated in WT but up-regulated in at least three GABA mutants from Group I. They mainly included defence response (fungus, virus and bacterium) genes (e.g. *CAD8*, *HMP19*, *YSL7*, *NIT2*), ethylene and auxin responsive genes (*RAP2-6*, *ACS2*).

**The ERF-VII transcription factors for oxygen sensing**. RAP2.12 , a member of the ERF (ethylene response factor) subfamily AP2 transcription factor family (RAP), and its homologues RAP2.2 and RAP2.3 act redundantly in multiple stress responses.

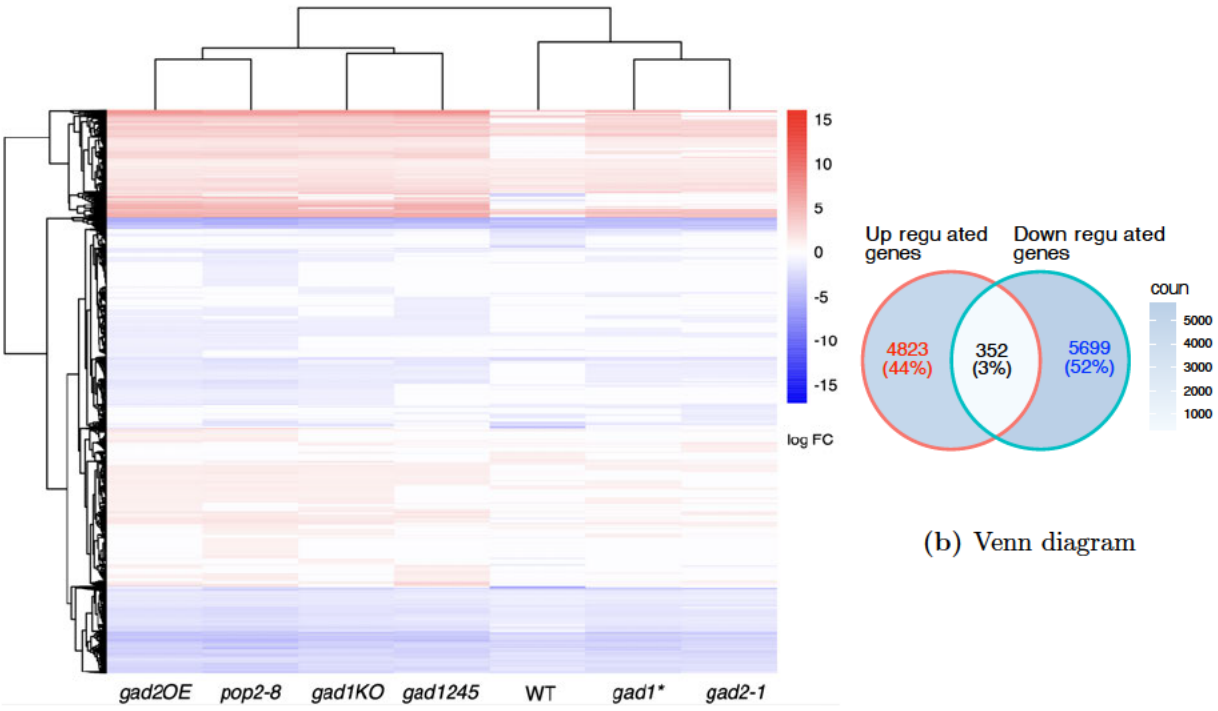


(a) Expression pattern of DEGs

(b) Venn diagram

**Figure 3.16:** Differentially expressed genes (DEGs) after submergence in WT and GABA mutants. (a): Hierarchical clustering of log2 fold change. (b): Venn diagram. Up- and down-regulated genes of (a) log2 fold change and (b) DEGs number/proportion were indicated by red and blue, respectively. The fold change in each genotype was normalised against its corresponding control plants.

In *Arabidopsis*, an effective low oxygen-sensing response requires RAP2.12 stabilization followed by HRA1 induction to modulate the extent of the anaerobic response by negative feedback regulation of RAP2.12. This mechanism is crucial for plant survival under suboptimal oxygenation conditions. The discovery of the feedback loop regulating the oxygen-sensing mechanism in plants opens new perspectives for breeding flood-resistant crops (Licausi et al., 2011). The ERF-VII genes could be classified into two groups based on their transcriptional responses to hypoxia and ABA (Papdi et al., 2015). *RAP2.12*, *RAP2.2* and *RAP2.3* can all be activated by ABA, but they were repressed or unaffected under low oxygen. In contrast, *HRE1* and *HER2* were repressed by ABA but induced by anoxia. Papdi et al. (2015) observed 9 h anoxia treatment led to a gradual reduction of RAP2.12 and RAP2.2 mRNA levels, in contrast HRE1 and HRE2 genes were inducted. In this study, *RAP2.3*, had significantly higher expression in *gad1245* than in *pop2-8* under control conditions (Fig 3.18, C.21). However, after 6 d submergence in all lines RAP2.3 expression was up-regulated to the same level as for WT. Similar patterns of expression could be seen in *RAP2.2* but not for *RAP2.12* nor *RAP2.6*. These data suggest that the oxygen sensing system in the seven lines responded differently to submergence.
Autophagy plays an essential role in plant development and stress responses, and a recent study suggested that the fermentation product ethanol promotes autophagy-mediated

**(a)** Clustering of oppositely regulated 352 DEGs

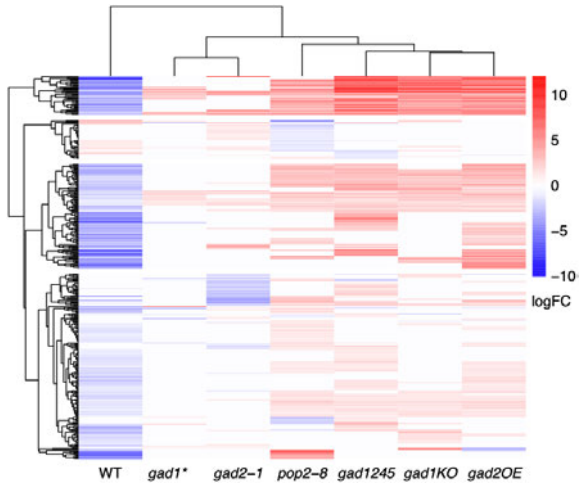


**(b)** 25 oppositely regulated DEGs

| Gene ID | Gene info |
|---|---|
| AT1G43160 | Ethylene-responsive transcription factor RAP2-6 |
| AT4G24000 | Glycosyltransferase (Fragment) CSLG2 |
| AT5G13170 | Bidirectional sugar transporter SWEET15 |
| AT1G04580 | Benzaldehyde dehydrogenase (NAD(+)) AAO4 |
| AT2G03850 | Late embryogenesis abundant (LEA) family protein |
| AT1G01480 | 1-aminocyclopropane-1-carboxylate synthase 2 ACS2 |
| AT1G17020 | Senescence-related gene SRG1 |
| AT1G80160 | F18B13.24 protein; GLYOXYLASE I 7 Vicinal oxygen chelate (VOC) superfamily member |
| AT2G15780 | F19G14.22 Cupredoxin superfamily protein |
| AT2G45570 | Cytochrome P450, family 76, subfamily C, CYP76C2 |
| AT4G21680 | Protein NRT1/ PTR FAMILY 7.2 NPF7.2 |
| AT4G37990 | Cinnamyl alcohol dehydrogenase 8 CAD8 Elicitor-activated gene 3 ELI3 |
| AT2G35730 | Heavy metal associated protein 19 HMP19 |
| AT3G45130 | Terpene cyclase/mutase family member. lanosterol synthase 1 LAS1 |
| AT1G65730 | Probable metal-nicotianamine transporter YSL7 |
| AT3G44300 | Nitrilase 2 NIT2 |
| AT2G36780 | UDP-glycosyltransferase family protein UGT73C3 |
| AT4G33150 | Lysine-ketoglutarate reductase (LKR)/saccharopine dehydrogenase (SDH) bifunctional enzyme LKR/SDH |
| AT5G56200 | C2H2 type zinc finger transcription factor family |
| AT1G79900 | Mitochondrial arginine transporter BAC2 |
| AT3G57380 | Glycosyltransferase |
| AT3G46680 | UGT76E6 UDP-glycosyltransferase 76E6 |
| AT1G69480 | Phosphate transporter PHO1 homolog 10 PHO1-H10 |
| AT1G05340 | Cysteine-rich TM module stress tolerance protein |
| AT3G06490 | Transcription factor MYB108 |

**Figure 3.17:** Oppositely regulated 352 genes among WT and GABA mutants after submergence. (a) Clustering of 352 DEGs with different expression patterns. (b) List of 25 oppositely regulated genes in (a). The fold change in each genotype was normalised against its corresponding control plants.

submergence tolerance in *Arabidopsis* (Yuan et al., 2020). In the current study, submergence significantly induced *ATG8E* expression in all lines, and *gad1** and *gad1245* had a greater than 2.1 fold change.

WRKY transcription factors play important roles in a large number of plant processes, including senescence, seed development, seed dormancy and germination, biotic and abiotic stress responses. Xiao et al. (2013) found that the antagonistic cross talk between abiotic and biotic stresses (drought and disease) in rice is regulated by WRKY13, which autoregulates its own expression and represses the expression of *SNAC1* and *WRKY45-1* through selectively binding to different cis-elements in the promoter regions of these genes. Stress responsive No Apical meristem, *STRESS RESPONSIVE NO APICAL MERISTEM, ARABIDOPSIS TRANSCRIPTION ACTIVATION FACTOR1/2* (*SNAC1*, *CUP-SHAPED COTYLEDON*) promotes stomatal closure and its over-expression increased drought resistance while knockouts of *WRKY45-1* increased both drought and bacterial resistance (Xiao et al., 2013). In this study, *WRKY13* in *pop2-8* leaves had increased expression over WT under control conditions. After submergence, the expression of *WRKY13* in *gad1245* and *pop2-8* both decreased. However, *WRKY45* in all 6 control mutants had

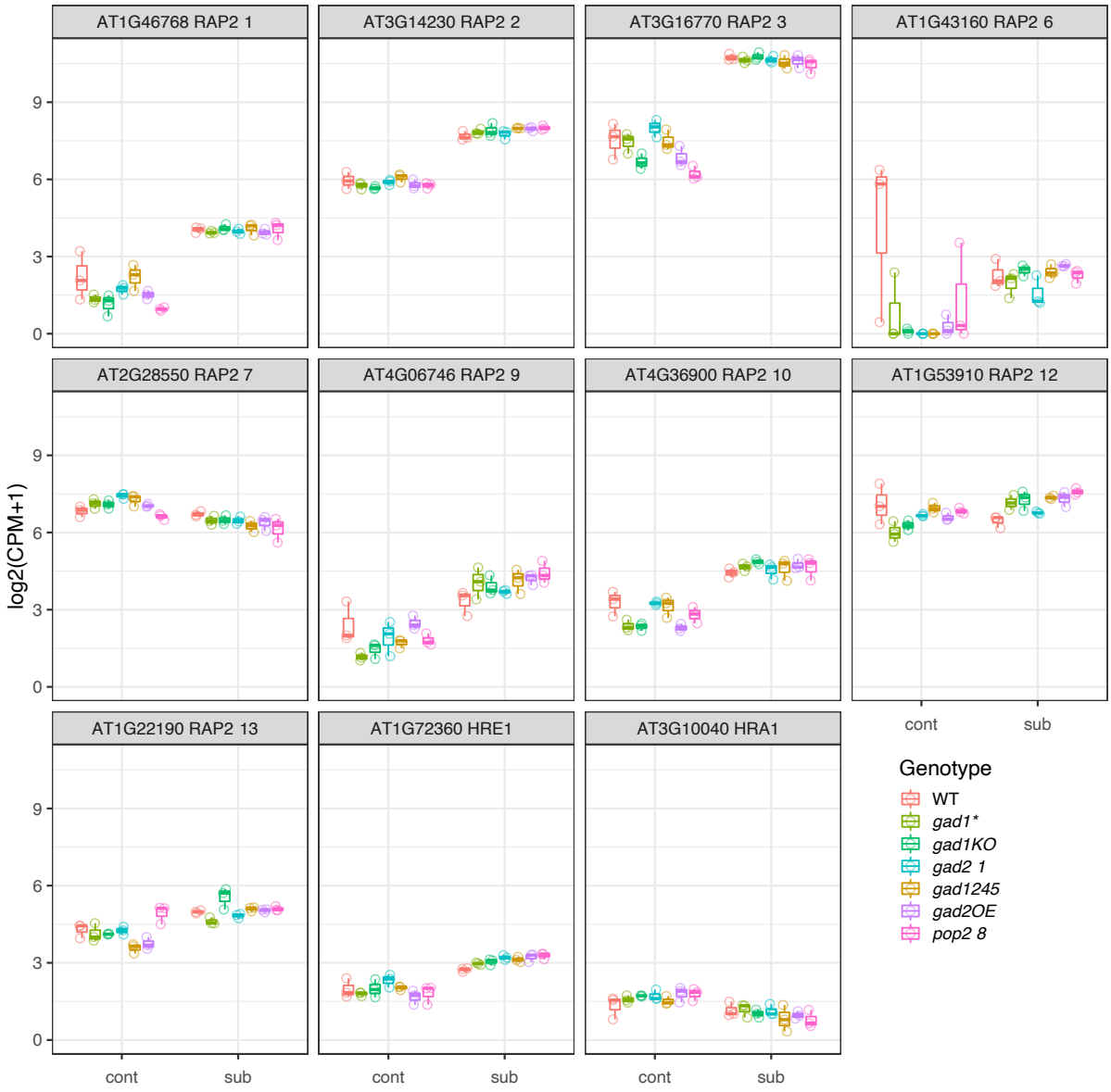


**Figure 3.18:** Expression of oxygen-sensing gens (RAP2, HRE1, HRA1) in WT and GABA mutants. CPM: counts per million.

lower expression compared to WT, but its expression in all 7 lines were promoted after flooding.

**Expression of core HRGs in WT and GABA mutants after submergence**. Over two thirds of the 52 core hypoxia response genes (Table A.1) changed significantly in one or more lines after 6 d submergence (Fig 3.19), mostly up-regulated. Interestingly, transcripts of *AlaAT2*, *HRE1* and plasma membrane-bound *NADPH oxidase* (also known as *RESPIRATORY BURST OXIDASE HOMOLOG D* [*RBOHD*] in plants) were not affected in WT, but were enhanced in all mutants after submergence. *HYPOXIA RESPONSE ATTENUATOR1* (*HRA1*) was also not significantly affected in WT, but decreased in mutants other than *gad1** and *gad2-1*. RAP1.12 is the upstream regulator of HRA1,

and its steady-state levels could be impacted by HRA1. HRA1 protein is active in cells experiencing hypoxia despite of whether the plants are under normal growth or low oxygen conditions. For example, Giuntoli et al. (2014) reported that in non-stressed *Arabidopsis*, *HRA1* expression was restricted to the shoot apical region, leaf vascular and roots, where hypoxia occurred due to high oxygen need and low diffusion. Some hypoxia unknown

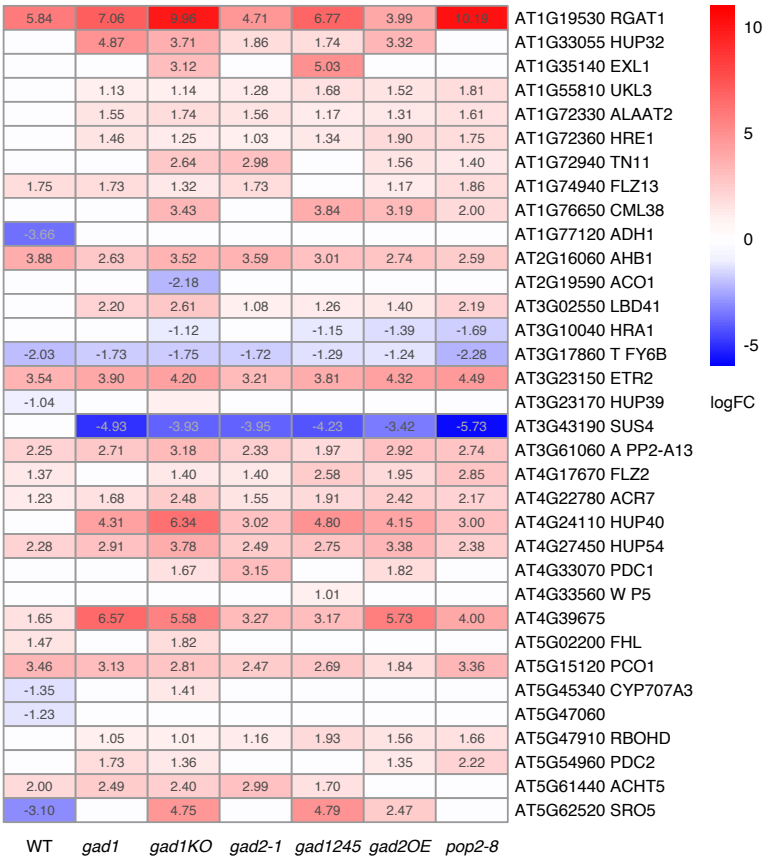


**Figure 3.19:** Log2 fold change of core hypoxia-responsive genes among WT and GABA mutants after submergence. The fold change in each genotype was normalised against its corresponding control plants.

proteins (*HUPs*) reported by previous work also appeared to be regulated differently in the current research (*HUP32*, *HUP39*, *HUP40* and *HUP54*) between WT and GABA mutants (Fig 3.19).

#### 3.1.3.2 Expression of GABA metabolism related genes under control and submergence

Gene related to GABA-metabolism were checked for their expression under control and submergence conditions, including GABA-shunt genes and GABA-transport related genes. As shown in Fig 3.20, knockout of certain *GAD* isoform(s) usually resulted in a lower expression of that gene in GABA mutants, however *gad1** had a higher *GAD1* expression which was not changed by submergence, possibly due to its T-DNA insertion was at a large intron (over 1000 bp) and was rather short (51 bp). It is also possible that alter-

native promoters exist in the *GAD1* gene, and the T-DNA insertion somehow promoted its expression which was otherwise usually relatively low in the leaves, this need to be examined in the future work.

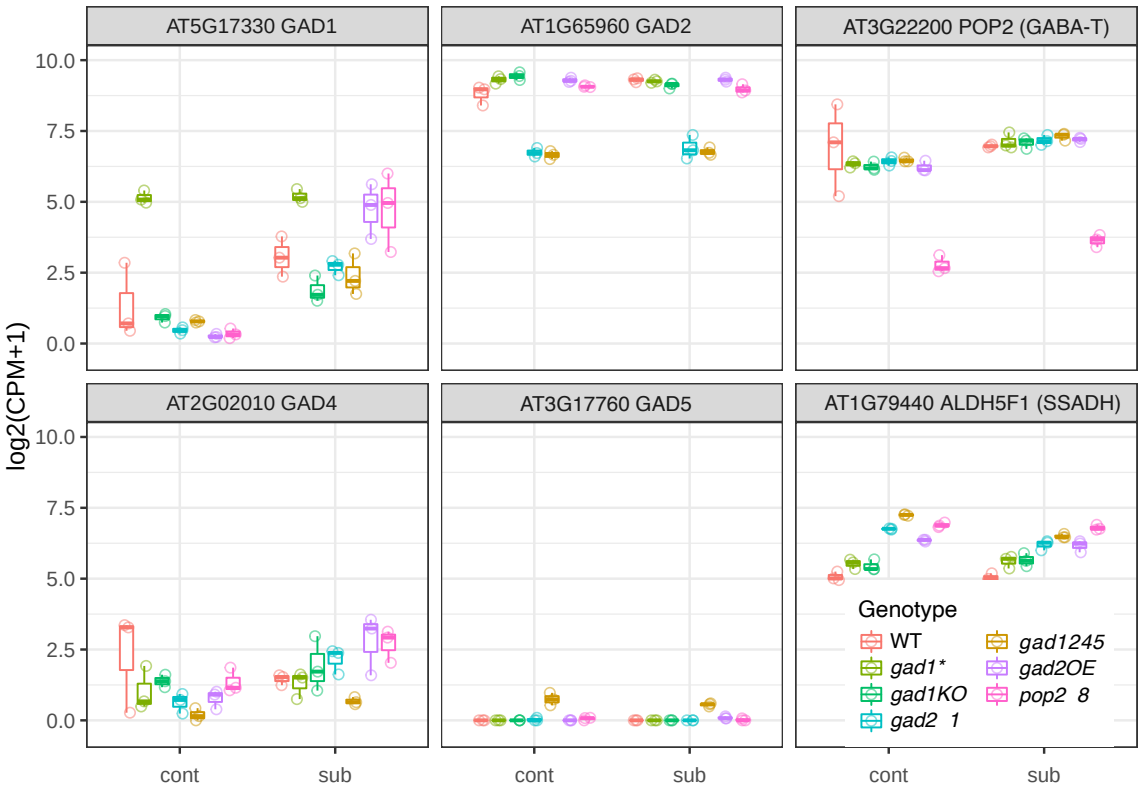


**Figure 3.20:** Expression of GABA-shunt genes in WT and GABA mutants under control and submerged conditions (n=3, Boxplot).

*SSADH* (ALDH5F1) expression was not affected by submergence, and all mutants except for the two *GAD1* lines had a higher expression than WT under both control and submerged conditions. Submergence induced the expression of both *GAD1* and *GAD4* in most GABA mutants, especially *GAD1* expression in *gad2OE* and *pop2-8*. Miyashita and Good (2008) also found that after 2, 8, 24 h hypoxia treatment, *GAD4* expression increased to approximately 3-, 19- and 13-fold in *Arabidopsis* roots, in the meantime the authors found suppressed expression of *GAD2* and no changes of *GAD1* in response to hypoxia. However, in my research *GAD1* as also highly inducible by hypoxia in non-*GAD1* lines while *GAD4* only induced among three lines (*gad2-1*, *gad2OE* and *pop2-8*). Recently, Meng et al. (2020) also reported light/dark submergence induced *GAD1* and *GAD4* expression in wild type leaves (various ecotypes), and also *GAD1* had a much higher fold change than *GAD4*; moreover, the sensitive WT lines induced more *GAD1* expression than the tolerant ones, no matter whether submerged or recovered plants (both compared to control plants). They found only *GAD1* was strongly induced in mitochondrial mutants after submergence. Clearly, leaf *GAD1* played a role under hypoxia, probably more important than that of

*GAD4*. The reason why *gad1** had a promoted *GAD1* expression in the shoots is yet to be uncovered, but its large biomass and fully recovery of Fv/Fm from de-submergence suggests this feature benefits plants to coping with hypoxia during both submergence and recovery phrases. A further quantitative PCR will be able to confirm whether the shoot *GAD1* expression is higher than WT in *gad1**. All of these results suggested that the levels of GABA need to be tightly controlled through the modulation of transcript abundance of the different *GAD* genes during standard growth conditions or in response to stress.

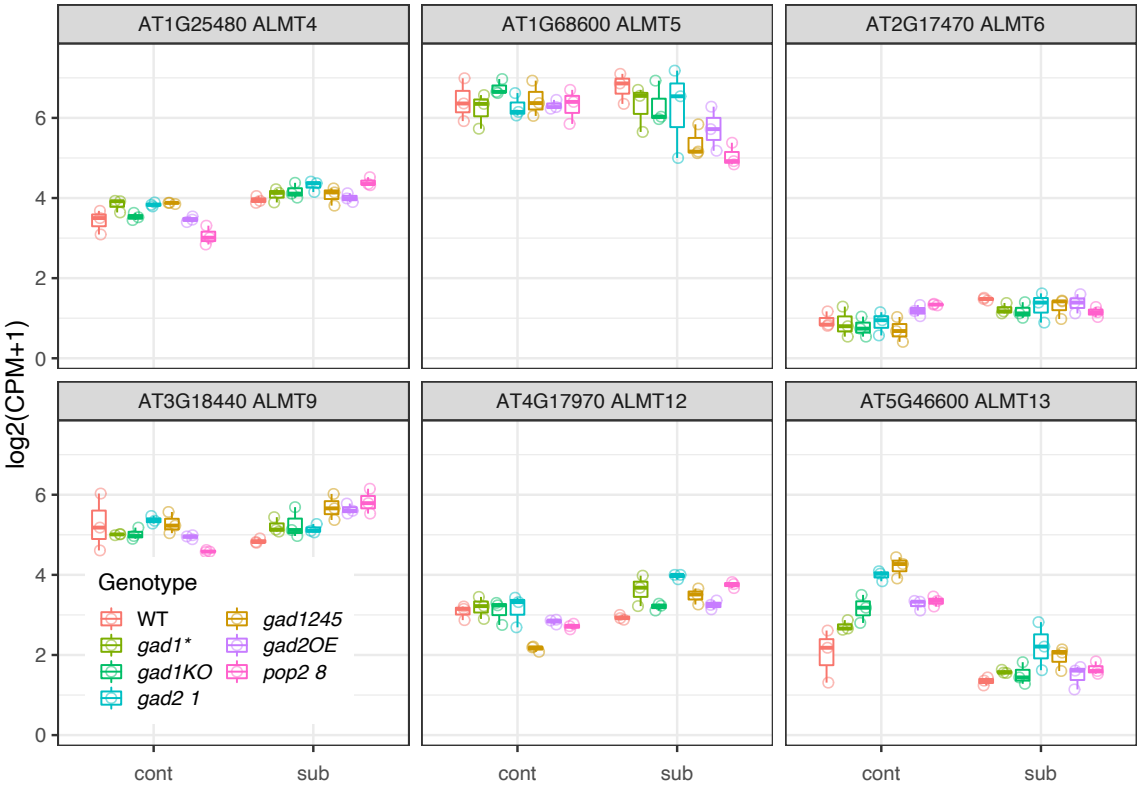


**Figure 3.21:** Expression of ALMT genes in WT and GABA mutants under control and submerged conditions (n=3). The DEGs and log2 fold change were shown in Fig C.15

The aluminum-activated malate transporters (ALMTs) belong to a protein family of anion channels that contribute to a plants' tolerance towards toxic aluminum ions in the soil, but not all 14 ALMTs in the *Arabodipsis* have the same function, for example, some of them are involved in stomata regulation (Sharma et al., 2016) . ABA-induced stomatal closure involves ALMT4; ALMT12 is also involved in stomata closure; while the vacuolar ALMT6 and tonoplast ALMT9 are both involved in stomata opening (Eisenach et al., 2017; Meyer et al., 2011; Jaślan and De Angeli, 2022; Luu et al., 2019). In wheat GABA negatively regulates TaALMT1 activity to prevent malate efflux from roots to soil under acidic/$Al^{3+}$ conditions (Ramesh et al., 2015), and this is also likely to occur under other stresses, e.g. cold, heat, salinity as GABA accumulation is induced. Klecker et al. (2014) proposed 53

shoot-specific hypoxic-responsive genes in *Arabidopsis*: at least 2-fold induction and 2-fold higher expression in hypoxic leaves (versus aeration leaves and hypoxic roots, respectively), these genes also had significantly higher ratio of gene induction during hypoxia in shoots, i.e. [shoot Hypoxia/shoot Control]/[root Hypoxia/root Control] >2. ALMT5 is among those shoot-specific genes, but in my experiment, it was found to be down-regulated in *gad2OE* and *pop2-8* after submergence while unaffected in other lines, this could be due to the plant age as they used young seedlings (7 d), and hypoxia was not induced by submergence. However, the decreased expression in the two GABA-accumulating lines may be one of the reasons that these two lines did not cope with submergence as well as the other lines. As shown in Fig 3.21 and Fig C.15, *gad1245* had a lower expression of *ALMT12* than WT under control conditions, while all mutants had a lower expression of *ALMT13* except for *gad1** than WT. After submergence, *ALMT13* expression in all seven lines decreased, *ALMT5* and *ALMT12* only significantly altered in *gad1245* and *pop2-8*; in addition, *ALMT4* and *ALMT9* in *pop2-8* as well as *ALMT6* in *gad1245* were also up-regulated. These results strongly suggested that the role of GABA in response to submergence is closely related to regulating *ALMT* mRNA levels.

#### 3.1.3.3 GO enrichment analysis of WT and GABA mutants after submergence

DEGs in each line were split into up- and down- regulated genes and went through separate GO enrichment analyses, resulting in 93 (Fig 3.22a GO-Up results) and 166 (Fig 3.22b GO-Down results) over-represented GO terms, respectively. In general, a wide spectrum of physiological processes were greatly affected by submergence, as evidenced by the over-representation of the corresponding GO terms. A full list of these GO terms was shown (Table C.5) in the corresponding order as in the heatmap (Fig 3.22).

Seven common GO terms appeared in both GO-Up and GO-Down but with distinct patterns: only WT in GO-Up but mutants were in GO-Up (all or at least four GABA mutants), suggesting an opposite regulation of genes involved in these processes in response to submergence. This could be correlated with the earlier shown opposite regulated patterns by submergence between WT and GABA mutants (Fig 3.17). These processes were: cellular response to hormone stimulus; response to jasmonic acid and fatty acid; secretory vesicle; response to ABA, alcohol and lipid. The last three processes were already over-represented under control conditions in all GABA mutants by down-regulated genes as well as in *gad1245* by up-regulated genes (Fig C.8, Section 3.1.2.2). Twenty-two terms in GO-Up and 32 terms in GO-Down were shared between all accessions, suggesting commonly affected processes of all seven lines to cope with submergence. Up-regulated genes enriched GO terms mainly included response to hypoxia, decreased oxygen and nutrient levels; cellular response to hormone/ethylene stimulus and organic substance; response to ethylene and ethylene-activated signalling pathway; response to chitin and

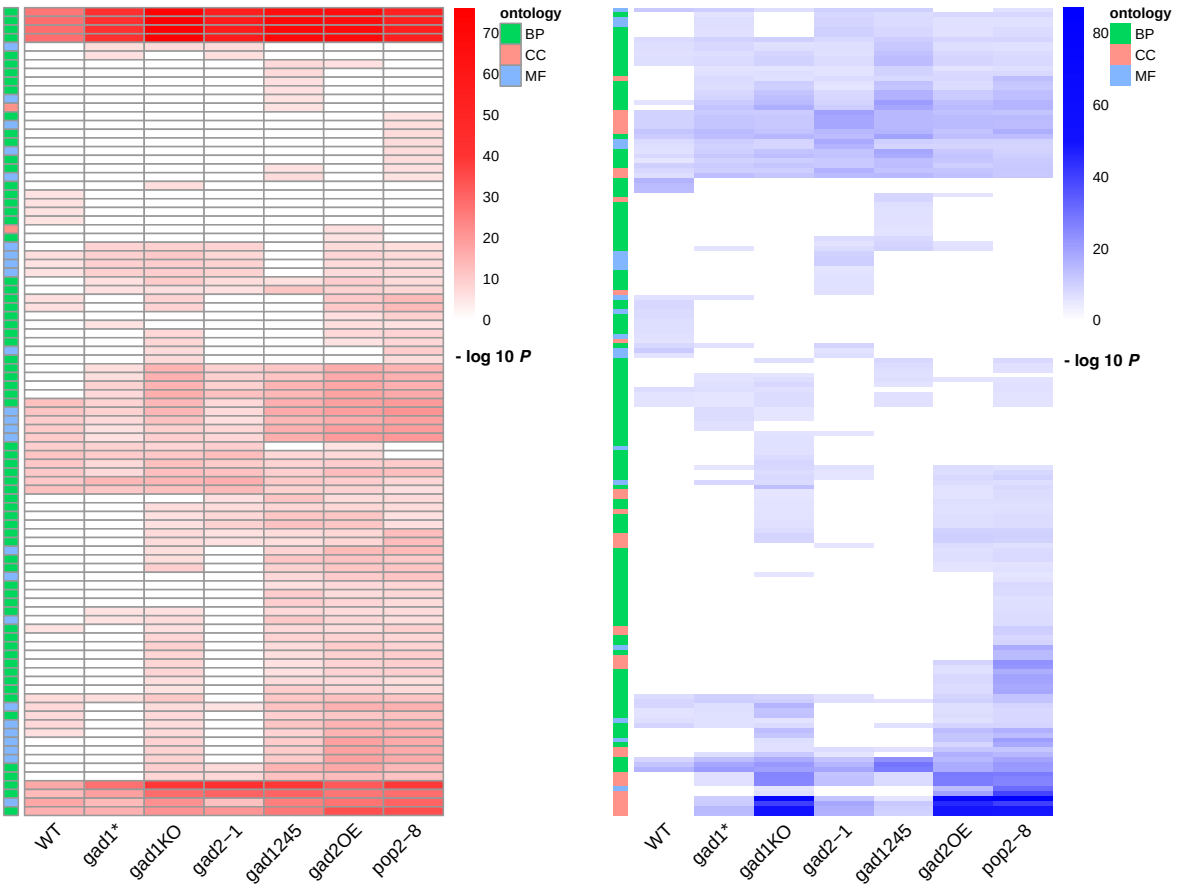


**(a)** Up-regulated genes enriched 93 GO terms **(b)** Down-regulated genes enriched 166 GO terms

**Figure 3.22:** Clustering patterns of GO terms enriched through up- or down-regulated genes in WT and GABA mutants after submergence. GO terms with Bonferroni adjusted $P < 0.01$ was considered significantly enriched and -log10 $P$ was presented in the heat maps. (a) 93 terms enriched by up-regulated genes. (b) 166 terms enriched by down-regulated genes.

organonitrogen compound; protein serine/threonine kinase activity; defense response to bacterium; nucleosidase activity; protein phosphorylation; phosphotransferase activity, adenyl nucleotide binding and adenyl ribonucleotide binding. Down-regulated genes enriched GO terms mainly included cell wall and polysaccharide metabolic processes, i.e. galacturonan and pectin metabolic processes, cell wall polysaccharide and macromolecule biosynthetic processes, hemicellulose metabolic process, microtubule cytoskeleton, anchored component of plasma membrane and external encapsulating structure organization (Table C.5).

In GO-Up results, all GABA mutants were enriched in leaf senescence (GO:0010150), and three of them (*gad1**, *gad1KO* and *gad2-1*) were also enriched in positive regulation of leaf senescence (GO:1900057). In GO-Down results, all GABA mutants were enriched in water (GO:0006833) and fluid (GO:0042044) transport, and water transmembrane transporter (GO:0005372) and water channel (GO:0015250) activity. However, submerged WT plants was not significantly impacted in these processes (Table C.5). Fig C.16 showed the four

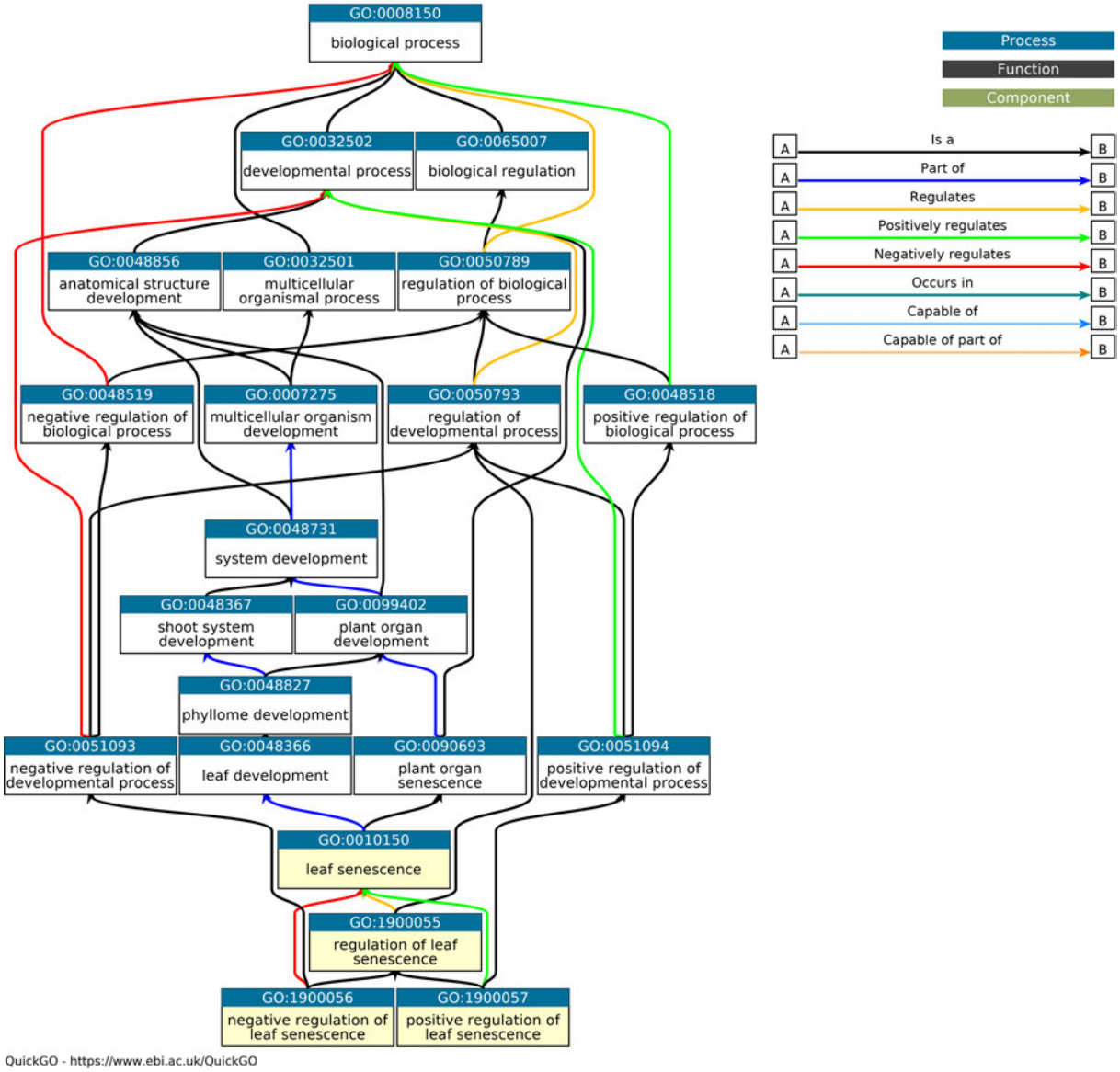


**Figure 3.23:** Four GO terms related to leaf senescence, including leaf senescence (GO:0010150) and its three child terms: regulation (GO:1900055), positive (GO:1900057) and negative (GO:1900056) regulation of leaf senescence.

water and fluid transport related terms and Fig C.17 showed DEGs in WT and GABA mutants involved, Most of them were genes encoding aquaporins (AQPs), the protein in plants facilitating across membrane water transport, e.g. plasma membrane intrinsic proteins (PIPs), tonoplast intrinsic proteins (TIPs), nodulin-26 like intrinsic proteins (NIPs), and small basic intrinsic proteins (SIPs) . Regulation of water uptake is closely related to plant growth under normal and stress conditions, and reduced root water uptake and impaired root hydraulic conductivity (mediated by AQPs) were proposed to be the reason why flooded plants experience wilting (Tan et al., 2018). Fig 3.23 showed the four senescence related terms and Fig C.18 showed DEGs in WT and GABA mutants involved in these processes, such as indole-3-acetic acid inducible 17 (IAA17), small auxin upregulated 36 (SAUR36). As the last step of leaf development, senescence is featured by

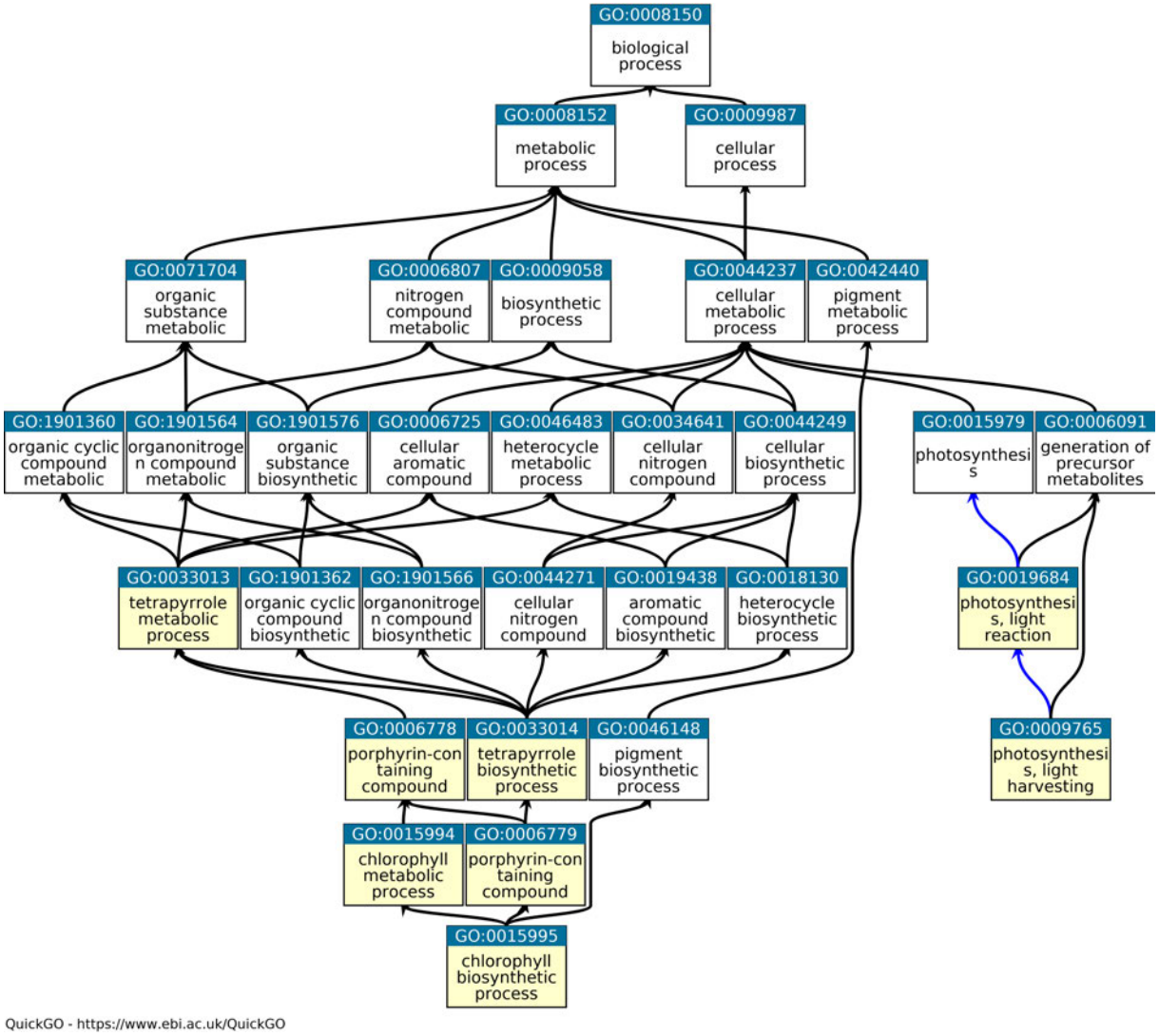


**Figure 3.24:** Six chlorophyll and photosynthesis related processes enriched by down-regulated genes in GABA mutants (not *gad1** and *gad1245*) after submergence. Legend the same as in Fig 3.23.

degradation and recycling processes, which involves degrading chlorophyll, protein, nucleic acid and lipid, transporting nutrients to growing tissues, and finally producing fruits and seeds (Ansari et al., 2014). The previous section 3.1.2 has shown that a large amount of senescence related genes had decreased expression in GABA mutants under non-stressed conditions. Here, it shows that after 6 d submergence, many of these genes and more others in the mutants were up-regulated (Fig C.18).

The GABA mutants also had different PSII sensitivity to submergence (Fig 3.3), together with the down-regulation of AQP genes and up-regulation of leaf senescence genes, it is not surprising in the mutants, many photosynthesis related biological processes (16 terms in GO-Down) happened in chloroplast and plastid (15 out of 32 of the ontology 'CC'), as shown in Fig C.19. *pop2-8* were enriched in all these processes, and *gad1KO* and *gad2OE* most of them, while *gad1245* only in photosystem I (GO:0009522), chlorophyll metabolic

(GO:0015994) and biosynthetic (GO:0015994) processes (Table C.5). Establishment of protein localization to chloroplast (GO:0072596) and light harvesting during photosynthesis (GO:0009765) were significantly impacted in *gad2OE* and *pop2-8* leaves after submergence. Six of these process were shown in Fig 3.24.

#### 3.1.3.4 KEGG enrichment analysis of WT and GABA mutants after submergence

The DEGs in each line were than sent through KEGG pathway analyses, resulting in 57 enriched pathways (Fig 3.25) with distinct patterns as summarised in Table C.6. Although the GABA-shunt pathway were impaired in different ways, these mutants experienced some common changes after 6d submergence as with WT, with other distinguishable responses as well. Six pathways were commonly significantly enriched across all seven lines (Fig 3.25), suggesting these pathways to be greatly affected by submergence regardless of GABA shunt capability. These processes included metabolism of porphyrin, ascorbate and aldarate, elongation of fatty acid, MAPK signalling pathway and plant hormone signal transduction.

Thirty-five pathways were partially shared across the seven lines. Plant-pathogen interaction was enriched in five lines, especially *gad2-1* and *gad1245*, but not in *gad1** or *pop2-8*. However, it was already promoted in non-stressed *pop2-8* plants (Fig 3.11). The other 34 pathways all belong to metabolism-related processes, e.g. energy, carbohydrate, amino acids, cofactors and vitamin, terpenoids and polyketides as well as secondary metabolites biosynthesis, suggesting profound metabolic responses to submergence among two or more lines. Moreover, beta-Alanine metabolism show up in all mutants but not WT, while glucosinolate biosynthesis and secondary metabolites biosynthesis were both in all lines other than *gad2-1* but all other lines.

In terms of *gad1245* and its two parent lines *gad1KO* and *gad2-1*, there were also some differences between them. Fatty acid degradation and cyanoamino acid metabolism were promoted in *gad1245*, *gad2OE* and *pop2-8* but neither parent line. There were six more pathways that were also promoted in *gad1245* (also in WT) but neither of its parent lines: pentose and glucuronate interconversions, indole alkaloid biosynthesis, isoquinoline alkaloid biosynthesis, and metabolism of three amino acids (tyrosine, phenylalanine and tryptophan). On the contrary, 3 pathways showed up in both *gad1KO and gad2-1* but not *gad1245*. They also didn't show up in some other lines, i.e. zeatin biosynthesis not in *pop2-8*, nitrogen metabolism not in *pop2-8* and *gad2OE*, and carbon fixation not in WT and *gad2OE*. It is worth exploring the above processes as *gad1245* seemed to be not behaving like its parental lines. Collectively, these discrepancies suggested distinct strategies in reconfiguration of metabolic processes in response to submergence among

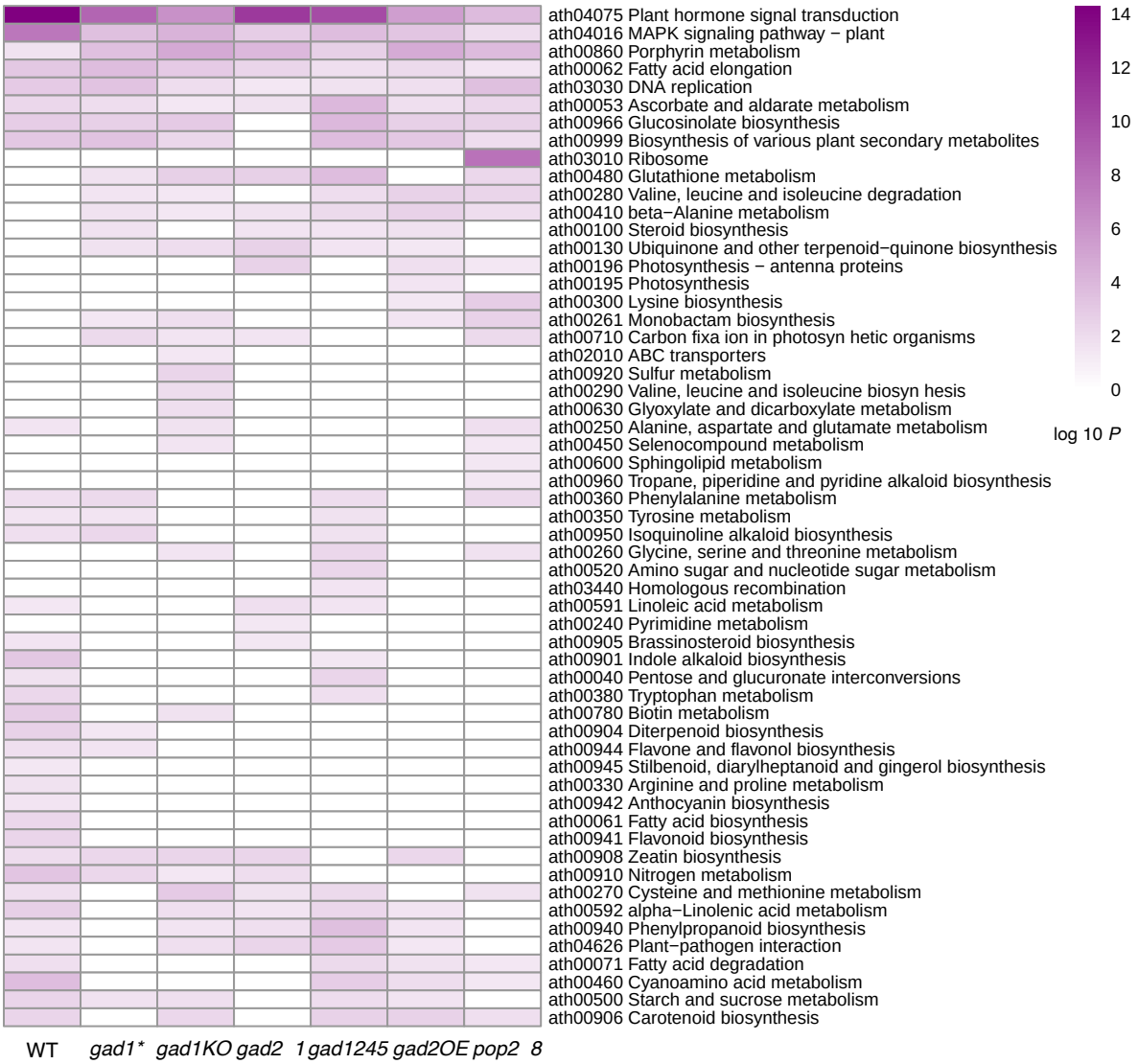


**Figure 3.25:** KEGG pathway analysis of WT and GABA mutants after submergence. The clustered enrichment pattern displayed the -log 10 $P$ value. All coloured cells represented significantly enriched terms with Bonferroni adjusted $P < 0.05$.

WT, GABA-deficient and GABA-accumulating lines.

Sixteen pathways were uniquely enriched in one specific line. Five in WT: biosynthesis of fatty acid, flavonoid and anthocyanin; arginine and proline metabolism; stilbenoid, diarylheptanoid and gingerol biosynthesis. Four in *gad1KO*: ABC transporters; sulfur metabolism; glyoxylate and dicarboxylate metabolism; valine, leucine and isoleucine biosynthesis. One in *gad2-1*: pyrimidine metabolism. Two in *gad1245*: homologous recombination; amino sugar and nucleotide sugar metabolism. One in *gad2OE*: ath00195 photosynthesis (light reaction). Three in *pop2-8*: ribosome; sphingolipid metabolism; tropane, piperidine and pyridine alkaloid biosynthesis. The following pathways, which related to energy production and amino acid metabolism, were checked for details of DEGs in each line.

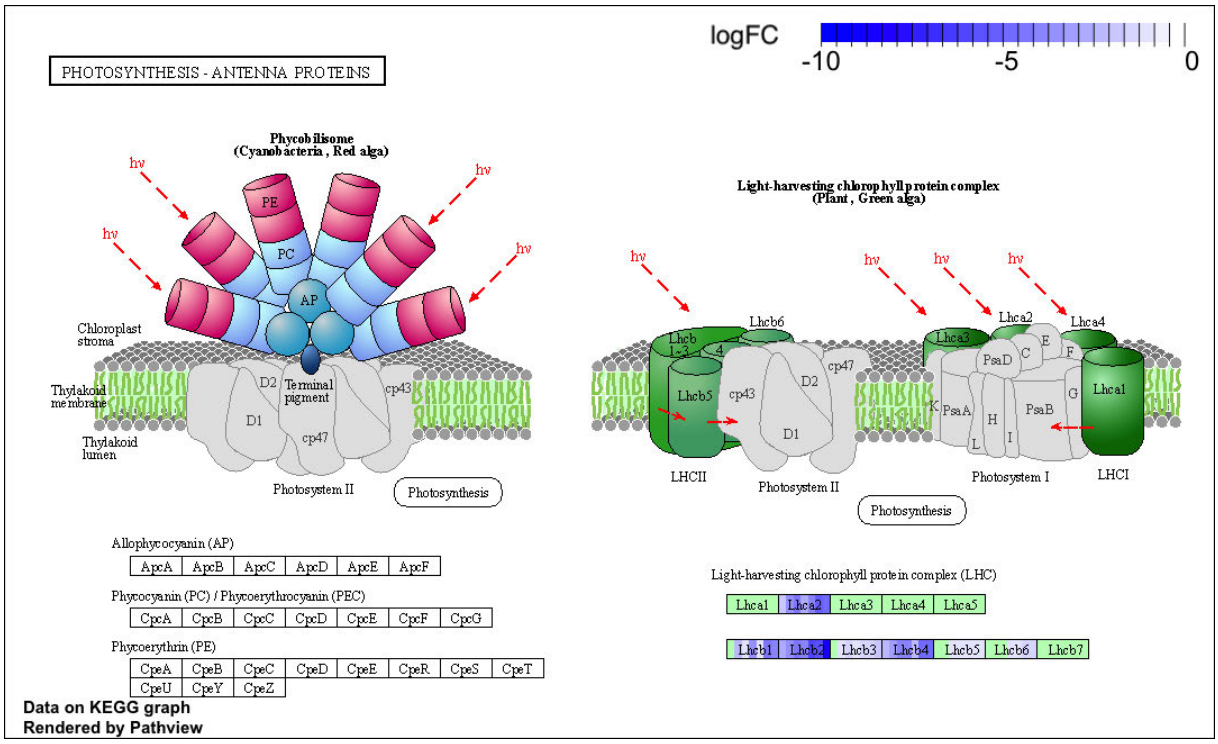


**Figure 3.26:** Differentially expressed genes of WT and GABA mutants in photosynthesis (antenna proteins ath00196) after submergence. Highlighted boxes are light-harvesting chlorophyll protein complex (LHC) in *Arabidopsis*. From left to right in a box: WT, *gad1*, gad1KO, gad2-1, gad1245, gad2OE, pop2-8.*

**Photosynthesis - antenna proteins**. *gad2-1*, *gad2OE* and *pop2-8* were significantly affected in this pathway with 10, 12 and 12 DEGs, respectively (Table C.6). On the contrary, WT only had three genes down-regulated (Fig 3.26). Photosystems I (PSI) and II (PSII) are both crucial for the light-dependent reactions in plants, and they each consists of a reaction centre core and antenna complexes that enhance light harvesting (Leister, 2016). The light harvesting chlorophyll protein complex (LHC) includes chlorophyll and carotenoids, which are situated inside the chloroplasts and transfer harvested light to the reaction centre. LhcA and LhcB are associated with PSI and PSII, respectively, and they are important for photosynthetic efficiency, photoprotection, and photoacclimation (Jansson, 1999). Of the six LHCB isoforms only Lhcb2 can be phosphorylated, which is central to state transition, and Lhcb1 and Lhcb2 proteins have different yet complementary functional role (Pietrzykowska et al., 2014). Chloroplastic serine-threonine protein kinase STN7 phosphorylates Lhcb1 and Lhcb2 proteins at a threonine (Thr) residue near their near N terminus during their state transitions, and thylakoid-associated phosphatase 38 (also named protein phosphatase 1, TAP38/PPH1) catalyzes the reverse reaction. Collectively the balance between these two enzymes activities determines the phosphorylation state of LHCII. de Bianchi et al. (2011) showed that Lhcb4 proteins specifically function in protecting PSII from photoinhibiton using single or triple knockout of *Lhcb4* mutants. The triple knockout mutant (*koLhcb4*) didn't alter electron transport rates, but

it showed a disrupted PSII macrostructure and is defective in photoprotection as the single knockouts. *koLhcb4* also had a compensatory increase of Lhcb1 and a slightly reduced photosystem II/I ratio than wild type, and an increased sensitivity to high light stress. Studies also suggest that LHCBs are involved in ABA signalling partly by modulating ROS homestasis, supported by the fact that down-regulation or disruption of any LHCB isoforms reduced ABA-regulated stomatal movement while overexpression *LHCB6* enhanced the sensitivity to ABA (Xu et al., 2011). In current study, *gad2OE* and *pop2-8* had the most decreased expression of *Lhca2* and several *Lhcbs*, which is in agreement with the GO enrichment results. As their Fv/Fm also decreased the most after 6 d submergence (Fig 3.3), thus their photosynthesis capacity being the most inhibited during hypoxia.

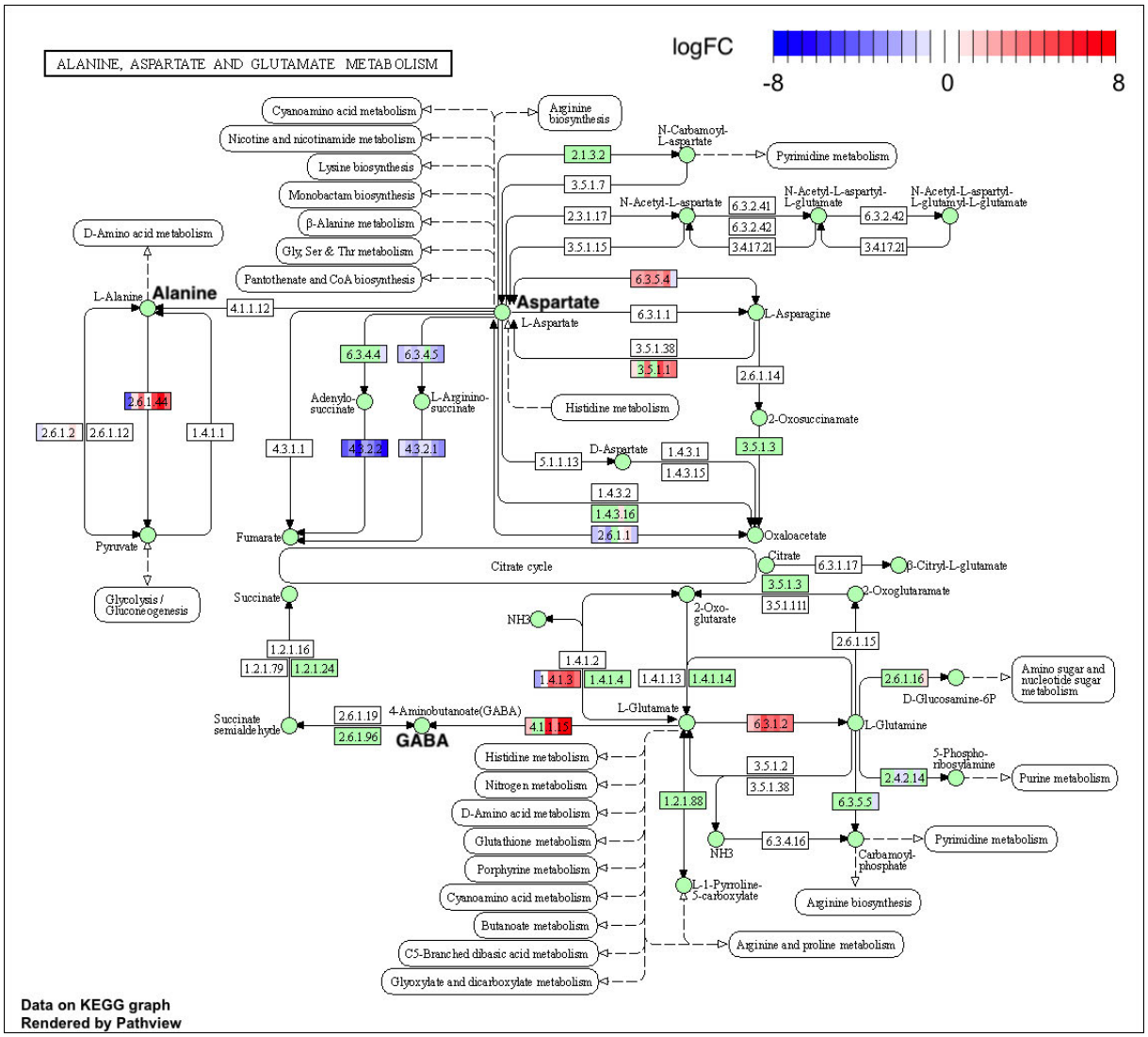


**Figure 3.27:** Differentially expressed genes of WT and GABA mutants in alanine, aspartate and glutamate metabolism (ath00250) after submergence. From left to right in a box: WT, *gad1*, gad1KO, gad2-1, gad1245, gad2OE, pop2-8.*

**Alanine, aspartate and glutamate metabolism**. All non-stressed mutants (except *pop2-8*) showed significantly enrichment in alanine, aspartate and glutamate metabolism

(Fig 3.11). However after submergence, only WT, *gad1KO* and *pop2-8* were enriched in the metabolism of these three amino acids, so whether prior-flooding changes contribute to their acclimation to stress is worth looking into.

Submergence didn't alter alanine:glyoxylate aminotransferase encoding gene *AGT3* expression in WT, but down-regulated its expression in all six mutants. Except for *gad1** and *gad2-1*, the other four mutants also showed increased expression of *AGT2*, but repressed expression in WT.

Submergence up-regulated GLN-dependent cytosolic *ASN1;1* expression in all seven lines, with *gad1KO* and *gad2OE* being the most affected, probably due to their prior-stress lower expression of this gene (Fig 3.14). In contrast *ASN2* show no changes in WT but down-regulated in all GABA mutants, and *ASN3* expression was decreased only in *pop2-8*. Collectively, *ASN* genes were induced by submergence in all lines except for *pop2-8*, in which the three genes in total turned out to be slightly down-regulated. Maaroufi-Dguimi et al. (2011) subjected one month old hydroponic plants to 6-24h 100 mM NaCl, and showed the T-DNA insertion *asn2-1* mutant had higher ammonium level and lower salinity tolerance than WT, due to impaired nitrogen assimilation and translocation. They also found increased ASN1 mRNA level in both WT and mutant leaves upon salinity, but inhibited transcript and protein levels of chloroplastic GLN2 in both lines. Asp and Pro accumulation in response to salinity provided evidence for their roles as prevailing stress responding amino acids. In the current study flooding also inhibited Glutamine synthetase 2 GLN2 (GS2) gene expression in the two *GAD1* lines (*gad1** and *gad1KO*) and two GABA-accumulating lines (*gad2OE* and *pop2-8*). By contrast, GS1 encoding genes *GLN1;1* and *GLN1;4* were induced in all seven lines, and submergence oppositely regulated *GLN1;3* in WT (down-) and *gad1KO* (up-). GS2-KO barley and Lotus were unable to grow under photorespiratory conditions but not GS2-KO *Arabidopsis* (Ferreira et al., 2019), as GLN1;3 acts redundantly with GDH in assimilating photorespiratory ammonium in the mutant, which also has increased salt tolerance. A recent study on *AtGS2-KO* plants by Hachiya et al. (2021) suggested that acidic stress through ammonium assimilation by GLN2 is the primary cause of ammonium toxicity in *Arabidopsis*, rather than its accumulation, which challenges previous knowledge.

**Arginine and proline metabolism**. Polyamine pathway can contribute to the hypoxia-induced GABA accumulation, too. A study on Fava bean seeds germination showed that under hypoxia, despite of GABA shunt, at least 30% of GABA formation is supplied by polyamine degradation pathway (Yang et al., 2013). In current study, there is a strong induction of genes related to arginine and proline in some GABA mutants, however, this pathway showed only to be in WT that was significantly affected by submergence, none of the GABA mutants, this is probably due to the mutants have already be greatly impacted (most DEGs repressed in nearly all GABA mutants as shown in Fig 3.13) in these processes under control conditions (Fig 3.11), and the changes induced by submergence were not

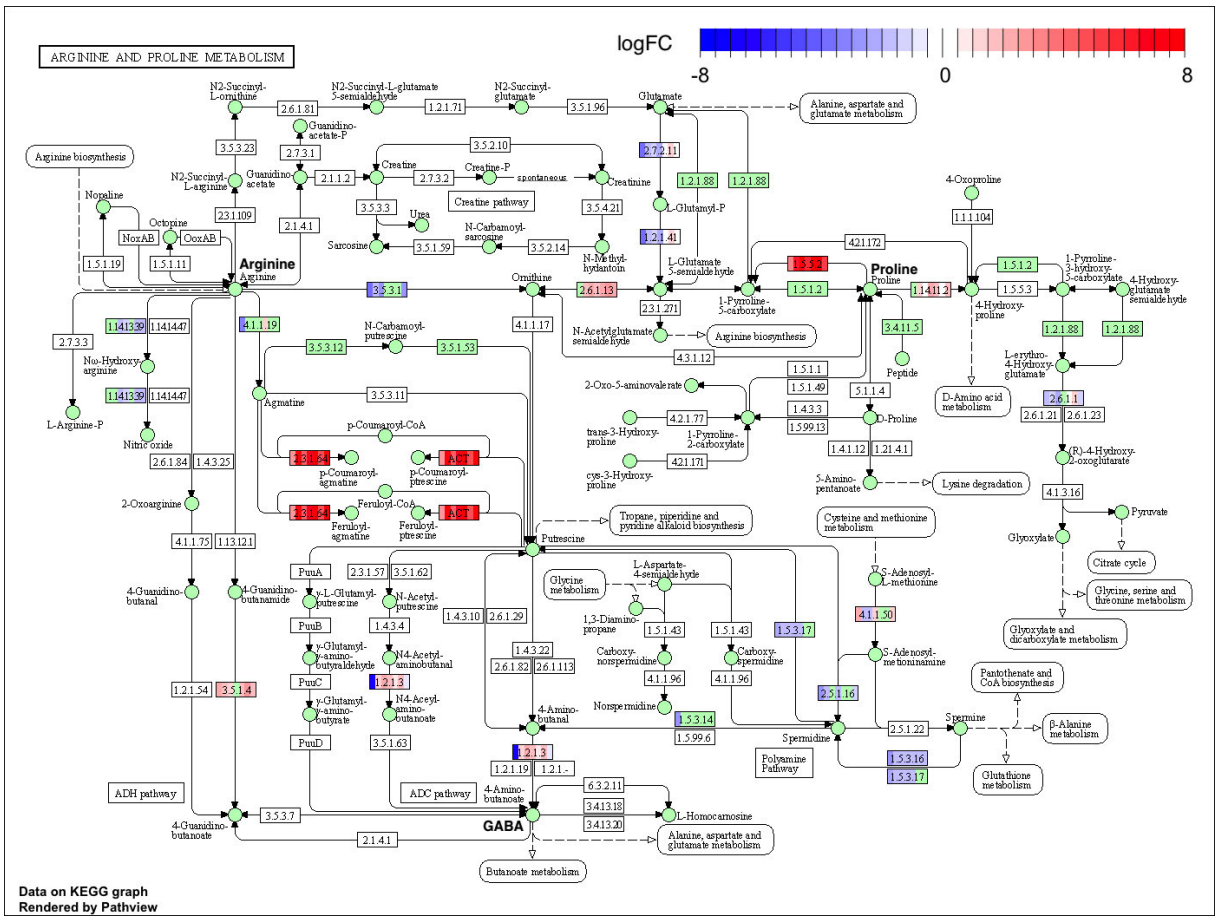


**Figure 3.28:** Differentially expressed genes of WT and GABA mutants in arginine and proline metabolism (ath00330) after submergence. From left to right in a box: WT, *gad1*, gad1KO, gad2-1, gad1245, gad2OE, pop2-8.*

as significant as in other pathways. After submergence, ADC, which functions in PA biosynthesis, was found to be down-regulated in WT and up-regulated in *gad1245*, but not altered in other mutants. This suggested the alternative PA pathway for GABA biosynthesis is promoted in this line as it could not use the GADs to produce GABA. An elevated *ALDH* expression was also seen, in all *GAD* mutants, but it was repressed strongly in WT and slightly in *pop2-8*, suggested the promoted mRNA from 4-ABAL to GABA in *GAD* mutants.

### 3.1.4 Mutation-specific transcriptional response to submergence

The previous section examined the submergence responses for each of the 7 lines, including WT and GABA mutants. However, further investigation was needed in order to ascertain how the GABA mutants respond to submergence due to disturbed GABA shunt capability. Therefore, common submerge responses as WT should be excluded, their transcriptomic differences to WT under control conditions should also be considered in order to get the mutation-specific submerge-response (MutSub).

### 3.1.4.1 Identification of mutation-specific differentially expressed genes in GABA mutants responding to submergence

In total there were 5878 mutation-specific submerge-response (MutSub) genes across all GABA mutants. As shown in Fig C.7, *pop2-8* still obtained the largest number of responsive genes (4679), followed by *gad2OE* (3277), *gad1245* (2859) and *gad1KO* (2242), while much less MutSub genes were found in *gad1** (578) and *gad2-1* (689). A similar pattern was seen in the UpSet plot (Fig 3.29). Most of the MutSub genes, either shared or unique, belonged to the four lines that had the most DE genes. For example, 790 DEGs were identified in *gad1KO*, *gad1245*, *gad2OE* and *pop2-8*. On the contrary, *gad2-1* and *gad1** only contain 48 and 12 DE genes, respectively. There were 2291 DEGs (39.0%) that exclusively belonged to either one of the six mutants, suggesting the plants underwent quite distinctive processes in response to submergence. Among them, 1466 DEGs belong to *pop2-8*.

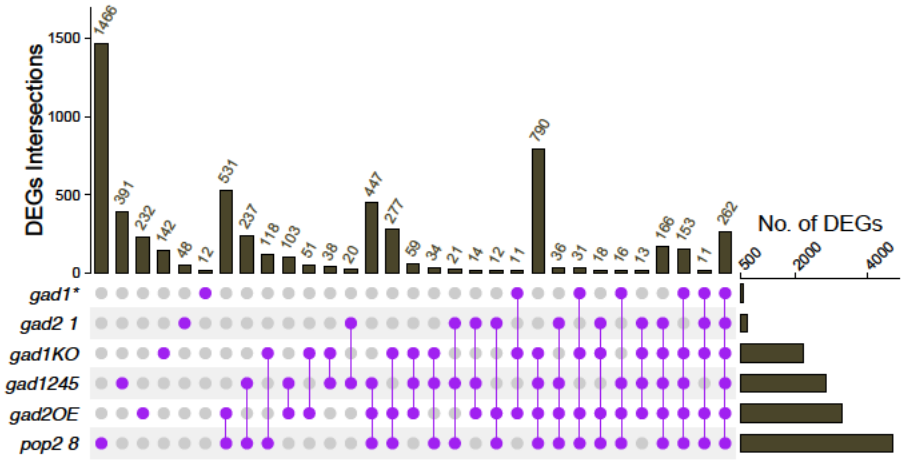


**Figure 3.29:** UpSet plot of intersected mutation-specific differentially expressed genes (DEGs) in GABA mutants after submergence. The number of DEGs in each mutant and overlapping DEGs across different mutants are shown in the bottom right bar chart and top bar chart, respectively. The dot matrix at the bottom left indicates the respective overlaps by connected purple circles. For example, *pop2-8* had the highest number of uniquely-regulated genes (1466 DEGs), while 790 DEGs were shared in four GABA mutants (not in *gad1** and *gad2-1*). Only overlaps with more than 10 DEGs were presented here.

The 5878 Mutation-specific submerge-responsive DEGs which appeared in at least one of the six GABA mutants were applied to the analysis of hierarchical clustering. Fig 3.30 showed that most of these genes followed the same up- (3147) or down- (2716) expression patterns in all six mutants, although some genes could be missing or more-/less- expressed in specific line(s). Only 15 shared genes showed had opposite expression between mutants, this is consistent with the previous section, as the majority of oppositely regulated genes by submergence was between WT and the GABA mutants (Fig 3.17). As Fig 3.31 showed, these DEGs were oppositely regulated between *pop2-8* and the other three GABA-deficient

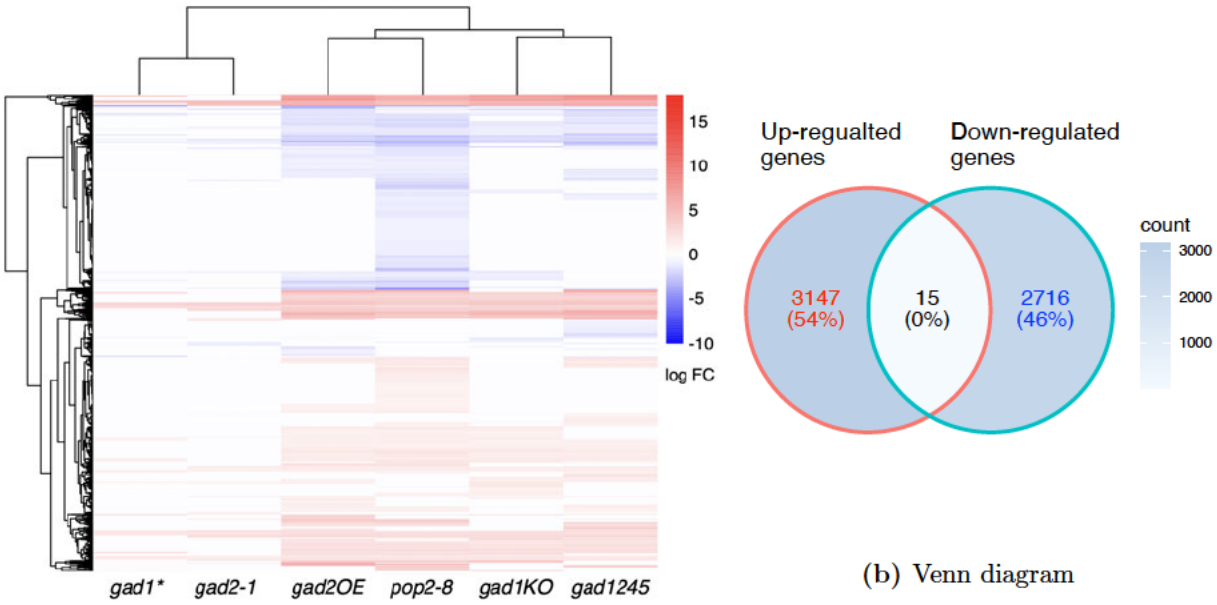


(a) Expression pattern of DEGs

(b) Venn diagram

**Figure 3.30:** Mutation-specific differentially expressed genes (DEGs) after submergence in GABA mutants. (a): Hierarchical clustering of log2 fold change. (b): Venn diagram. Up- and down- regulated genes of (a) log2 fold change and (b) DEGs number/proportion were indicated by red and blue, respectively. The fold change in each genotype was normalised against WT.

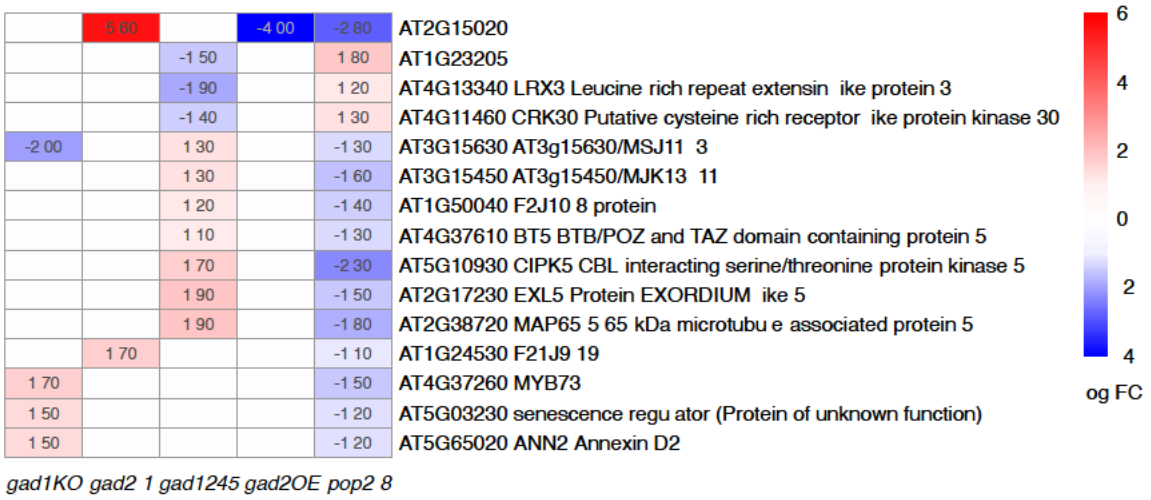


**Figure 3.31:** Oppositely regulated MutSub DEGs in GABA mutants after submergence.

lines, mainly *gad1245*.

**Mutation-specific expression of core HRGs in GABA mutants after submergence.** In the current study, half of the 52 core hypoxia-responsive genes were also mutation specific responsive (Fig 3.32). *gad1** and *gad2-1* only contained 5 and 3 MutSub DEGs, suggesting their response to flooding were more like wild type than the other mutants.

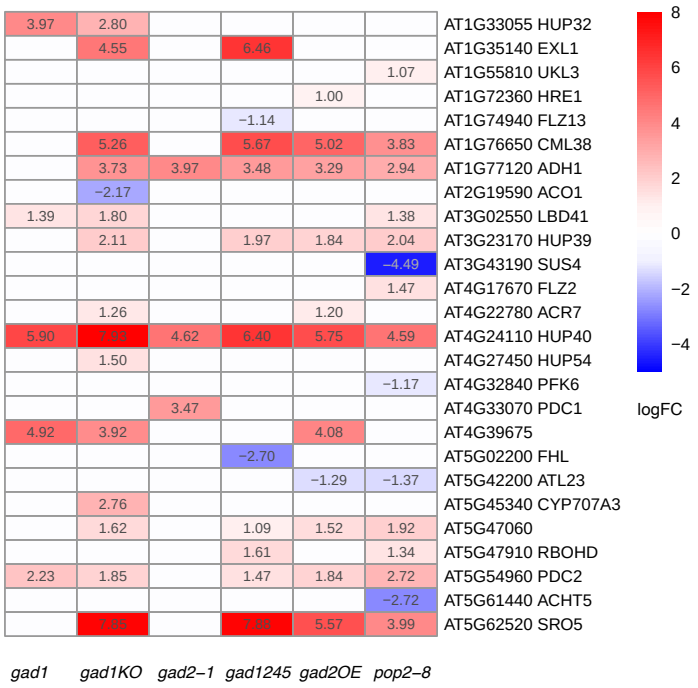


**Figure 3.32:** Log2 fold change of core hypoxia-responsive genes among MutSub DEGs in GABA mutants after submergence.

#### 3.1.4.2 GO enrichment analysis of mutation-specific submergence-responsive genes in GABA mutants

The mutation-specific submergence-responsive DEGs in each GABA mutant were split into up- and down- regulated genes and went through separate GO enrichment analyses, resulting in 101 (Fig 3.33a GO-Up results) and 98 (Fig 3.33b GO-Down results) enriched GO terms, respectively. A complete list of these terms is shown in Table C.7 in the same order as in the heat maps of Fig 3.33.

GO-Up results included 12 terms shared in all six GABA mutants, mainly response to ABA, JA, lipid, alcohol, fatty acid and decreased oxygen level, oxoacid metabolic process and carboxylic acid catabolic process. GO-Down results included five terms shared across all GABA mutants: polysaccharide metabolic process, external encapsulating structure organization, and auxin related processes such as response to auxin, cellular response to auxin stimulus, auxin-activated signalling pathway. As in Fig C.20, *gad1245* and the two GABA-accumulating lines shared 8 GO terms in GO-Up results. They were glutathione transferase activiy, protein serine/threonine kinase and flavin adenine dinucleotide binding, and five metabolic processes including alpha-amino acid, aromatic amino acid, indolalkylamin and tryptophan. In GO-Up results, response to reactive oxygen species (GO:0000302) and hydrogen peroxide (GO:0042542) were not enriched in *gad1** and *gad2-1*, and positive regulation of leaf senescence (GO:1900057) was also not enriched in *gad1245* (Table C.7), indicating that in response to submergence, these two lines were likely to experience less

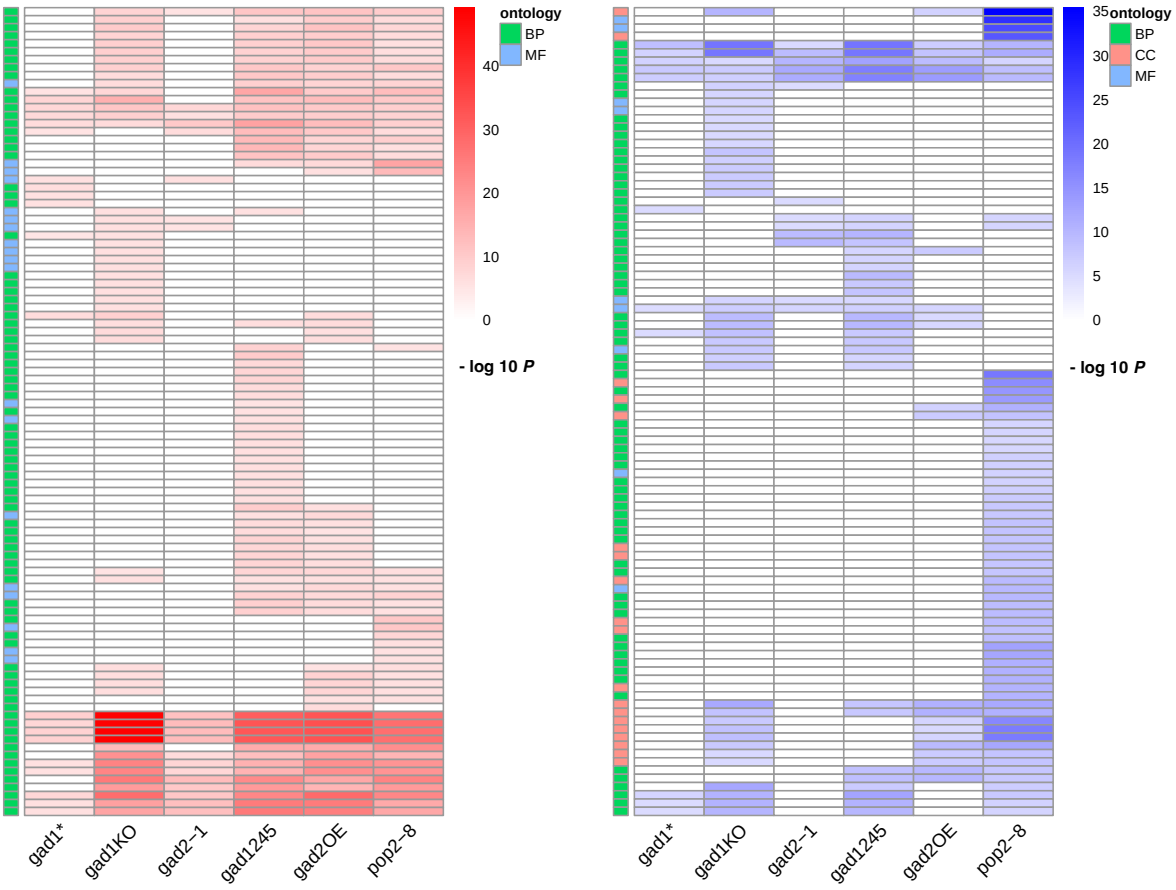


**(a)** Up-regulated genes enriched 101 terms

**(b)** Down-regulated genes enriched 98 terms

**Figure 3.33:** Clustering patterns of GO terms enriched through up- or down-regulated MutSub DE genes in GABA mutants after submergence. GO terms with Bonferroni adjusted $P < 0.01$ was considered significantly enriched and -log10 $P$ was presented in the heat maps. (a) 101 terms enriched by up-regulated genes. (b) 98 terms enriched by down-regulated genes.

ROS damage and senescence than WT, in contrast to the other mutants.

In GO-Down results, 15 out of 98 terms were related to chlorophyll biosythetic and metabolic processes or took place in plastid and chloroplast, which is similar to the previous section 3.1.3 where mainly *gad1KO*, *gad2OE* and *pop2-8* were greatly affected in these processes. Nine terms belong to 'CC' still showed up in all three lines, suggesting their DEGs function in these cell components, but mostly only *pop2-8* were enriched in the 6 biological processes (Fig C.22). In addition, dark reaction of photosynthesis (GO:0019685) were enriched in *gad1KO*, meaning the six DEGs involved in this process were more down-regulated than WT in response to submergence than the other mutants. *pop2-8* had 8 DEGs, but its total number of DEGs were larger, thus this process were not calculated as significantly over-represented, but still, these down-regulated genes suggest the mutants had less transcription related to the photosynthetis dark reaction, which could affect carbon fixation (Table C.7).

#### 3.1.4.3 KEGG enrichment analysis of mutation-specific submergence-responsive genes in GABA mutants

The mutation-specific submergence-responsive DEGs in each GABA mutant went through KEGG pathway analyses, resulting in 49 enriched pathways with distinct patterns (Fig 3.34) as summarised in Table C.8. Although the GABA-shunt pathway were affected differently in the mutants, the six enriched pathways shared across all six mutants suggested that: disturbed GABA shunt in general have these processes significantly affected by submergence and they were different from WT. These pathways were: plant hormone signal transduction and five metabolic processes involved lipids (fatty acid degradation and alpha-Linolenic acid metabolism), amino acids (valine, leucine and isoleucine degradation; beta-alanine metabolism), as well as terpenoids and polyketides (zeatin biosynthesis). Although all affected, *gad2-1*, *gad1245* and *gad2OE* were more promoted in some of the pathways than the other mutants.

Twenty-five pathways were partially shared across the mutants, which belonged to nine sub classes: "Amino acid metabolism" (×8), "Biosynthesis of other secondary metabolites" (×5), "Carbohydrate metabolism" (×3), "Energy metabolism" (×2), "Lipid metabolism" (×1), "Metabolism of cofactors and vitamins" (×2), "Metabolism of other amino acids" (×2), "Metabolism of terpenoids and polyketides" (×1), and "Signal transduction" (×1). Most of them showed up in *gad1245* (×19), *gad2OE* (×18) and *pop2-8* (×19) while *gad1KO*, *gad1** and *gad2-1* only had 12, 7 and 5 enriched pathways, respectively. This suggested that the strategies of *gad2-1* and *gad1** plants to cope with submergence were the least different from WT than the other four mutants.

Five pathways were shared among five mutants, leaving only one line not affected. "Glycine, serine and threonine metabolism" and "Tryptophan metabolism" were not in *gad2-1*; "Cysteine and methionine metabolism" and "Cyanoamino acid metabolism" were not in *gad1**; "Arginine and proline metabolism" not in *gad1KO*.

Once again, *gad1245* had some different response compared to its two parent lines. Three pathways were not enriched in *gad2-1* but they showed up in *gad1KO*, *gad1245*, *gad2OE* and *pop2-8*, i.e. starch and sucrose metabolism, glycerolipid metabolism and indole alkaloid biosynthesis. Pentose and glucuronate interconversions was not enriched in *gad1245* but it was in the two parent lines (*gad1KO* and *gad2-1*) of *gad1245*, as well as in *gad1**. On the contrary, eight pathways were enriched in *gad1245* but neither of its parent lines (Fig 3.34, Table C.8). Among them one was also enriched in *gad1** plants: lysine degradation; three also appeared in *pop2-8* plants: phenylalanine metabolism, isoquinoline alkaloid biosynthesis, glucosinolate biosynthesis; the other four also showed up in *gad2OE* and *pop2-8* plants: glutathione metabolism, tyrosine metabolism, limonene and pinene degradation,

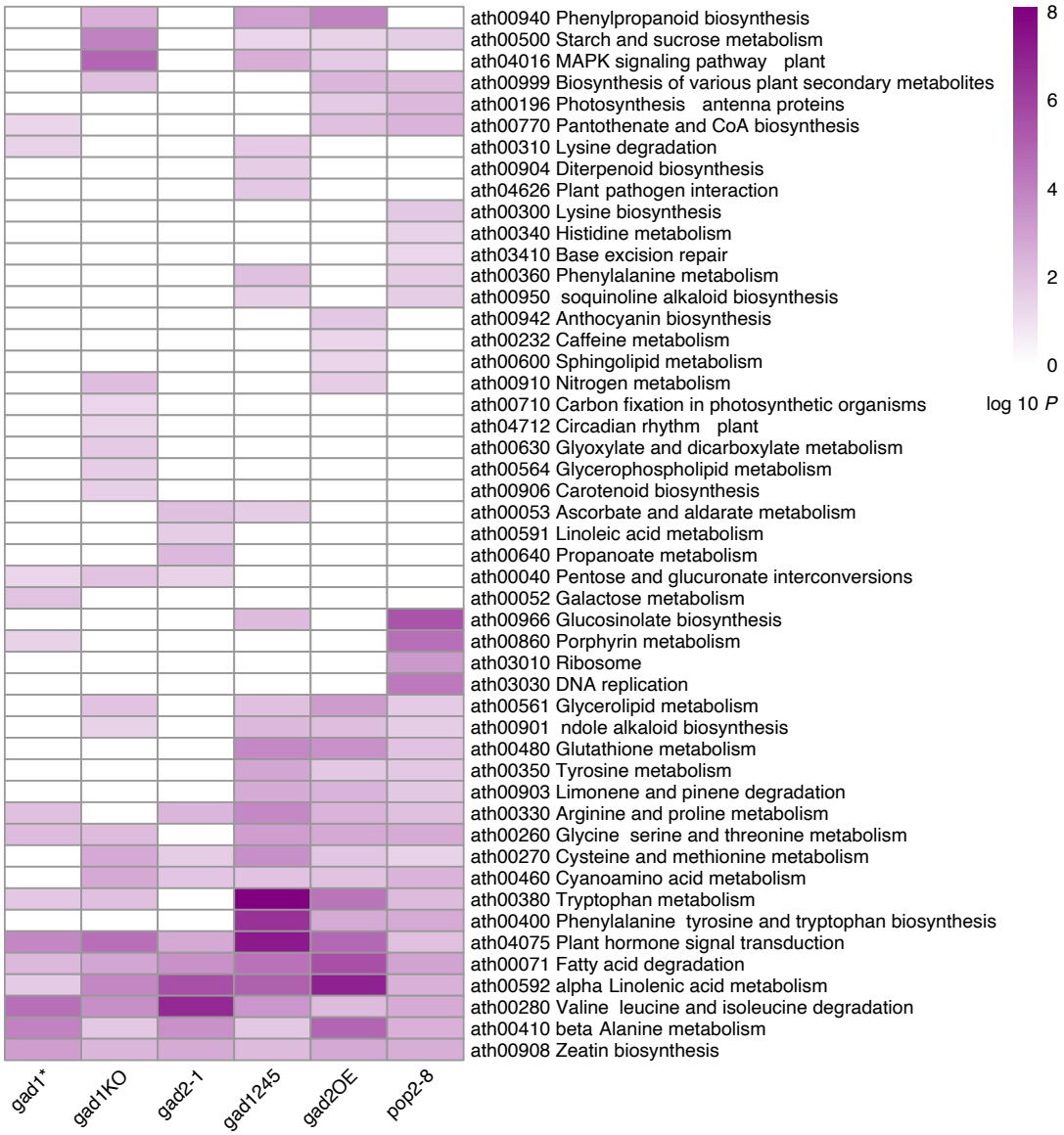


**Figure 3.34:** KEGG pathway analysis of mutation-specific responsive DE genes in GABA mutants after submergence. The clustered enrichment pattern displayed the -log 10 $P$ value. All coloured cells represented significantly enriched pathways with Bonferroni adjusted $P < 0.05$.

and phenylalanine, tyrosine and tryptophan biosynthesis. These results suggested that although the GABA content was significantly lower in *gad1245* than in either *gad2OE* or *pop2-8*, somehow they were still able to regulate similar processes in order to cope with submergence.

Eighteen pathways were uniquely enriched in one specific GABA mutants, with most metabolism related. The four GABA-deficient lines mainly involved in metabolism of carbohydrate, energy, lipid, terpenoids and polyketides while *gad2OE* and *pop2-8* participated mostly in secondary metabolites, amino acid and lipid metabolism. Other than the above metabolic processes, *gad1KO* and *gad1245* also corresponded to environmental adaptation, and *pop2-8* promoted genetic information processing (replication

and repair as well as translation). Specifically, they were: "Galactose metabolism" in *gad1**; "Propanoate metabolism" and "Linoleic acid metabolism" in *gad2-1*; "Diterpenoid biosynthesis" and "Plant-pathogen interaction" in *gad1245*; "Caffeine metabolism", "Anthocyanin biosynthesis" and "Sphingolipid metabolism" in *gad2OE*; "Glyoxylate and dicarboxylate metabolism", "Carbon fixation in photosynthetic organisms", "Glycerophospholipid metabolism", "Carotenoid biosynthesis" and "Plant circadian rhythm" in *gad1KO*; "Lysine biosynthesis", "Histidine metabolism", "DNA replication", "Base excision repair" and "Ribosome" in *pop2-8*. Only *pop2-8* plants involved in changed translation processes in response to flooding, suggesting a change of post-transcriptional in this line may happen.

**Tryptophan metabolism**. *gad1245* had greatly affected tryptophan metabolism compared to its two parent lines: *gad1KO* only enriched in a less extent while *gad2-1* not significantly affected at all. Tryptophan metabolism is pathogen-triggered and regulated by MYB transcription factors as well as products during indole glucosinate conversion. CYP79B2 and CYP79B3 enzymes work redundantly converting tryptophan to indole-3-acetaldoxime (IAOx). IAOx represents a branching point for indolic glucosinolate (IG) biosynthesis, camalexin and indole-carboxylic acids (ICA) pathways. As a secondary metabolite, camelexin functions as antimicrobial and antioxidative substances. In all GABA mutants except for *gad1** and *gad2-1*, the expression of *CYP79B2* was found to be up-regulated. *CYP79B3* was also up-regulated in *gad1245*, suggesting an increased production of IAOx and promoted pathogen response. Thus *gad2-1* plants may not experience as severe fungal attack than other lines, which could potentially be an advantage during the following recovery period.

### 3.1.5 Metabolomics response of GABA mutants before and after submergence

Although increased transcript abundance is usually regarded as induced gene expression, due to the variance of post-transcriptional regulation between different genes, transcript abundance may not necessary represent actual increased/decrease rates of gene transcription or reflect the amount of final active protein product. For example, Taylor et al. (2010) reported that anoxia altered abundance of mitochondrial proteins were not reflected in transcript levels. Therefore, a metabolomics analyses was conducted to determine if gene expression correlated with cellular metabolite changes in response to hypoxia stress.

#### 3.1.5.1 TCA intermediates content under control, submergence and recovery

For all mutants, the content of citrate, isocitrate and fumarate were significantly lower than WT under control, suggesting that the TCA cycle were affected due to disturbed GABA shunt efficiency.

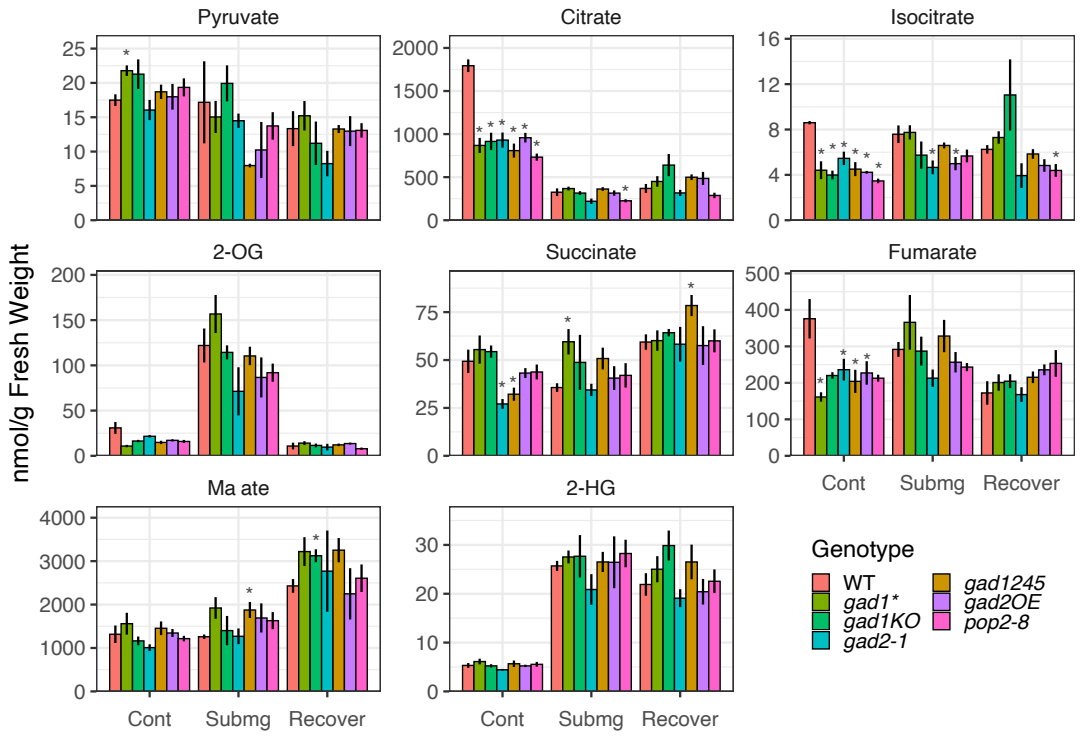


**Figure 3.35:** TCA intermediates content under control, submergence and recovery in WT and GABA mutants. Stars showed significance between WT and mutant under the same treatment ($P < 0.05$) using student t-test.

Pyruvate content was significantly higher in *gad1** compared to WT under control conditions. No significant differences in pyruvate were observed between mutants and WT under other conditions, except for *gad1245* pyruvate decreased greatly after flooding and then increased when returned to normal conditions, a different trend to other lines. Under control conditions, citrate and isocitrate content in all six GABA mutants, and fumarate content in four mutants were lower than that in WT, which could be due to decreased succinate levels as in the case of *gad2-1* and *gad1245* plants (Fig 3.35). After submergence, citrate levels in all lines largely decreased, with only *pop2-8* significantly lower than WT; after recovery no mutants showed significant differences compared to WT, although *gad1245* and *pop2-8* had relatively lower levels of citrate. The precursor of citrate, isocitrate content were not dramatically altered in most lines, still *gad2-1* and *gad2OE* under submergence and *pop2* after recovery still had lower levels of isocitrate than in WT under the same conditions. Succinate in *gad2-1* and *gad1245* under control conditions was significantly lower than WT, however, after 6d flooding, only *gad1** contained a higher level of succinate than WT. After a further 2d recovery, *gad1245* maintained the highest succinate content.

#### 3.1.5.2 Amino acid content under control, submergence and recovery conditions

Previous sections of this chapter have shown that there were significant changes in the transcriptome profiles between WT and GABA mutants even under control conditions, and many metabolic processes involving amino acid metabolism were significantly altered, however, the content of many amino acids were not (Fig 3.36).

Not surprisingly, *pop2-8* had the greatest GABA content under any conditions due to the block of GABA catabolism through the main GABA shunt pathway, while *gad2-1* and *gad1245* had minimal GABA content in all conditions. The extremely high accumulated GABA in *pop2-8* plants but none other lines also suggests that no matter under control or submerged conditions, GABA metabolism is a finely tuned and seems to be rapidly produced and catalysed if needed. In fact, GABA accumulation has also been reported in response to hypoxia within 24 h but it also decreased shortly after (Miyashita and Good, 2008), suggesting the fast catabolism of GABA. The expression of GAD1 in *gad1** leaves was much higher than in WT (Fig 3.20) but GABA concentration were not significantly higher than in WT leaves, which might be due to a much higher flux through the GABA shunt in *gad1** than in WT, resulting in a similar steady state GABA levels. This higher flux through the GABA shunt can be beneficial for carbon metabolism (Michaeli et al., 2011), which contributed to hypoxia tolerance of *gad1**. Previous studies have shown that except for the GABA shunt, other pathways such as polyamine oxidation could also contribute to GABA accumulation upon stresses, thus here the net minimal GABA observed in these two lines can either mean the GABA produced by the other pathway was efficiently consumed (as in Fig 3.35 higher succinate levels were seen in *gad1245*), or there may not be that much GABA produced under the condition of this experiment. *gad2OE* mutant didn't show a significant higher GABA concentration than WT under control and submergence, but only under recovery, suggesting that the driving promoter probably could contribute more to GABA accumulation during the post-hypoxic period rather than non-stress or submerged conditions. These observations confirmed that as the major pathway for GABA metabolism, a disturbed GABA shunt significantly changed the concentration of GABA either under normal or stressed conditions.

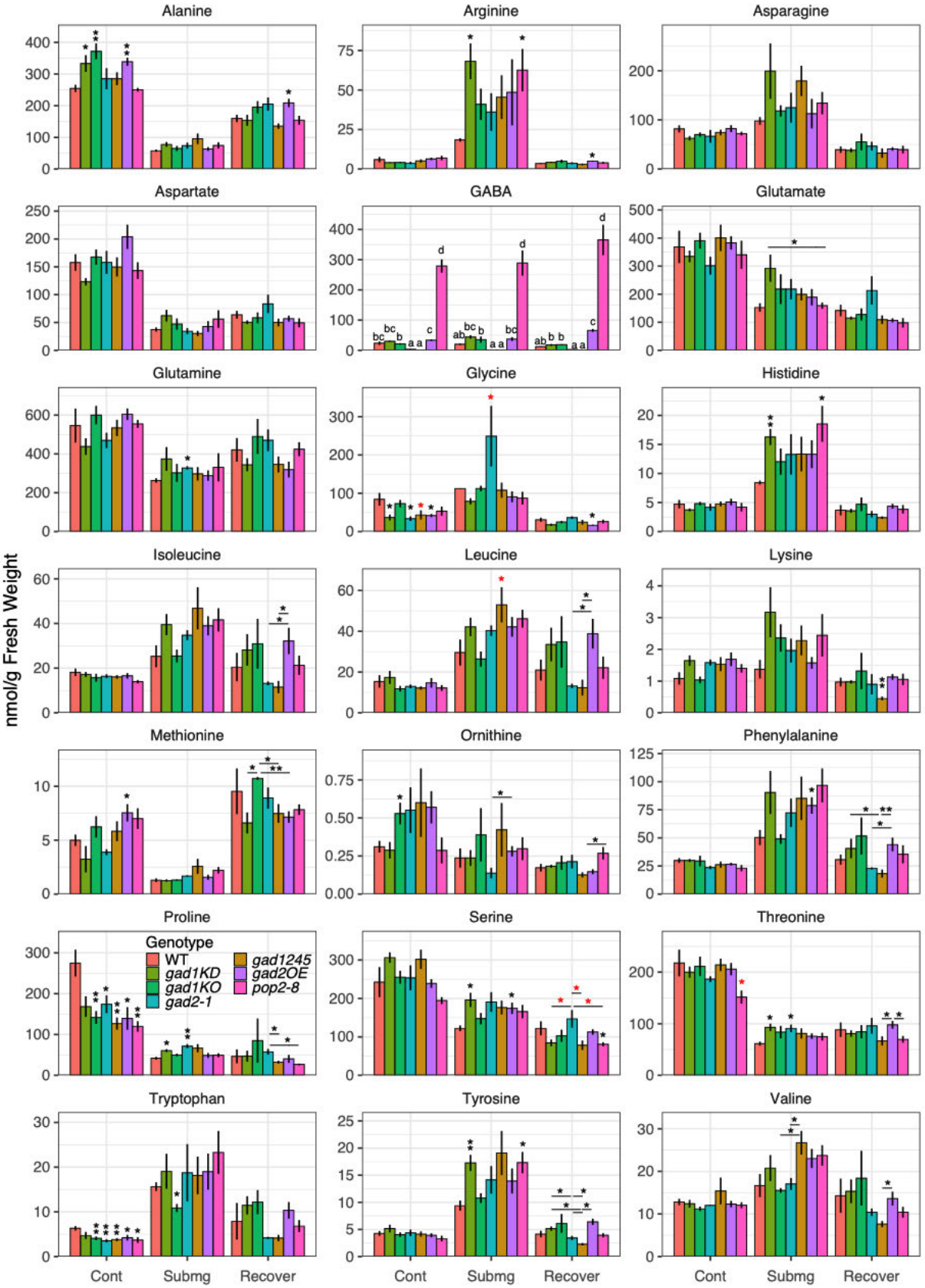


**Figure 3.36:** Amino acids content under control, submergence and recovery in WT and GABA mutants. Stars represent significance between WT and mutant under the same treatment ($P < 0.05$) using student t-test (black) or one way ANOVA (red). Different letters represent significant differences under the same conditions using one way ANOVA.

Alanine content was higher in control plants of the two *GAD1* lines and *gad2OE*, then it dramatically decreased in all lines after submergence, and increased to some extent after returning to normal conditions, with only *gad2OE* containing higher alanine than WT at the end of recovery. The observation of elevated/reduced Ala could be related to its decreased/increased catabolism to pyruvate, which involves several alanine aminotransferases that play important roles in amino acid metabolism and are closely related to the GABA shunt. When alanine is converted to Pyruvate, 2-OG is also converted to Glu, which is the substrate for GABA biosynthesis. For example, *alanine–glyoxylate aminotransferase 3* (*AGT3*) and the mitochondrial *AGT2 homolog 3* (*PYD4*) expresson in all control mutants was found to be repressed (Fig 3.14). However, after 6 d submergence, *AGT3* and *alanine aminotransferase 2* (*AlaAT2*) had promoted expression in all mutants but was not affected in WT, while *PYD4* expression was decreased in WT and increased in four mutants (not *gad1** and *gad2-1*).

Glutamate and glutamine content both decreased after submergence and in most cases there were not big differences between mutants and WT, this suggested that although glutamate metabolism in GABA shunt was affected in different manner, the mutants were able to adjusting other metabolic processes on their own need, through other pathways.

Methionine is the precursor of ethylene, and it could also be eventually converted into Spm and Spd, which play a role in polyamine pathway of GABA production. In the current study, *gad2OE* leaves had a higher Met content than WT leaves under control conditions, and there was no difference between all submerged leaves, while at the end of recovery, *gad1KO* had a higher Met content than three mutants (*gad1**, *gad1245* and *gad2OE*).

## 3.2 Conclusion

Under standard growth conditions, all GABA mutants showed normal development although GABA-deficient lines had significantly lower GABA content than both WT and *gad2OE*, while *pop2-8* maintained the highest content of GABA (Fig 3.36). In terms of biomass and PSII photosynthesis, there were also no significant differences between WT and the GABA mutants. The mutants do have differences in terms of water management, as the two GABA accumulating lines *gad2OE* and *pop2-8* had higher relative water content than the *GAD1* lines, especially *gad1KO* (Fig 3.2).

**Impaired GABA shunt pathway regulate submergence responses and recovery**. Under submergence, shoots tend to maintain a higher oxygen level than the other organs due to both the night-time inward diffusion from the water column and daytime endogenous production from underwater photosynthesis (Winkel et al., 2013; Rich et al., 2013).

After 6 d submergence, potential quantum efficiency of PS II (Fv/Fm) was significantly decreased (Fig 3.3), indicating less efficient use of light energy and more photoinhibition damage in all accessions under submergence. However, the different degree of Fv/Fm inhibition between all seven lines suggested the submerged plants could have maintained some oxygen in their leaves due to underwater photosynthesis, but it can be very different. In other words, the actually 'hypoxia' challenge each line faced was not exactly the same, although they were all subjected to submergence. Submergence affected the photosynthesis related process in GABA mutants more than WT, as all mutants "carbon fixation in photosynthetic organisms" was enriched except for *gad1245* and *gad2OE*, "Photosynthesis - antenna proteins" was also affected in *gad2-1*, *gad2OE* and *pop2-8* and the genes encoding LHC proteins were down-regulated in these lines (Fig 3.25), suggesting these mutants differ to WT in terms of photosynthesis. In agreement with the physiological results, GO enrichment analysis revealed that three of the GABA mutants, *gad1KO*, *gad2OE* and *pop2-8* differentially regulated genes were over-represented in the chlorophyll biosynthetic and metabolic process, suggesting the importance of *GAD1* and *GABA-T* in submerged plants to maintain underwater photosynthesis. As under control conditions, these processes were not significantly altered compared to WT (Fig 3.11), it seems submergence greatly impaired the capability of GABA mutants to maintain photosynthesis. This is in corresponding with the Fv/Fm results as *gad1245* and *pop2-8*, which had the most disturbed GABA shunt, decreased more than the other mutants in Fig 3.3 after submergence.

**Transcriptionally primed GABA mutants before submergence**. Under abiotic stress, transcription factors that are hormone- and stress-responsive participate in the regulation of plant hormone signalling pathways. Current results showed that although physiologically no significant differences could be observed, the transcripts of GABA mutants have shown acclimation to multiple stresses/hormones under control conditions. Promoted oxygen sensing in GABA mutants under control conditions may occur due to altered GO processes related to oxygen levels, as well as the *RAP2* family related genes expression. Enhanced response to plant hormones in GABA mutants under control were also seen, except for *gad2-1* which showed less impact in these two pathways. In addition, altered circadian rhythm (not *GAD1* mutants), and greatly affected metabolic processes especially the two most closely related to the GABA shunt (alanine, aspartate and glutamate; arginine and proline) occurred in non-stressed GABA mutants. All of these transcriptome adapatations could be correlated to the hypoxia tolerance. Moreover, the importance of *GAD1* in leaves was shown in response to light submergence, as its expression dramatically increased in all lines, more than that of *GAD4* (Fig 3.20), while *GAD4* induction was reported previously (Miyashita and Good, 2008; Wang et al., 2014) but not for *GAD1*. This is supported by the fully recovery of Fv/Fm (Fig 3.3) in the *gad** plants which had high *GAD1* expression in leaves and shoots, and the relative higher tolerance in the *gad2-1* plants than the mutants that had *GAD1* knockout such

as *gad1KO* and *gad1245*. Also, *gad1** and *gad2-1* plants have less transcripts related to responses to ROS and hydrogen peroxide, which potentially mean these two lines experienced less oxidative stress than the other lines. This could be due to the current submergence experiment was not under complete darkness, which could induce more severe leaf senescence in the two GABA accumulating lines than in *gad2-1* and WT as shown in Fig C.2a. The greatly increased *GAD1* expression after submergence were also reported recently in WT and some mitochondrial mutants when submerged under day/light cycles which was of greater fold change than *GAD4* (Meng et al., 2020).

**An impaired GABA shunt pathway affects metabolic profiles before, during and after submergence**. The reconfiguration of N metabolism upon hypoxia and recovery is critical, during which alanine aminotransferase (AlaAT) and glutamate Dehydrogenase (GDH) both play important roles (Diab and Limami, 2016), and these genes were also DEGs in GABA mutants. Liu et al. (2021) studied two peanut cultivars after 12d waterlogging and found that differentially accumulated proteins (DAPs) uniquely in the roots of the tolerant line were related to malate metabolism and glyoxylic acid cycle, e.g. L-lactate dehydrogenase (LDH), $NAD^+$-dependent malic enzyme (NAD-ME), aspartate aminotransferase (AspAT) and glutamate dehydrogenase (GDH). The tolerant line also had higher activity of alcohol dehydrogenase (ADH) and malate dehydrogenase (MDH), and prolonged activity of LDH than the sensitive line upon waterlogging. It acquired a better tolerance to waterlogging due to efficiently using various carbon sources (through enhanced anaerobic respiration, malate metabolism and glycoylic acid cycle) to maintain energy and thus decreasing the accumulation of toxic substances upon stress (Liu et al., 2021). In the current study, the higher accumulation of alanine could contribute to plants adaptation under submergence and recovery. Proline accumulation under stresses is related to control the stability or activity of ROS scavenging enzymes (e.g. APX, GSH) in the glutathione-ascorbate cycle (Székely et al., 2008). In this study, most of the mutants had lower proline than WT before submergence, but after submergence, only in *gad1** and *gad2-1* was the proline content higher than submerged WT plants. This is in line with altered expression of genes related in these metabolic processes(Fig 3.13, 3.28), and also with the better overall performance of these two lines, again with the GO enrichment results, suggesting them experiencing less ROS-induced damage than other lines. Alanine metabolism is closely related to GABA metabolism and it was transcriptionally affected under both normal and submergence (Fig 3.14, 3.27). The hypoxia induced alanine accumulation was reported to be important for tolerance of plants, and it could be partially derived from the GABA shunt pathway (Miyashita and Good, 2008). Under submergence, the rapid accumulated GABA could be converted to SSA by GABA-T (the *pop2-8* plants could accumulate higher level of GABA), using pyruvate as the amino receptor and thus produce alanine in the same time. The alanine concentration in *gad1245* and *pop2-8* were both lower compared to *GAD1* lines under control conditions, and to *gad2OE* after

recovery. One reason could be in these two lines the flow of the GABA shunt pathway is reduced, due to *GADs* knockout and *GABA-T* knockout, respectively.

The current study showed different tolerance and strategies of the GABA mutants to cope with submergence, illustrated their physiological, transcriptional and metabolic responses, suggested the essential nature of *GAD1* and *GABA-T* in regulating GABA concentration to submergence and the post-hypoxia stresses.

## 3.3 Materials and methods

### 3.3.1 Plant material and growth conditions

Seven lines of *Arabidopsis* were used in the experiment as described previously (Table 1.2). The mutants were:
GAD1 T-DNA insertion which did not result in GABA-deficient: *gad1**. GABA-deficient lines: *gad1KO, gad2-1*, and *gad1245*.
GABA-accumulating line by GAD2 over expression: *gad2OE*.
GABA-accumulating line through GABA-T deficiency: *pop2-8*.

Seeds were sown in pots containing vermiculite, perlite and soil in a 1:1:3 volume mixture and cold stratified in the dark for 3 d. The pot plants were transferred to a climate-controlled chamber. The temperature was 22°C/22°C (day/night), relative humidity was 65%, and photoperiod was 14 h/10 h (day/night) at 120 $\mu$mol $m^{-2}sec^{-1}$ photosynthetic photon flux density (PPFD). The pots were wrapped with a black mesh with a small hole for the seedling to grow through at the four-leaf stage. This was to prevent the leaching of soil material during subsequent submergence.

For the submergence treatment, 4.5 weeks old plants were completely submerged for 6 d in transparent bins (volume: 75 L; height: 50 cm) filled with 40 cm of water, and the light was slightly dimmed to 100 $\mu$mol PPFD. For de-submergence (Recovery) treatment, the plants were removed from the water and transferred back to standard growth conditions as above for 2 d.

Leaf tissue of six individual *Arabidopsis* plants was harvested at midday for total RNA and metabolites extraction before (Day 0, Control) and after submergence (Day 6, Submergence) as well as after de-submergence (Day 8, Recover). Samples were weighed, sealed in 1.5 mL Eppendorf tube, and quickly snap frozen using liquid nitrogen. All samples were stored in -80°C until extraction.

The main experiment of this chapter was conducted in the Whelan lab at La Trobe

University, and the other independent submergence and recovery experiments were repeated afterwards in the Gilliham lab at the University of Adelaide in a short-day growth room (10/14 h day/night cycles instead of 14h/10h, Fig C.1, C.2).

### 3.3.2 Biomass and maximum quantum yield

Rosette fresh weight (FW), turgid weight (TW) and dry weight (DW) and relative water content (RWC) were measured and calculated using equation 3.1 (Yeung et al., 2018).

$$RWC(100\%) = \frac{FW - DW}{TW - DW} \times 100 \tag{3.1}$$

Maximum quantum yield (Fv/Fm, variable fluorescence/maximal fluorescence) were determined according to Rossel et al. (2006). Briefly, after short (5 min) dark acclimation, pulsed actinic light at 120 $\mu$mol $m^{-2}sec^{-1}$ were applied to the plants using the IMAGING-PAM M-series Chlorophyll Fluorescence System according to the manufacturer's instructions (Walz). Leaves with an Fv/Fm below detection level were marked as dead.

### 3.3.3 RNA-seq and bioinformatic analyses

Mature leaf tissue of three biological replicates from the control and submergence treatments for each line were used. Five to ten leaves from each plant were pooled and ground using a Tissue Lyser II (Qiagen). Total RNA was isolated using the Spectrum™ Plant Total RNA Kit (Sigma) according to the manufacturer's instructions, and DNA was removed via on-column DNase digestion using the RNase-Free DNase kit (Sigma). The RNA was eluted in molecular grade DNase- and RNase-free water (Sigma) and integrity validated on agarose gels. The libraries for RNA-seq were constructed according to the manuals provided by the TruSeq Stranded mRNA Library Prep Kit (Illumina, Scoresby, Victoria, Australia) and then sequenced on the NextSeq 500 system platform (Illumina) as 76-bp single-end reads with an average quality score (Q30) of above 95% and on average 23M reads per sample. Libraries were prepared and sequenced in the Whelan lab at La Trobe University.

To process raw sequencing data to gene counts, multiple tools were used for checking the read quality and trimming, mapping and counting. Raw sequencing reads were checked for quality using FastQC (version 0.11.8) and adapters trimmed with Trimmomatic (version 0.39) (Bolger et al., 2014). The trimmed FASTQ reads were mapped to the TAIR10 reference genome (`https://www.arabidopsis.org`) using STAR (version 2.7.3a) (Dobin et al., 2012). Aligned reads of each gene were counted based on the Araport11 genome annotation by featureCounts in Subread (version 1.6.4) (Liao et al., 2013b) The mapping of raw sequencing data to gene counts were performed by Charlotte Sai in Snakemake (Köster and Rahmann, 2012) and processed on the University of Adelaide's

High Performance Compute (HPC) Service - 'Phoenix' (https://www.adelaide.edu.au/technology/research/high-performance-computing/phoenix-hpc).

The following analysis includes differential gene expression, functional and pathway analysis conducted in R (version 4.0.3). The R package 'edgeR' (version 3.34.1) was used to test for differential gene expression (Chen et al., 2016). Lowly expressed genes (less than five counts in a quarter of all samples per line) were eliminated using the *filterByExpr()* function in the edgeR. Genes had absolute log2 Fold Change $> 1$ and Bonferroni adjusted $P$ value $adj.P < 0.05$ were regarded as differentially expressed genes (DEGs). Overlaps in the list of DEGs across different comparison groups were identified and visualised by UpSet plots using R function *UpSetR* (version 1.4.0) in the package 'ComplexHeatmap' (Conway et al., 2017). Heatmaps were drawn using R function *pheatmap* (version 1.0.12) in the ComplexHeatmap (Kolde, 2019). Gene Ontology analysis was performed using biomaRt (Durinck et al., 2009), GO.db (Carlson, 2021) and annotate (Gentleman, 2021) to determine the genotype specific functional enrichment (i.e. over-represented processes). KEGG (Kyoto Encyclopedia of Genes and Genomes) pathway analysis (using KEGGREST) was performed to determine pathway enrichment between WT and GABA mutants under control and submerged conditions (Tenenbaum and Maintainer, 2021). Detailed parameter settings are contained within R code and R session information available on GitHub (https://github.com/LillyCollins/ArabidopsisRNAseq_Control.git for control plants, https://github.com/LillyCollins/ArabidopsisRNAseq_Submergence.git for submergence response of WT and GABA mutants, https://github.com/LillyCollins/ArabidopsisRNAseq_MutSubmg.git for mutation-specific submergence response of GABA mutants).

### 3.3.4 Metabolite extraction and quantification

Metabolite extraction was conducted at Metabolomics Australia Perth according to the protocol they provided. They provided: (1) extraction buffer, chloroform/methanol/water (1 : 2.5 : 1, vvv); and (2) Mastermix, 0.5 mL ice cold extraction buffer and 0.5$\mu$L each internal standard (sorbitol and valine) per sample. After weighing out frozen leaf sample (normally >30 mg) as quick and cold as possible, 2 beads were added to the tube and the tissues were ground with Retsch Mill for 1 min (up to 3 min for larger sample) using pre-frozen trays. Then immediately mastermix was added to the ground sample, vortexed for 15 min, shaken at 4°C for 15 min in ice blocks on the Multitube vortexer, centrifuged at 14,500g for 3 min at 4°C to remove debris, and all of the supernatant was transferred to clean 1.5 mL tube on ice (Tube 'A'). Metabolites were extracted again from the remaining pellet by adding 0.5 mL cold extraction buffer (without internal standards), vortexing for 15 sec, repetition of the above shake and centrifuge processes, and the supernatant was also transferred to Tube 'A'. Tube 'A' was centrifuged again and 0.8mL supernatant were transferred to a new labelled 1.5 $\mu$L tube (Tube 'B'). 0.4 mL of water was added

to Tube 'B', which was then vortexed for 1 min and centrifuged for 3 min. Then 700 $\mu$L of the extract's polar (upper) phase was transferred to a clean 1.5 mL tube (Tube 'C'), and 60 $\mu$L was aliquoted into glass insert placed inside of a labelled 1.5ml tube (Tube 'D'). 20 $\mu$L of every sample was transferred into a new 2 mL Eppendorf tube for pooling and with 5x 60 $\mu$L aliquoted as a pool. All pulled samples were dried down in speed vac overnight at room temperature together with remaining extract tubes, as metabolites degrade completely within 24 h in extraction buffer. Once completely dry, samples were stored at -80°C and they were re-dried for 30 min before GC-MS run.

Semi-quantitative analysis of polar metabolites were conducted by Metabolomics Australia Perth using TMS derivatisation and Gas Chromatography–Mass Spectrometry (GCMS) instrumentation, and the results were divided into metabolites within the TCA cycle and other metabolites. Vendor software and databases for the analysis and identification of the metabolites were used, and used the quality control standard mix from Metabolomics Australia Perth were used to validate the results. The results (arbitrary numbers without a unit) represented the area below the compound peak in the chromatogram of the GCMS analysis, also referred to as the abundance. The results were normalised to an internal standard to compare one compound within several samples, adjusted for 100mg fresh weight of each sample, and then the percentage of the metabolite abundance per total abundance was calculated for metabolites in each sample.

Quantitative analyses were also conducted by Alex Lee (ARC Centre of Excellence in Plant Energy Biology) using liquid chromatography selective reaction monitoring mass spectrometry (LC-SRM-MS). For organic acids, 50 µL of 250 mM 3-nitrophenylhydrazine in 50% methanol, 50 µL of 150 mM 1-ethyl-3-(3-dimethylaminopropyl) carbodiimide in methanol, and 50 µL of 7.5% pyridine in 75% methanol were mixed and allowed to react on ice for 60 minutes for each of 100 µL of sample. 50 µL of 2 mg mL-1 butylated-hydroxytoluene in methanol was added to terminate the reaction, followed by the addition of 700 µL of water. Derivatized organic acids were separated on a Phenomenex Kinetex XB-C18 column (50 x 2.1mm, 5µm particle size) using 0.1% formic acid in water and methanol with 0.1% formic acid as the mobile phase. For amino acid, dried samples were re-suspended in 50 mL water. Chromatographic separation was performed using Agilent Poroshell 120 HILIC-Z column, using mobile phases of 20 mM ammonium formate in water and 20 mM ammonium formate in acetonitrile. The Agilent 6430 Triple Quadrupole mass spectrometer (QQQ-MS) was operated in negative (organic acids) or positive (amino acids) ion mode in selective reaction monitoring (SRM) mode. For each sample, 1 $\mu$L or a 15 $\mu$L aliquot was injected and analysed using an Agilent 1100 HPLC system coupled to QQQ-MS an equipped with an electrospray ion source. Data acquisition and LC-MS control were done using the Agilent MassHunter Data Acquisition software. Data acquisition and analysis were carried out using Agilent MassHunter Data Acquisition and MassHunter

Quantitative Analysis Softwares. Metabolites were quantified by comparing the integrated peak area with a calibration curve obtained using authentic standards, and normalised against fresh weight and internal standards.

CHAPTER 4

# The role of the putative GABA binding motif in regulating pH-dependent anion transport

The gamma-aminobutytic acid, GABA, was found to be rapidly accumulated in plants under stresses (Loreti et al., 2016). The aluminum-activated malate transporters (ALMTs) contribute to plants' tolerance towards toxic aluminum ions in the soil (Meyer et al., 2011; Luu et al., 2019). GABA can reduce the anion transport activity of ALMT and the inhibition was proposed to occur via a direct interaction with the putative binding motif (12 amino acids) (Ramesh et al., 2015). A substitution in the first amino acid residue of ALMT could abolish the its sensitivity to GABA, and the interaction was proposed to be in the cytosolic site of the membrane (Ramesh et al., 2015; Long et al., 2019). For detailed review see Chapter 1 Section 1.5. In this chapter, the potential role of this putative plant GABA biding motif in regulating anion transport under different pH was explored, to better understand how GABA signalling through ALMT. Substitution of the last residue was conducted and whole cell currents under different solution and pH combinations were investigated. The channel activity and pH sensitivity of both wild type and mutants were studied.

## 4.1 Results

After site-directed mutagenesis PCR, cDNA of the two mutants were sequenced and confirmed the mutation at the site of H224 (Fig D.1) into alaninie (H224A, FigD.1a) and arginine (H224R, FigD.1b). Then the cRNA of TaALMT1 WT and three mutants ($TaALMT1^{F213C}$, $TaALMT1^{H224A}$ and $TaALMT1^{H224R}$) were injected into *X. laevis* oocytes to express for 1-2 d. All control or gene-expressing oocytes were pre-loaded with 10 mM malate via injection 1-4h before testing them in different solutions (low or high pH with

or without 10 mM malate).

### 4.1.1 External malate activated TaALMT1-mediated currents were altered by site-mutations at alkaline pH

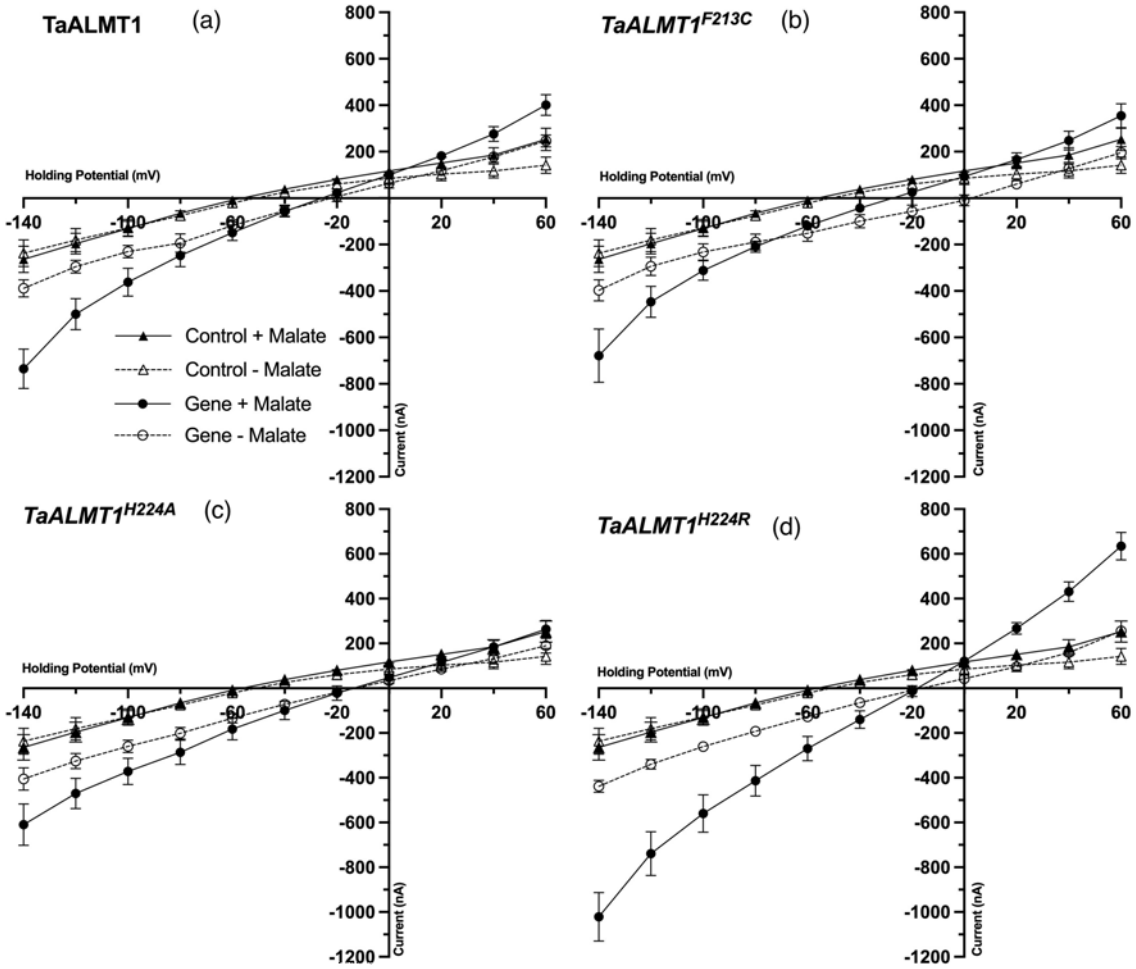


**Figure 4.1:** Electrophysiological characterisation of control (i.e. not injected with cRNA, triangles) and gene-expressing (circles) *X. laevis* oocytes preloaded with malate at pH 7.5. Mean I/V relationship of n $\geq$ 6 oocytes recorded in the absence (white symbols) and presence (black symbols) of 10 mM malate in the recording solutions. Data show mean $\pm$ SEM. Oocytes were injected with water or cRNA of TaALMT1 wildtype or site-directed mutants.

The ionic conductance of TaALMT1, $TaALMT1^{F213C}$, $TaALMT1^{H224A}$ and $TaALMT1^{H224R}$ were examined firstly under pH 7.5 with and without external malate. Adding 10 mM malate to the pH 7.5 solution resulted in significantly enhanced inward negative currents in the wildtype TaALMT1-expressing cells but not in water injected control cells at holding potential $\leq$ -100 mV, suggesting that malate efflux can be activated by external malate through TaALMT1 (Fig 4.1(a), 4.4a), as expected. The increased current magnitude due to to external malate in the media was significant at holding potentials more negative than -60 mV in $TaALMT1^{H224R}$ injected cells while in $TaALMT1^{F213C}$ injected cells the differences

were evident at more negative holding potential (-140 mV) and in $TaALMT1^{H224A}$ injected cells this was not seen.

A closer examination of currents at -120 mV were conducted for all genotypes under either solution (Fig 4.4a). Compared to TaALMT1, $TaALMT1^{F213C}$ and $TaALMT1^{H224A}$ abolished the malate-activation at -120 mV, while $TaALMT1^{H224R}$ showed a significant and an approximately 2.5 fold greater malate efflux due to the addition of malate to the basal solution. This indicates the substitution of the first or last residue of the putative GABA binding motif changed its channel activity in response to external malate. In accordance with this, in pH 7.5 solutions containing malate, $TaALMT1^{H224R}$ also had larger negative currents than the other two mutants, however there were no significant differences between TaALMT1 and any of the mutants in non-malate solutions (Fig 4.4a). These results suggested that both TaALMT1$^{F213C}$ and TaALMT1$^{H224A}$ have a severely diminished ability to transport anions at alkaline pH. However, substituting an Arginine for the Histidine residue somehow enhances the malate-activated anion efflux.

In addition, whether in the presence or absence of 10 mM malate in the recording solution, there was a positive shift (20∼40 mV) of reversal potential (i.e. the voltage at which the net current is zero, $E_{rev}$) in all the gene-injected cells compared to control cells ($E_{rev}$ = -10 mV). This shift of $E_{rev}$ of the inward current maybe due to TaALMT1 currents being mediated by anion efflux, suggesting larger malate efflux due to TaALMT channel functioning well regardless of the substitution of an amino acid, or may be due to a consequence of mRNA injection – which is common. Further, examination would need to be undertaken to differentiation of these two possibilities. For $TaALMT1^{F213C}$-expressing cells the addition of external malate to the media resulted in a negative 20 mV shift of $E_{rev}$, from 0 mV to -20 mV, suggesting that the external malate enhanced malate efflux in these two lines is due to both the altered transporter's selectivity and its increased anion permeability. This may explain the larger malate activated currents detected from this construct shown previously (Ramesh et al., 2015), although this was not observed here at -120 mV (Fig 4.4a). On the contrary, all other constructs didn't have an altered $E_{rev}$ upon exposure to malate, suggesting that external malate enhanced malate efflux is not due to an altered transporter's selectivity but solely due to its increased anion permeability. On the contrary, water-injected cells didn't show a significant shift of reversal potential whether the media contains malate or not.

Taken together, and the previous results of Ramesh et al. (2015), where $TaALMT1^{F213C}$ had enhanced malate active currents, the increased/decreased magnitude of both negative and positive currents and the shifted reversal potential indicate that TaALMT1 can regulate an external malate enhanced malate efflux from the cell. This regulation may be altered by a cysteine substitution of the first residue (Phenylalanine) of the GABA-binding

motif although the contradiction in my data and that of Ramesh et al. (2015) needs to be further explored. Substitution of the histidine with an alanine inhibited transport capacity. Furthermore, currents were promoted by an arginine substitution of the histidine residue. This may be a result of alanine being uncharged and hydrophobic, while arginine are positively charged and hydrophillic and therefore the H224R substitution could help stabilise the protein. Alanine also has a much smaller molecular weight compared to the other two amino acids, which could affect the structure of the protein more.

### 4.1.2 External malate activated TaALMT1-mediated currents were altered by site-mutations at acidic pH

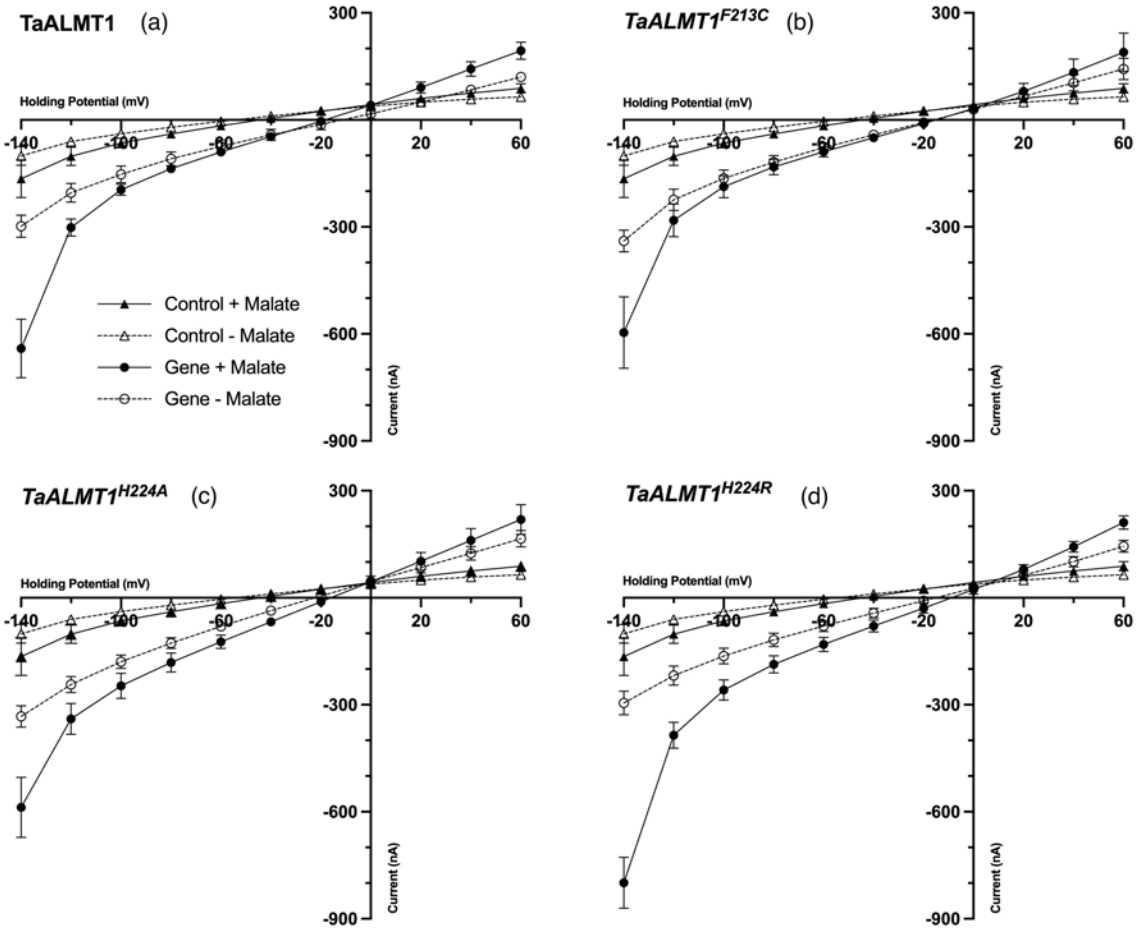


**Figure 4.2:** I-V plots of water-injected (control) and gene-injected *X. laevis* oocytes preloaded with malate and tested at pH 5.5. Oocytes were injected with water or cRNA of TaALMT1 wildtype or site-directed mutants. Two types of recording solutions were used, either plus 10 mM malate or without malate. n $\geq$ 6, data showed mean $\pm$ SEM.

In terms of how WT and site-directed TaALMT1 mutants facilitated malate efflux in response to acidic pH, similar patterns could be observed as that for alkaline pH, but with some differences. Oocytes injected with TaALMT1 WT or mutants were tested in the acidic media at pH 4.5 (Fig 4.2) and pH 5.5 (Fig 4.3). Generally both pH conditions resulted

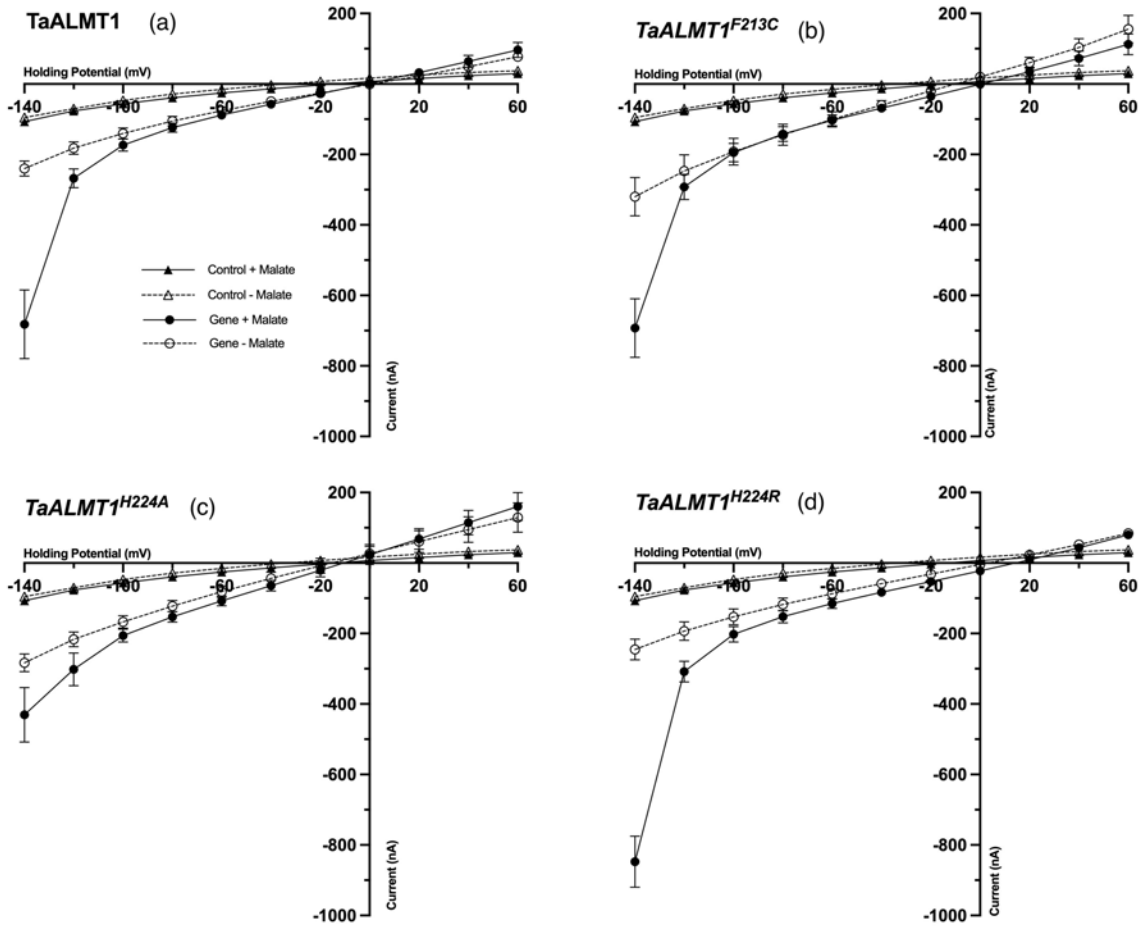


**Figure 4.3:** I-V plots of water-injected (control) and gene-injected *X. laevis* oocytes preloaded with malate and tested at pH 4.5. Oocytes were injected with water or cRNA of TaALMT1 wildtype or site-directed mutants. Two types of recording solutions were used, either plus 10 mM malate or without malate. n $\geq$ 6, data showed mean $\pm$ SEM.

in a decrease in the magnitude of the TaALMT1-mediated inward current compared to at pH 7.5 (Fig 4.1), whether with external malate in the solutions or not. Compared to control cells, both WT and the three mutants still maintained the activation of the channel at the most negative holding potential (-140 mV) when malate was added to the solution (Fig 4.2, 4.3) under acidic conditions. The cells expressing TaALMT1 wildtype or mutants at acidic pH (pH 4.5 and 5,5) still had greater negative currents compared to control cells, especially at the most negative holding potentials, no matter whether there was external malate or not. $TaALMT1^{H224R}$ expressed cells were the most responsive, with a more than 2-fold increase of negative currents (Fig 4.2(d), 4.2(d)), in contrast to TaALMT1$^{H224A}$ which was the least responsive (Fig 4.3). These results indicates that TaALMT1 has intrinsic properties and allows the protein to function as a malate efflux transporter (at least in oocytes).

In terms of reversal potential at pH 5.5, all gene-expressing cells had a positive 20-30 mv shift compared to control cells upon the addition of malate (Fig 4.2), which is not the

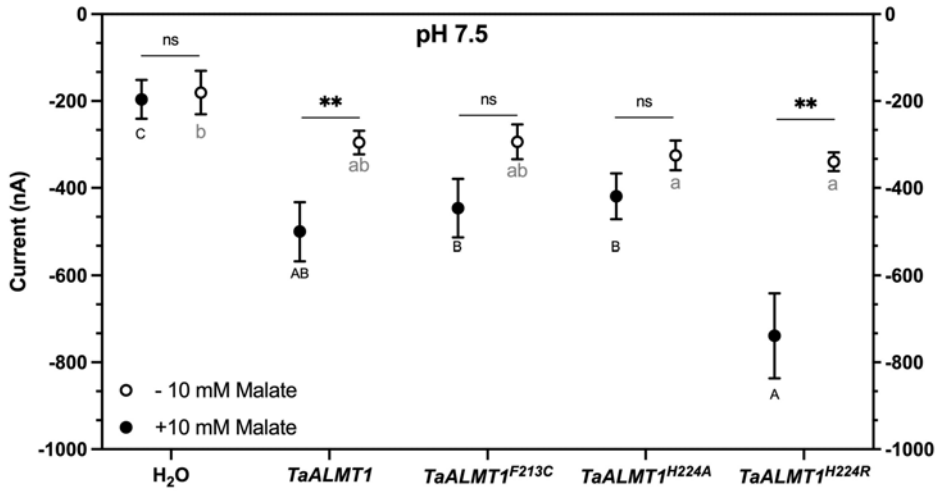


**(a)** Malate efflux at -120 mV (pH 7.5)

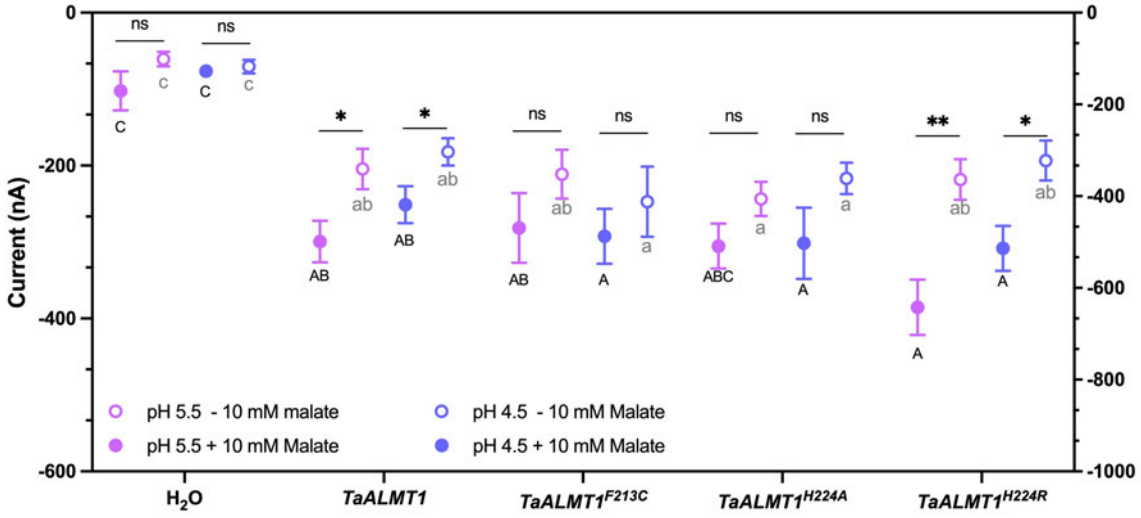


**(b)** Malate efflux at -120 mV (pH 5.5 and 4.5)

**Figure 4.4:** Malate efflux at -120 mV of control and gene-expressing *X. laevis* oocytes ( n $\geq$ 6) in alkaline (a) and acidic (b) solutions. Cells were injected with water or cRNA of TaALMT1 wildtype or site-directed mutants and incubated for 24-36 h, then preloaded with malate 1-4 h before clamping. Two types of recording solutions were used, either plus 10 mM malate or with no addition of malate. Different letters indicate significant differences between genotypes in a particular solution using one-way ANOVA, with uppercase and lowercase representing solution with or without 10 mM malate, respectively ($P$ <0.05). Stars indicate student t-test significance. * $P$ <0.05, ** $P$ <0.01.

same for at pH 7.5 (Fig 4.1). No shifts in reversal potential upon addition of malate were shown for any of the constructs including TaALMT$^{F213C}$, which showed a shift at pH7.5, indicating the low probability of opening at acidic pH of all channels.

The currents at a holding potential of -120 mV holding potential were also examined (Fig 4.4b). In the same solution at -120 mV, compared to WT, none of the mutants showed significantly altered negative currents (either pH 5.5 or pH 4.5), and there were also no significant differences between the mutants (Fig 4.4b). However, when adding

malate to the solution, once again, both TaALMT1 and $TaALMT1^{H224R}$ showed significant activation (i.e. larger negative currents in malate-containing solution than non-malate solution), while $TaALMT1^{F213C}$ and $TaALMT1^{H224A}$ had no activation at -120 mV (Fig 4.4b), similar to the alkaline results (Fig 4.4a).

Taken together, it seems the substitution of one amino acid in the putative GABA-binding motif, did not significantly change the ALMT-regulated currents directly at either alkaline or acidic pH when malate is not added. However, it does affect ALMT-regulated channel activation and malate efflux when malate is added to the solutions: the F213 and H224A mutation both reduced the activation, while the H224R mutation promoted this activation (Fig 4.4).

### 4.1.3 pH sensitivity of TaALMT1 was affected by site-mutations

It has been shown earlier that the mutants had altered channel activation capability in both alkaline and acidic solutions in response to the addition of malate, although no significant changes could be seen between mutants and WT when they were subjected to the non-malate solution. Next the question is if that is also the case of pH sensitivity for ALMT? The currents at -120 mV holding potential in response to pH changes were examined and compared within each gene-expressing cells, to find out the pH response of WT and mutants (Fig 4.5).

ALMT-mediated currents were significant upon addition of malate in both TaALMT1- and $TaALMT1^{H224R}$-expressing cells at both pH, but not significant in the other two mutants-expressing cells (Fig 4.5), regardless of the presence of malate in the solution. Although the currents were inhibited by acidic pH, compared to TaALMT1-expressing cells, $TaALMT1^{H224R}$-expressing cells had a greater activation when the solution contained malate (Fig 4.5). These observations could probably be due to altered channel activation or open probability. However, no altered pH sensitivity could be observed with the mutations present using this analysis.

Previous results have shown that adding malate to the solution resulted in the channel activation for oocytes injected with TaALMT1 WT and H224R cNDA. Next the percent activation at both alkaline and acidic pH for TaALMT1 WT and mutants were cacculated to reveal if there were significant differences in activating the channels. As shown in Fig 4.6, the H224R substitution had a greater percent activation than the other two mutants at pH 7.5, and it also had significantly higer percent activation than F213C at pH 5.5, but no differences at pH 4.5 could be observed. This could be due to the channel at pH 4.5 has already very low affinity for anion transport.

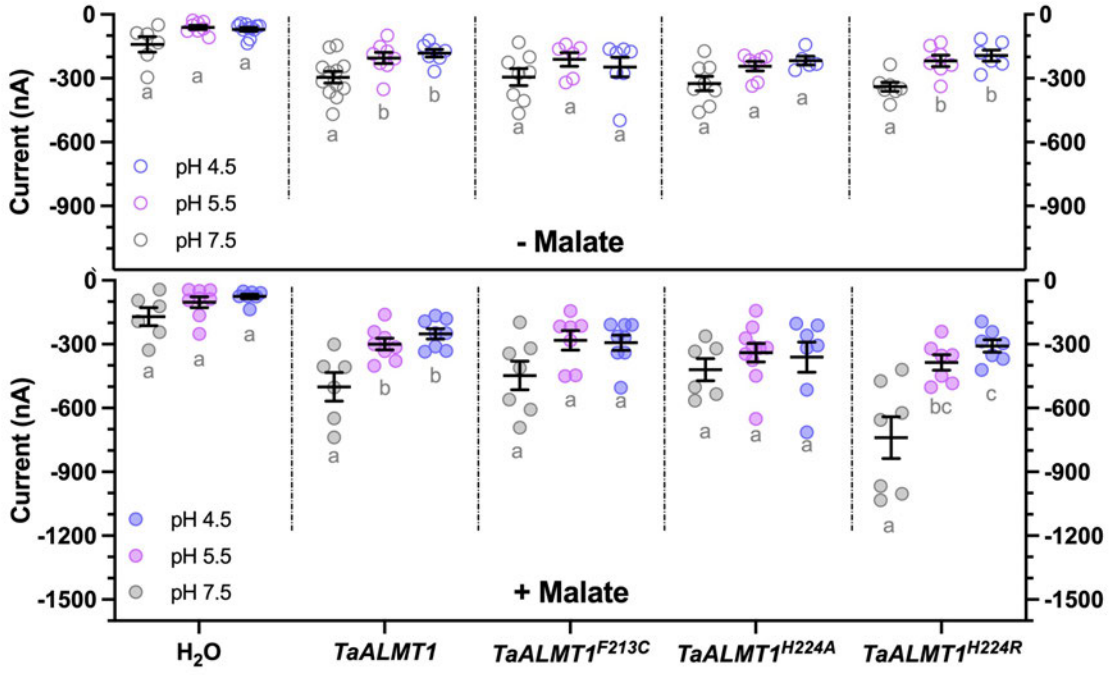


**Figure 4.5:** Malate efflux at -120 mV of control and gene-expressing *X. laevis* oocytes (n $\geq$ 6) at different pHs. All cells were injected with water or cRNA of TaALMT1 wildtype or site-directed mutants and incubated for 24-36 h, then preloaded with malate 1-4 h before clamping. Two types of recording solutions were used, either with or without 10 mM malate. Different lowercase letters indicate significant differences within a genotype between solutions with different pH ($P$ <0.05) one-way ANOVA.

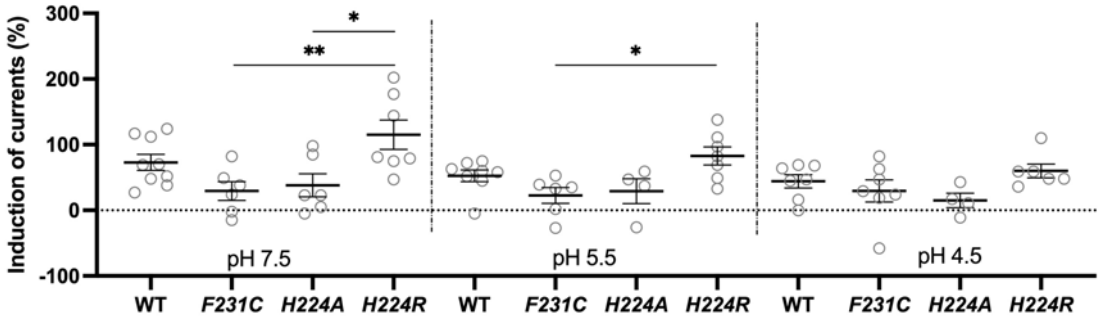


**Figure 4.6:** Percentage activation (%) of control and gene-expressing *X. laevis* oocytes at different pH (n $\geq$ 4) at different pHs. All cells were injected with water or cRNA of TaALMT1 wildtype or site-directed mutants and incubated for 24-36 h, then preloaded with malate 1-4 h before clamping. The percent activation of channel was calculated as the percent of current increased due to the addition of malate to the solution. Stars indicate significant differences in channel activation between genotypes within the same pH condition (* $P$ <0.05. * $P$ <0.05) one-way ANOVA.

### 4.1.4 Structural analysis of TaALMT1 based on the resolved AtALMT1 structure

The sequence of TaALMT1 was firstly aligned to AtALMT1 sequence (4.7). Based on the resolved secondary structure AtALMT1's structure ((Wang et al., 2021a)), the putative

GABA binding site of TaALMT1 is predicted to be localised in the conjunction of TM6 and H1 at the intracellular side.

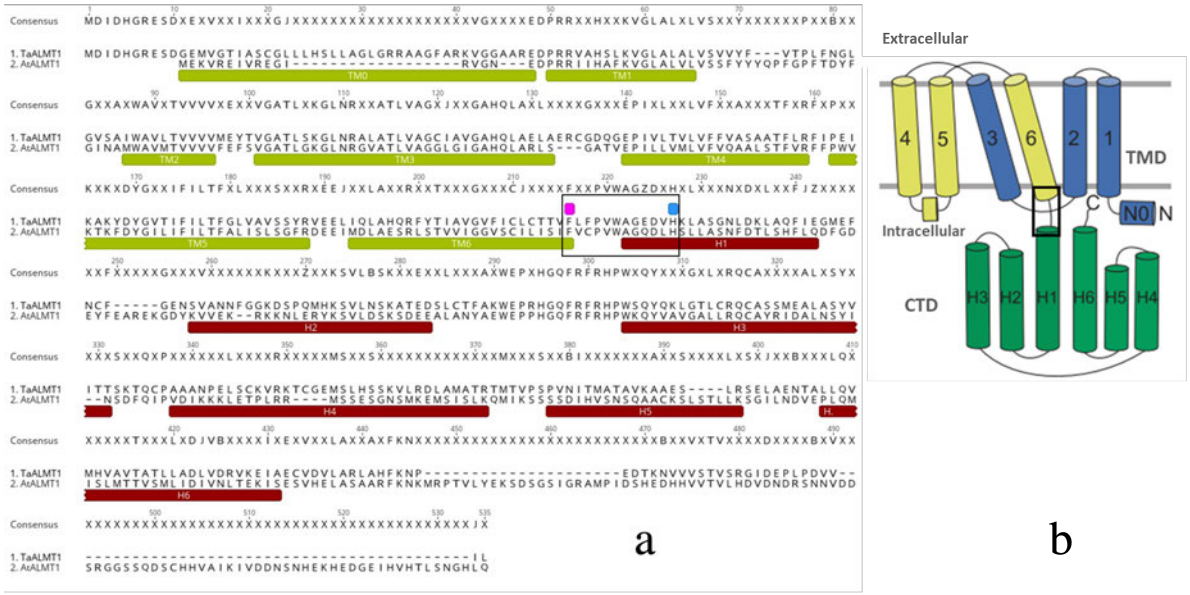


**Figure 4.7:** Structural alignment of wheat TaALMT1 to Arabidopsis AtALMT1. (a) Sequence alignment of AtALMT1 and TaALMT1. The secondary structure (TM0-6, H1-6) of TaALMT1 are assigned based on the structure of AtALMT1 (Wang et al., 2021a). The black box indicated the conserved GABA binding motif according to Ramesh et al. (2015). The purple dot represents F213 and the blue dot represents the H224 residue of the TaALMT1 protein. The alignment was performed using MUSCLE alignment in Geneious Prime software. (b) Schematic representation of the domain arrangement in one AtALMT1 subunit, adopted from (Wang et al., 2021a). The black box represents the conserved GABA binding motif.

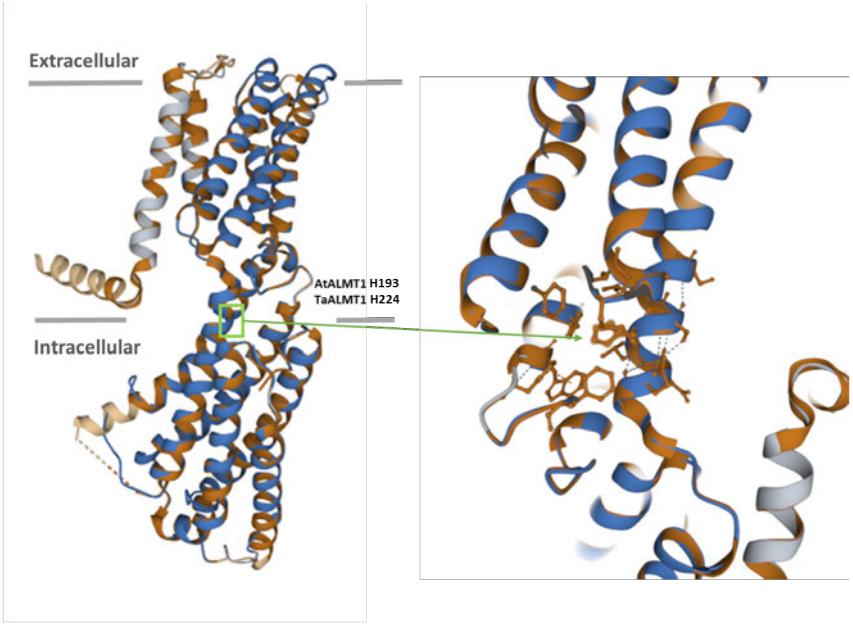


**Figure 4.8:** Structural alignment of wheat TaALMT1 to Arabidopsis AtALMT1 (apo/pH7.5, PDB ID: 7vq4) using SWISS-model. Regions of the polymer chain that are not aligned are coloured in lighter shades of orange and blue. AtALMT1H193/TaALMT1H224 (green box) is shaded with dark blue/orange, indicating a similar fold.

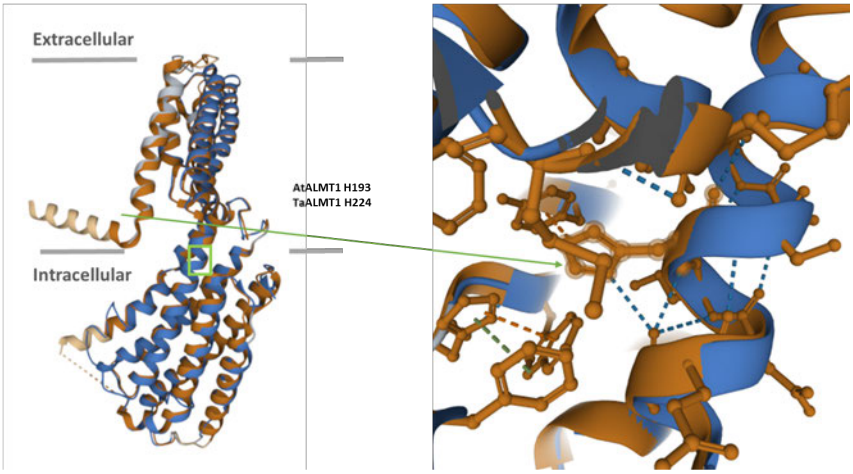


**Figure 4.9:** Structural alignment of wheat TaALMT1 to Arabidopsis AtALMT1 (apo/pH5, PDB ID: 7vq3) using SWISS-model. The pairwise structure alignment was performed using Protein data bank analyze tool. Regions of the polymer chain that are not aligned are coloured in lighter shades of orange and blue. AtALMT1H193/TaALMT1H224 (green box) is shaded with dark blue/orange, indicating a similar fold. Blue dashed line: hydrogen bond; orange dashed line: cation-$\pi$ interaction; green dashed line: $\pi$-stacking.

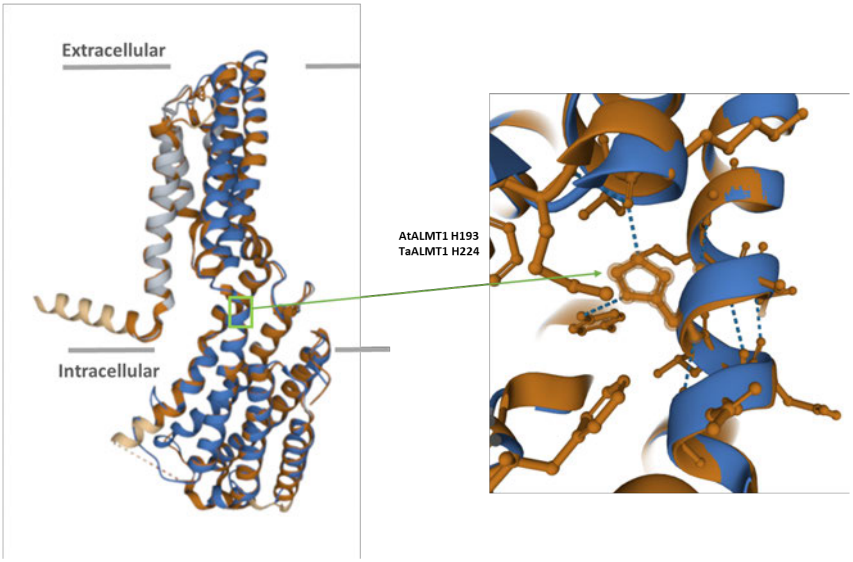


**Figure 4.10:** Structural alignment of wheat TaALMT1 to Arabidopsis AtALMT1 (malate/pH7.5, PDB ID: 7vq5) using SWISS-model. The pairwise structure alignment was performed using Protein data bank analyze tool. Regions of the polymer chain that are not aligned are coloured in lighter shades of orange and blue. AtALMT1H193/TaALMT1H224 (green box) is shaded with dark blue/orange, indicating a similar fold. Blue dashed line: hydrogen bond

TaALMT1 was then structurally aligned to the recently solved AtALMT1 structure of Wang et al. (2021a)) to examine predicted similarity at a protein fold level under various ligand binding and pH conditions. In detail, single subunit of TaALMT1 was aligned to AtALMT1 apo/pH7.5 (Fig 4.8), AtALMT1 apo/pH5.0 (Fig 4.9) and AtALMT1 malate/pH7.5 (Fig 4.10), respectively. All alignment models indicate the putative GABA binding motif is very well aligned with the AtALMT1 structure (as shown in dark blue and orange in Fig 4.8, 4.9 and 4.10). Based on the predicted homology model of TaALMT1,

under alkaline pH conditions (pH 7.5) without ligand binding, the TaALMT1H224 was not forming any chemical bonds with adjacent amino acids (Fig 4.8). Interestingly, under acidic conditions, a cation-pi (cation-$\pi$) interaction was formed between TaALMT1 H224 and Y299, corresponding to AtALMT1 H193 and Y271 within AtALMT1 (Fig 4.9). When a malate binding model at pH 7.5 was used, instead of having the cation-$\pi$ interaction, a few hydrogen bonds were formed between TaALMT1H224 with neighbouring amino acids (Fig 4.10).

The H224A mutation may change the conformation of these hydrogen bonds as alanine is uncharged, thereby inhibiting the proper function of the protein. The AtALMT1 H193 can also form cation-$\pi$ interactions with tyrosine (Y266 and Y271) to stabilise the protein structure at pH 5.0 (Fig 4.9), which could possibly be happening in TaALMT1 with H224. At pH 5.0, the imidazole side chain of histidine is protonated and hydrophilic, so the H224R mutation did not alter the cation-$\pi$ interaction of the TaALMT1 protein as much as the non-charged and hydrophobic H224A mutation. Therefore, H224A could also affect the stability of the protein and result in decreased sensitivity to pH, in contrast to H224R.

## 4.2 Discussion

ALMT1-mediated malate efflux was reported previously (Pietrzykowska et al., 2014). In the current study, the biophysical properties of oocytes expressing TaALMT1 demonstrate that TaALMT1-mediated current was activated due to addition of malate into the solution or due to an increase in pH. The substitution of one amino acid resulted in reduced or enhanced activation, depending on the specific mutation and pH of the solution. Both histidine and arginine are positively charged amino acids, while hydrophobic alanine and hydrophilic cysteine are uncharged. This could potentially result in a conformational change of the ALMT protein and contribute to their inconsistent functional responses to pH changes as well as the absence/presence of malate in the solution.

The substitute of cysteine and histidine did not directly alter the ALMT channel activity significantly under either alkaline or acidic conditions that did not contain malate, however, in response to the addition of malate or to pH change, the mutation resulted in different ALMT channel regulated currents. Under both acidic and alkaline conditions, the TaALMT1 protein activation was significantly inhibited by the substitution of phenylalanine 213 to cysteine (F213C) as well as Histidine 224 to Alanine (H224A) but not to Arginine (H224R). The H224R mutation of TaALMT1 can enhance malate-activated currents at alkaline pH, but to a lesser extent under acidic conditions as decreasing pH inhibited malate efflux in general. Similarly, whether the solution contained malate or not, the alkaline pH-induced currents were abolished by the F213C and H224A but not by the

H224R substitution.

GABA was proposed to inhibit anion transport by TaAMLT1 in membrane patches from the cytosolic rather than extracellular membrane face via reducing the channel open probability ($NP_{50}$) instead of inhibiting channel current magnitude (Long et al., 2019). As there is only one pore (Wang et al., 2021a) it is likely that this occurs by GABA permeation through the same pore competitively with malate that resulted in inhibiting the malate conductance. As the wheat ALMT1 shares 63% similarity with Arabidopsis ALMT1, they likely share a similar mechanism in GABA-regulated ALMT function. Further investigation is needed to confirm the mutant responses in the presence of $Al^{3+}$ under different pH and/or malate conditions. As the rapid accumulation of GABA in response to abiotic and biotic stress is common (Loreti et al., 2016), and GABA biosynthesis consumes protons which results in an increased cytosolic pH. The GABA shunt also changes organic acids concentrations in plants, so the negative regulation of ALMT channels by GABA could be due to altering ALMT pH sensitivity by affecting its structure. Further investigation of how the mutants respond to the addition of GABA is needed to confirm if the H224 mutants behave like F213C which has decreased GABA sensitivity. This will shed light on the pH sensitive histidine residue and its potential role in GABA regulated ALMT function.

The current study only tested the anion transport activity of TaALMT F213 or TaALMT1 H224A/R mutants. It is possible that mutating H224 into other titratable amino acids such as Aspartate (H224D) or Leucine (H224L) could also change its pH sensitivity. So far, we've only tested the malate transport activity of TaALMT1 mutants upon the external malate activation. It also has been suggested that the CTD of AtALMT1 is involved in homodimer assembly; therefore mutation in the CTD may affect the correct dimerization (Wang et al., 2021a). More work needs to carry out to test whether the abolished anion conductance observed in $TaALMT1^{H224A}$ injected oocytes is correlated to the incorrect dimer assembly. Despite the tested TaALMT1H224 site, there are extra six histidine residues located on the CTD of TaALMT1. The pKa value of each histidine can be further determined to select the potential pH sensing site that accessible for the proton moieties. In addition, the pKa of histidine could be influenced by the adjacent interacting amino acid, therefore losing the pH sensitivity. For instance, AtKAT1F266 shifts the pKA of AtKAT1H266 by forming a cation-$\pi$ interaction, consequently, mutation of H267 did not affect the pH dependency of KAT1 (González et al., 2012). In the predicted model of TaALMT1 (aop/pH5) (Fig 4.9), a cation-$\pi$ interaction was formed between TaALMT1H224 and TaALMT1Y299; more work needs to be done to explore whether it's the similar scenario as for KAT1.

ALMT is also reported to selectively transport other anions such as $NO_3^-$, $SO_4^{2-}$, $Cl^-$ although to a lesser degree, apart from facilitating organic acids (as malate in this case)

efflux to chelate the $Al^{3+}$ (Piñeros et al., 2008). Therefore, it could create a charge gradient for the plasma membrane which can have further effects on the physiological response of plants. Malate or other anions/cations-efflux/influx of various plant mutants that have altered GABA-shunt genes expression could also be examined, combined with the expression of other *ALMT* genes, would also provide more information of GABA and ion transport. These could also be examined in the future to better understand how GABA signalling through ALMT.

## 4.3 Materials and methods

### 4.3.1 TaALMT1 site-directed mutagenesis

TaALMT1 and $TaALMT1^{F213C}$ in pGEMHE-DEST were provided by Long et al. (2019), and TaALMT1 was used as a template for generating $TaALMT1^{H224R}$ and $TaALMT1^{H224R}$ mutants.

**Site-directed Mutagenesis PCR**. Primers were designed based on the Quik Change Site Directed Mutagenesis Kit PCR protocol (Stratagene, USA). Histidine 224 of the wheat ALMT1 was mutated to alanine and arginine using the mutagenic primer 5'-GTC TGG GCC GGA GAG GAC GTC GCC AAG CTC GCC TCC-3' and 5'-GTC TGG GCC GGA GAG GAC GTC CGC AAG CTC GCC TCC-3', respectively. The PCR was 36 cycles and altered bases are underlined. A Mini Prep kit (PureLink Pro Quick96, Sigma) was used to extract plasmid DNA (according to high copy protocol) from the *E.coli* transformation, of which 4-5 ug was linearized with the restriction enzyme *NheI* (New England Biolabs). The 105 $\mu$L reaction system included: 10 $\mu$L CutSmart Bufffer, 13-15 $\mu$L DNA template, 2 $\mu$L *NheI* and Nuclease-free water (calculated). The mixture was incubated at 37 °C for 2.5 hours, and isolated plasmid DNA was sequenced (Sangers sequensing, AGRF) to confirm the presence and correct orientation of the mutation.

**cRNA preparation and purification**. The mMESSAGE mMACHINE™ T7 Transcription Kit (Invitrogen, Sigma) was used to synthesize the capped complementary RNA (cRNA) for oocyte expression. The 20 $\mu$L reaction system was used for capped transcription reaction assembly, which included around 1000 $\mu$g linearised plasmid DNA (2 to 4 $\mu$L) and Nuclease-free water (calculated), 2 $\mu$L 10× Reaction Buffer, 10 $\mu$L 2× NTP/CAP, and 2 $\mu$L Enzyme Mix. The reaction tube was gently flicked and briefly centrifuged and then incubated at 37 °C for 2 hours. 1 $\mu$L TURBO DNase was added to the reaction, mixed well and incubated for a further 15 min at 37 °C to remove any template DNA presented. Recovery and purification of the RNA was as following. 115 $\mu$L Nuclease-free water and 15 $\mu$L ammonium acetate stop solution was added and mixed through, then 150 $\mu$L phenol/chloroformIAA was added and centrifuged at mixmam speed for 5 min.

The upper aqueous phrase was recovered, equal volume of isopropanol was added, and the mixture was chilled at -20 °C for 20 min, followed by 15 min centrifuge at 4 °C. The upper phrase was removed, and 70% ethanol (molecular grade) was added and centrifuged for 15 min. Remove the upper phrase and root dry the RNA, then aliquet 15 $\mu$L Nuclease-free water to desolve the purified RNA. After recovery of the RNA, the reaction product was quantified through denaturing gel electrophoresis and RNA concentration was measured.

### 4.3.2 Electrophysiological expreiment

**Gene expression in *X. laevis* oocytes**. The incubation solution used was Ringer's solution which contains 96 mM NaCl, 2 mM KCl, 5 mM $MgCl_2$, 5 mM HEPES, 0.6 mM $CaCl_2$, 5% w/v horse serum, 500 $\mu$g/mL tetracycline and 1× penicillin-streptomycin (Sigma P4333). Stage IV and V *X. laevis* oocytes were maintained in the incubation solution overnight, then selected and injected with 46 nl UltraPure distilled water (DNAse, RNase-free, Invitrogen) or 32 ng cRNA using a micro-injector (Nanoject II, automatic nanolitre injector, Drummond Scientific) and incubated in Ringer's solution for 1-2 d at 18 °C.

**Electrophysiology**. Whole cell currents of oocytes were recorded under constant perfusion of the recording solutions at room temperature (22 °C) using conventional two-electrode voltage-clamp (TEVC) techniques. An Oocyte Clamp OC-725C amplifier (Warner Instruments) were used to record the currents, which were digitised using an Axon Digidata 1400A (Molecular Devices) and the software Clampex 10.2 (Molecular Devices). Recording electrodes were filled with 3 M KCl and had resistances between 0.5 and 1.2 megaaohms. The TEVC method measured the net currents in the oocytes expressing TaALMT1 wild-type and mutation genes both in the presence and absence of malate in either acidic (pH 4.5, pH 5.5) or alkaline (pH 7.5) recording solutions (Table 4.1).

For oocytes preloaded with malate, 46 nl of 100 mM pH 7.5 Na-malate was injected to the oocytes 1-4 h prior to electrophysiological recordings, which theoretically results in an increase of 9.0 mM in the intracellular Na-malate concentration assuming a cell diameter of 1.0 mm. The ionic composition of the recording solutions was chosen to attenuate the major voltage-dependent, hyperpolarized-induced, and volume-sensitive endogenous oocyte malate currents. The holding potential was set to 0 mV, and voltage test pulses (400 ms in duration) were stepped between +60 mV and -140 mV (in 20-mV increments) with a 10s resting phase at 0 mV between each voltage pulse. Representative current traces under the above range of voltages were recorded and the Current-Voltage ($I$-$V$) relationships measured under different recording solutions were constructed by measuring the current amplitude at the steady states of the test pulses.

**Table 4.1:** Basic recording solutions

| Chemical | Final Conc | Quantity |
|---|---|---|
| Milli-Q water | - | 900 - 950 ml |
| 60 mM Ca-stock | 0.7 or 0.5 mM | For pH7.5, 11.67 ml; For pH4.5 or pH5.5, 8.33 ml |
| 1 M Malic acid stock | 10 or 0 mM | 10 ml or 0 ml |
| 0.5 M MES stock | 5 mM | 10 ml, and adjust pH with 0.5 M BTP |
| Mannitol | 220 mosmol/kg | 36 - 38 g |
| Milli-Q water | - | Top up to 1000 ml |

### 4.3.3 TaALMT1 protein structural modelling

The full-length sequence of TaALMT1 was used to build the homology model based on the resolved AtALMT1 structure under different ligand binding and pH conditions using SWISS-MODEL online tool and the Protein Data Base (PDB). Three TaALMT1 models were established based on: AtALMT1 (apo/pH5, PDB ID: 7vq3), AtALMT1 (apo/pH7.5, PDB ID: 7vq34) and AtALMT1 (malate/pH7.5, PDB ID: 7vq5) respectively. The generated model of TaALMT1 was then structurally alignment to each corresponding AtALMT1 model for comparison. The Pairwise structure alignment was performed using protein data bank online analyze tool. Figure images were created with Pairwise structure alignment tool.

# CHAPTER 5

# General discussion and future work

Gamma-aminobutyric acid (GABA), a four carbon nonproteinogenic amino acid, rapidly accumulates in plant tissues under biotic and abiotic stress. GABA has long been studied for its role in regulating carbon and nitrogen metabolism, which impacts the ability of plants to respond to stress (Al-Quraan and Al-Omari, 2017). The GABA-shunt is the main metabolic pathway for GABA synthesis, where cytosolic GAD catalyses the conversion of glutamate into GABA, GABA-permease transports GABA into the mitochonidria where it is catabolised by GABA-T into SSA and finally into succinate (by SSA dehydrogenase), where it enters the TCA cycle (Fig 1.1). Putrescine can be used for the GABA synthesis in the peroxisome instead of glutamate in the polyamine pathway (Fig 1.1). Recently it was suggested that GABA may exert its effects through a not yet completely defined signalling pathway which involves the negative regulation of anion channels from the plant aluminum-activated malate transporter (ALMT) protein family (Ramesh et al., 2015). In the current study, the role of GABA under two of the most common abiotic stresses, salinity and flooding (submerged plants mainly experience hypoxia and post-hypoxia stress), were explored. In *Arabidopsis* mutants with altered endogenous GABA concentration and a disturbed GABA-shunt pathway (Table 1.2, Fig 3.36), it appears that GABA differentially impacts responses in terms of these two abiotic stresses. Decreasing or blocking GABA production from glutamate by knocking down single or multiple *GAD*s (*gad1KO, gad2-1, gad1245*), or totally inhibiting GABA catabolism by *GABA-T* knockout (*pop2-8*), resulted in distinctive transcriptomic and metabolic profiles under both control and stressed conditions.

## 5.1 Transcriptional "pre-adapted" plants

Upon submergence, 25% of genes detected by transcriptomics in WT were significantly affected. The GABA mutants were more affected with up to 1.8-folder higher transcriptional change compared to WT (Fig C.6), indicating more profound alterations when the GABA shunt pathway was disturbed. Interestingly, some of the GABA mutants seemed to be able to "pre-adapt" themselves even prior to stress, as they have at least over 900 genes differentially regulated compared to WT (Fig C.4). Many of the DEGs are involved in stress response, including salt response. Some of the proteins and enzymes encoded by these genes were: BTB and TAZ domain protein 2 (BT2), similar to RCD5 (SR5), and Δ-*1-pyrroline-5-carboxylate* (P5C) synthetase, P5CS. *BT2* regulates responses to various hormones, stress and metabolic conditions in *Arabidopsis*, and loss of *BT2* causes hypersensitivity and decreased germination rate in response to sugar, ABA and $H_2O_2$ (Misra et al., 2018). P5C, an intermediate in proline biosynthesis and catabolism, can be reduced to glutamate (the precursor of GABA, Fig 1.1) by P5C dehydrogenase P5CDH, or be oxidased into proline (Delauney and Verma, 1993). Glutamate can be converted to P5C by P5CS. Both P5C and proline play a key role in stress response and ROS accumulation. *SRO5* and *P5CDH* are natural *cis*-antisense gene pairs, which is named nat-siRNAs as they are derived from natural transcripts (Borsani et al., 2005). Salinity induced *SRO5* expression is important to salt tolerance, and the *SRO5-P5CDH* nat-siRNAs together with their proteins formed key components of a regulatory loop that controls ROS production and stress response (Borsani et al., 2005). *SRO5* was down-regulated in all mutants under control conditions except for *pop2-8*, and *BT2* was up-regulated in *pop2-8* (Fig 3.6). *P5CS1* was also down-regulated in the two GABA accumulating lines *gad2OE* and *pop2-8* but not altered in other lines. Collectively, these genes could be correlated with the faster root growth of the two GABA accumulating lines under control conditions.

The other "pre-adapted" gene expression enriched processes in non-stressed GABA mutants include: impaired circadian rhythms in all mutants except for the two *GAD1* lines, promoted cellular response to decreased oxygen in *gad2-1*, and plant hormone and signal transduction in all mutants except for *gad2-1* (Fig 3.11, Table C.3). In addition, down-regulation of defense response to fungus was found in *gad1KO*, *gad2OE* and *pop2-8*; down-regulation of defense response to bacterium was found in *gad2OE* and *pop2-8*; and amino acid and carbohydrate metabolic processes were also differently affected between the GABA mutants (Fig 3.11, Table C.3). As plants under hypoxia experienced a much severe energy crisis and co-occurring biotic stresses (infection and pathogen attack), the down-regulated defense and bacteria response in these three lines suggesting they would be more vulnerable to the upcoming submergence than *gad1**, *gad2-1* and *gad1245*.

It is unclear why in *gad2-1* genes involved in low oxygen sensing had been up-regulated even non-stressed conditions (Fig 3.8a, 3.9), but this may contribute to the overall better performance of *gad2-1* under hypoxia (Fig 3.3), and can be correlated with the less induced ROS and defense genes by submergence. *gad2-1* was not significantly impacted in plant hormone and plant signal transduction as the other mutants (Fig 3.11), which means they were less disturbed in these processes and can cope with stress better. As it has been recently shown that there is a second mutation in *gad2-1* (Fig C.14), all the transcriptional and metabolic responses of this line may be a combined result of losing both genes. This could be further examined by investigating mutants in these pathways in *gad2*, or induction of these pathways in a non-*gad2* background and examining these impacts on hypoxia tolerance.

***GAD4* and *GABA-T* both impact the regulation of the circadian rhythm**. The KEGG pathway analysis showed in control plants, *gad1245* and *pop2-8* were affected much more than the other mutants in circadian rhythm regulation (Fig 3.11). As the expression of many genes involved in this pathway were not altered in *gad2-1*, *gad2OE* nor the two *GAD1* lines (Fig 3.12), and the expression of *GAD5* is minimal (Fig 3.20), it seemes that additional knockout of *GAD4* has a large impact. Whether this is due to an additive effect of knocking out the *GAD*s or a specific response in *gad4* plants will need to be tested. Further, whether it was a direct or indirect impact of the high GABA, or knockout of *GABA-T* would also need to be examined by studies supplying GABA and examination of the *gaba-t* mutant alleles. As an autoregulatory endogenous mechanism which controls numerous physiological and molecular processes, circadian rhythms regulate many other genes and processes, such as stomatal movement, starch degradation, photosynthesis and gene expression (Yakir et al., 2006). In *Arabidopsis*, CIRCADIAN CLOCK ASSOCIATED1 (CCA1) and LATE ELONGATED HYPOCOTYL (LHY) are MYB-related proteins that function close to the central oscillator and they function synergistically in regulating circadian rhythms, by binding to the same region of the promoter of a Light-harvesting chlorophyll a/b protein (LHCA/B) (Lu et al., 2009). The *cca1* mutant shows a short period rhythm while the *cca1 lhy* double mutants shows an even shorter period (Lu et al., 2009). Both *CCA1* and *LHY*, and *HY5* (important for photomorphogenesis) were down-regulated in *gad1245* and *pop2-8*. Accordingly, genes encoding leaf starch degradation were greatly up-regulated in these two lines, such as *STARCH EXCESS 1* (*SEX1/GWD1*), *ALPHA-AMYLASE-LIKE 3* (*AMY3*) and *GWD3*. This could be correlated with the greater biomass than WT and faster root growth in these two lines (Fig 2.4a, 3.2) under control conditions. However, this could mean they could experience greater photosynthesis inhibition in response to stress and greater inhibition of Fv/Fm under submergence, due to the light harvesting capacity could be lower already without an obvious phenotype under control conditions. This was the case of *pop2-8* (Fig 3.3) but not for *gad1245*, as it had a higher Fv/Fm than WT under submergence, but still

both *gad1245* and *pop2-8* did not show the recovery of Fv/Fm while all the other lines including WT did, indicating they were sensitive to post-hypoxia stress (including higher light and oxidative stress). As *gad1245* and *pop2-8* has extremely low and high GABA concentration (Fig 3.36) respectively, this suggests that GABA may signalling through circadian genes. This needs further exploration, which initially could be by studying the circadian period in these mutants (Sharma and Bhatt, 2014).

**$H^+$-ATPase and CIPKs**. Increased proton pumping activities are always associated with cell expansion and improved salinity tolerance. The reason that some mutants were more resistant to salinity could be due to their higher proton transport capacity than WT even under non-stressed conditions. The mRNA expression profiles of genes encoding $H^+$-ATPase and CIPK proteins in leaves of 4.5 weeks old plants were explored to assess their predisposition to tolerate stress without the interfering stress-adaptive responses. The proton transporters include P-type ATPase which are characterised by forming a phosphorylated intermediate and contain five subfamilies (Axelsen and Palmgren, 2001), and V-type ATPases. ACA8 and ACA1 are P-type ATPases localised to plasma membrane and chloroplast envelope (plastids), respectively. Mediated by calcineurin B-like protein (CBL) and CBL-interacting protein kinase (CIPK) complexes, ACA8 has crucial functions in the termination of $Ca^{2+}$ signals by removing excess $Ca^{2+}$ from the cytosol to the extracellular apoplast (Costa et al., 2017). In Arabidopsis, BONZAI1 (BON1) physically interacts with ACA10 and ACA8 to regulate cytosol calcium signals, which are critical for stomatal closure as well as plant immunity (Yang et al., 2017). ACA10/8 are negative regulators of plant immunity responses. Several P-type 2B subfamilies of autoinhibited calmodulin-regulated $Ca^{2+}$-transporting ATPases were up-regulated in *pop2-8* and *gad1245*, this could be correlated to their faster root growth and greater biomass than WT under control conditions (Fig C.23).

## 5.2 The GABA shunt pathway functions differently in response to salinity and hypoxia

Although both *gad1245* and *pop2-8* had faster root growth than WT under control conditions, *gad1245* had greater percent reduction (70.4% ) following salinity treatment and thus can be classified as less tolerant to salt stress compared to *pop2-8*, suggesting the importance of producing GABA through the GADs for salt-stressed plants (Fig 2.4a, 2.3). In contrast, *pop2-8* was more tolerant to mild salinity (<100 mM) because root growth was maintained under salt stress (Fig 2.4a). It is possible that higher GABA concentrations in *pop2-8* could improve salinity tolerance by conferring better tolerance to reactive oxygen species (Li et al., 2016a), membrane potential maintenance and optimal $Na^+/K^+$ ratio (mainly through regulating ion transporters). Su et al. (2019) also reported that the *gad1,2*

double mutant to be more sensitive than *pop2-5* to salt stress, which is in accordance to the ovservations in the current research.

Unlike under salt stress, the potential quantum efficiency of PS II (Fv/Fm) results showed that *pop2-8* and *gad2OE* was greatly inhibited in response to submergence. During the subsequent 2 d recovery period *pop2-8* had a further decreased Fv/Fm, while *gad2OE* could restore to a certain extent. For the *GAD* lines, *gad1** which has *GAD1* expression in both roots and shoots, had the lowest decrease and showed a full recovery of Fv/Fm; *gad1KO* was more impaired by submergence than the other GABA deficient lines, and Fv/Fm could be restored to some extent in *gad2-1* (Fig 3.3). However, unlike its parent lines, *gad1245* did not show an increase in Fv/Fm during the recovery period, although it was not inhibited as much by submergence as *gad1KO* (Fig 3.3). In line with the physiological results, functional analysis of differentially expressed genes by submergence also showed that the three lines *gad1KO*, *gad2OE* and *pop2-8* down-regulated genes were significantly enriched in photosynthetic processes (Fig 3.24). *gad2OE* and *pop2-8* had more severe impairment of genes related to photosynthesis light reaction compare to other mutants, e.g. light signal consumption, phyA and phyB light harvesting (Fig 3.25, 3.26, Table C.5), while *gad1KO* had the most impaired photosynthesis dark reaction (Table C.7). These three lines (*gad1KO*, *gad2OE* and *pop2-8*) had the most upregulation in genes related to protein ubiquitination and ubiquitin-protein transferase activity, cellular response to lipid, alcohol, starvation, nutrient levels and abscisic acid stimulus as well (Table C.5). Except for WT and *gad1**, in all the other five lines, up-regulated genes were significantly enriched in processes like programmed cell death induced by symbiont (Table C.5). These results indicate the importance of both GABA synthesis and catabolism through the GABA shunt pathway when plants were subjected to hypoxia and post-hypoxia stress.

Taken together, it seems that the inability to utilise GABA (*pop2-8*) does more harm to plants during flooding and recovery than not being able to produce GABA (*gad1245* in the extreme case) through the GABA shunt pathway, while under salt stress it is the other way around. Several reasons could be underlying these observations: (i) GABA concentration has an optimal functional range; (ii) as the energy crisis for plants under submergence is more severe than under salt stress, GABA signalling may play a key role in salinity tolerance, but it is a different scenario in flooding tolerance, which is a combination of stresses.

Hypoxia-induced GABA accumulation in plants is much higher than under other stresses. In 3 to 4 week old *Arabidopsis* leaves, a 2-fold increase of GABA was induced after 4 d salt stress (Zarei et al., 2016), while hypoxia could induce up to 12-fold (Allan et al., 2012) and 6-fold GABA (Breitkreuz et al., 2003) within a couple of hours (Table 1.1). Thus, in submerged and recovered *pop2-8* leaves, the concentration of GABA could be too high and beyond the optimal functioning range, which may be one of the reasons why *pop2-8*

copes with salt stress better than submergence. In fact, even *pop2-1* from the a different ecotype, Lansberg *erecta* (Ler) rather than Columbia, was reported to be more sensitive to salinity compared to WT and, to 1 mM GABA treatment compared to *pop2-8* which could also be due to the same reason (Renault et al., 2010, 2011). GABA accumulates in *pop2-1* causes cell elongation defects and represses the expression of genes encoding secreted and cell-wall related proteins (Renault et al., 2011). In the current study, the root growth of wild type and *pop2* mutants from the two ecotypes were compared, and *pop2-1* was also more sensitive to salt stress than *pop2-8* (Fig 2.7). In response to submergence, there were more cell wall biogenesis encoding genes down-regulated in *pop2-8* than in other GABA mutants (including *gad1245*) as shown in Table C.5, correlating with the less hypxoia tolerance of *pop2-8*. A further study to compare the GABA concentration in WT and *pop2* leaves and roots from the two ecotypes under both salt stress and submergence could test this hypothesis.

The submerged plants face greater energy crisis, which differs from salinity. *pop2-1* and *pop2-3* (Ler ecotype) were also reported to have early leaf senescence under various stress conditions, including dark, cold, wounding, dehydration and ABA treatment (Jalil et al., 2017). The two *pop2* lines had rapidly decreased photosynthesis and chlorophyll content but increased membrane ion leakage and malondialdehyde concentration under stress conditions (Jalil et al., 2017). The dark treatment alone in the current study suggested that the *gad2OE* and *pop2-8* developed more leaf senescence phenotype than the *gad2-1*, while WT was the least affected (Fig C.2a), suggesting the essential role of *GABA-T* in leaf senescence and C:N re-allocation. After submergence, the down-regulated genes were significantly enriched in cellular response to starvation (GO:0009267) in four mutants (not *gad1** and *gad2-1*), and *pop2-8* had the greatest number of DEGs involved, suggesting it experienced a more severe energy crisis (Fig C.5).

The hypoxia induced alanine accumulation was reported to be important for tolerance of plants, and it could be partially derived from the GABA shunt pathway (Miyashita and Good, 2008). Under submergence, the rapid accumulated GABA could be converted to SSA by GABA-T (thus *pop2-8* plants could accumulate higher level of GABA), using pyruvate as the amino receptor and produce alanine at the same time (the GABA shunt pathway in Fig 1.1). The alanine concentration in *gad1245* and *pop2-8* were both lower compared to *GAD1* lines under control conditions, and to *gad2OE* after recovery (Fig 3.36). One reason could be that in these two lines the flow of the GABA shunt pathway is reduced, due to *GADs* knockout and *GABA-T* knockout, respectively. So, it is possible that in the *pop2-8* plants upon submergence, the lack of GABA catabolism is vital, and other transcriptional and metabolic adjustments were not enough to compensate this loss. Further exploration on how the carbon and nitrogen flow by tracking metabolite labeling from stable isotope tracers can add addition information and reveal more specific pathway

activities (Allen and Young, 2020).

Under hypoxia, the accumulation of GHB was reported in *Arabidopsis* and other species (Breitkreuz et al., 2003; Allan et al., 2008), suggesting the SSA derived from the GABA shunt pathway was converted to GHB instead of succinate (Fig 1.1). In the meantime, the *Arabidopsis ssadh* mutants (T-DNA insertion) accumulated higher GHB, ROS and were dwarf, but the *ssadh pop2* mutant did not alleviated these changes, indicating less toxic SSA accumulation in the double mutant (Bouché et al., 2003; Ludewig et al., 2008). However, *SSADH*-silenced tomato (by virus-induced gene silencing) was reported to be less sensitive to salinity than WT, although they cannot degrade GABA and had a dwarf phenotype and elevated ROS levels under normal conditions (Bao et al., 2015), indicating salt-induced toxic SSA could be lower under salinity than under hypoxia. The differed tolerance of *GAD* and *GABA-T* mutant lines in the current study could be due to differences in the accumulation of GHB and other aldehydes, which not only come from from the GABA shunt pathway. This need to be further explored by measuring the GHB concentration of *ssadh gad* and *ssadh pop2* double mutants under both stress conditions.

It is also possible that GABA signalling plays a key role in salinity tolerance and regulation of ion transport. Whereas GABAs role in hypoxia tolerance is not limited to signalling, which may include the need for catabolism. In the current study, under salinity, the *pop2-8* had relative less $Na^+$ accumulation (Fig 2.10), in agreement to what Su et al. (2019) had reported. In contrast, *gad1245* did not accumulate significantly higher concentrations of $Na^+$ compared to WT under salinity, which is the opposite to what was reported in the *gad1,2* double mutant (Su et al., 2019). The reason could be that they used 4 week-old soil-grown plants which were treated for two weeks, while in my experiments plants were hydroponically grown for 5.5 weeks and treated for 6 d. During different vegetative growth stage, the tolerance of plants could vary. In the earlier stages, the growth of *gad1,2* in their study (on salt media) and *gad1245* and *gad1KO* in my study (either on control or salt media) were significantly inhibited (Fig B.2, B.3). This could be mainly due to the *GAD1* gene having higher expression in the roots, as the *gad2-1* mutant maintained higher root growth than *gad1KO* and *gad1245* (Fig B.2, B.3).

Another key difference between *gad1245* and *pop2-8* is that the former could still use the GABA produced from the other pathway such as polyamine degradation (as shown in Fig 3.28 the expression *ADC2* was induced by submergence in *gad1245* but not other mutants), while *pop2-8* totally blocked the catabolism of GABA. Xing et al. (2007) proposed PA degradation could contribute to about 39% of salt-induced GABA in soybean roots. Studies also show that hypoxia- and anoxia-induced accumulation of GABA in fava bean and tea leaves are reduced by 32% and 25%, respectively by aminoguanidine, a diamine oxidase inhibitor that represses the production of putrescine which is the precursor for GABA

biosynthesis through the polyamine pathway (Yang et al., 2013; Liao et al., 2017). This may be why *gad1245* could maintain the same root growth rate as WT under salinity (Fig 2.4a) and it could also cope with hypoxia, while *pop2-8* could not compensate the loss of GABA catabolism. Overall *pop2-8* showed the least tolerance in both the submergence and the recovery phases. Further exploration of the polyamine concentration is needed to verify if that is also the case in *Arabidopsis* under these two types of stresses. The next step should include looking into specific mutants of key genes revealed in the current study in more details, constructing co-expression networks of the DEGs to illustrate how specific mutation(s) resulted in these different observations.

## 5.3 The role of GABA binding motif in regulating anion transport

GABA was reported to be negatively regulating the aluminum-activated malate transporter 1 (TaALMT1) via a direct interaction with the putative binding motif (12 amino acids) in the protein (Ramesh et al., 2015). The inhibition was proposed to be from the cytosol through a reduction of channel open probability instead of changing the channel current magnitude (Long et al., 2019). Chapter 4 of this thesis mainly explored the anion transport and pH sensitivity by substituting the last residue in the putative plant GABA binding motif. This showed that substituting the histidine to alanine abolished the channel activation by external malate and pH sensitivity of the protein, while the H224R maintained/enhanced the channel activation and pH sensitivity (Fig 4.5). Further investigation is needed to confirm the mutant responses in the presence of $Al^{3+}$ and the addition of GABA, under different pH and/or malate conditions, in order to confirm if the H224 mutants behave like F213C which has decreased GABA sensitivity. This will improve the understanding on the pH sensitive histidine residue and its potential role in GABA regulated ALMT function.

The TaALMT1 was structurally aligned to the recently solved AtALMT1 structure (Wang et al., 2021a)) and predicted homology model of TaALMT1 was constructed. It showed that without ligand binding, under acidic conditions, a cation-pi (cation-$\pi$) interaction was formed between TaALMT1 H224 and Y299 (Fig 4.9) while there is no bond at pH 7.5 (Fig 4.8); but when with malate binding at pH 7.5, a few hydrogen bonds were formed between TaALMT1H224 with neighbouring amino acids instead of the cation-$\pi$ interaction (Fig 4.10). As GABA production consums protons in the cytosol, GABA could regulate the ALMT channel through altering the conformation of the channel due to pH changes. More work needs to be conducted to test whether the abolished anion conductance observed in $TaALMT1^{H224A}$ injected oocytes is correlated to the incorrect dimer assembly.

The regulation of cytoplasmic pH is an important factor in survival under hypoxia, as it

serves as a signal between lactic and ethanolic fermentation (Roberts et al., 1984). As the production of GABA in the cytosol consumes protons and the catabolism of GABA in the mitochondria produces protons, it is likely that GABA signalling through directly regulating pH to further influence other signal and metabolic pathways or protein functions. The Arabidopsis *AtALMT1* is mainly expressed in the roots, so it was not detected in the RNAseq results (leave tissue). However, several other *ALMT* genes were found to be among the DEGs in GABA mutants (Fig 3.21, C.15) as well as genes that regulate *AtALMT1*. The transcription factor SENSITIVE TO PROTON RHIZOTOXICITY 1 (STOP1) was identified to be directly involved in plant response to acidic stress, and it also regulates the expression of *AtALMT1* (Iuchi et al., 2007). STOP1 regulates acidic stress and aluminum stress differently, as the sensitive phenotype of the *stop1* mutant to aluminum stress can be rescued by overexpression of *ALMT1*, but its sensitivity to acidic stress cannot (Kobayashi et al., 2014). Submergence induced the expression of *STOP1* in all mutants but in WT the induction was much smaller. *ALMT12* which is involved in stomatal closure, was repressed in *gad1245* under control conditions, but greatly increased in response to submergence. In contrast, *ALMT13* expression was largely induced in non-stressed *gad1245* compared to WT and was decreased down by submergence (Fig 3.21, C.15). While *ALMT12* expression was not affected by submergence in WT, and *ALMT13* decreased to a much lesser degree compared to *gad1245*. All these results revealed a link between GABA concentration and *ALMT* expression, which may be indirect evidence for GABA signalling. In the future, measuring the impact of *almt* knockout on plant responses to salt and hypoxia may better reveal a link between the GABA shunt and the ALMT protein function.

## 5.4 Conclusion

Overall, this thesis explored the role of GABA when plants are exposed to salinity and hypoxia, revealed that GABA differentially affected plants in response to these two types of stress. Furthermore I explored the pH sensitivity of a protein that is regulated by GABA. I found that a disturbed GABA shunt pathway under control conditions impacted many processes, including stress response, circadian rhythm regulation, plant hormone and MAPK signalling. The two lines with the most disturbed GABA shunt capacity, *gad1245* and *pop2-8* were impacted the most, but they showed opposite tolerance under salt stress and submergence (*pop2-8* being more tolerant to salinity but less tolerant to hypoxia and vice versa). I propose that this could relate to their differential capacity to detoxify reactive oxygen species, the ability to use GABA as an energy source, photosynthetic capacity, amino acid metabolism and pathogen resistance (Fig 5.1).

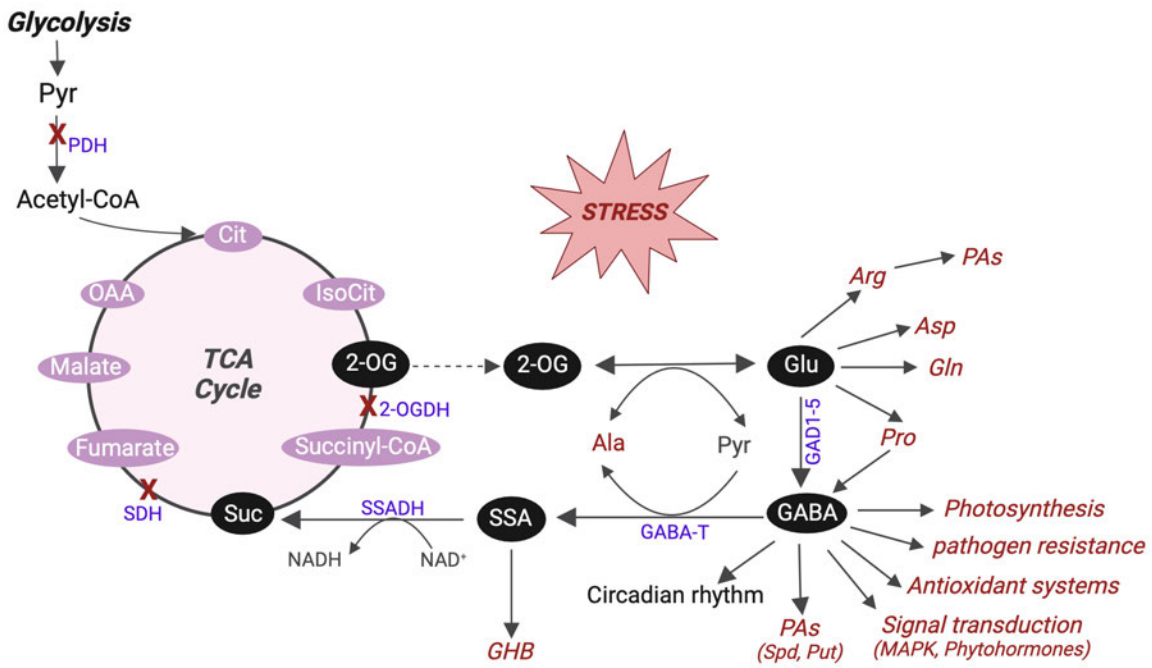


**Figure 5.1:** Schematic model of the GABA shunt involved processes under stress conditions. Two enzymes in the TCA cycle, 2-OG dehydrogenase and succinate dehydrogenase, as well as the entry of pyruvate into the TCA cycle via pyruvate dehydrogenase, were inhibited under stress conditions. Under both control and stressed conditions, the modified GABA shunt pathway in different lines, especially in *gad1245* and *pop2-8*, has distinct responses in terms of amino acid metabolism, energy metabolism, pathogen resistance, signal transduction and pathogen resistance. These were indicated in red. 2-OGDH, 2-oxoglutarate dehydrogenase; IsoCit, isocitrate; PAs, polyamines; PDH, pyruvate dehydrogenase; SDH, Succinate dehydrogenase; see Fig 1.1 for the remaining abbreviations.

# APPENDIX A

# SUPPLEMENTARY DATA FOR CHAPTER 1

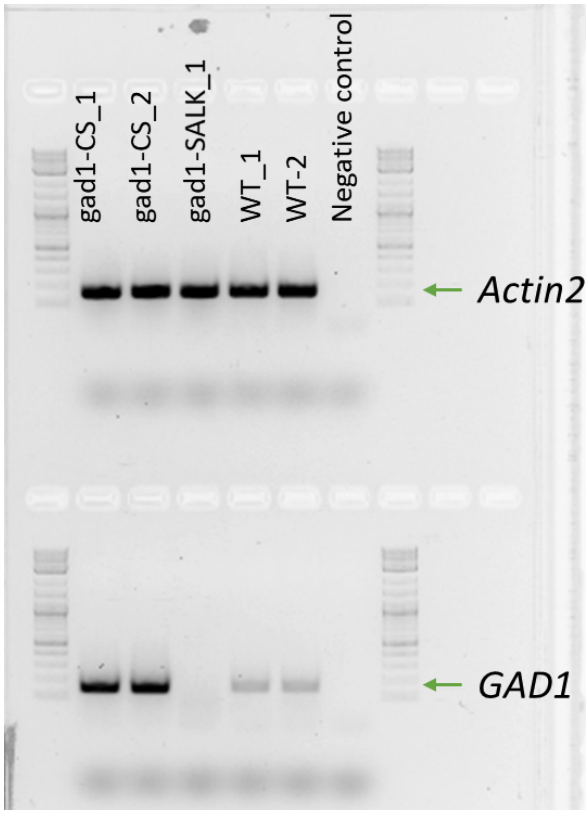


**(a)** Shoot *GAD1* expression

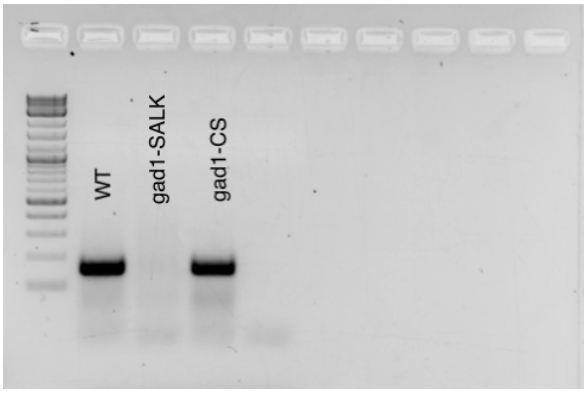


**(b)** Root *GAD1* expression

**Figure A.1:** Shoot and root *GAD1* expression in WT and the two *GAD1* lines for 2 weeks old plants. The leaf PCR and root qPCR (35 × cycles) results confirmed *gad1-SALK* to be a *GAD1* knockout while *gad1-CS* had *GAD1* expression in leaves and roots. So in this thesis they were named *gad1KO* and *gad1**, respectively.

**Table A.1:** A list of 52 core hypoxia-responsive genes (Mustroph et al., 2009)

| Gene ID | Gene Name | Gene Description |
|---|---|---|
| AT1G17290 | *ALAAT1* | Alanine aminotransferase 1, mitochondrial |
| AT1G72330 | *ALAAT2* | alanine aminotransferase 2 |
| AT1G19530 | *RGAT1* | DNA polymerase epsilon catalytic subunit A; RGA TARGET 1 |
| AT1G26270 | *PI4KG5* | Phosphatidylinositol 4-kinase gamma 5 |
| AT1G33055 | *HUP32* | Uncharacterized protein unannotated coding sequence from BAC F9L11 |
| AT1G35140 | *EXL1* | Protein EXORDIUM-like 1 |
| AT1G43800 | *S-ACP-DES6* | Stearoyl-[acyl-carrier-protein] 9-desaturase 6, chloroplastic |
| AT1G55810 | *UKL3* | uridine kinase-like 3 |
| AT1G63090 | *PP2A11* | F-box protein PP2-A11 |
| AT1G72360 | *HRE1* | Integrase-type DNA-binding superfamily protein |
| AT1G72940 | *TN11* | F3N23_14; Nucleotide-binding, leucine-rich repeat (NLR) gene regulated by nonsense-mediated mRNA decay (NMD) genes UPF1 and UPF3 |
| AT1G74940 | *FLZ13* | FCS-Like Zinc finger 13 |
| AT1G76650 | *CML38* | calcium-binding EF hand family protein |
| AT1G77120 | *ADH1* | Alcohol dehydrogenase class-P |
| AT2G16060 | *AHB1* | NSHB1; ARABIDOPSIS HEMOGLOBIN 1; oxygen binding/transporter |
| AT2G17850 | - | Rhodanese/Cell cycle control phosphatase superfamily protein |
| AT2G19590 | *ACO1* | 1-aminocyclopropane-1-carboxylate oxidase 1 |
| AT2G29870 | - | Aquaporin-like superfamily protein |
| AT2G34390 | *NIP2-1* | Aquaporin NIP2-1 |
| AT2G47520 | *ERF071* | Ethylene-responsive transcription factor ERF071 |
| AT3G02550 | *LBD41* | LOB domain-containing protein 41 |
| AT3G10040 | *HRA1* | Hypoxia response attenuator 1, a low oxygen-inducible transcription factor |
| AT3G17860 | *TIFY6B* | JAI3; JAZ3 (JASMONATE-ZIM-DOMAIN PROTEIN 3) |
| AT3G23150 | *ETR2* | Ethylene receptor 2 |
| AT3G23170 | *HUP39* | Proline/serine-rich PRP, Hypoxia response unknow protein 39 |
| AT3G27220 | - | Kelch repeat-containing protein At3g27220 |
| AT3G43190 | *SUS4* | Sucrose synthase 4 |
| AT3G61060 | *AtPP2-A13* | Phloem protein 2-A13 |
| AT4G10270 | - | wound-responsive family protein |
| AT4G17670 | *FLZ2* | FCS-Like Zinc finger 2, senescence-associated protein-related |
| AT4G22780 | *ACR7* | ACT domain-containing protein ACR7 |
| AT4G24110 | *HUP40* | NADP-specific glutamate dehydrogenase |
| AT4G27450 | *HUP54* | Hypoxia response unknow protein 54 |
| AT4G32840 | *PFK6* | ATP-dependent 6-phosphofructokinase |
| AT4G33070 | *PDC1* | Pyruvate decarboxylase 1 |
| AT4G33560 | *WIP5* | Member of the wound-induced polypeptide (WIP) family |
| AT4G39675 | - | At4g39675 |
| AT5G02200 | *FHL* | Protein FAR-RED-ELONGATED HYPOCOTYL 1-LIKE |
| AT5G10040 | - | At5g10040 |
| AT5G15120 | *PCO1* | Plant cysteine oxidase 1 |
| AT5G26200 | - | Mitochondrial substrate carrier family protein, T19G15_50 |
| AT5G39890 | *PCO2* | Plant cysteine oxidase 2 |
| AT5G42200 | *ATL23* | E3 ubiquitin-protein ligase ATL23 |
| AT5G44730 | - | Haloacid dehalogenase-like hydrolase family protein |
| AT5G45340 | *CYP707A3* | Abscisic acid 8'-hydroxylase 3 |
| AT5G47060 | - | Putative uncharacterized protein |
| AT5G47910 | *RBOHD* | Respiratory burst oxidase homolog protein D |
| AT5G54960 | *PDC2* | Pyruvate decarboxylase 2 |
| AT5G58070 | *TIL* | TEMPERATURE-INDUCED LIPOCALIN; binding / transporter |
| AT5G61440 | *ACHT5* | Thioredoxin-like 1-2, chloroplastic |
| AT5G62520 | *SRO5* | Probable inactive poly [ADP-ribose] polymerase SRO5 |
| AT5G66985 | - | At5g66985 |

# appendix B

# Supplementary data for Chapter 2

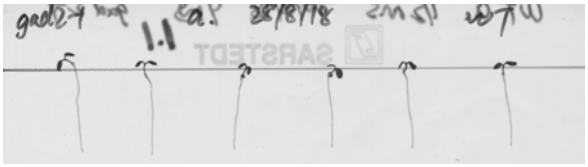

**(a)** Transfer to new media (0 d)

**(b)** Transfer to new media (4 d)

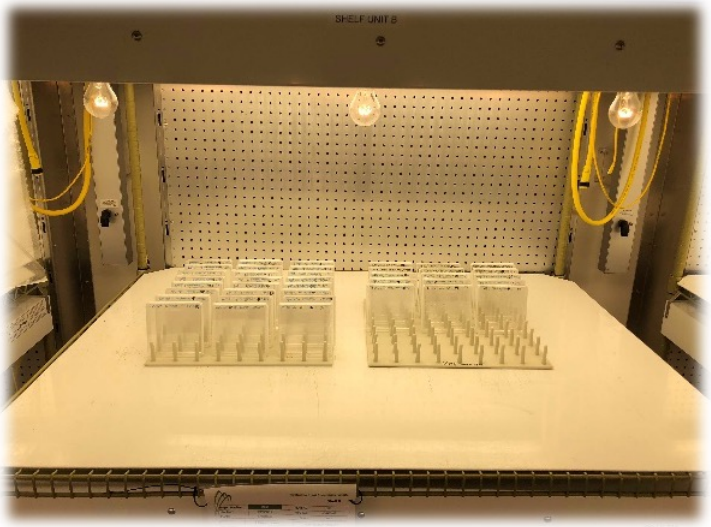

**(c)** Plates in short day growth room

**Figure B.1:** *Arabidopsis* plants grown on 1/2 MS media in short day growth room and representative photo of scanned plates for root assay. (a) The seedlings were just transferred to new media. (b) Four days after transfer to new media of the same plate. (c) Plates in a rack. For each plate, half WT and half GABA mutants.

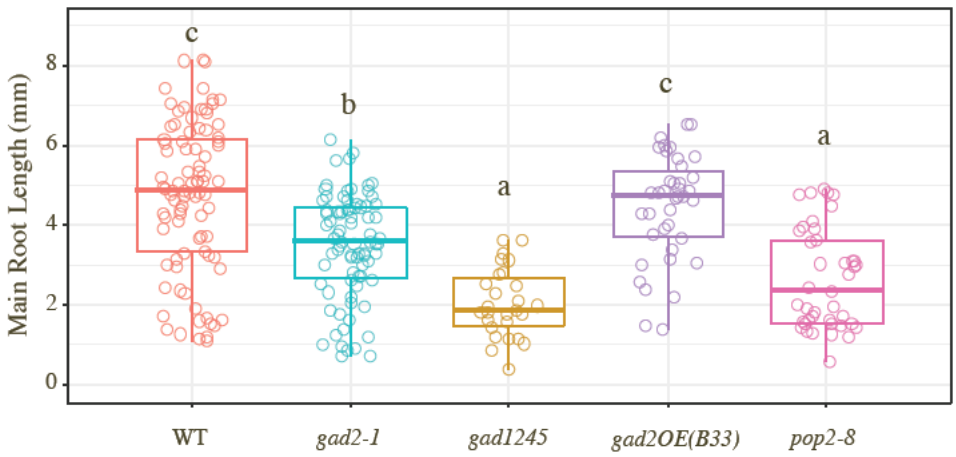


**Figure B.2:** Main root length of DAG4 WT and GABA mutants on 1/2 MS (- sucrose) in short day growth room. Letters represent one-way ANOVA significance.

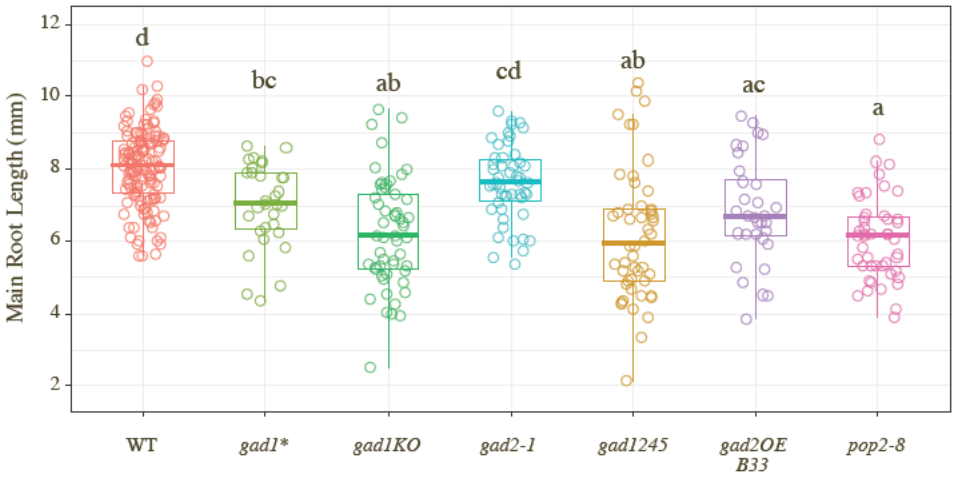


**Figure B.3:** Main root length of WT and GABA mutants on 1/2 MS + 100 mM NaCl (- sucrose) at DAG7 in short day growth room. Letters represent one-way ANOVA significance.

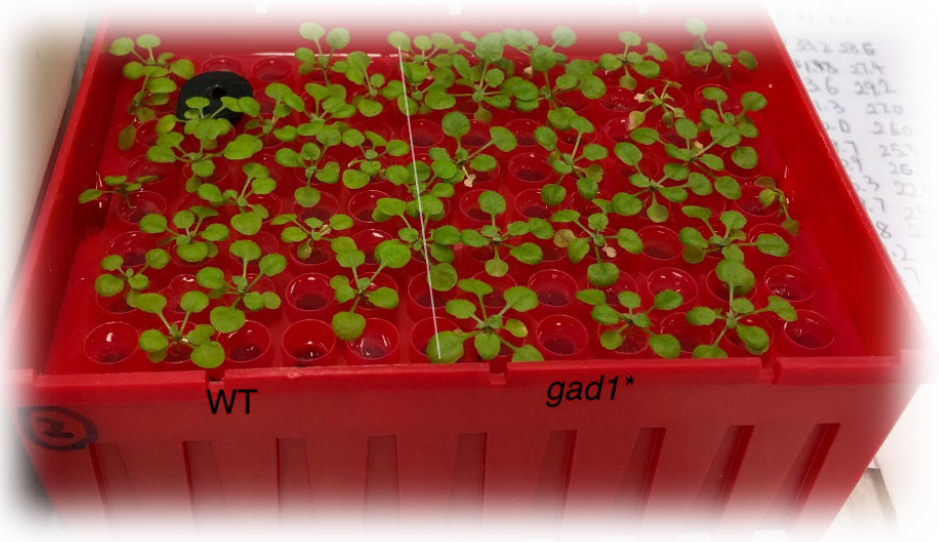


**Figure B.4:** After 7d salt stress leaves of *gad1** (on the right) were greener than WT. Plants were grown under short day conditions. The chlorophyll content will need to be quantified to confirm.

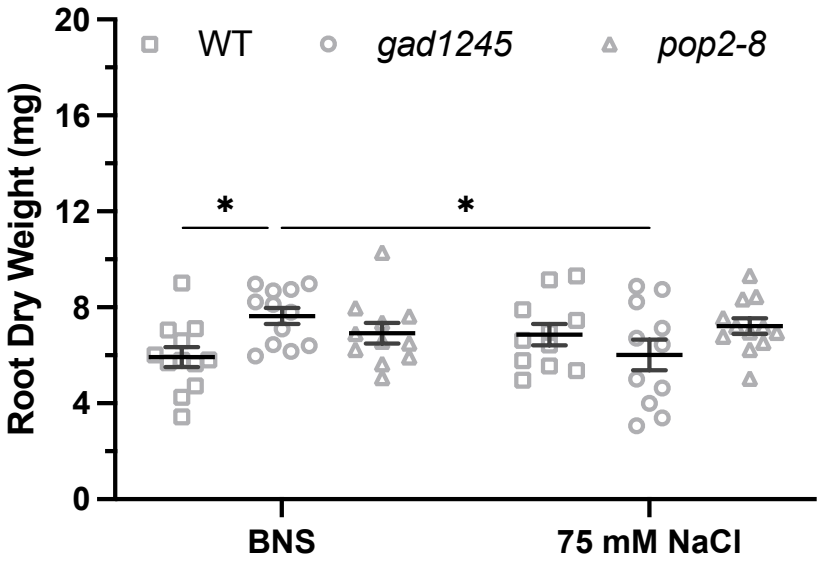


**Figure B.5:** Root dry weight of hydroponically grown WT and GABA mutants in BNS ± 75 mM NaCl. Plants were corresponding to those in Fig 2.9 at DAG46. Data show mean ± SE. Number of biological replicates n ∈ [8 ∼ 13]. Stars show significant difference between genotypes with in the same treatment or between treatments within a genotype using two-way ANOVA. * $P < 0.05$.

# APPENDIX C

# SUPPLEMENTARY DATA FOR CHAPTER 3

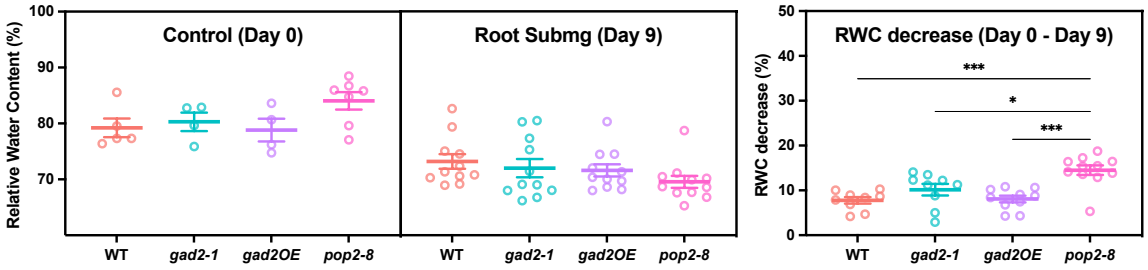


**Figure C.1:** Relative water content before and after 9 d root submergence and the % decrease. Data showes mean ± SE and stars represent statistical significance using one way ANOVA. n = 4, 5 or 7 for control plants and n = 11 for stressed plants. * $P < 0.05$, *** $P < 0.001$.

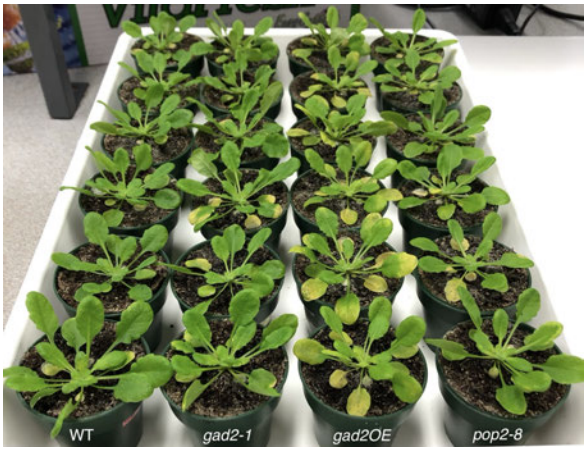


**(a)** Leaf senescence after darkness

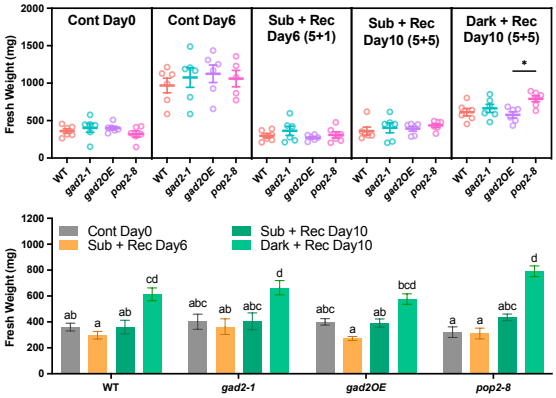


**(b)** Rosette fresh weight

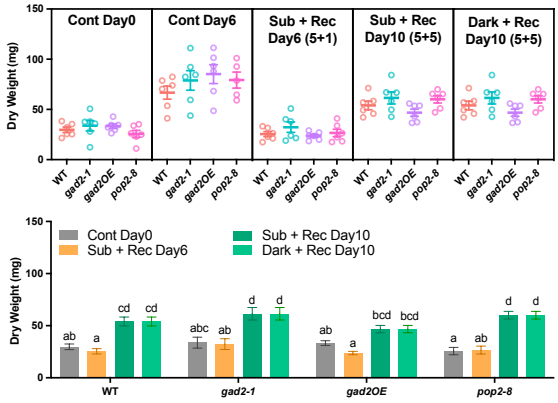


**(c)** Rosette dry weight

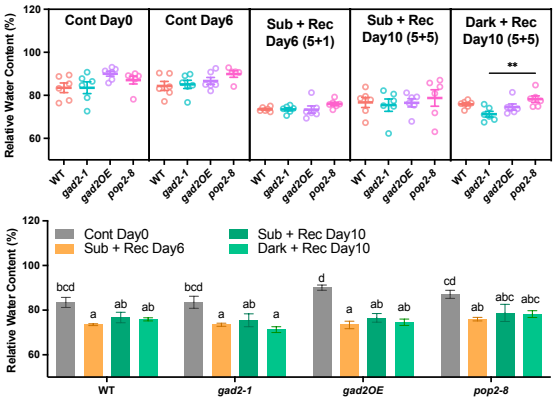


**(d)** Rosette relative water content

**Figure C.2:** WT and GABA mutants under control conditions and following recovery from darkness or light submergence. (a) Representative phenotypes after 5 d dark treatment. Changes of (b) Rosette fresh weight, (c) Rosette dry weight and (d) relative water content (d) in WT and GABA mutants under control conditions, recovery for 1 d or 5 d from submergence, and recovery for 5 d from darkness. Plants were subjected to stresses for 5 d. Data showed mean ± SE of 6 biological replicates (except for *pop2-8* Control Day6, n = 5). Stars and letters represent statistical significance using one way and two-way ANOVA, respectively. * $P < 0.05$, ** $P < 0.01$.

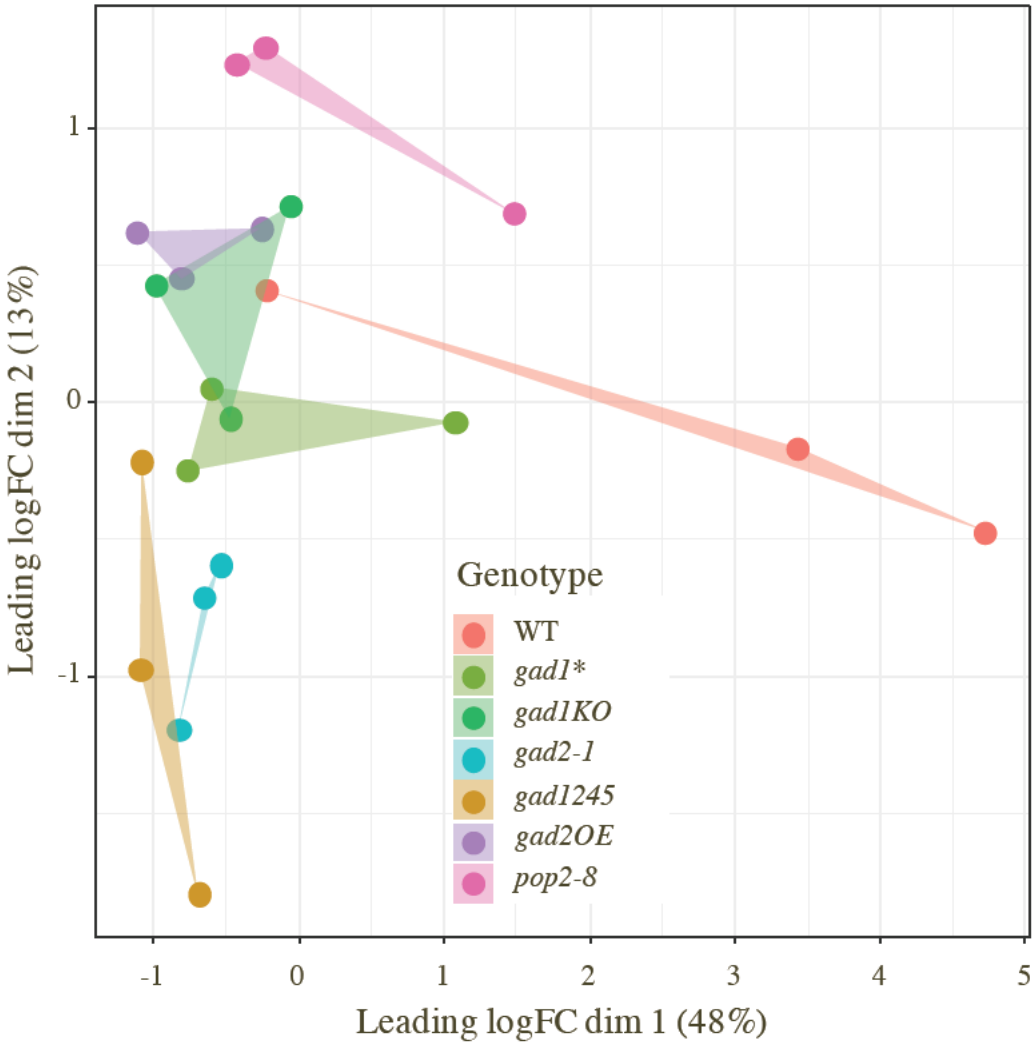


**Figure C.3:** Multi-dimensional scaling (MDS) principal coordinate plot for WT and GABA mutants under control conditions with n = 3 biological representatives for each line. This plot visualises the differences (*leading log2-fold-change* between each pair of samples) between the expression profiles of all samples in two dimensions.

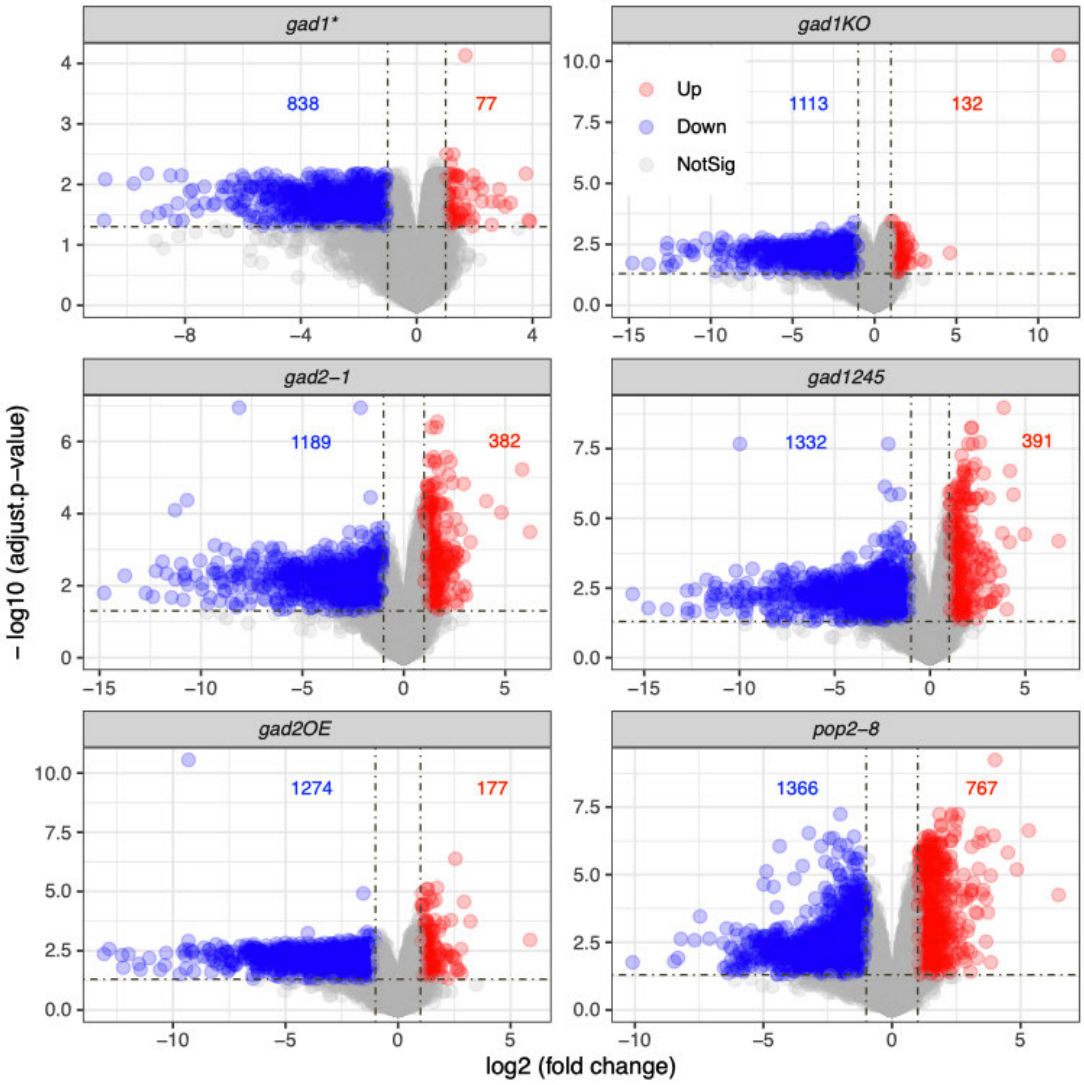


**Figure C.4:** Volcano plot of gene expression in GABA mutants compared to WT under control conditions. Vertical and horizontal dashed lines denote $|log2FC| > 1$ and $adj.P < 0.05$, respectively. Genes that were significantly up-/down- regulated are highlighted in red and blue, respectively, and the numbers of DEGs are also displayed in each sub-figure.

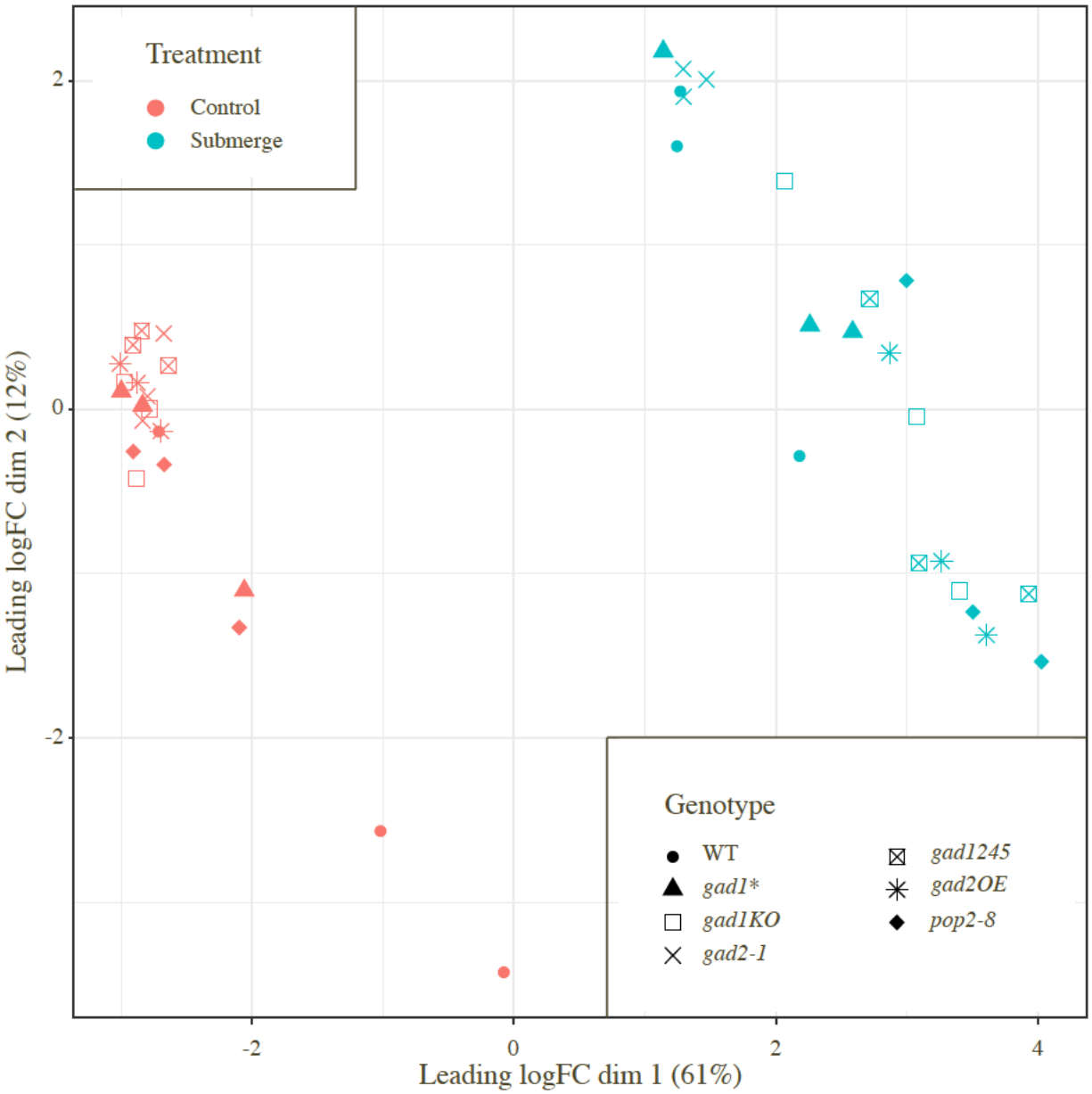


**Figure C.5:** Multi-dimensional scaling (MDS) principal coordinate plot for WT and GABA mutants under control and submerged conditions (n = 3 biological representatives). This plot visualises the differences (*leading log2-fold-change* between each pair of samples) between the expression profiles of all samples in two dimensions.

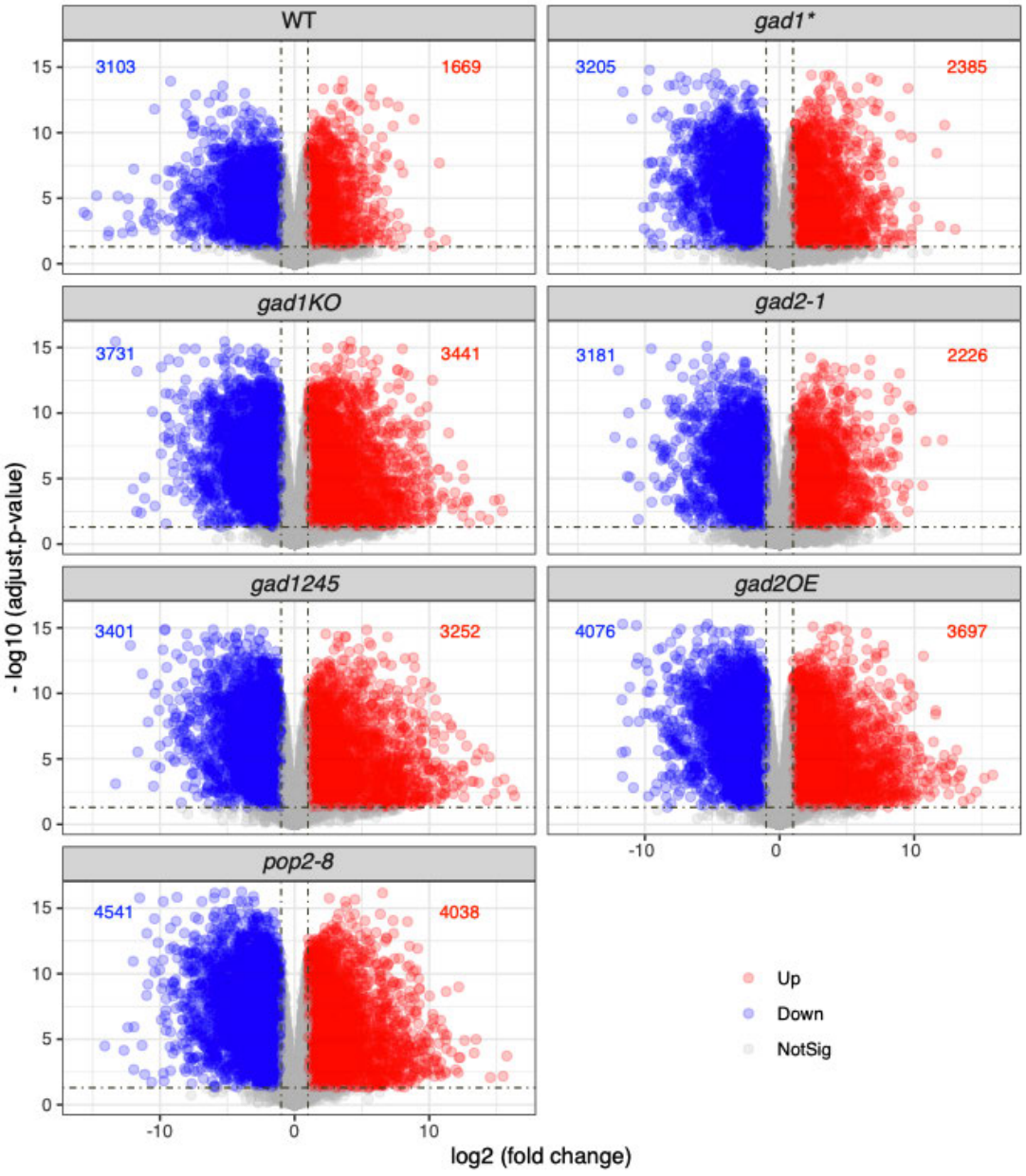


**Figure C.6:** Volcano plot of gene expression in WT and GABA mutants after submergence. Genes that are significant up-/down- regulated ($|log2FC| > 1$ and $adj.P < 0.05$) as well as their number are highlighted in red/blue, respectively.

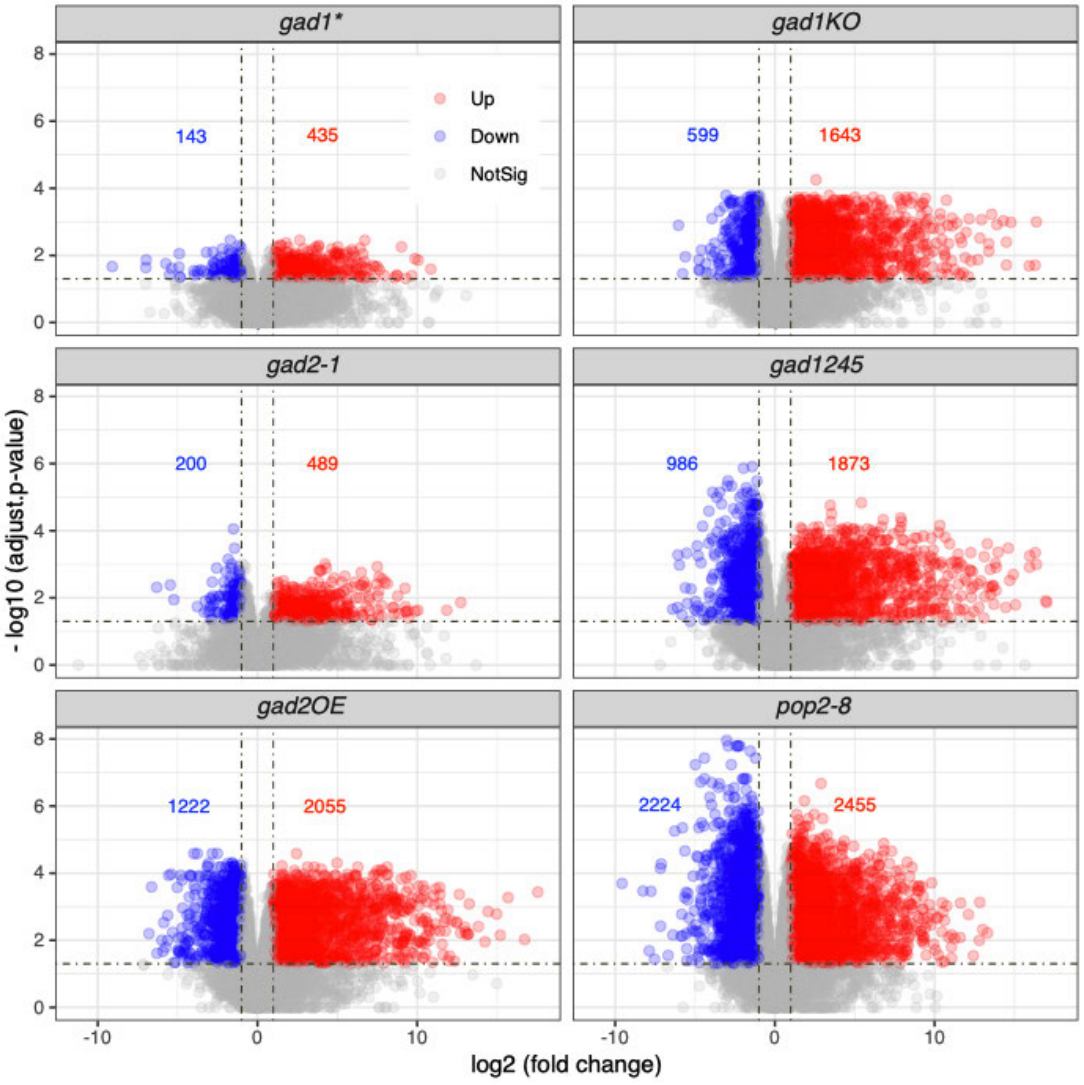


**Figure C.7:** Volcano plot of MutSub gene expression in WT and GABA mutants after submergence.. Genes that are significant up-/down- regulated ($|log2FC| > 1$ and $adj.P < 0.05$) as well as their number are highlighted in red/blue, respectively.

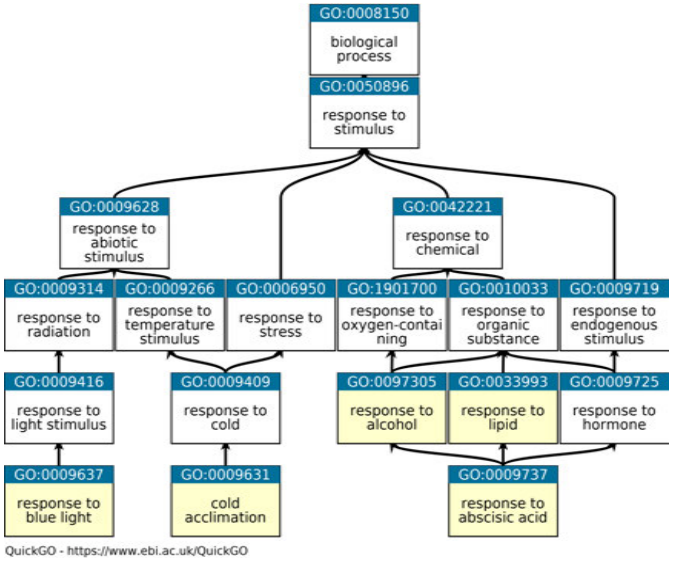


**(a)** Response to stimulus (light, cold, ABA, alcohol and lipid)

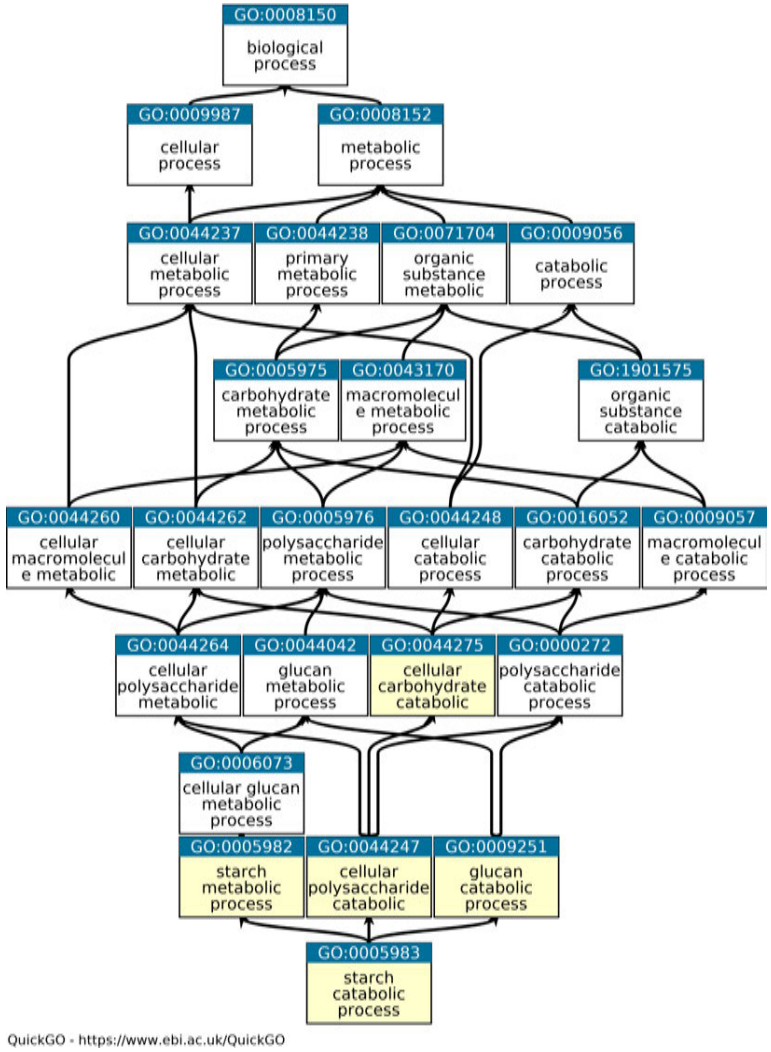


**(b)** Starch catabolic pathways

**Figure C.8:** *gad1245* up-regulated genes exclusively enriched GO terms under control conditions. (a) Response to stimulus (Class I category B/C and Class III category 3B in Table C.3). (b) Starch catabolic processes (Class III category 3C in Table C.3). Legend is the same as Fig 3.9.

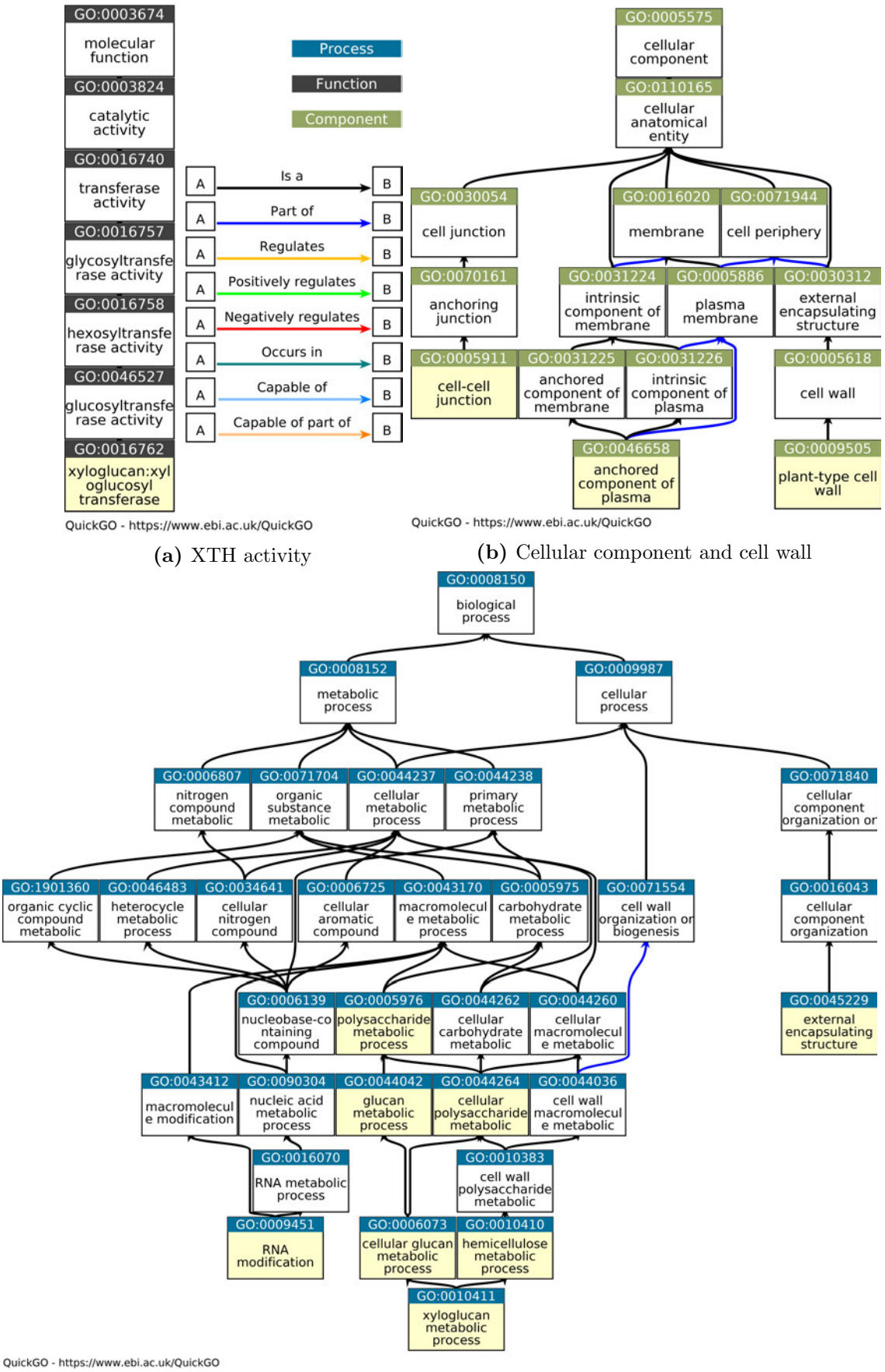


**(a)** XTH activity

**(b)** Cellular component and cell wall

**(c)** RNA modification, xyloglucan metabolic and external encapsulating structure

**Figure C.9:** *pop2-8* up-regulated genes enriched GO terms under control conditions, including 5 Group II terms that it shared with other mutants (Fig 3.8a).


**Figure C.10:** Log2 fold change (normalised against WT) of DEGs related to Class I category A (oxygen/hypoxia response) in GABA mutants under control conditions.

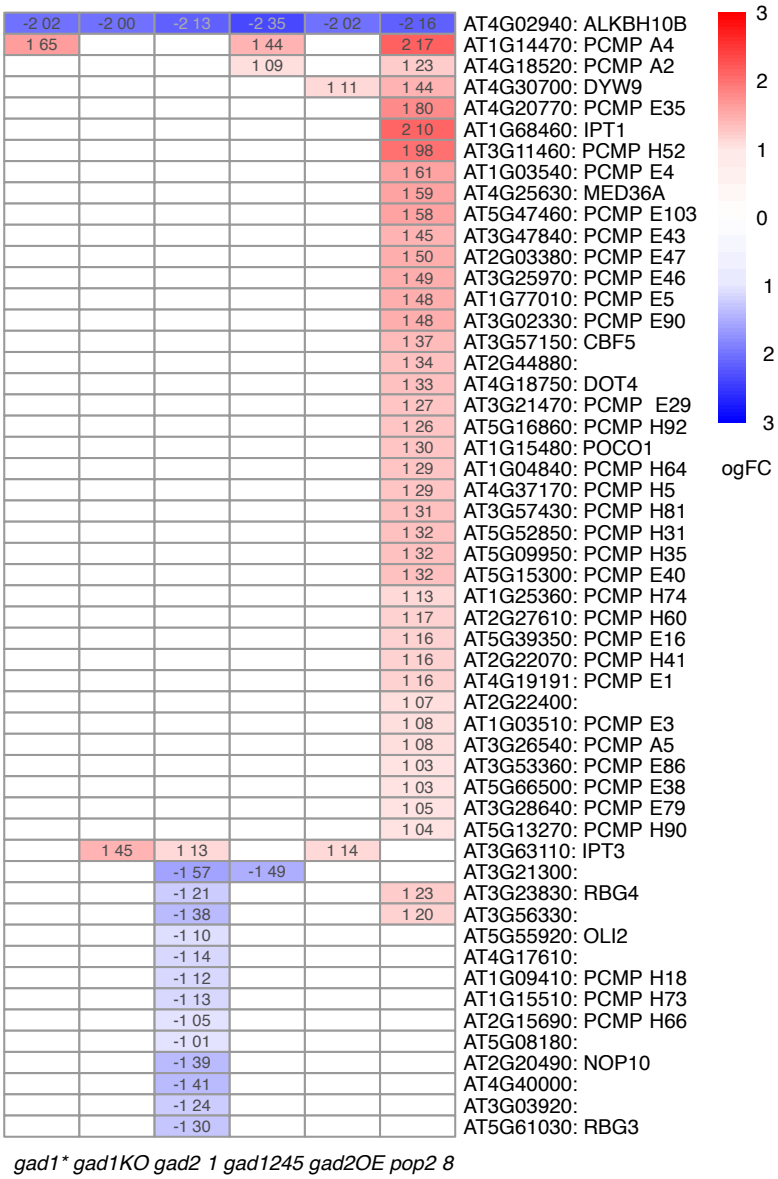


**Figure C.11:** Log2 fold change (normalised against WT) of 53 DEGs related to RNA modification (GO:0009451, Table C.1 Group 3G) in GABA mutants under control conditions.

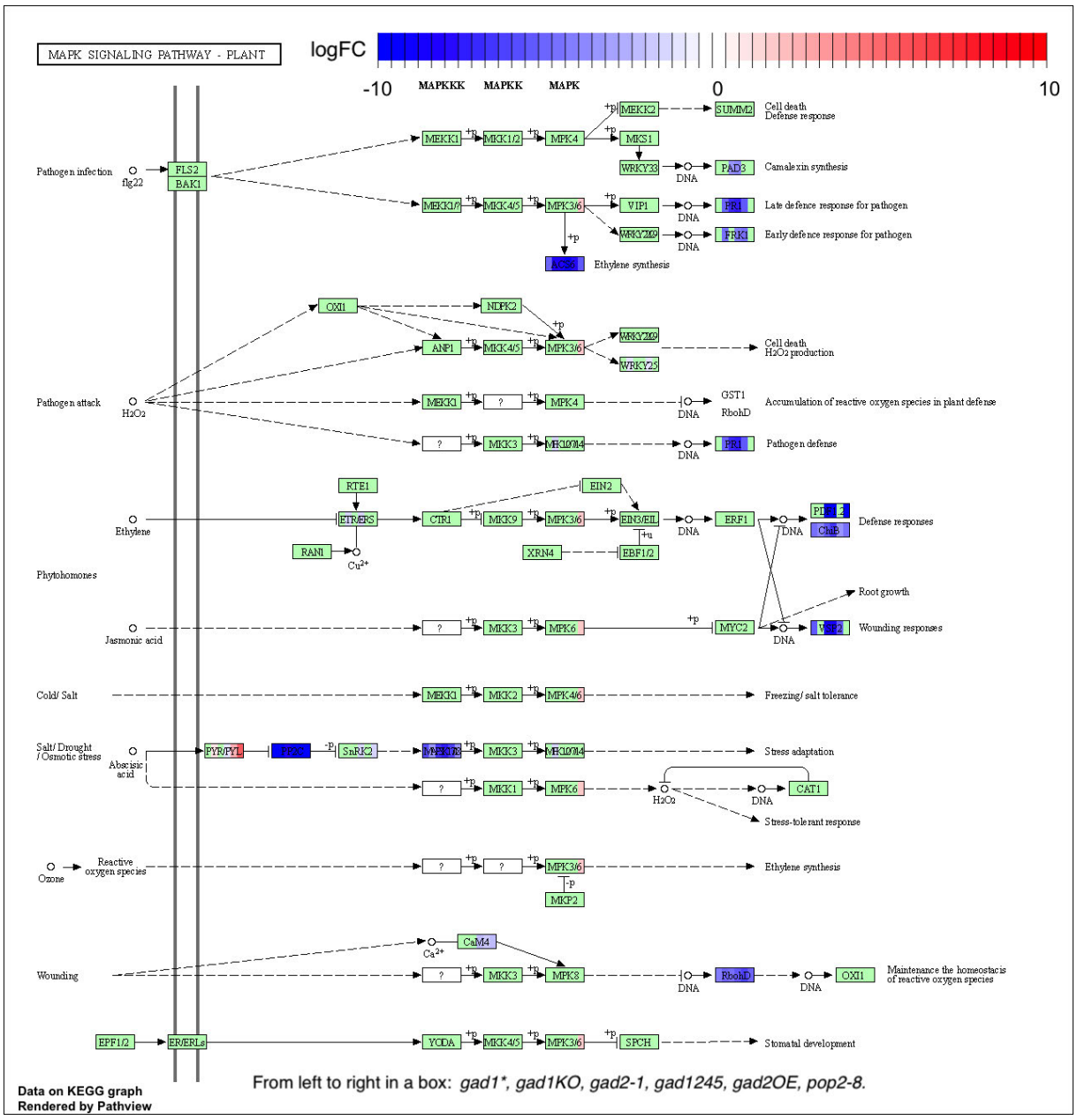


**Figure C.12:** Differentially expressed genes in GABA mutants associated with plant hormone signal transduction under control conditions. From left to right in a box: *gad1*, gad1KO, gad2-1, gad1245, gad2OE, pop2-8.*

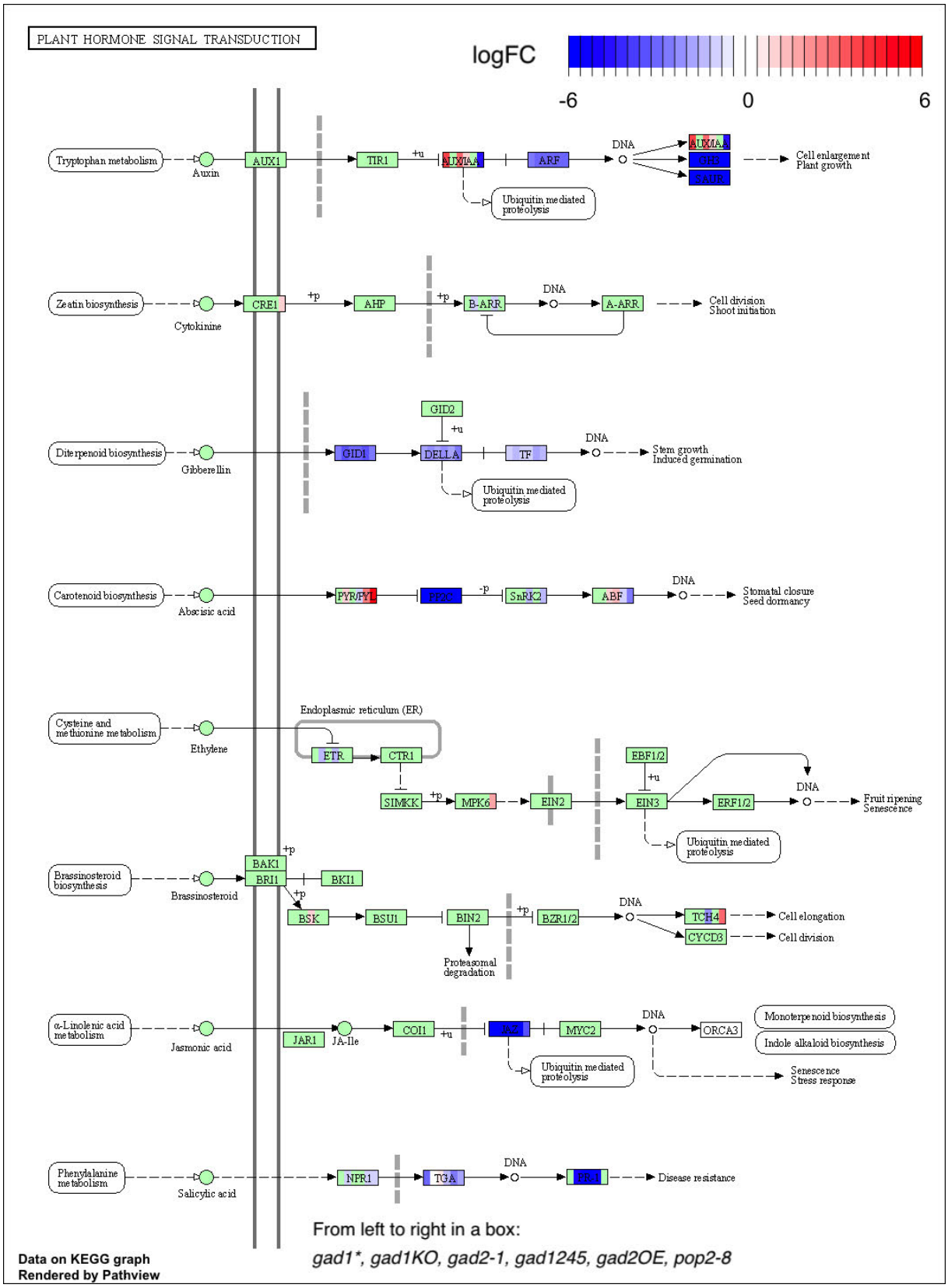


**Figure C.13:** Differentially expressed genes in GABA mutants associated with plant hormone signal transduction under control conditions. From left to right in a box: *gad1*, gad1KO, gad2-1, gad1245, gad2OE, pop2-8.*

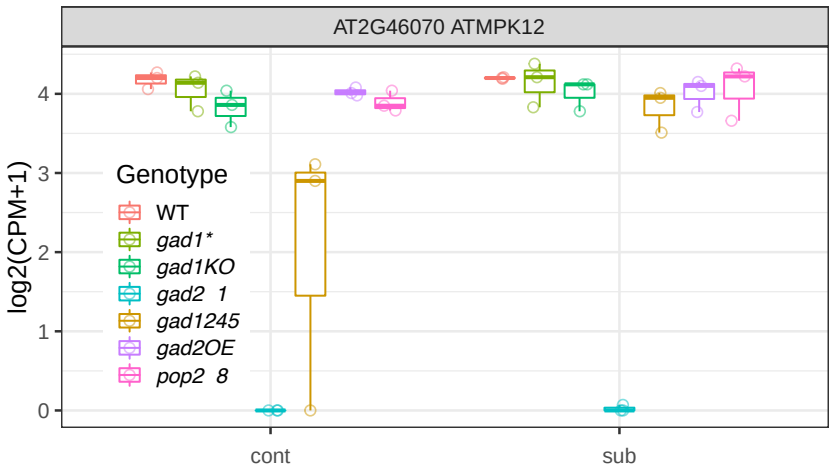


**Figure C.14:** *MPK12* Expression in WT and GABA mutants under control and submerged conditions. (n=3). Boxplot shows median (Q2, 50th percentile) with interquartile range (IQR, Q3 - Q1). Whiskers represent ranges from Q3 to Q3+1.5*IQR, and from Q1-1.5*IQR to Q1.

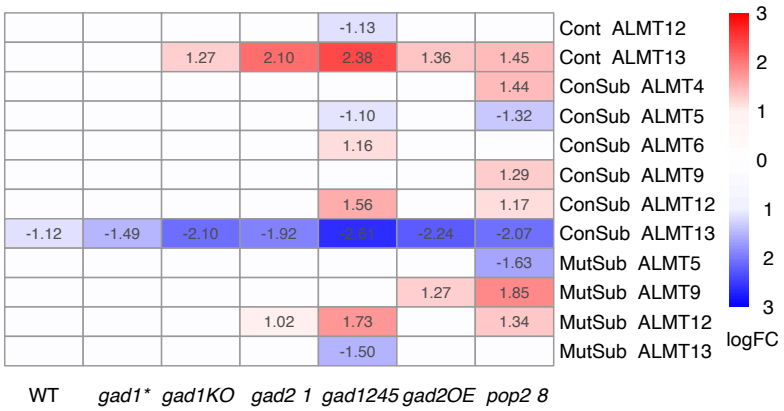


**Figure C.15:** Log2 fold change of *ALMT* genes in WT and GABA mutants under control and submerged conditions.

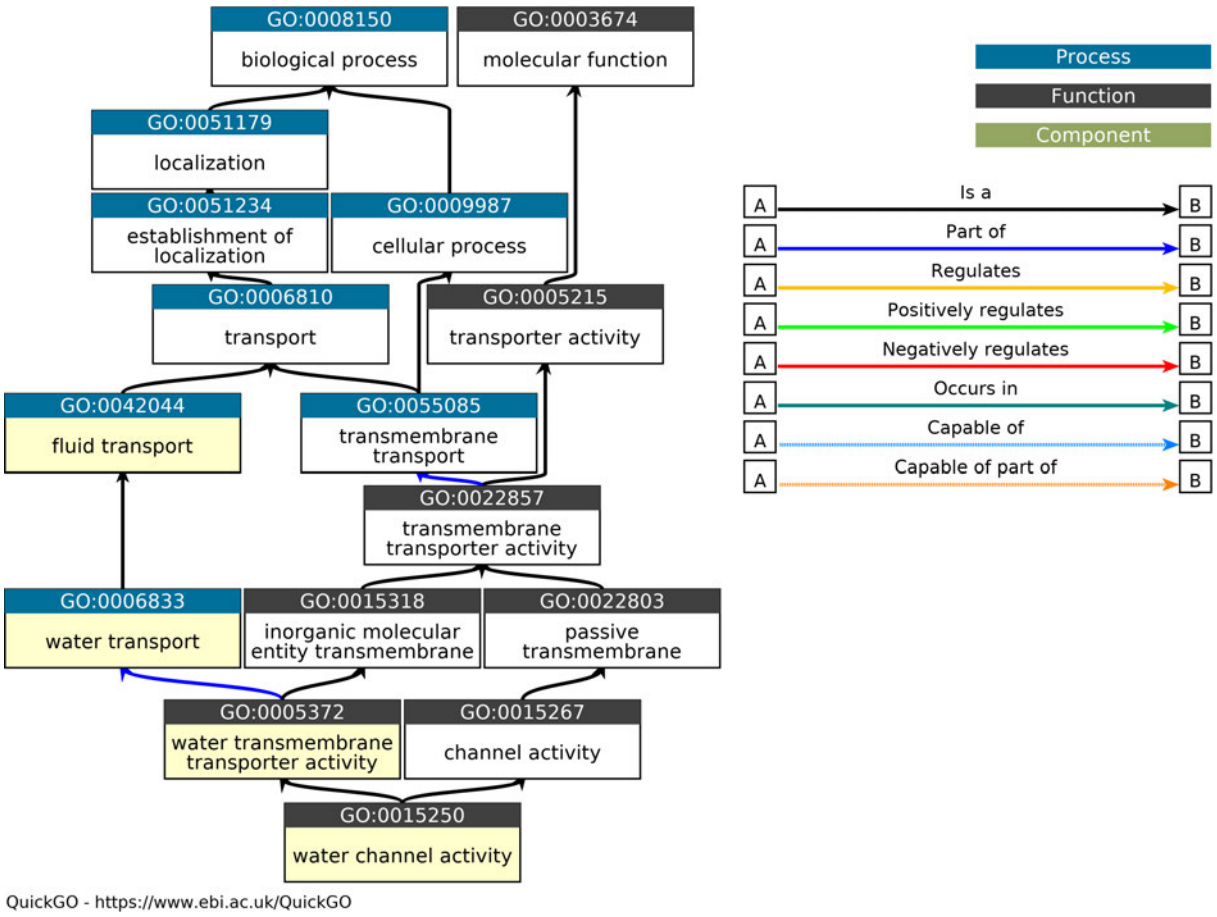


**Figure C.16:** Four GO terms related to water transport, including water transport (GO:0006833), fluid (GO:0042044) transport, water transmembrane transporter activity (GO:0005372) and water channel activity (GO:0015250).

| GeneName | WT | *gad1** | *gad1KO* | *gad2-1* | *gad1245* | *gad2OE* | *pop2-8* |
|---|---|---|---|---|---|---|---|
| ***PIP1-1*** | | | | -1.19 | -1.4 | | -1.34 |
| ***PIP1-2*** | | -1.09 | | -1.21 | -1.46 | -1.24 | -1.42 |
| ***PIP1-3*** | -1.5 | -2.18 | -2.34 | -2.65 | -3.33 | -3.15 | -3.92 |
| ***PIP1-4*** | -2.3 | -1.72 | -1.9 | -1.77 | -1.88 | -2.28 | -2.75 |
| ***PIP1-5*** | -1.1 | -1.6 | -1.3 | -1.6 | -1.76 | -1.76 | -1.69 |
| ***PIP2-1*** | -1.5 | -2.15 | -2.32 | -2.58 | -2.87 | -2.24 | -3.01 |
| ***PIP2-2*** | | -1.31 | -1.14 | -1.67 | -2.18 | -1.25 | -1.88 |
| ***PIP2-3*** | -3.3 | -3.88 | -3.53 | -4.21 | -3.81 | -3.1 | -4.38 |
| ***PIP2-4*** | -4.4 | -3.8 | -3.84 | -4.85 | -5.32 | -2.63 | -3.89 |
| ***PIP2-5*** | -1.9 | -1.9 | -2.17 | -1.65 | -2.75 | -2.69 | -2.7 |
| ***PIP2-6*** | -1.1 | -1.47 | -1.15 | -1.52 | -1.7 | -1.39 | -1.07 |
| ***PIP2-7*** | -2.6 | -3.03 | -2.99 | -3.18 | -3.99 | -4.02 | -5.13 |
| ***PIP2-8*** | -3.3 | -4.11 | -4.74 | -3.35 | -4.62 | -5.25 | -6.36 |
| ***TIP1-1*** | -1.9 | -2.94 | -2.66 | -2.94 | -3.66 | -3.96 | -4.56 |
| ***TIP1-2*** | | | | -1.09 | | -1.08 | -1.16 |
| ***TIP2-1*** | -4.8 | -5.56 | -5.85 | -5.76 | -6.18 | -7.36 | -7.46 |
| ***TIP2-2*** | | -1.75 | -1.61 | -2.15 | -2.61 | -1.68 | -2 |
| ***SIP1-2*** | 1.16 | | | 1.8 | 1.2 | | |
| ***NIP5-1*** | 3.64 | 3.15 | 4.16 | | 2.79 | 3.79 | 4.17 |
| *SYP121* | 1.27 | 1.23 | 1.71 | 1.51 | 1.5 | 1.47 | 1.39 |
| *ERECTA* | -1 | -1.77 | -2.27 | -2.09 | -2.85 | -2.54 | -3.4 |
| *BDG1* | -1.9 | -2.74 | -3.57 | -3.52 | -4.54 | -4.97 | -4.56 |
| *ABCG22* | | | -1.23 | -2.46 | -2.15 | -1.01 | -2.3 |
| *NIP6-1* | | | | -1.13 | -1.82 | | -1.05 |
| *GSO1* | | | | | | | -1.71 |

**Figure C.17:** Log2 fold change of DEGs related to water and fluid transport in WT and GABA mutants after submergence. The gene names belong to the two child term (Fig C.16), i.e. the activity of transporter and water channels were in bold.

| GeneID | GeneName | WT | gad1* | gad1KO | gad2-1 | gad1245 | gad2OE | pop2-8 | GeneID | GeneName | WT | gad1* | gad1KO | gad2-1 | gad1245 | gad2OE | pop2-8 |
|---|---|---|---|---|---|---|---|---|---|---|---|---|---|---|---|---|---|
| AT1G77450 | NAC032 | -1.91 | | | | | | | | | | | | | | | |
| AT1G05100 | MAPKKK18 | -4.42 | | | | | | | AT5G44610 | PCAP2 | 10.01 | 9.78 | 9.17 | | 12.33 | 12.31 | 12.2 |
| AT1G04250 | IAA17 | -1.4 | -3.11 | -3.4 | -2.49 | -3.23 | -3.44 | -4.88 | AT5G45890 | SAG12 | | | 14.43 | | 16.33 | 13.64 | 15.49 |
| AT3G63530 | BB | | | | -1.04 | -1.31 | -1.03 | -1.75 | AT1G73220 | OCT1 | | | 8.27 | | 9.96 | 8.53 | 8.38 |
| AT4G36900 | RAP2-10 | 1.19 | 2.52 | 2.79 | 1.39 | 1.58 | 2.72 | 2.02 | AT3G11340 | UGT76B1 | | | 5.63 | | 6.48 | 4.72 | 3.21 |
| AT5G14930 | SAG101 | 1.52 | 1.48 | 1.85 | 1.64 | 1.61 | 1.87 | 1.53 | AT3G02150 | TCP13 | | | 1.71 | | 1.3 | 1.74 | 1.91 |
| AT5G39610 | NAC92 | 3.09 | 6.11 | 6.98 | 5.36 | 5.4 | 7.42 | 6.42 | AT5G45900 | ATG7 | | | 1.69 | | 1.69 | 1.36 | 1.63 |
| AT3G29035 | NAC59 | 3.54 | 5.11 | 6.03 | 4.08 | 4.23 | 5.41 | 5.3 | AT5G51640 | YLS7 | | | 1.61 | | 1.48 | 1.8 | 2.18 |
| AT1G34180 | anac016 | 2.38 | 3.21 | 4.53 | 3.61 | 3.74 | 4.43 | 4.08 | AT2G39200 | MLO12 | | 2.59 | 4.69 | | 4.53 | 4.54 | 4.6 |
| AT3G04060 | anac046 | | 3.73 | 5.53 | 3.32 | 3.36 | 4.93 | 4.5 | AT3G16857 | ARR1 | 1.2 | 1.17 | 1.38 | | 1.19 | 1.48 | 1.25 |
| AT2G45210 | SAUR36 | | 3.89 | 5.89 | 5.58 | 6.01 | 5.48 | 4.33 | AT1G73680 | ALPHA DOX2 | | 1.26 | 1.55 | | 1.34 | 1.98 | 1.82 |
| AT4G18170 | WRKY28 | | 3.13 | 4.49 | 3.91 | 3.96 | 3.74 | 3.48 | AT2G13790 | SERK4 | 1.04 | | 1.23 | | 1.31 | 1.6 | 1.73 |
| AT1G19270 | DA1 | | 1.11 | 1.61 | 1.25 | 1.68 | 2.07 | 1.95 | AT5G24530 | DMR6 | | | | 1.02 | 1.05 | 1.42 | 1.58 |
| AT3G19290 | ABF4 | | 1.48 | 1.74 | 1.01 | | 1.61 | 1.47 | AT1G11190 | ENDO1 | | | | | 4.1 | 3.46 | 2.32 |
| AT2G43000 | JUB1 | 2.24 | 3.5 | 5.41 | 3.09 | 5.68 | 5.17 | 6.22 | AT3G25010 | AtRLP41 | | | | | 1.64 | 2 | 2.34 |
| AT3G56400 | WRKY70 | | | 1.55 | 1.36 | 1.25 | 1.26 | | AT1G64360 | SAQR | 1.59 | | 1.96 | 1.27 | | 1.11 | 1.1 |
| AT5G62620 | GALT6 | | | 1.27 | 1.57 | 1.9 | 1.45 | 1.54 | AT2G22300 | CAMTA3 | | | 1.21 | | | 1.33 | 1.01 |
| AT1G70170 | 2MMP | | 4.65 | 6.22 | | 9 | 9.36 | 9.55 | AT3G52430 | PAD4 | | | | | | 1.21 | 1.63 |
| AT3G27010 | TCP20 | | | | | | | 1.05 | AT4G12570 | UPL5 | | 1.07 | 1.31 | 1.03 | | 1.34 | 1.38 |
| AT5G02760 | APD7 | 1.53 | | | | | | | AT4G16690 | PPD | -1.49 | 1.56 | 2.19 | 1.8 | 2.95 | 2.23 | 2.14 |
| AT2G20570 | GPRI1 | | | | -1.17 | -1.32 | | | AT4G18980 | AtS40-3 | -3.57 | 3.23 | 5.62 | | 5.01 | 5.75 | 4.06 |
| AT5G22070 | RSE1 | | | | | -1.24 | -1.06 | | AT1G17020 | SRG1 | -4.03 | | 7.35 | | 6.39 | 5.42 | 3.06 |
| AT4G02380 | SAG21 | | 3.96 | 4.61 | 4.62 | 5.94 | 5.31 | 4.55 | AT2G13810 | ALD1 | -3.07 | | | | 3.95 | 4.93 | 2.38 |
| AT1G73980 | TTM1 | | | 1.28 | | | 1.28 | 1.4 | AT5G13170 | SWEET15 | -9.22 | | 5.56 | | 7.08 | 8.33 | |
| AT3G52250 | PWR | | | | | | | 1.06 | AT1G27320 | AHK3 | | | | | | 1.13 | 1.05 |
| AT5G16470 | MBS2 | | | 1.04 | | 1.06 | | | AT5G17290 | ATG5 | | | 1.06 | | | | 1.01 |
| AT3G10985 | SAG20 | 2.17 | 3.34 | 3.61 | 2.6 | 3.25 | 3.15 | 2.81 | AT4G30790 | ATG11 | | | | | | 1.06 | |
| AT1G20900 | AHL27 | 4.8 | 7.64 | 6.4 | 8.29 | 6.37 | 5.16 | 8.24 | AT5G24110 | WRKY30 | | | | | 2.56 | | 3.05 |
| AT1G54130 | RSH3 | 1.13 | 1.45 | 1.99 | 1.18 | 1.4 | 1.77 | 1.98 | AT5G11520 | ASP3 | -1.64 | | | | 1.64 | 1.1 | 1.22 |
| AT1G69490 | NAC029 | 2.52 | 4.32 | 5.23 | 4.05 | 3.94 | 5.03 | 5.5 | AT5G59220 | SAG113 | -5.73 | | 4.2 | | | 5.69 | |
| AT1G73500 | MKK9 | 1.67 | 2.75 | 3.25 | 3.05 | 2.38 | 2.9 | 2.56 | AT1G32450 | NPF7.3 | -2.36 | | | | | | |
| AT4G32940 | GAMMA-VPE | 2.76 | 3.79 | 4.08 | 2.71 | 2.56 | 3.68 | 3.27 | AT1G05620 | URH2 | -1.12 | | | | | | |
| AT5G08790 | NAC081 | 1.53 | 2.5 | 3.12 | 2.47 | 2.84 | 2.78 | 2.57 | AT1G53230 | TCP3 | | | | | -1.43 | -1.03 | |
| AT5G37600 | GLN1-1 | 1.35 | 1.83 | 2.78 | 1.98 | 2.41 | 2.46 | 3.02 | AT3G15030 | TCP4 | | -1.05 | -1.31 | -1.59 | -1.31 | -2.02 | -1.75 |
| AT4G01250 | WRKY22 | 2.27 | 2.66 | 4.14 | 2.49 | 3.4 | 3.05 | 2.72 | AT5G64940 | ATATH13 | | -1.25 | -1.65 | -1.28 | -1.2 | -1.32 | -2.01 |
| AT4G23810 | WRKY53 | 2.5 | 2.78 | 4.14 | 2.75 | 3.98 | 4.14 | 4.31 | AT1G54040 | ESP | -7.35 | -8.2 | -9.33 | -7.19 | -8.77 | -8.73 | -10.41 |
| AT3G10500 | NAC053 | | 1.39 | 1.93 | 1.66 | 1.87 | 2.12 | 2.75 | AT5G51720 | NEET | -5.73 | -3.93 | -4.5 | -5.81 | -5.34 | -5.92 | -5.8 |
| AT3G19190 | ATG2 | | 1.17 | 1.47 | 1.15 | 1.14 | 1.63 | 1.39 | AT2G42530 | COR15B | -2.92 | -2.85 | -2.48 | -3.37 | -3.55 | -2.89 | -2.94 |
| AT3G62770 | ATG18A | | 1.22 | 1.48 | 1.13 | 1.18 | 1.48 | 1.6 | AT2G42540 | COR15A | -7.1 | -5.12 | -4.47 | -5.32 | -5.85 | -4.3 | -4.97 |
| AT5G13180 | NAC083 | | 1.5 | 1.76 | 1.31 | 1.45 | 1.87 | 2.25 | AT2G44300 | LTPG14 | -2.06 | -2.96 | -3.78 | -3.23 | -3.46 | -3.2 | -4.9 |
| AT2G35980 | NHL10 | | 2.91 | 8.53 | 6.3 | 9.67 | 8.37 | 6.7 | AT4G30520 | SARK/CIK3 | -1.24 | -2.02 | -2.08 | -1.75 | -2.88 | -2.2 | -2.45 |
| AT5G39520 | CSAP | | 8.12 | 9.84 | 7.24 | 9.44 | 8.7 | 7.39 | AT5G12080 | MSL10 | -1.04 | -1.85 | -2.24 | -1.45 | -2.02 | -2.04 | -2.52 |
| AT4G10500 | DLO1 | | | 1.42 | 2.61 | 3.92 | 3.3 | 4.21 | AT5G52300 | LTI65 | -7.69 | | | | | | |
| AT2G43570 | CHI | | | 3.18 | 3.82 | 5.1 | 4.35 | 2.53 | AT5G52310 | RD29A | -5.18 | -2.81 | | -3.28 | -3.4 | | |

**Figure C.18:** Log2 fold change of 87 DEGs related to leaf senescence (GO:0010150) in WT and GABA mutants after submergence. The gene names belong to the 3 child terms (Fig 3.23) were in bold, and red/green gene names indicates positive/negative regulation of leaf senescence.

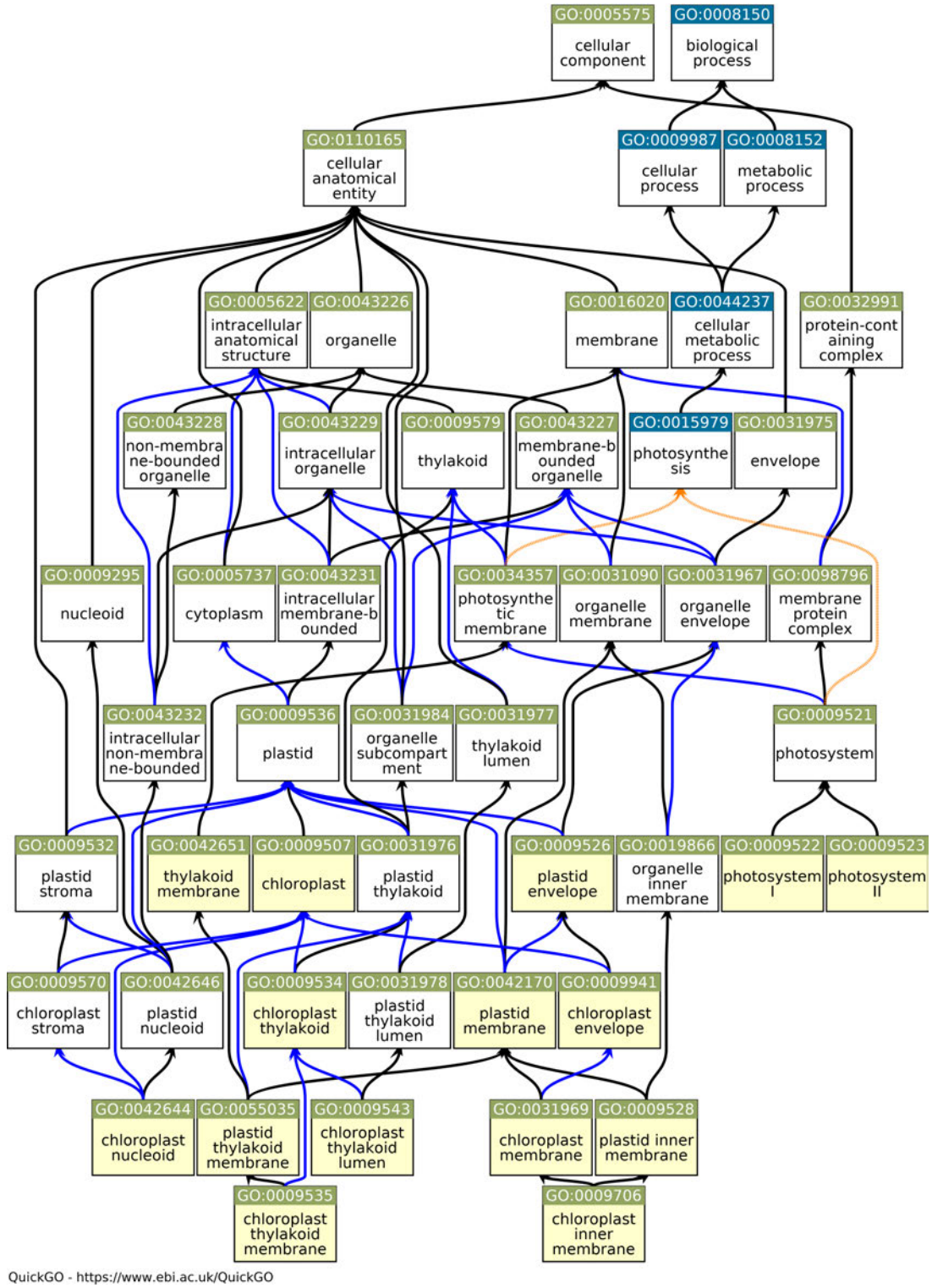


**Figure C.19:** 15 GO terms in GO-Down results after submergence. They all belong to ontology cell component ('CC'), where many enriched process took place in plastid and chloroplast. Legend the same as Fig C.16

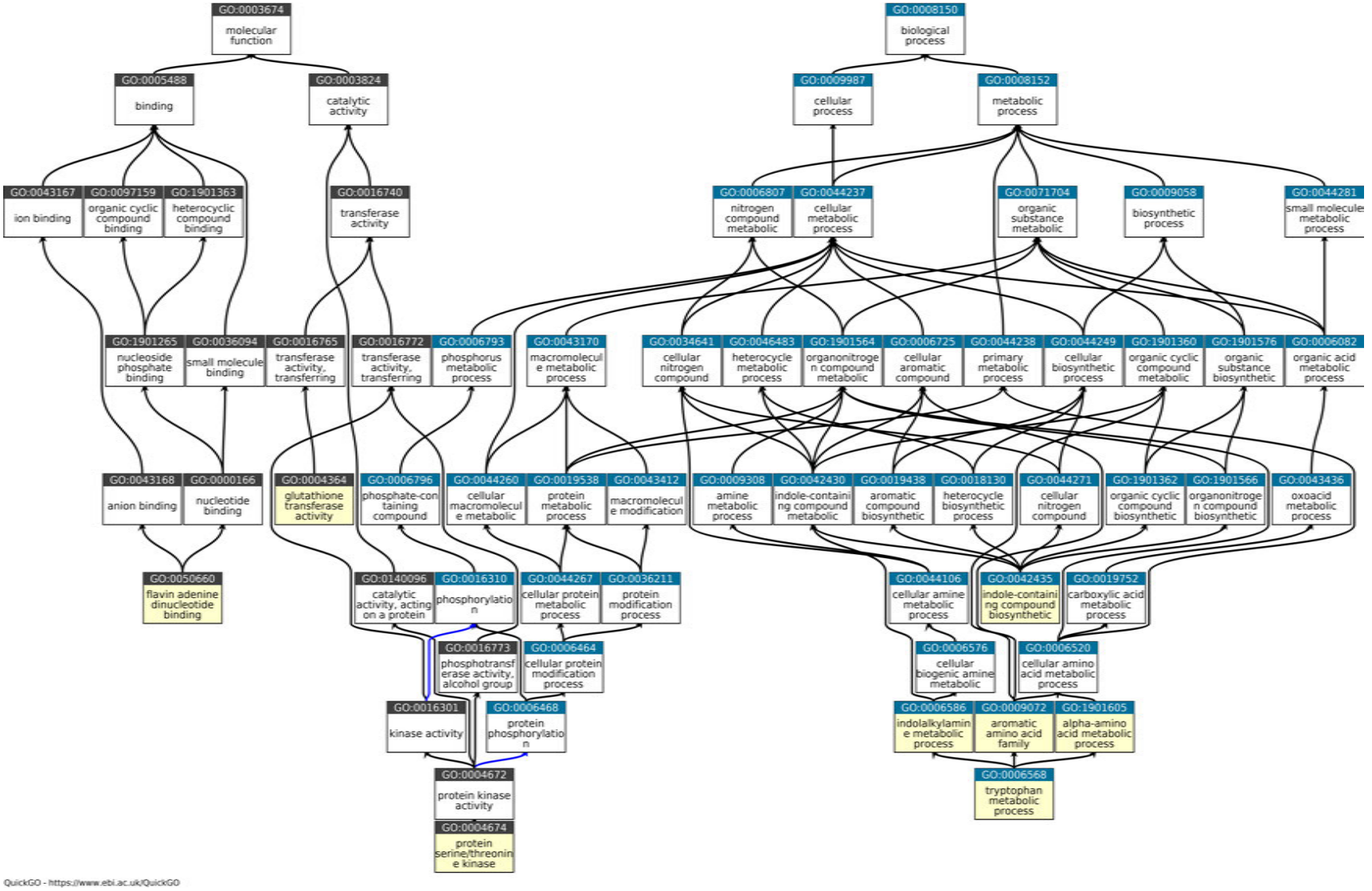


**Figure C.20:** Shared terms through up-regualated MutSub DE genes in *gad1245*, *gad2OE* and *pop2-8*. Legend the same as in Fig C.16.

| GeneName | WT | *gad1** | *gad1KO* | *gad2-1* | *gad1245* | *gad2OE* | *pop2-8* | DEGs |
|---|---|---|---|---|---|---|---|---|
| *RAP2-1* | | | -1.77 | | | | -2.2 | Cont |
| *RAP2-3* | | | | | | | -1.4 | Cont |
| *RAP2-6* | | | -9.39 | -12.72 | -12.72 | -7.55 | | Cont |
| *RAP2-9* | | -2.01 | -1.5 | | | | | Cont |
| *RAP2-10* | | -1.13 | -1.17 | | | -1.21 | | Cont |
| *RAP2-12* | | -1.23 | | | | | | Cont |
| *RAP2-1* | 1.85 | 3.18 | 3.66 | 2.65 | 2.09 | 2.94 | 4.06 | ConSub |
| *RAP2-2* | 1.73 | 2.11 | 2.27 | 1.89 | 1.93 | 2.19 | 2.26 | ConSub |
| *RAP2-3* | 3.11 | 3.17 | 4.08 | 2.64 | 3.05 | 3.75 | 4.25 | ConSub |
| *RAP2-6* | -3.5 | | 6.03 | 8.38 | 9.4 | 4.41 | | ConSub |
| *RAP2.7* | | | | | -1.04 | | | ConSub |
| *RAP2-9* | | 3.73 | 3.04 | 1.96 | 2.91 | 1.93 | 3.05 | ConSub |
| *RAP2-10* | 1.19 | 2.52 | 2.79 | 1.39 | 1.58 | 2.72 | 2.02 | ConSub |
| *RAP2-12* | | 1.15 | 1.02 | | | | | ConSub |
| *RAP2-13* | | | 1.52 | | 1.6 | 1.35 | | ConSub |
| *HRE1* | | 1.46 | 1.25 | 1.03 | 1.34 | 1.9 | 1.75 | ConSub |
| *HRA1* | | | -1.12 | | -1.15 | -1.39 | -1.69 | ConSub |
| *RAP2-1* | | | 1.81 | | | | 2.21 | MutSub |
| *RAP2-3* | | | | | | | 1.13 | MutSub |
| *RAP2-6* | | | 9.51 | 11.86 | 12.88 | 7.88 | | MutSub |
| *RAP2-9* | | 2.78 | 2.09 | | 1.96 | | 2.1 | MutSub |
| *RAP2-10* | | 1.34 | 1.6 | | | 1.53 | | MutSub |
| *RAP2-12* | | 1.92 | 1.79 | | 1.18 | 1.51 | 1.53 | MutSub |
| *HRE1* | | | | | | 1 | | MutSub |

**Figure C.21:** Log2 fold change of RAP2, HRE1 and HRA1 genes in WT and GABA mutants under control and submerged conditions.

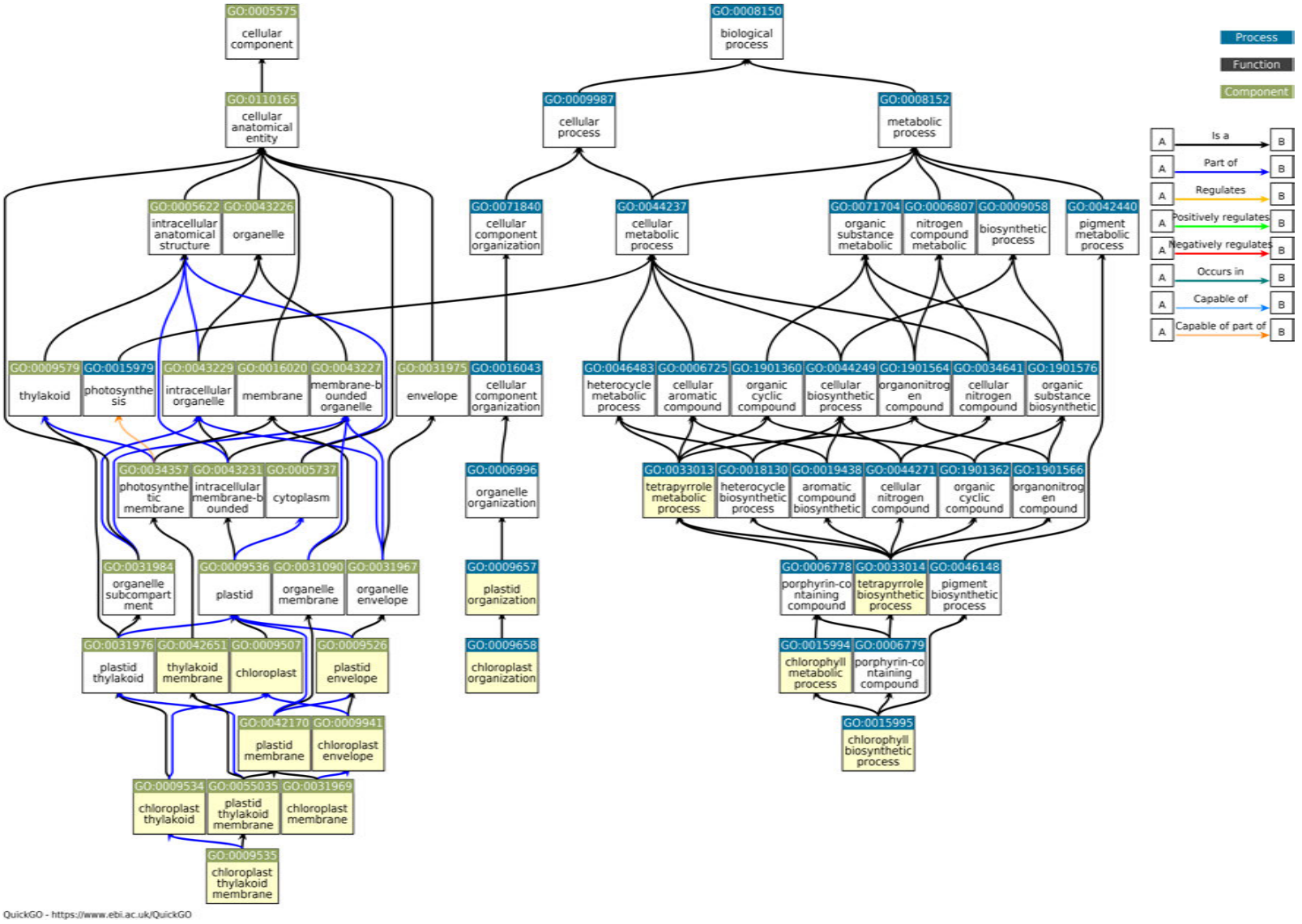


**Figure C.22:** 15 chloroplast biosynthesis related terms through up-regulated MutSub DEGs in *gad1KO*, *gad2OE* and *pop2-8* after submergence.

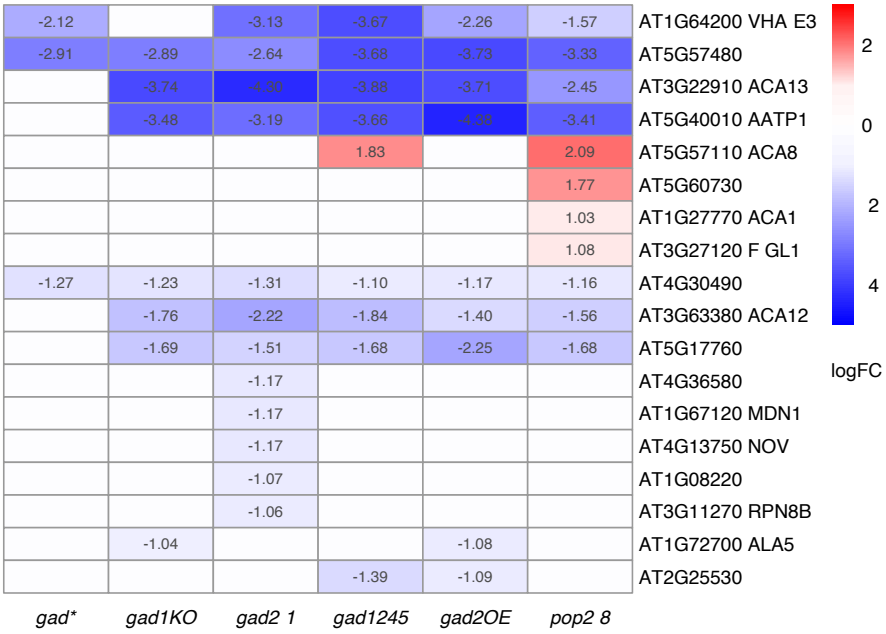


**Figure C.23:** Log fold change of ATPase genes in GABA mutants compared to WT under control conditions. Genes significant up-/down- regulated ($|log2FC| > 1$ and $adj.P < 0.05$) were highlighted in red/blue, respectively.

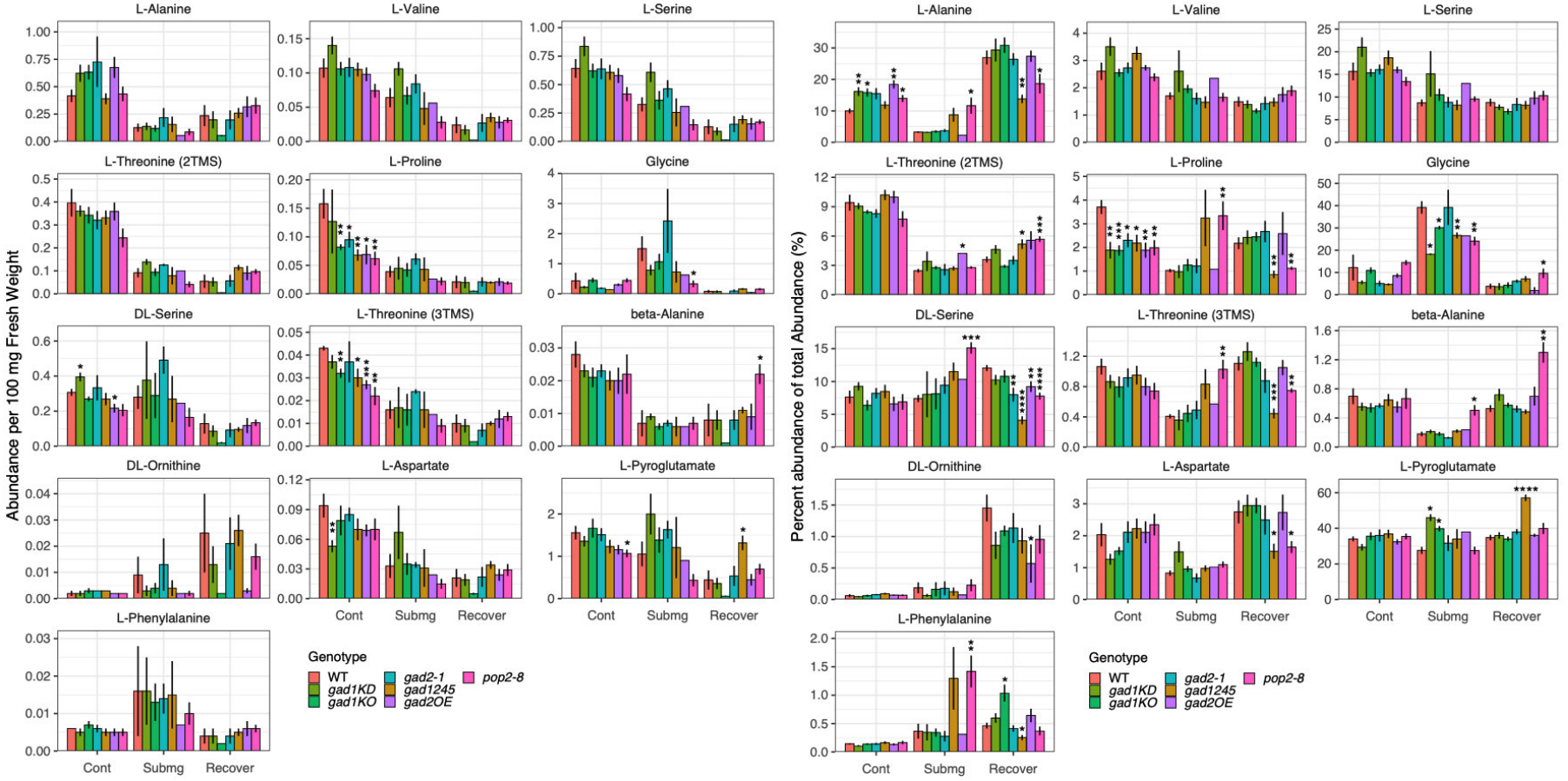


**(a)** Abundance per 100 mg Fresh Weight

**(b)** Percent abundance of total abundance

**Figure C.24:** Abundance of amino acids under control, submergence and recovery in WT and GABA mutants using GCMS. Stars denoted significance between WT and mutant under the same treatment ($P < 0.05$) using student t-test.

**Table C.1:** List of 134 DEGs in GABA mutants under control conditions, with category B and D corresponding to the venn diagram in Fig 3.10a.

| Gene ID | Gene Info | Category |
|---|---|---|
| AT1G02340 | HFR1: Transcription factor HFR1 | B, D |
| AT1G05100 | MAPKKK18: Mitogen-activated protein kinase kinase kinase 18 | B, D |
| AT1G05680 | UGT74E2: Glycosyltransferase (Fragment) | B, D |
| AT1G07430 | AIP1: Protein phosphatase 2C 3 | B, D |
| AT1G10560 | PUB18: U-box domain-containing protein 18 | B, D |
| AT1G12240 | BFRUCT4: Acid beta-fructofuranosidase 4, vacuolar | B, D |
| AT1G15100 | RHA2A: E3 ubiquitin-protein ligase RHA2A | B, D |
| AT1G15520 | ABCG40: ABC transporter G family member 40 | B, D |
| AT1G16060 | ADAP: AP2-like ethylene-responsive transcription factor | B, D |
| AT1G18390 | Protein kinase superfamily protein | B, D |
| AT1G43160 | RAP2-6: Ethylene-responsive transcription factor RAP2-6 | B, D |
| AT1G45249 | ABF2: abscisic acid responsive elements-binding factor 2 | B, D |
| AT1G48630 | RACK1B: RACK1B_AT | B, D |
| AT1G49720 | ABF1: Abscisic acid responsive element-binding factor 1 | B, D |
| AT1G51800 | IOS1: LRR receptor-like serine/threonine-protein kinase IOS1 | B, D |
| AT1G51940 | LYK3: LysM domain receptor-like kinase 3 | B, D |
| AT1G52400 | BGLU18: Beta-D-glucopyranosyl abscisate beta-glucosidase | B, D |
| AT1G54160 | NFYA5: Nuclear transcription factor Y subunit A-5 | B, D |
| AT1G59870 | ABCG36: ABC transporter G family member 36 | B, D |
| AT1G62660 | BFRUCT3: Acid beta-fructofuranosidase 3, vacuolar | B, D |
| AT1G65690 | NHL6: NDR1/HIN1-like protein 6 | B, D |
| AT1G65790 | SD17: Receptor-like serine/threonine-protein kinase SD1-7 | B, D |
| AT1G67120 | AT1G67120: MDN1: ATPases; nucleotide, ATP and transcription factor binding | B, D |
| AT1G69260 | AFP1: Ninja-family protein AFP1 | B, D |
| AT1G69270 | RPK1: Probable LRR receptor-like serine/threonine-protein kinase RPK1 | B, D |
| AT1G72770 | HAB1: Protein phosphatase 2C 16 | B, D |
| AT1G75750 | GASA1: Gibberellin-regulated protein 1 | B, D |
| AT2G01540 | CAR10: Protein C2-DOMAIN ABA-RELATED 10 | B, D |
| AT2G26040 | PYL2: Abscisic acid receptor PYL2 | B, D |
| AT2G30020 | PP2C-type phosphatase AP2C1 | B, D |
| AT2G32510 | MAPKKK17: Mitogen-activated protein kinase kinase kinase 17 | B, D |
| AT2G33150 | PED1: PKT3 | B, D |
| AT2G38310 | PYL4: Abscisic acid receptor PYL4 | B, D |
| AT2G40180 | PP2C5: PP2C-type phosphatase AP2C3 | B, D |
| AT2G40330 | PYL6: Abscisic acid receptor PYL6 | B, D |
| AT2G40340 | DREB2C: Integrase-type DNA-binding superfamily protein | B, D |
| AT2G46510 | AIB: Transcription factor ABA-INDUCIBLE bHLH-TYPE | B, D |
| AT3G01420 | DOX1: Alpha-dioxygenase 1 | B, D |
| AT3G02140 | AFP4: TMAC2 | B, D |
| AT3G03450 | RGL2: RGL2 | B, D |
| AT3G11410 | PP2CA: Protein phosphatase 2C 37 | B, D |
| AT3G18130 | RACK1C: Receptor for activated C kinase 1C | B, D |
| AT3G19580 | AZF2: ZF2 | B, D |
| AT3G22231 | PCC1: Cysteine-rich and transmembrane domain-containing protein PCC1 | B, D |
| AT3G25010 | AtRLP41: Receptor like protein 41 | B, D |
| AT3G26790 | FUS3: B3 domain-containing transcription factor FUS3 | B, D |
| AT3G48360 | BT2: BTB/POZ and TAZ domain-containing protein 2 | B, D |
| AT3G59220 | PRN1: Pirin-1 | B, D |
| AT3G63060 | EDL3: EID1-like F-box protein 3 | B, D |
| AT4G11890 | Protein kinase superfamily protein | B, D |
| AT4G18010 | IP5P2: Type I inositol polyphosphate 5-phosphatase 2 | B, D |
| AT4G21534 | SPHK2: Sphingosine kinase 2 | B, D |
| AT4G23450 | AIRP1: RING/U-box superfamily protein | B, D |
| AT4G26080 | ABI1: Protein phosphatase 2C 56 | B, D |
| AT4G33780 | ATP phosphoribosyltransferase regulatory subunit | B, D |
| AT4G34000 | ABF3: ABSCISIC ACID-INSENSITIVE 5-like protein 6 | B, D |
| AT5G01520 | AIRP2: AtAIRP2 | B, D |
| AT5G01550 | LECRKA4.2: lectin receptor kinase a4.1 | B, D |
| AT5G01810 | CIPK15: CBL-interacting serine/threonine-protein kinase 15 | B, D |
| AT5G05440 | PYL5: Abscisic acid receptor PYL5 | B, D |
| AT5G11260 | HY5: Basic-leucine zipper (bZIP) transcription factor family protein | B, D |
| AT5G13170 | SWEET15: Bidirectional sugar transporter SWEET15 | B, D |
| AT5G13330 | ERF113: Rap2.6L | B, D |
| AT5G14920 | GASA14: Gibberellin-regulated protein 14 | B, D |
| AT5G17490 | RGL3: DELLA protein RGL3 | B, D |
| AT5G25980 | TGG2: Myrosinase 2 | B, D |
| AT5G35750 | AHK2: Histidine kinase 2 | B, D |
| AT5G45830 | DOG1: delay of germination 1 | B, D |
| AT5G46590 | anac096: NAC domain-containing protein 96 | B, D |

Continuation of Table C.1

| Gene ID | Gene Info | Category |
|---|---|---|
| AT5G52300 | LTI65: Low-temperature-induced 65 kDa protein | B, D |
| AT5G52900 | MAKR6: Probable membrane-associated kinase regulator 6 | B, D |
| AT5G57050 | ABI2: AtABI2 | B, D |
| AT5G58670 | PLC1: Phosphoinositide phospholipase C 1 | B, D |
| AT5G59220 | SAG113: Probable protein phosphatase 2C 78 | B, D |
| AT5G62470 | MYB96: Transcription factor MYB96 | B, D |
| AT5G64750 | ABR1: Ethylene-responsive transcription factor ABR1 | B, D |
| AT5G65310 | ATHB-5: Homeobox-leucine zipper protein ATHB-5 | B, D |
| AT5G67300 | MYB44: MYBR1 | B, D |
| AT5G67450 | AZF1: ZF1 | B, D |
| AT1G05010 | ACO4: 1-aminocyclopropane-1-carboxylate oxidase 4 | B, D |
| AT1G09530 | PIF3: Transcription factor PIF3 | B, D |
| AT1G17380 | TIFY11A: Protein TIFY 11A | B, D |
| AT1G19180 | TIFY10A: TIFY10A | B, D |
| AT1G19570 | DHAR1: Glutathione S-transferase DHAR1, mitochondrial | B, D |
| AT1G21910 | ERF012: DREB26 | B, D |
| AT1G28480 | GRXC9: Glutaredoxin-C9 | B, D |
| AT1G30135 | TIFY5A: Protein TIFY 5A | B, D |
| AT1G48500 | TIFY6A: Protein TIFY 6A | B, D |
| AT1G56650 | MYB75: Transcription factor MYB75 | B, D |
| AT1G63100 | SCL28: Scarecrow-like protein 28 | B, D |
| AT1G65390 | PP2A5: Protein PHLOEM PROTEIN 2-LIKE A5 | B, D |
| AT1G70700 | JAZ9: TIFY7 | B, D |
| AT1G72450 | TIFY11B: TIFY11B | B, D |
| AT1G74950 | TIFY10B: TIFY10B | B, D |
| AT1G79460 | GA2: KS1 | B, D |
| AT2G14900 | GASA7: Gibberellin-regulated protein 7 | B, D |
| AT2G16750 | | B, D |
| AT2G34070 | TBL37: Protein trichome birefringence-like 37 | B, D |
| AT2G34600 | TIFY 5B: Protein TIFY 5B | B, D |
| AT2G38240 | ANS: Probable 2-oxoglutarate-dependent dioxygenase ANS | B, D |
| AT2G40750 | WRKY54: Probable WRKY transcription factor 54 | B, D |
| AT2G42580 | TTL3: Inactive TPR repeat-containing thioredoxin TTL3 | B, D |
| AT3G05800 | BHLH150: Transcription factor bHLH150 | B, D |
| AT3G14395 | | B, D |
| AT3G15356 | LEC: Lectin-like protein LEC | B, D |
| AT3G15500 | NAC055: NAC3 | B, D |
| AT3G16570 | RALF23: RALF23 | B, D |
| AT3G16770 | RAP2-3: Ethylene-responsive transcription factor RAP2-3 | B, D |
| AT3G17860 | TIFY6B: Protein TIFY 6B | B, D |
| AT3G19100 | CRK2: CDPK-related kinase 2 | B, D |
| AT3G43440 | TIFY3A: Protein TIFY 3A | B, D |
| AT3G50660 | CYP90B1: Cytochrome P450 90B1 | B, D |
| AT3G50700 | GAF1: Protein indeterminate-domain 2 | B, D |
| AT3G54030 | BSK6: BSK6 | B, D |
| AT3G55970 | JRG21: JRG21 | B, D |
| AT3G63010 | GID1B: Gibberellin receptor GID1B | B, D |
| AT4G18890 | BEH3: BES1/BZR1 homolog protein 3 | B, D |
| AT4G26120 | Ankyrin repeat family protein / BTB/POZ domain-containing protein | B, D |
| AT4G26150 | GATA22: Putative GATA transcription factor 22 | B, D |
| AT4G30610 | SCPL24: Serine carboxypeptidase 24 | B, D |
| AT4G39070 | BBX20: B-box zinc finger protein 20 | B, D |
| AT5G05600 | Probable 2-oxoglutarate-dependent dioxygenase | B, D |
| AT5G13220 | JAZ10: jasmonate-zim-domain protein 10 | B, D |
| AT5G20900 | TIFY3B: Protein TIFY 3B | B, D |
| AT5G26230 | MAKR1: Probable membrane-associated kinase regulator 1 | B, D |
| AT5G39760 | ZHD10: Zinc-finger homeodomain protein 10 | B, D |
| AT5G39860 | PRE1: Transcription factor PRE1 | B, D |
| AT5G41260 | BSK8: Serine/threonine-protein kinase BSK8 | B, D |
| AT5G41315 | GL3: MYC6.2 | B, D |
| AT5G54060 | A3G2XYLT: Glycosyltransferase (Fragment) | B, D |
| AT5G56860 | GATA21: GATA transcription factor 21 | B, D |
| AT5G59845 | GASA10: Gibberellin-regulated protein 10 | B, D |
| AT5G60300 | LECRK19: L-type lectin-domain containing receptor kinase I.9 | B, D |
| AT5G63970 | RGLG3: E3 ubiquitin-protein ligase RGLG3 | B, D |

**Table C.2:** Direct GO terms of oppositely regulated DEGs in GABA mutants under control. BP: biological process. CC: cell component. MF: molecular function.

| Gene ID | GO term | Ontology |
|---|---|---|
| AT1G02340 | GO:0000976 transcription regulatory region sequence-specific DNA binding | MF |
| | GO:0006355 regulation of transcription, DNA-templated | BP |
| | GO:0009642 response to light intensity | BP |
| | GO:0010218 response to far red light | BP |
| AT1G04570 | GO:0031969 chloroplast membrane | CC |
| AT1G15580 | GO:0006355 regulation of transcription, DNA-templated | BP |
| AT1G25510 | GO:0004190 aspartic-type endopeptidase activity | MF |
| AT1G28330 | GO:0009744 response to sucrose | BP |
| | GO:0009750 response to fructose | BP |
| | GO:0009749 response to glucose | BP |
| AT1G29395 | GO:0009528 plastid inner membrane | CC |
| | GO:0009706 chloroplast inner membrane | CC |
| | GO:0009535 chloroplast thylakoid membrane | CC |
| | GO:0031357 integral component of chloroplast inner membrane | CC |
| | GO:0009941 chloroplast envelope | CC |
| AT1G48570 | GO:0003729 mRNA binding | MF |
| AT1G51440 | GO:0004620 phospholipase activity | MF |
| | GO:0004806 triglyceride lipase activity | MF |
| | GO:0008970 phospholipase A1 activity | MF |
| | GO:0047714 galactolipase activity | MF |
| AT1G56110 | GO:0042254 ribosome biogenesis | BP |
| | GO:0030515 snoRNA binding | MF |
| AT1G58520 | GO:0005227 calcium activated cation channel activity | MF |
| AT1G64780 | GO:0008519 ammonium transmembrane transporter activity | MF |
| | GO:0015696 ammonium transport | BP |
| | GO:0072488 ammonium transmembrane transport | BP |
| | GO:0015843 methylammonium transport | BP |
| AT1G69200 | GO:0042793 plastid transcription | BP |
| | GO:0009662 etioplast organization | BP |
| | GO:0016310 phosphorylation | BP |
| | GO:0006355 regulation of transcription, DNA-templated | BP |
| | GO:0009658 chloroplast organization | BP |
| AT1G70090 | GO:0045489 pectin biosynthetic process | BP |
| | GO:0047262 polygalacturonate 4-alpha-galacturonosyltransferase activity | MF |
| AT1G80270 | GO:0003729 mRNA binding | MF |
| | GO:0009941 chloroplast envelope | CC |
| | GO:0005874 microtubule | CC |
| | GO:0043015 gamma-tubulin binding | MF |
| AT2G44500 | GO:0006004 fucose metabolic process | BP |
| AT3G05640 | GO:0016791 phosphatase activity | MF |
| | GO:0006470 protein dephosphorylation | BP |
| | GO:1904526 regulation of microtubule binding | BP |
| | GO:0016311 dephosphorylation | BP |
| AT3G05880 | GO:0042538 hyperosmotic salinity response | BP |
| AT3G06530 | GO:0006364 rRNA processing | BP |
| | GO:0042254 ribosome biogenesis | BP |
| | GO:0000462 maturation of SSU-rRNA from tricistronic rRNA transcript | BP |
| | GO:0030515 snoRNA binding | MF |
| | GO:0045943 positive regulation of transcription by RNA polymerase I | BP |
| AT3G17830 | GO:0009535 chloroplast thylakoid membrane | CC |
| AT3G18600 | GO:0000463 maturation of LSU-rRNA from tricistronic rRNA transcript | BP |
| | GO:0004386 helicase activity | MF |
| | GO:0016887 ATPase activity | MF |
| AT3G20440 | GO:0005978 glycogen biosynthetic process | BP |
| | GO:0003844 1,4-alpha-glucan branching enzyme activity | MF |
| | GO:0019252 starch biosynthetic process | BP |
| | GO:0102752 1,4-alpha-glucan branching enzyme activity | MF |
| AT3G23830 | GO:0003697 single-stranded DNA binding | MF |
| | GO:0003690 double-stranded DNA binding | MF |
| | GO:1900864 mitochondrial RNA modification | BP |
| AT3G44750 | GO:0016575 histone deacetylation | BP |
| | GO:0045892 negative regulation of transcription, DNA-templated | BP |
| AT3G48360 | GO:0016567 protein ubiquitination | BP |
| | GO:0006355 regulation of transcription, DNA-templated | BP |
| | GO:0051973 positive regulation of telomerase activity | BP |
| AT3G54810 | GO:0043565 sequence-specific DNA binding | MF |
| | GO:0006355 regulation of transcription, DNA-templated | BP |
| | GO:0008270 zinc ion binding | MF |
| | GO:0045893 positive regulation of transcription, DNA-templated | BP |

Continuation of Table C.2

| Gene ID | GO term | Ontology |
|---|---|---|
| | GO:0000976 transcription regulatory region sequence-specific DNA binding | MF |
| AT3G56330 | GO:0008033 tRNA processing | BP |
| | GO:0030488 tRNA methylation | BP |
| | GO:0000049 tRNA binding | MF |
| | GO:0004809 tRNA (guanine-N2-)-methyltransferase activity | MF |
| | GO:0002940 tRNA N2-guanine methylation | BP |
| | GO:0006400 tRNA modification | BP |
| AT4G01950 | GO:0016311 dephosphorylation | BP |
| | GO:0016024 CDP-diacylglycerol biosynthetic process | BP |
| | GO:0004366 glycerol-3-phosphate O-acyltransferase activity | MF |
| | GO:0102420 sn-1-glycerol-3-phosphate C16:0-DCA-CoA acyl transferase activity | MF |
| | GO:0016791 phosphatase activity | MF |
| | GO:0090447 glycerol-3-phosphate 2-O-acyltransferase activity | MF |
| | GO:0010143 cutin biosynthetic process | BP |
| AT4G11460 | GO:0016310 phosphorylation | BP |
| | GO:0006468 protein phosphorylation | BP |
| AT4G25480 | GO:0006355 regulation of transcription, DNA-templated | BP |
| | GO:0000987 cis-regulatory region sequence-specific DNA binding | MF |
| | GO:0000976 transcription regulatory region sequence-specific DNA binding | MF |
| AT4G31210 | GO:0006265 DNA topological change | BP |
| | GO:0003729 mRNA binding | MF |
| AT5G03350 | GO:0009627 systemic acquired resistance | BP |
| | GO:0016310 phosphorylation | BP |
| | GO:0071446 cellular response to salicylic acid stimulus | BP |
| AT5G08610 | GO:0004386 helicase activity | MF |
| | GO:0003729 mRNA binding | MF |
| | GO:0016887 ATPase activity | MF |
| AT5G14580 | GO:0006402 mRNA catabolic process | BP |
| | GO:0090503 RNA phosphodiester bond hydrolysis, exonucleolytic | BP |
| | GO:0008033 tRNA processing | BP |
| | GO:0006396 RNA processing | BP |
| | GO:0006397 mRNA processing | BP |
| | GO:0090305 nucleic acid phosphodiester bond hydrolysis | BP |
| | GO:0004654 polyribonucleotide nucleotidyltransferase activity | MF |
| | GO:0006364 rRNA processing | BP |
| | GO:0004527 exonuclease activity | MF |
| | GO:0000175 3'-5'-exoribonuclease activity | MF |
| | GO:0006401 RNA catabolic process | BP |
| | GO:0000957 mitochondrial RNA catabolic process | BP |
| | GO:0000958 mitochondrial mRNA catabolic process | BP |
| | GO:0000965 mitochondrial RNA 3'-end processing | BP |
| | GO:0000963 mitochondrial RNA processing | BP |
| AT5G15340 | GO:0008270 zinc ion binding | MF |
| AT5G15970 | GO:0003729 mRNA binding | MF |
| AT5G17330 | GO:0019752 carboxylic acid metabolic process | BP |
| | GO:0004351 glutamate decarboxylase activity | MF |
| | GO:0006536 glutamate metabolic process | BP |
| | GO:0006538 glutamate catabolic process | BP |
| | GO:0046686 response to cadmium ion | BP |
| AT5G41080 | GO:0008081 phosphoric diester hydrolase activity | MF |
| | GO:0008889 glycerophosphodiester phosphodiesterase activity | MF |
| | GO:0006071 glycerol metabolic process | BP |
| | GO:0046475 glycerophospholipid catabolic process | BP |
| AT5G45080 | GO:0061809 NAD+ nucleotidase, cyclic ADP-ribose generating | MF |
| | GO:0050135 NAD(P)+ nucleosidase activity | MF |
| | GO:0003953 NAD+ nucleosidase activity | MF |
| AT5G48470 | GO:0006355 regulation of transcription, DNA-templated | BP |
| | GO:0009658 chloroplast organization | BP |
| AT5G54470 | GO:0008270 zinc ion binding | MF |
| | GO:0006355 regulation of transcription, DNA-templated | BP |
| | GO:0000976 transcription regulatory region sequence-specific DNA binding | MF |
| AT5G55250 | GO:0103007 indole-3-acetate carboxyl methyltransferase activity | MF |
| | GO:0051749 indole acetic acid carboxyl methyltransferase activity | MF |
| | GO:0000287 magnesium ion binding | MF |
| | GO:0008757 S-adenosylmethionine-dependent methyltransferase activity | MF |
| | GO:0010252 auxin homeostasis | BP |
| AT5G57560 | GO:0016762 xyloglucan:xyloglucosyl transferase activity | MF |
| | GO:0006073 cellular glucan metabolic process | BP |
| | GO:0010411 xyloglucan metabolic process | BP |

**Table C.3:** Shared or unique GO terms in GABA mutants under control conditions. Red/blue indicate up-/down-regulated genes, respectively.

| GO accession | Description | Ontology | DEGs ratio: No. of DEGs divided by total genes | | | | | | Group |
|---|---|---|---|---|---|---|---|---|---|
| | | | *gad1** | *gad1KO* | *gad2-1* | *gad1245* | *gad2OE* | *pop2-8* | |
| GO:0071456 | cellular response to hypoxia | BP | 39/242 | 42/242 | (15+40)/242 | 53/242 | 47/242 | 41/242 | 1A |
| GO:0036294 | cellular response to decreased oxygen levels | BP | 39/244 | 43/244 | (15+40)/244 | 53/244 | 47/244 | 41/244 | 1A |
| GO:0071453 | cellular response to oxygen levels | BP | 39/244 | 43/244 | (15+40)/244 | 53/244 | 47/244 | 41/244 | 1A |
| GO:0036293 | response to decreased oxygen levels | BP | 41/272 | 45/272 | (15+40)/272 | 53/272 | 48/272 | 43/272 | 1A |
| GO:0033993 | response to lipid | BP | 86/982 | 120/982 | 118/982 | (35+145)/982 | 137/982 | 118/982 | 1B |
| GO:0009737 | response to abscisic acid | BP | 56/615 | 85/615 | 67/615 | (25+80)/615 | | 86/615 | 1B |
| GO:0097305 | response to alcohol | BP | 56/622 | 85/622 | 67/622 | (25+80)/622 | 89/622 | 87/622 | 1B |
| GO:0009631 | cold acclimation | BP | | 12/56 | | 7/56 | | | 1C |
| GO:0071310 | cellular response to organic substance | BP | 12/1218 | 84/1218 | | 102/1218 | 96/1218 | 104/1218 | 1D |
| GO:0016762 | xyloglucan:xyloglucosyl transferase activity | MF | | 4/33 | | | | 8/33 | 2A |
| GO:0005976 | polysaccharide metabolic process | BP | | | | 22/504 | | 37/504 | 2B |
| GO:0006073 | cellular glucan metabolic process | BP | | | | 16/251 | 10/251 | 23/251 | 2B |
| GO:0044042 | glucan metabolic process | BP | | | | 16/257 | 10/257 | 23/257 | 2B |
| GO:0044264 | cellular polysaccharide metabolic process | BP | | | | 18/329 | 11/329 | 26/329 | 2B |
| GO:0004553 | hydrolase activity, hydrolyzing O-glycosyl compounds | MF | | 11/418 | | | | | 3A |
| GO:0009416 | response to light stimulus | BP | | | 28/763 | | | | 3B |
| GO:0009637 | response to blue light | BP | | | | 9/94 | | | 3B |
| GO:0005982 | starch metabolic process | BP | | | | 8/76 | | | 3C |
| GO:0005983 | starch catabolic process | BP | | | | 6/18 | | | 3C |
| GO:0009251 | glucan catabolic process | BP | | | | 8/56 | | | 3C |
| GO:0044247 | cellular polysaccharide catabolic process | BP | | | | 8/48 | | | 3C |
| GO:0044275 | cellular carbohydrate catabolic process | BP | | | | 8/74 | | | 3C |
| GO:0046658 | anchored component of plasma membrane | CC | | | | | | 21/173 | 3D |
| GO:0005911 | cell-cell junction | CC | | | | | | 58/971 | 3D |
| GO:0009505 | plant-type cell wall | CC | | | | | | 36/406 | 3D |
| GO:0010410 | hemicellulose metabolic process | BP | | | | | | 13/114 | 3E |
| GO:0010411 | xyloglucan metabolic process | BP | | | | | | 10/61 | 3E |
| GO:0045229 | external encapsulating structure organization | BP | | | | | | 37/586 | 3F |
| GO:0009451 | RNA modification | BP | | | | | | 40/322 | 3G |
| GO:0009651 | response to salt stress | BP | 45/474 | 65/474 | 61/474 | 69/474 | 75/474 | 70/474 | 4A |
| GO:0009753 | response to jasmonic acid | BP | 31/196 | 36/196 | 56/196 | 64/196 | 53/196 | 33/196 | 4A |
| GO:0070542 | response to fatty acid | BP | 31/200 | 36/200 | 56/200 | 65/200 | 53/200 | 33/200 | 4A |

Continuation of Table C.3

| GO accession | Description | Ontology | DEGs ratio: No. of DEGs divided by total genes | | | | | | Group |
|---|---|---|---|---|---|---|---|---|---|
| | | | *gad1** | *gad1KO* | *gad2-1* | *gad1245* | *gad2OE* | *pop2-8* | |
| GO:1901701 | cellular response to oxygen-containing compound | BP | 47/761 | 69/761 | 67/761 | 84/761 | 78/761 | 71/761 | 4A |
| **GO:0010150** | **leaf senescence** | BP | 27/149 | 28/149 | 24/149 | 26/149 | 33/149 | 30/149 | 4B |
| GO:0016054 | organic acid catabolic process | BP | 26/172 | 30/172 | 31/172 | 33/172 | 34/172 | 29/172 | 4C |
| GO:0019752 | carboxylic acid metabolic process | BP | 65/1070 | 78/1070 | 99/1070 | 115/1070 | 94/1070 | 89/1070 | 4C |
| GO:0043436 | oxoacid metabolic process | BP | 80/1201 | 95/1201 | 114/1201 | 136/1201 | 112/1201 | 103/1201 | 4C |
| GO:0046395 | carboxylic acid catabolic process | BP | 23/158 | 27/158 | 28/158 | 30/158 | 31/158 | 26/158 | 4C |
| GO:0072329 | monocarboxylic acid catabolic process | BP | 12/69 | 14/69 | 13/69 | 15/69 | 15/69 | 15/69 | 4C |
| GO:0050660 | flavin adenine dinucleotide binding | MF | 18/173 | 21/173 | 24/173 | 28/173 | 31/173 | 27/173 | 4D |
| GO:0032787 | monocarboxylic acid metabolic process | BP | | 48/547 | 53/547 | 61/547 | 52/547 | 53/547 | V |
| GO:0002213 | defense response to insect | BP | 8/33 | 10/33 | 13/33 | 13/33 | 11/33 | | V |
| GO:0031347 | regulation of defense response | BP | 23/281 | 30/281 | 35/281 | 43/281 | 37/281 | | V |
| GO:0016844 | strictosidine synthase activity | MF | 6/15 | 6/15 | 7/15 | 8/15 | 8/15 | | V |
| GO:0046527 | glucosyltransferase activity | MF | 22/181 | 21/181 | 25/181 | 27/181 | | 28/181 | V |
| GO:0008194 | UDP-glycosyltransferase activity | MF | 27/312 | 30/312 | | 36/312 | 35/312 | 39/312 | V |
| GO:0031667 | **response to nutrient levels** | BP | 22/238 | 32/238 | | | 29/238 | 30/238 | V |
| **GO:1900057** | **positive regulation of leaf senescence** | BP | 8/18 | 8/18 | | | 9/18 | 7/18 | V |
| GO:0015996 | **chlorophyll catabolic process** | BP | 8/21 | 7/21 | | | 8/21 | 8/21 | V |
| **GO:1900055** | **regulation of leaf senescence** | BP | 10/48 | 11/48 | | | 12/48 | 11/48 | V |
| GO:0000302 | response to reactive oxygen species | BP | 18/163 | | 26/163 | 27/163 | 26/163 | 22/163 | V |
| GO:0042542 | response to hydrogen peroxide | BP | 13/73 | | 15/73 | 15/73 | 14/73 | | V |
| GO:1901605 | alpha-amino acid metabolic process | BP | 24/296 | | 38/296 | 44/296 | 36/296 | | V |
| GO:0016843 | amine-lyase activity | MF | 6/20 | | 7/20 | 8/20 | 8/20 | | V |
| GO:0010279 | indole-3-acetic acid amido synthetase activity | MF | 4/6 | 5/6 | 5/6 | 5/6 | | | V |
| GO:1901606 | alpha-amino acid catabolic process | BP | | 12/68 | 15/68 | 15/68 | 15/68 | | V |
| GO:0009751 | response to salicylic acid | BP | | 21/178 | 29/178 | 33/178 | 30/178 | | V |
| GO:0071395 | cellular response to jasmonic acid stimulus | BP | | 16/103 | 19/103 | 24/103 | 22/103 | | V |
| GO:0071398 | cellular response to fatty acid | BP | | 16/107 | 19/107 | 25/107 | 22/107 | | V |
| GO:0009867 | jasmonic acid mediated signaling pathway | BP | | 16/98 | 18/98 | 22/98 | 21/98 | | V |
| GO:2000022 | regulation of jasmonic acid mediated signaling pathway | BP | | 10/41 | 11/41 | 14/41 | 13/41 | | V |
| GO:0071396 | cellular response to lipid | BP | | 51/552 | | 60/552 | 60/552 | 53/552 | V |
| GO:0032870 | cellular response to hormone stimulus | BP | | 74/1023 | | 85/1023 | 83/1023 | 93/1023 | V |
| GO:0071310 | cellular response to organic substance | BP | | 84/1218 | | 102/1218 | 96/1218 | 104/1218 | V |
| GO:0010243 | response to organonitrogen compound | BP | | | 29/267 | 43/267 | 34/267 | | V |
| GO:0009627 | systemic acquired resistance | BP | | | 19/84 | 20/84 | 17/84 | | V |

Continuation of Table C.3

| GO accession | Description | Ontology | DEGs ratio: No. of DEGs divided by total genes | | | | | | Group |
|---|---|---|---|---|---|---|---|---|---|
| | | | *gad1** | *gad1KO* | *gad2-1* | *gad1245* | *gad2OE* | *pop2-8* | |
| GO:0014070 | response to organic cyclic compound | BP | | | 37/326 | 45/326 | 37/326 | | V |
| GO:0099503 | secretory vesicle | CC | | | 26/173 | 31/173 | 24/173 | | V |
| GO:0009813 | flavonoid biosynthetic process | BP | | | 14/81 | 18/81 | 15/81 | | V |
| GO:0009063 | cellular amino acid catabolic process | BP | | | 17/89 | 16/89 | 17/89 | | V |
| GO:0004364 | glutathione transferase activity | MF | | | 13/68 | 14/68 | 14/68 | | V |
| GO:0006749 | glutathione metabolic process | BP | | | 15/85 | 16/85 | 16/85 | | V |
| GO:0050832 | defense response to fungus | BP | | 48/576 | | 63/576 | 54/576 | | V |
| GO:0015291 | secondary active transmembrane transporter activity | MF | | 31/317 | | 38/317 | 38/317 | | V |
| GO:0071949 | FAD binding | MF | | 14/85 | | 16/85 | 19/85 | | V |
| GO:0010200 | response to chitin | BP | | | | 29/136 | 21/136 | | V |
| GO:0009718 | anthocyanin-containing compound biosynthetic process | BP | | | | 10/33 | 9/33 | | V |
| GO:0042742 | defense response to bacterium | BP | | | | 50/463 | 49/463 | | V |
| GO:0071215 | cellular response to abscisic acid stimulus | BP | | 29/301 | | | 35/301 | 37/301 | V |
| GO:0097306 | cellular response to alcohol | BP | | 29/301 | | | 35/301 | 37/301 | V |
| GO:0006972 | hyperosmotic response | BP | | 14/68 | | | 17/68 | 17/68 | V |
| GO:0042538 | hyperosmotic salinity response | BP | | 12/57 | | | 15/57 | 15/57 | V |
| GO:0080043 | quercetin 3-O-glucosyltransferase activity | MF | 10/64 | | | 14/64 | | 14/64 | V |
| GO:0031669 | cellular response to nutrient levels | BP | 19/184 | 24/184 | | | | | V |
| GO:0009267 | cellular response to starvation | BP | 17/169 | 22/169 | | | | | V |
| GO:0042537 | benzene-containing compound metabolic process | BP | 12/78 | 14/78 | | | | | V |
| GO:0006787 | porphyrin-containing compound catabolic process | BP | 8/26 | | | | 8/26 | | V |
| GO:0033015 | tetrapyrrole catabolic process | BP | 8/26 | | | | 8/26 | | V |
| GO:0006561 | proline biosynthetic process | BP | | | | | 5/8 | 5/8 | V |
| GO:0009738 | abscisic acid-activated signaling pathway | BP | | | | | 33/270 | 34/270 | V |
| GO:0035251 | UDP-glucosyltransferase activity | MF | 17/143 | | 22/143 | 21/143 | | 26/143 | V |
| GO:0080044 | quercetin 7-O-glucosyltransferase activity | MF | 10/55 | | 13/55 | 13/55 | | 12/55 | V |
| GO:0006576 | cellular biogenic amine metabolic process | BP | | | 16/72 | 16/72 | | | V |
| GO:0044106 | cellular amine metabolic process | BP | | | 17/83 | 17/83 | | | V |
| GO:0010112 | regulation of systemic acquired resistance | BP | | | 8/23 | 9/23 | | | V |
| GO:0006568 | tryptophan metabolic process | BP | | | 10/37 | 12/37 | | | V |
| GO:0006586 | indolalkylamine metabolic process | BP | | | 10/37 | 12/37 | | | V |
| GO:0000325 | plant-type vacuole | CC | | | 69/828 | 73/828 | | | V |
| GO:0010193 | response to ozone | BP | | | 9/33 | 10/33 | | | V |
| GO:0010597 | green leaf volatile biosynthetic process | BP | | | 4/4 | 4/4 | | | V |

Continuation of Table C.3

| GO accession | Description | Ontology | DEGs ratio: No. of DEGs divided by total genes | | | | | | Group |
|---|---|---|---|---|---|---|---|---|---|
| | | | *gad1** | *gad1KO* | *gad2-1* | *gad1245* | *gad2OE* | *pop2-8* | |
| GO:0009072 | aromatic amino acid family metabolic process | BP | | | 15/84 | 21/84 | | | V |
| GO:0042430 | indole-containing compound metabolic process | BP | | | 19/81 | 22/81 | | | V |
| GO:0042435 | indole-containing compound biosynthetic process | BP | | | 15/57 | 18/57 | | | V |
| GO:0009064 | glutamine family amino acid metabolic process | BP | | | 16/97 | | 18/97 | | V |
| GO:0009065 | glutamine family amino acid catabolic process | BP | | | 8/18 | | 7/18 | | V |
| GO:0043562 | cellular response to nitrogen levels | BP | 9/48 | | | | | | VI |
| GO:0009631 | cold acclimation | BP | | 12/56 | | | | | VI |
| GO:0003978 | UDP-glucose 4-epimerase activity | MF | | 5/8 | | | | | VI |
| GO:0050373 | UDP-arabinose 4-epimerase activity | MF | | 4/5 | | | | | VI |
| GO:0046379 | extracellular polysaccharide metabolic process | BP | | 4/5 | | | | | VI |
| GO:0045230 | capsule organization | BP | | 4/5 | | | | | VI |
| GO:0045227 | capsule polysaccharide biosynthetic process | BP | | 4/5 | | | | | VI |
| GO:0033358 | UDP-L-arabinose biosynthetic process | BP | | 4/5 | | | | | VI |
| GO:0045226 | extracellular polysaccharide biosynthetic process | BP | | 4/5 | | | | | VI |
| GO:0006536 | glutamate metabolic process | BP | | | 8/27 | | | | VI |
| GO:0019372 | lipoxygenase pathway | BP | | | 4/5 | | | | VI |
| GO:0030515 | snoRNA binding | MF | | | 8/25 | | | | VI |
| GO:0009309 | amine biosynthetic process | BP | | | 11/50 | | | | VI |
| GO:0042401 | cellular biogenic amine biosynthetic process | BP | | | 11/50 | | | | VI |
| GO:0010120 | camalexin biosynthetic process | BP | | | | 6/13 | | | VI |
| GO:0052317 | camalexin metabolic process | BP | | | | 6/13 | | | VI |
| GO:0016616 | oxidoreductase activity, acting on the CH-OH group of donors, NAD or NADP as acceptor | MF | | | | 25/181 | | | VI |
| GO:0080061 | indole-3-acetonitrile nitrilase activity | MF | | | | 4/4 | | | VI |
| GO:0047427 | cyanoalanine nitrilase activity | MF | | | | 4/4 | | | VI |
| GO:0018822 | nitrile hydratase activity | MF | | | | 4/4 | | | VI |
| GO:0000257 | nitrilase activity | MF | | | | 4/4 | | | VI |
| GO:0016815 | hydrolase activity, acting on carbon-nitrogen (but not peptide) bonds, in nitriles | MF | | | | 4/4 | | | VI |
| GO:0008652 | cellular amino acid biosynthetic process | BP | | | | 30/234 | | | VI |
| GO:0015297 | antiporter activity | MF | | | | 28/209 | | | VI |
| GO:0000162 | tryptophan biosynthetic process | BP | | | | 9/27 | | | VI |
| GO:0046219 | indolalkylamine biosynthetic process | BP | | | | 9/27 | | | VI |
| GO:0015116 | sulfate transmembrane transporter activity | MF | | | | 7/15 | | | VI |

Continuation of Table C.3

| GO accession | Description | Ontology | DEGs ratio: No. of DEGs divided by total genes | | | | | | Group |
|---|---|---|---|---|---|---|---|---|---|
| | | | *gad1** | *gad1KO* | *gad2-1* | *gad1245* | *gad2OE* | *pop2-8* | |
| GO:1902358 | sulfate transmembrane transport | BP | | | | 7/15 | | | VI |
| GO:0046394 | carboxylic acid biosynthetic process | BP | | | | 57/546 | | | VI |
| GO:0016143 | S-glycoside metabolic process | BP | | | | 22/121 | | | VI |
| GO:0019760 | glucosinolate metabolic process | BP | | | | 22/121 | | | VI |
| GO:0042908 | xenobiotic transport | BP | | | | 16/74 | | | VI |
| GO:1901607 | alpha-amino acid biosynthetic process | BP | | | | 27/191 | | | VI |
| GO:0008272 | sulfate transport | BP | | | | 8/18 | | | VI |
| GO:0016053 | organic acid biosynthetic process | BP | | | | 58/582 | | | VI |
| GO:0006560 | proline metabolic process | BP | | | | | 9/16 | | VI |
| GO:0008509 | anion transmembrane transporter activity | MF | | | | | 46/482 | | VI |
| GO:0000976 | transcription regulatory region sequence-specific DNA binding | MF | | | | | | 90/1012 | VI |
| GO:0001067 | regulatory region nucleic acid binding | MF | | | | | | 90/1012 | VI |
| GO:0043565 | sequence-specific DNA binding | MF | | | | | | 108/1312 | VI |
| GO:0009639 | response to red or far red light | BP | | | | | | 32/235 | VI |
| GO:1990837 | sequence-specific double-stranded DNA binding | MF | | | | | | 90/1038 | VI |
| GO:0003690 | double-stranded DNA binding | MF | | | | | | 93/1155 | VI |
| GO:0005506 | iron ion binding | MF | | | | | | 40/370 | VI |
| GO:0047893 | flavonol 3-O-glucosyltransferase activity | MF | | | | | | 6/11 | VI |
| GO:0071483 | cellular response to blue light | BP | | | | | | 9/31 | VI |
| GO:0009733 | response to auxin | BP | | | | | | 43/433 | VI |
| GO:0016709 | oxidoreductase activity, acting on paired donors, with incorporation or reduction of molecular oxygen, NAD(P)H as one donor, and incorporation of one atom of oxygen | MF | | | | | | 21/151 | VI |

**Table C.4:** Shared or uniquely enriched pathways among GABA mutants under control conditions.

| Class | Sub Class | Description | DEGs ratio: No. of DEGs divided by total genes | | | | | |
|---|---|---|---|---|---|---|---|---|
| | | | *gad1** | *gad1KO* | *gad2-1* | *gad1245* | *gad2OE* | *pop2-8* |
| **Metabolism** | Lipid metabolism | Fatty acid degradation | 8/47 | 9/47 | 10/47 | 12/47 | 9/47 | 10/47 |
| | | alpha-Linolenic acid metabolism | 9/43 | 9/43 | 15/43 | 16/43 | 14/43 | 10/43 |
| | Amino acid metabolism | Valine, leucine and isoleucine degradation | 11/52 | 10/52 | 10/52 | 9/52 | 10/52 | 10/52 |
| | | Arginine and proline metabolism | 8/54 | 8/54 | 11/54 | 10/54 | 12/54 | 10/54 |
| | Metabolism of other amino acids | beta-Alanine metabolism | 8/47 | 8/47 | 12/47 | 10/47 | 10/47 | 8/47 |
| | Biosynthesis of other secondary metabolites | Indole alkaloid biosynthesis | 3/4 | 3/4 | 3/4 | 3/4 | 3/4 | 2/4 |
| | Metabolism of terpenoids and polyketides | Zeatin biosynthesis | 7/32 | 7/32 | 9/32 | 7/32 | 8/32 | 9/32 |
| **Metabolism** | Lipid metabolism | Cutin, suberine and wax biosynthesis | | 5/37 | 7/37 | | | |
| | Metabolism of cofactors and vitamins | Ubiquinone and other terpenoid-quinone biosynthesis | | 6/39 | | 8/39 | 7/39 | |
| | Amino acid metabolism | Alanine, aspartate and glutamate metabolism | 6/51 | 7/51 | 12/51 | 11/51 | 10/51 | |
| | | Cysteine and methionine metabolism | 11/124 | | | 16/124 | 14/124 | |
| | | Tyrosine metabolism | | 7/41 | | 9/41 | 8/41 | 7/41 |
| | | Tryptophan metabolism | 7/64 | 7/64 | 11/64 | 14/64 | | |
| | | Phenylalanine, tyrosine and tryptophan biosynthesis | | | 10/56 | 14/56 | | |
| | Metabolism of other amino acids | Cyanoamino acid metabolism | 7/70 | 10/70 | 10/70 | 12/70 | 10/70 | |
| | | Glutathione metabolism | | | 14/103 | 14/103 | 15/103 | |
| | Carbohydrate metabolism | Starch and sucrose metabolism | | 17/171 | 21/171 | | 20/171 | 23/171 |
| | Metabolism of terpenoids and polyketides | Diterpenoid biosynthesis | 4/21 | | 5/21 | 5/21 | 4/21 | |
| | | Carotenoid biosynthesis | | | | | 5/29 | 7/29 |
| | Energy metabolism | Nitrogen metabolism | 5/43 | | 8/43 | | 6/43 | 8/43 |
| | Biosynthesis of other secondary metabolites | Phenylpropanoid biosynthesis | | 19/128 | 20/128 | 22/128 | 20/128 | |
| | | Anthocyanin biosynthesis | | | 2/2 | 2/2 | 2/2 | |
| **Environmental Information Processing** | Signal transduction | MAPK signaling pathway - plant | 11/139 | 15/139 | | 20/139 | 18/139 | 18/139 |
| | | Plant hormone signal transduction | 29/289 | 36/289 | | 37/289 | 38/289 | 50/289 |
| **Organismal Systems** | Environmental adaptation | Circadian rhythm - plant | | | 8/39 | 15/39 | 8/39 | 15/39 |
| **Metabolism** | Lipid metabolism | Fatty acid elongation | | | | | | 7/36 |
| | | Steroid biosynthesis | | | | | | 7/36 |
| | | Linoleic acid metabolism | | | | 3/9 | | |

Continuation of Table C.4

| Class | Sub Class | Description | DEGs ratio: No. of DEGs divided by total genes | | | | | |
|---|---|---|---|---|---|---|---|---|
| | | | *gad1** | *gad1KO* | *gad2-1* | *gad1245* | *gad2OE* | *pop2-8* |
| | Amino acid metabolism | Phenylalanine metabolism | | | | | 5/33 | |
| | Metabolism of other amino acids | Taurine and hypotaurine metabolism | | | 3/9 | | | |
| | Carbohydrate metabolism | Amino sugar and nucleotide sugar metabolism | | 13/133 | | | | |
| | Metabolism of cofactors and vitamins | Pantothenate and CoA biosynthesis | | | | | | 7/34 |
| | Biosynthesis of other secondary metabolites | Flavonoid biosynthesis | | | | 5/25 | | |
| | | Flavone and flavonol biosynthesis | | | | 2/4 | | |
| | | Isoquinoline alkaloid biosynthesis | | | | | 4/22 | |
| | | Glucosinolate biosynthesis | | | | 7/26 | | |
| **Genetic Information Processing** | Translation | Ribosome biogenesis in eukaryotes | | | 13/98 | | | |
| **Cellular Processes** | Transport and catabolism | Peroxisome | | 9/87 | | | | |
| **Organismal Systems** | Environmental adaptation | Plant-pathogen interaction | | | | | | 26/204 |

**Table C.5:** Shared or unique GO terms in WT and GABA mutants after submergence. Red/blue indicate up-/down-regulated genes, respectively. The GO terms are in the same order as in Fig 3.22.

| **GO term** | **Ontology** | **DEGs ratio: No. of DEGs divided by total genes** | | | | | | |
|---|---|---|---|---|---|---|---|---|
| | | *WT* | *gad1** | *gad1KO* | *gad2-1* | *gad1245* | *gad2OE* | *pop2-8* |
| GO:0036293 response to decreased oxygen levels | BP | 71/269 | 104/269 | 157/269 | 115/269 | 147/269 | 155/269 | 145/269 |
| GO:0071456 cellular response to hypoxia | BP | 69/239 | 98/239 | 149/239 | 110/239 | 142/239 | 147/239 | 137/239 |
| GO:0036294 cellular response to decreased oxygen levels | BP | 69/241 | 99/241 | 150/241 | 111/241 | 143/241 | 148/241 | 138/241 |
| GO:0071453 cellular response to oxygen levels | BP | 69/241 | 99/241 | 150/241 | 111/241 | 143/241 | 148/241 | 138/241 |
| GO:0003690 double-stranded DNA binding | MF | | 147/1147 | 200/1147 | 142/1147 | | | |
| **GO:1900057 positive regulation of leaf senescence** | BP | | 10/18 | 10/18 | 10/18 | | | |
| GO:0050832 defense response to fungus | BP | | | | | 111/562 | 116/562 | |
| GO:0009063 cellular amino acid catabolic process | BP | | | | | 30/89 | 28/89 | 29/89 |
| GO:0042435 indole-containing compound biosynthetic process | BP | | | | | 21/55 | | |
| GO:1901606 alpha-amino acid catabolic process | BP | | | | | 23/68 | | |
| GO:0004364 glutathione transferase activity | MF | | | | | 22/64 | | 24/64 |
| GO:0099503 secretory vesicle | CC | | | | | 43/173 | | |
| GO:0070647 protein modification by small protein conjugation or removal | BP | | | 164/959 | | | | 191/959 |
| GO:0019199 transmembrane receptor protein kinase activity | MF | | | | | | | 34/96 |
| GO:0043412 macromolecule modification | BP | | | | | | 557/3561 | 615/3561 |
| GO:0007178 transmembrane receptor protein serine/threonine kinase signaling pathway | BP | | | | | | 21/59 | 25/59 |
| GO:0004675 transmembrane receptor protein serine/threonine kinase activity | MF | | | | | | 21/59 | 25/59 |
| GO:0007167 enzyme linked receptor protein signaling pathway | BP | | | | | | 21/59 | 25/59 |
| GO:0042908 xenobiotic transport | BP | | | | | 24/74 | 25/74 | 28/74 |
| GO:0050660 flavin adenine dinucleotide binding | MF | | | | | 45/169 | 45/169 | 48/169 |
| GO:0009814 | BP | | | 16/33 | | | | |
| GO:0009061 anaerobic respiration | BP | 6/9 | | 7/9 | | 7/9 | | |
| GO:1900426 positive regulation of defense response to bacterium | BP | 10/27 | | | | | | |
| GO:0010105 negative regulation of ethylene-activated signaling pathway | BP | 8/17 | | | | | | |
| GO:0070298 negative regulation of phosphorelay signal transduction system | BP | 8/17 | | | | | | |
| GO:0005776 autophagosome | CC | | | | | | 15/29 | |
| GO:0044242 cellular lipid catabolic process | BP | | | 30/108 | | | 33/108 | |
| GO:1990837 sequence-specific double-stranded DNA binding | MF | 97/1035 | 144/1035 | 193/1035 | 137/1035 | | 196/1035 | 208/1035 |
| GO:0043565 sequence-specific DNA binding | MF | 122/1301 | 175/1301 | 239/1301 | 162/1301 | | 245/1301 | 257/1301 |
| GO:0000976 transcription regulatory region sequence-specific DNA binding | MF | 96/1010 | 143/1010 | 192/1010 | 136/1010 | | 195/1010 | 207/1010 |
| GO:0001067 regulatory region nucleic acid binding | MF | 96/1010 | 143/1010 | 192/1010 | 136/1010 | | 195/1010 | 207/1010 |
| GO:0009651 response to salt stress | BP | | 71/470 | 108/470 | 72/470 | 92/470 | 114/470 | 110/470 |
| GO:0016054 organic acid catabolic process | BP | | 34/167 | 44/167 | 33/167 | 53/167 | 52/167 | 53/167 |
| GO:0006464 cellular protein modification process | BP | 253/3200 | | 495/3200 | | 456/3200 | 548/3200 | 606/3200 |
| GO:0036211 protein modification process | BP | 253/3200 | | 495/3200 | | 456/3200 | 548/3200 | 606/3200 |
| GO:0002238 response to molecule of fungal origin | BP | | | | | | 12/19 | 15/19 |
| GO:1900424 regulation of defense response to bacterium | BP | 13/52 | 16/52 | 19/52 | | | 22/52 | 22/52 |
| GO:0009738 abscisic acid-activated signaling pathway | BP | | | 65/262 | | 56/262 | 68/262 | 75/262 |
| GO:0016567 protein ubiquitination | BP | | | 158/833 | | | 158/833 | 179/833 |
| GO:0004842 ubiquitin-protein transferase activity | MF | | | 100/487 | | | 102/487 | 123/487 |

Continuation of Table C.5

| GO term | Ontology | DEGs ratio: No. of DEGs divided by total genes | | | | | | |
|---|---|---|---|---|---|---|---|---|
| | | *WT* | *gad1** | *gad1KO* | *gad2-1* | *gad1245* | *gad2OE* | *pop2-8* |
| GO:0032446 protein modification by small protein conjugation | BP | | | 159/866 | | | 160/866 | 181/866 |
| GO:0009737 response to abscisic acid | BP | | 88/603 | 144/603 | 93/603 | 130/603 | 156/603 | 161/603 |
| GO:0097305 response to alcohol | BP | | 89/610 | 146/610 | 94/610 | 132/610 | 158/610 | 163/610 |
| **GO:0010150 leaf senescence** | BP | | 36/143 | 55/143 | 36/143 | 54/143 | 61/143 | 61/143 |
| GO:0033993 response to lipid | BP | | 132/966 | 207/966 | 142/966 | 197/966 | 228/966 | 237/966 |
| GO:0006468 protein phosphorylation | BP | 141/1277 | 169/1277 | 249/1277 | 157/1277 | 250/1277 | 284/1277 | 305/1277 |
| GO:0016773 phosphotransferase activity, alcohol group as acceptor | MF | 141/1303 | 173/1303 | 255/1303 | 159/1303 | 257/1303 | 290/1303 | 315/1303 |
| GO:0016301 kinase activity | MF | 151/1514 | 188/1514 | 277/1514 | 175/1514 | 280/1514 | 316/1514 | 343/1514 |
| GO:0030554 adenyl nucleotide binding | MF | 234/2625 | 288/2625 | 421/2625 | 287/2625 | 444/2625 | 506/2625 | 541/2625 |
| GO:0032559 adenyl ribonucleotide binding | MF | 234/2614 | 288/2614 | 421/2614 | 287/2614 | 444/2614 | 506/2614 | 541/2614 |
| GO:0000160 phosphorelay signal transduction system | BP | 44/260 | 53/260 | 66/260 | 53/260 | 56/260 | 63/260 | |
| GO:0009873 ethylene-activated signaling pathway | BP | 41/203 | 48/203 | 61/203 | 51/203 | 54/203 | 57/203 | 54/203 |
| GO:0032870 cellular response to hormone stimulus | BP | 114/999 | 136/999 | 200/999 | 140/999 | 181/999 | 205/999 | 219/999 |
| GO:0071310 cellular response to organic substance | BP | 128/1182 | 154/1182 | 230/1182 | 164/1182 | 213/1182 | 247/1182 | 261/1182 |
| GO:0009723 response to ethylene | BP | 49/281 | 66/281 | 83/281 | 67/281 | 74/281 | 78/281 | 77/281 |
| GO:0071369 cellular response to ethylene stimulus | BP | 43/210 | 50/210 | 65/210 | 53/210 | 57/210 | 61/210 | 58/210 |
| GO:0042430 indole-containing compound metabolic process | BP | | | | 21/79 | 34/79 | 29/79 | 31/79 |
| GO:0000302 response to reactive oxygen species | BP | | 32/159 | 44/159 | 34/159 | 46/159 | 49/159 | 49/159 |
| GO:0009753 response to jasmonic acid | BP | | | 48/196 | 41/196 | 59/196 | 63/196 | 54/196 |
| GO:0070542 response to fatty acid | BP | | | 49/200 | 43/200 | 61/200 | 64/200 | 56/200 |
| GO:0009626 plant-type hypersensitive response | BP | | | 30/88 | 22/88 | 29/88 | 33/88 | 42/88 |
| GO:0034050 programmed cell death induced by symbiont | BP | | | 30/89 | 22/89 | 29/89 | 33/89 | 42/89 |
| GO:0016799 hydrolase activity, hydrolyzing N-glycosyl compounds | MF | | | 45/167 | | 48/167 | 61/167 | 64/167 |
| GO:0014070 response to organic cyclic compound | BP | | | 71/316 | | 83/316 | 90/316 | 91/316 |
| GO:1901701 cellular response to oxygen-containing compound | BP | | | 149/741 | | 144/741 | 166/741 | 177/741 |
| GO:0035639 purine ribonucleoside triphosphate binding | MF | 220/2790 | | | | 423/2790 | 484/2790 | 527/2790 |
| GO:0006796 phosphate-containing compound metabolic process | BP | | | | | 376/2517 | 426/2517 | 461/2517 |
| GO:0009627 systemic acquired resistance | BP | | | | 20/84 | 33/84 | 30/84 | 33/84 |
| GO:0042537 benzene-containing compound metabolic process | BP | | | | | 31/78 | 31/78 | 30/78 |
| GO:0009816 | BP | | 14/40 | 17/40 | | 19/40 | 19/40 | 20/40 |
| GO:0071949 FAD binding | MF | 16/80 | 21/80 | 28/80 | | 33/80 | 31/80 | 30/80 |
| GO:0002229 defense response to oomycetes | BP | 18/87 | | 28/87 | 20/87 | 30/87 | 31/87 | 36/87 |
| GO:0031669 cellular response to nutrient levels | BP | 26/179 | | 51/179 | | 50/179 | 55/179 | 56/179 |
| GO:0002237 response to molecule of bacterial origin | BP | | | 22/43 | 14/43 | 19/43 | 24/43 | 23/43 |
| GO:0071396 cellular response to lipid | BP | | | 113/540 | | 105/540 | 124/540 | 134/540 |
| GO:0071215 cellular response to abscisic acid stimulus | BP | | | 72/293 | | 64/293 | 77/293 | 84/293 |
| GO:0097306 cellular response to alcohol | BP | | | 72/293 | | 64/293 | 77/293 | 84/293 |
| GO:0009267 cellular response to starvation | BP | | | 44/164 | | 44/164 | 48/164 | 49/164 |
| GO:0046395 carboxylic acid catabolic process | BP | | 31/154 | 40/154 | 29/154 | 48/154 | 48/154 | 49/154 |
| GO:0031667 response to nutrient levels | BP | 36/232 | 44/232 | 66/232 | 39/232 | 66/232 | 73/232 | 75/232 |
| GO:0032555 purine ribonucleotide binding | MF | 241/2895 | | 442/2895 | 297/2895 | 462/2895 | 529/2895 | 566/2895 |
| GO:0016310 phosphorylation | BP | 158/1750 | 198/1750 | 289/1750 | | 293/1750 | 331/1750 | 359/1750 |
| GO:0017076 purine nucleotide binding | MF | 241/2907 | | 442/2907 | 297/2907 | 462/2907 | 529/2907 | 566/2907 |

Continuation of Table C.5

| GO term | Ontology | DEGs ratio: No. of DEGs divided by total genes | | | | | | |
|---|---|---|---|---|---|---|---|---|
| | | *WT* | *gad1** | *gad1KO* | *gad2-1* | *gad1245* | *gad2OE* | *pop2-8* |
| GO:0043531 ADP binding | MF | 31/200 | | 52/200 | 35/200 | 54/200 | 71/200 | 75/200 |
| GO:0061809 NAD+ nucleotidase, cyclic ADP-ribose generating | MF | 22/127 | 27/127 | 41/127 | 26/127 | 43/127 | 58/127 | 58/127 |
| GO:0003953 NAD+ nucleosidase activity | MF | 22/127 | 27/127 | 41/127 | 26/127 | 43/127 | 58/127 | 58/127 |
| GO:0050135 NAD(P)+ nucleosidase activity | MF | 22/127 | 27/127 | 41/127 | 26/127 | 43/127 | 58/127 | 58/127 |
| GO:0009751 response to salicylic acid | BP | | | 51/169 | 36/169 | 60/169 | 67/169 | 65/169 |
| GO:0031347 regulation of defense response | BP | | | 68/273 | 51/273 | 76/273 | 84/273 | 85/273 |
| GO:0010200 response to chitin | BP | 40/138 | 60/138 | 82/138 | 73/138 | 81/138 | 78/138 | 87/138 |
| GO:0010243 response to organonitrogen compound | BP | 51/261 | 71/261 | 103/261 | 86/261 | 104/261 | 105/261 | 112/261 |
| GO:0004674 protein serine/threonine kinase activity | MF | 122/896 | 144/896 | 212/896 | 135/896 | 217/896 | 240/896 | 261/896 |
| GO:0042742 defense response to bacterium | BP | 75/457 | 94/457 | 132/457 | 101/457 | 139/457 | 164/457 | 172/457 |
| GO:0016758 transferase activity, transferring hexosyl groups | MF | 87/366 | 88/366 | 89/366 | 86/366 | 89/366 | | 101/366 |
| GO:0090558 plant epidermis development | BP | | 62/282 | 67/282 | 68/282 | 68/282 | 81/282 | 88/282 |
| GO:0005372 water transmembrane transporter activity | MF | | 15/28 | 14/28 | 17/28 | 16/28 | 16/28 | 17/28 |
| GO:0015250 water channel activity | MF | | 15/28 | 14/28 | 17/28 | 16/28 | 16/28 | 17/28 |
| GO:0006833 water transport | BP | | 17/39 | 17/39 | 21/39 | 20/39 | 19/39 | 22/39 |
| GO:0042044 fluid transport | BP | | 17/39 | 17/39 | 21/39 | 20/39 | 19/39 | 22/39 |
| GO:0045491 xylan metabolic process | BP | 23/58 | 26/58 | 29/58 | 24/58 | 28/58 | 28/58 | 30/58 |
| GO:0010393 galacturonan metabolic process | BP | 44/171 | 48/171 | 50/171 | 45/171 | 56/171 | 53/171 | 57/171 |
| GO:0045488 pectin metabolic process | BP | 44/170 | 48/170 | 50/170 | 45/170 | 56/170 | 53/170 | 57/170 |
| GO:0070592 cell wall polysaccharide biosynthetic process | BP | 27/88 | 29/88 | 35/88 | 28/88 | 39/88 | 36/88 | 37/88 |
| GO:0044038 cell wall macromolecule biosynthetic process | BP | 29/91 | 31/91 | 37/91 | 30/91 | 41/91 | 38/91 | 39/91 |
| GO:0070589 cellular component macromolecule biosynthetic process | BP | 29/91 | 31/91 | 37/91 | 30/91 | 41/91 | 38/91 | 39/91 |
| GO:0009664 plant-type cell wall organization | BP | 36/153 | 40/153 | 44/153 | 39/153 | 48/153 | 47/153 | 53/153 |
| GO:0010087 phloem or xylem histogenesis | BP | | 36/124 | 40/124 | 34/124 | 42/124 | 45/124 | 48/124 |
| GO:0005911 cell-cell junction | CC | 152/967 | 172/967 | 192/967 | 169/967 | 180/967 | 213/967 | 257/967 |
| GO:0006073 cellular glucan metabolic process | BP | | 60/249 | 75/249 | 56/249 | 75/249 | 72/249 | 89/249 |
| GO:0044042 glucan metabolic process | BP | | 60/255 | 75/255 | 56/255 | 75/255 | 72/255 | 89/255 |
| GO:0033692 cellular polysaccharide biosynthetic process | BP | 44/198 | 54/198 | 68/198 | 52/198 | 70/198 | 68/198 | 78/198 |
| GO:0034637 cellular carbohydrate biosynthetic process | BP | | 63/240 | 79/240 | 60/240 | 79/240 | 78/240 | 90/240 |
| GO:0000271 polysaccharide biosynthetic process | BP | 53/239 | 67/239 | 81/239 | 62/239 | 86/239 | 83/239 | 94/239 |
| GO:0016051 carbohydrate biosynthetic process | BP | | 96/376 | 117/376 | 89/376 | 112/376 | 117/376 | 129/376 |
| GO:0005856 cytoskeleton | CC | 95/442 | 103/442 | 115/442 | 122/442 | 116/442 | 127/442 | 136/442 |
| GO:0005874 microtubule | CC | 62/242 | 70/242 | 76/242 | 81/242 | 77/242 | 86/242 | 92/242 |
| GO:0099512 supramolecular fiber | CC | 64/252 | 72/252 | 78/252 | 83/252 | 79/252 | 88/252 | 94/252 |
| GO:0099513 polymeric cytoskeletal fiber | CC | 64/252 | 72/252 | 78/252 | 83/252 | 79/252 | 88/252 | 94/252 |
| GO:0009505 plant-type cell wall | CC | 67/237 | 73/237 | 77/237 | 73/237 | 77/237 | 81/237 | 96/237 |
| GO:0010383 cell wall polysaccharide metabolic process | BP | 48/151 | 54/151 | 61/151 | 54/151 | 64/151 | 61/151 | 66/151 |
| GO:0008017 microtubule binding | MF | 45/169 | 52/169 | 55/169 | 64/169 | 53/169 | 58/169 | 63/169 |
| GO:0015631 tubulin binding | MF | 46/184 | 53/184 | 57/184 | 64/184 | 54/184 | 61/184 | 66/184 |
| GO:0009832 plant-type cell wall biogenesis | BP | 45/185 | 55/185 | 65/185 | 58/185 | 71/185 | 66/185 | 67/185 |
| GO:0009834 plant-type secondary cell wall biogenesis | BP | 30/87 | 36/87 | 42/87 | 37/87 | 44/87 | 42/87 | 41/87 |
| GO:0007010 cytoskeleton organization | BP | 64/318 | 78/318 | 89/318 | 81/318 | 89/318 | 98/318 | 103/318 |
| GO:0010410 hemicellulose metabolic process | BP | 38/112 | 41/112 | 46/112 | 41/112 | 46/112 | 45/112 | 50/112 |

Continuation of Table C.5

| GO term | Ontology | DEGs ratio: No. of DEGs divided by total genes | | | | | | |
|---|---|---|---|---|---|---|---|---|
| | | *WT* | *gad1** | *gad1KO* | *gad2-1* | *gad1245* | *gad2OE* | *pop2-8* |
| GO:0015630 microtubule cytoskeleton | CC | 70/305 | 77/305 | 86/305 | 89/305 | 85/305 | 96/305 | 102/305 |
| GO:0046658 anchored component of plasma membrane | CC | 44/173 | 59/173 | 61/173 | 59/173 | 62/173 | 66/173 | 67/173 |
| GO:0033993 response to lipid | BP | 195/966 | | | | | | |
| GO:0009753 response to jasmonic acid | BP | 63/196 | | | | | | |
| GO:0070542 response to fatty acid | BP | 63/200 | | | | | | |
| GO:0045489 pectin biosynthetic process | BP | | | | | 26/59 | 24/59 | 25/59 |
| GO:0000139 Golgi membrane | CC | | | | | 111/511 | | |
| GO:0010089 xylem development | BP | | | | 17/45 | 20/45 | 19/45 | 21/45 |
| GO:0030244 cellulose biosynthetic process | BP | | | | | 24/63 | | |
| GO:0051274 beta-glucan biosynthetic process | BP | | | | | 26/76 | | 29/76 |
| GO:0030865 cortical cytoskeleton organization | BP | | | | | 22/58 | 23/58 | |
| GO:1905177 tracheary element differentiation | BP | | | | | 11/17 | 11/17 | |
| GO:0010411 xyloglucan metabolic process | BP | | | | | 22/61 | | |
| GO:0097435 supramolecular fiber organization | BP | | | | | 45/173 | 49/173 | |
| GO:0009733 response to auxin | BP | | 81/415 | 91/415 | 87/415 | 93/415 | 97/415 | |
| GO:0009734 auxin-activated signaling pathway | BP | | 50/224 | | 52/224 | 61/224 | 62/224 | |
| GO:0071365 cellular response to auxin stimulus | BP | | 55/241 | | 58/241 | 66/241 | 66/241 | |
| GO:1990939 ATP-dependent microtubule motor activity | MF | | | | 27/62 | | | |
| GO:0003774 motor activity | MF | | | | 34/88 | | | |
| GO:0003777 microtubule motor activity | MF | | | | 28/63 | | | |
| GO:0016837 carbon-oxygen lyase activity, acting on polysaccharides | MF | 14/34 | 14/34 | | 15/34 | | | |
| GO:2000652 regulation of secondary cell wall biogenesis | BP | | | | 14/30 | 14/30 | | |
| GO:0000079 regulation of cyclin-dependent protein serine/threonine kinase activity | BP | 21/67 | | | 24/67 | 22/67 | | |
| GO:1904029 regulation of cyclin-dependent protein kinase activity | BP | 21/67 | | | 24/67 | 22/67 | | |
| GO:0061640 cytoskeleton-dependent cytokinesis | BP | | | | 20/53 | | | |
| GO:1902554 serine/threonine protein kinase complex | CC | | | | 26/79 | | | |
| GO:0004553 hydrolase activity, hydrolyzing O-glycosyl compounds | MF | 81/415 | 85/415 | | | | | |
| GO:0016143 S-glycoside metabolic process | BP | 37/119 | | 35/119 | | | | |
| GO:0019760 glucosinolate metabolic process | BP | 37/119 | | 35/119 | | | | |
| GO:0046527 glucosyltransferase activity | MF | 47/180 | | | | | | |
| GO:1901657 glycosyl compound metabolic process | BP | 51/202 | | 52/202 | | | | |
| GO:0009737 response to abscisic acid | BP | 111/603 | | | | | | |
| GO:0032870 cellular response to hormone stimulus | BP | 166/999 | | | | | | |
| GO:0097305 response to alcohol | BP | 112/610 | | | | | | |
| GO:0035251 UDP-glucosyltransferase activity | MF | 37/142 | | | | | | |
| GO:0099503 secretory vesicle | CC | 42/173 | | | | | | |
| GO:0044772 mitotic cell cycle phase transition | BP | 30/87 | 28/87 | 28/87 | 32/87 | | | |
| GO:0008194 UDP-glycosyltransferase activity | MF | 73/289 | 61/289 | | 62/289 | 62/289 | | |
| GO:0016538 cyclin-dependent protein serine/threonine kinase regulator activity | MF | 19/52 | | | 21/52 | 19/52 | 21/52 | |
| GO:0009250 glucan biosynthetic process | BP | | | 44/139 | | 43/139 | 42/139 | 52/139 |
| GO:0030243 cellulose metabolic process | BP | | 27/94 | | | 32/94 | | 36/94 |
| GO:0051273 beta-glucan metabolic process | BP | | 30/107 | | 29/107 | 34/107 | | 40/107 |
| GO:0000272 polysaccharide catabolic process | BP | 43/189 | 46/189 | 51/189 | | 49/189 | | 57/189 |

Continuation of Table C.5

| GO term | Ontology | DEGs ratio: No. of DEGs divided by total genes | | | | | | |
|---|---|---|---|---|---|---|---|---|
| | | *WT* | *gad1** | *gad1KO* | *gad2-1* | *gad1245* | *gad2OE* | *pop2-8* |
| GO:0045492 xylan biosynthetic process | BP | 15/37 | 16/37 | 19/37 | 15/37 | 18/37 | 18/37 | 19/37 |
| GO:1901659 glycosyl compound biosynthetic process | BP | 23/74 | 25/74 | 31/74 | | 25/74 | 27/74 | 31/74 |
| GO:0033260 nuclear DNA replication | BP | 12/18 | 12/18 | 12/18 | 10/18 | 10/18 | 11/18 | 13/18 |
| GO:0019761 glucosinolate biosynthetic process | BP | 18/46 | 18/46 | 22/46 | | 19/46 | | 22/46 |
| GO:0016144 S-glycoside biosynthetic process | BP | 18/46 | 18/46 | 22/46 | | 19/46 | | 22/46 |
| GO:0019758 glycosinolate biosynthetic process | BP | 18/46 | 18/46 | 22/46 | | 19/46 | | 22/46 |
| GO:0010233 phloem transport | BP | | 13/20 | 12/20 | 11/20 | 11/20 | 12/20 | |
| GO:0003018 vascular process in circulatory system | BP | | 13/20 | 12/20 | 11/20 | 11/20 | 12/20 | |
| GO:0010232 vascular transport | BP | | 13/20 | 12/20 | 11/20 | 11/20 | 12/20 | |
| GO:0019253 reductive pentose-phosphate cycle | BP | | 12/21 | 12/21 | 11/21 | | 12/21 | |
| GO:0019685 photosynthesis, dark reaction | BP | | 12/21 | 12/21 | 11/21 | | 12/21 | |
| GO:0072330 monocarboxylic acid biosynthetic process | BP | 55/262 | | 66/262 | 57/262 | | | |
| GO:0008652 cellular amino acid biosynthetic process | BP | | | 62/233 | | | | |
| GO:0032787 monocarboxylic acid metabolic process | BP | 95/538 | | 118/538 | | | | |
| GO:0005507 copper ion binding | MF | | | 54/197 | | | 54/197 | |
| GO:1901607 alpha-amino acid biosynthetic process | BP | | | 53/191 | | | | |
| GO:0006631 fatty acid metabolic process | BP | 56/274 | | 73/274 | 57/274 | | 70/274 | |
| GO:0044272 sulfur compound biosynthetic process | BP | | | 54/169 | | | | |
| GO:0006633 fatty acid biosynthetic process | BP | | 41/164 | 52/164 | 43/164 | | 52/164 | 55/164 |
| GO:0015994 chlorophyll metabolic process | BP | | | 33/90 | 27/90 | | 34/90 | 39/90 |
| GO:0015995 chlorophyll biosynthetic process | BP | | | 28/65 | 22/65 | | 29/65 | 33/65 |
| GO:0047259 glucomannan 4-beta-mannosyltransferase activity | MF | | 9/9 | 9/9 | | 7/9 | 9/9 | 9/9 |
| GO:0019752 carboxylic acid metabolic process | BP | 163/1049 | 172/1049 | 234/1049 | | | 215/1049 | 250/1049 |
| GO:0009528 plastid inner membrane | CC | | | 32/97 | | | 34/97 | 39/97 |
| GO:0009706 chloroplast inner membrane | CC | | | 31/93 | | | 33/93 | 38/93 |
| GO:0006778 porphyrin-containing compound metabolic process | BP | | | 34/106 | | | 38/106 | 41/106 |
| GO:0033013 tetrapyrrole metabolic process | BP | | | 34/107 | | | 38/107 | 41/107 |
| GO:0042644 chloroplast nucleoid | CC | | | 21/51 | | | 23/51 | 25/51 |
| GO:0033014 tetrapyrrole biosynthetic process | BP | | | 28/78 | | | 31/78 | 34/78 |
| GO:0006779 porphyrin-containing compound biosynthetic process | BP | | | 28/75 | | | 30/75 | 33/75 |
| GO:1901259 chloroplast rRNA processing | BP | | | 13/21 | | | 14/21 | 15/21 |
| GO:0019684 photosynthesis, light reaction | BP | | | 46/144 | | | 52/144 | 56/144 |
| GO:0031969 chloroplast membrane | CC | | | 81/294 | | | 88/294 | 95/294 |
| GO:0042170 plastid membrane | CC | | | 82/302 | | | 89/302 | 96/302 |
| GO:0009522 photosystem I | CC | | | | 17/43 | | 22/43 | 22/43 |
| GO:0072598 protein localization to chloroplast | BP | | | 20/51 | | | 23/51 | 26/51 |
| GO:0045036 protein targeting to chloroplast | BP | | | 20/49 | | | 23/49 | 26/49 |
| GO:0072596 establishment of protein localization to chloroplast | BP | | | 20/49 | | | 23/49 | 26/49 |
| GO:0009765 photosynthesis, light harvesting | BP | | | | | | 18/36 | 19/36 |
| GO:0010305 leaf vascular tissue pattern formation | BP | | | | | | 16/31 | 18/31 |
| GO:0032544 plastid translation | BP | | | 12/20 | | | 12/20 | 13/20 |
| GO:0000727 double-strand break repair via break-induced replication | BP | 8/12 | | | | | | 10/12 |
| GO:0042273 ribosomal large subunit biogenesis | BP | | | | | | | 45/114 |

Continuation of Table C.5

| GO term | Ontology | DEGs ratio: No. of DEGs divided by total genes | | | | | | |
|---|---|---|---|---|---|---|---|---|
| | | *WT* | *gad1** | *gad1KO* | *gad2-1* | *gad1245* | *gad2OE* | *pop2-8* |
| GO:0000724 double-strand break repair via homologous recombination | BP | | 27/94 | | | | | 39/94 |
| GO:0006364 rRNA processing | BP | | | | | | | 89/294 |
| GO:0009059 macromolecule biosynthetic process | BP | | | | | | | 824/4173 |
| GO:0010051 xylem and phloem pattern formation | BP | | | 24/68 | | | | 30/68 |
| GO:0045037 protein import into chloroplast stroma | BP | | | 15/30 | | | 15/30 | 18/30 |
| GO:0006996 organelle organization | BP | | | | | | | 423/1971 |
| GO:0016072 rRNA metabolic process | BP | | | | | | | 89/299 |
| GO:0042255 ribosome assembly | BP | | | | | | | 40/98 |
| GO:0015935 small ribosomal subunit | CC | | | | | | | 60/150 |
| GO:0022627 cytosolic small ribosomal subunit | CC | | | | | | | 49/113 |
| GO:0000725 recombinational repair | BP | | | | | | | 42/100 |
| GO:0022613 ribonucleoprotein complex biogenesis | BP | | | | | | | 147/535 |
| GO:0003723 RNA binding | MF | | | | | | | 472/1929 |
| GO:0042254 ribosome biogenesis | BP | | | | | | | 139/430 |
| GO:0042788 polysomal ribosome | CC | | | | | | | 51/98 |
| GO:0015934 large ribosomal subunit | CC | | | | | | 63/195 | 94/195 |
| GO:0022625 cytosolic large ribosomal subunit | CC | | | | | | 48/147 | 77/147 |
| GO:0043603 cellular amide metabolic process | BP | | | | | | 222/1068 | 291/1068 |
| GO:0006412 translation | BP | | | | | | 189/842 | 249/842 |
| GO:0043043 peptide biosynthetic process | BP | | | | | | 189/847 | 249/847 |
| GO:0006518 peptide metabolic process | BP | | | | | | 204/950 | 269/950 |
| GO:0043604 amide biosynthetic process | BP | | | | | | 200/916 | 263/916 |
| GO:0006260 DNA replication | BP | 49/195 | 56/195 | 60/195 | 48/195 | 47/195 | 63/195 | 76/195 |
| GO:0006261 DNA-dependent DNA replication | BP | 43/148 | 48/148 | 52/148 | 41/148 | 41/148 | 54/148 | 63/148 |
| GO:0043436 oxoacid metabolic process | BP | 200/1179 | 199/1179 | 265/1179 | | | 243/1179 | 281/1179 |
| GO:0016053 organic acid biosynthetic process | BP | 103/577 | 112/577 | 146/577 | 102/577 | | 135/577 | 153/577 |
| GO:0046394 carboxylic acid biosynthetic process | BP | 99/542 | 105/542 | 140/542 | | | 129/542 | 146/542 |
| GO:0003688 DNA replication origin binding | MF | 12/19 | 12/19 | 12/19 | | 11/19 | 13/19 | 15/19 |
| GO:0006270 DNA replication initiation | BP | 17/29 | 15/29 | 17/29 | | 15/29 | 19/29 | 20/29 |
| GO:0009657 plastid organization | BP | | | 95/310 | | | 101/310 | 115/310 |
| GO:0009658 chloroplast organization | BP | | | 76/239 | | | 80/239 | 91/239 |
| GO:0019843 rRNA binding | MF | | | 45/144 | | | 57/144 | 74/144 |
| GO:1901566 organonitrogen compound biosynthetic process | BP | | | 324/1790 | | | 359/1790 | 445/1790 |
| GO:0009523 photosystem II | CC | | 24/76 | 28/76 | 27/76 | 26/76 | 38/76 | 40/76 |
| GO:0009543 chloroplast thylakoid lumen | CC | | 20/47 | 27/47 | 18/47 | 18/47 | 33/47 | 33/47 |
| GO:0044264 cellular polysaccharide metabolic process | BP | 74/325 | 89/325 | 107/325 | 85/325 | 110/325 | 106/325 | 124/325 |
| GO:0005976 polysaccharide metabolic process | BP | 111/494 | 131/494 | 152/494 | 122/494 | 156/494 | 150/494 | 173/494 |
| GO:0045229 external encapsulating structure organization | BP | 134/582 | 152/582 | 166/582 | 145/582 | 171/582 | 169/582 | 193/582 |
| GO:0042651 thylakoid membrane | CC | | 92/466 | 154/466 | 110/466 | 101/466 | 166/466 | 178/466 |
| GO:0009535 chloroplast thylakoid membrane | CC | | 89/445 | 149/445 | 107/445 | 97/445 | 160/445 | 169/445 |
| GO:0055035 plastid thylakoid membrane | CC | | 89/446 | 149/446 | 107/446 | 97/446 | 160/446 | 169/446 |
| GO:0003729 mRNA binding | MF | | | 196/1030 | | | 248/1030 | 325/1030 |
| GO:0005840 ribosome | CC | | | 118/528 | | | 163/528 | 217/528 |

Continuation of Table C.5

| GO term | Ontology | DEGs ratio: No. of DEGs divided by total genes | | | | | | |
|---|---|---|---|---|---|---|---|---|
| | | *WT* | *gad1** | *gad1KO* | *gad2-1* | *gad1245* | *gad2OE* | *pop2-8* |
| GO:0009507 chloroplast | CC | | 393/2449 | 668/2449 | 398/2449 | 377/2449 | 701/2449 | 793/2449 |
| GO:0009534 chloroplast thylakoid | CC | | 119/540 | 198/540 | 137/540 | 124/540 | 216/540 | 222/540 |
| GO:0009526 plastid envelope | CC | | 162/736 | 265/736 | 166/736 | 152/736 | 272/736 | 292/736 |
| GO:0009941 chloroplast envelope | CC | | 158/717 | 257/717 | 161/717 | 147/717 | 267/717 | 286/717 |

**Table C.6:** Shared or uniquely enriched pathways among WT and GABA mutants after submergence.

| Class | Sub Class | Description | DEGs ratio: No. of DEGs divided by total genes | | | | | | |
|---|---|---|---|---|---|---|---|---|---|
| | | | WT | *gad1** | *gad1KO* | *gad2-1* | *gad1245* | *gad2OE* | *pop2-8* |
| **Metabolism** | Metabolism of cofactors and vitamins | Porphyrin metabolism | 15/53 | 22/53 | 29/53 | 22/53 | 22/53 | 30/53 | 31/53 |
| | Lipid metabolism | Fatty acid elongation | 14/36 | 17/36 | 19/36 | 14/36 | 15/36 | 18/36 | 18/36 |
| | Carbohydrate metabolism | Ascorbate and aldarate metabolism | 19/63 | 21/63 | 24/63 | 19/63 | 28/63 | 27/63 | 31/63 |
| **Environmental Information Processing** | Signal transduction | MAPK signaling pathway - plant | 49/139 | 45/139 | 59/139 | 41/139 | 51/139 | 59/139 | 60/139 |
| | | Plant hormone signal transduction | 99/289 | 99/289 | 115/289 | 101/289 | 113/289 | 119/289 | 124/289 |
| **Genetic Information Processing** | Replication and repair | DNA replication | 17/48 | 20/48 | 21/48 | 15/48 | 18/48 | 22/48 | 28/48 |
| **Metabolism** | Metabolism of terpenoids and polyketides | Diterpenoid biosynthesis | 9/21 | 8/21 | | | | | |
| | | Brassinosteroid biosynthesis | 4/8 | | | 4/8 | | | |
| | | Carotenoid biosynthesis | 11/29 | | 15/29 | | 14/29 | 16/29 | 16/29 |
| | | Zeatin biosynthesis | 11/32 | 13/32 | 16/32 | 13/32 | | 17/32 | |
| | Metabolism of other amino acids | beta-Alanine metabolism | | 16/47 | 19/47 | 15/47 | 19/47 | 23/47 | 24/47 |
| | | Selenocompound metabolism | | | 9/18 | | | | 10/18 |
| | | Cyanoamino acid metabolism | 24/70 | | | | 28/70 | 30/70 | 31/70 |
| | | Glutathione metabolism | | 30/103 | 42/103 | 32/103 | 40/103 | | 47/103 |
| | Metabolism of cofactors and vitamins | Ubiquinone and other terpenoid-quinone biosynthesis | | 14/39 | 18/39 | 15/39 | 15/39 | 17/39 | |
| | | Biotin metabolism | 8/16 | | 9/16 | | | | |
| | Lipid metabolism | Fatty acid degradation | 14/47 | | | | 19/47 | 21/47 | 22/47 |
| | | Steroid biosynthesis | | 13/36 | | 12/36 | 14/36 | 17/36 | |
| | | Linoleic acid metabolism | 4/9 | | | 5/9 | 5/9 | | |
| | | alpha-Linolenic acid metabolism | 15/43 | | 19/43 | 14/43 | 18/43 | 19/43 | |
| | Energy metabolism | Photosynthesis - antenna proteins | | | | 10/22 | | 12/22 | 12/22 |
| | | Carbon fixation in photosynthetic organisms | | 23/69 | 27/69 | 20/69 | | | 33/69 |
| | | Nitrogen metabolism | 16/43 | 16/43 | 18/43 | 15/43 | | | |
| | Carbohydrate metabolism | Pentose and glucuronate interconversions | 26/107 | | | | 37/107 | | |
| | | Starch and sucrose metabolism | 42/171 | 46/171 | 60/171 | | 53/171 | 62/171 | |
| | Biosynthesis of other secondary metabolites | Monobactam biosynthesis | | 6/14 | 8/14 | | | 8/14 | 10/14 |
| | | Indole alkaloid biosynthesis | 4/4 | | | | 3/4 | | |
| | | Phenylpropanoid biosynthesis | 30/128 | | 45/128 | 35/128 | 47/128 | 48/128 | |
| | | Flavone and flavonol biosynthesis | 3/4 | 3/4 | | | | | |
| | | Isoquinoline alkaloid biosynthesis | 8/22 | 10/22 | | | 10/22 | | |

Continuation of Table C.6

| Class | Sub Class | Description | DEGs ratio: No. of DEGs divided by No. of genes in pathway | | | | | | |
|---|---|---|---|---|---|---|---|---|---|
| | | | WT | *gad1** | *gad1KO* | *gad2-1* | *gad1245* | *gad2OE* | *pop2-8* |
| | | Glucosinolate biosynthesis | 11/26 | 12/26 | 15/26 | | 15/26 | 15/26 | 16/26 |
| | | Biosynthesis of various plant secondary metabolites | 21/64 | 25/64 | 27/64 | | 28/64 | 31/64 | 31/64 |
| | Amino acid metabolism | Alanine, aspartate and glutamate metabolism | 14/51 | | 21/51 | | | | 25/51 |
| | | Glycine, serine and threonine metabolism | | | 27/70 | | 26/70 | | 32/70 |
| | | Cysteine and methionine metabolism | 30/124 | | 50/124 | 33/124 | 41/124 | | 53/124 |
| | | Valine, leucine and isoleucine degradation | | 17/52 | 21/52 | | 20/52 | 25/52 | 27/52 |
| | | Lysine biosynthesis | | | | | | 8/15 | 11/15 |
| | | Tyrosine metabolism | 12/41 | 14/41 | | | 16/41 | | |
| | | Phenylalanine metabolism | 11/33 | 13/33 | | | 14/33 | | 18/33 |
| | | Tryptophan metabolism | 19/64 | | | | 23/64 | | |
| **Organismal Systems** | Environmental adaptation | Plant-pathogen interaction | 44/204 | | 70/204 | 54/204 | 66/204 | 72/204 | |
| **Metabolism** | Nucleotide metabolism | Pyrimidine metabolism | | | | 18/63 | | | |
| | Lipid metabolism | Fatty acid biosynthesis | 14/43 | | | | | | |
| | | Sphingolipid metabolism | | | | | | | 15/29 |
| | Energy metabolism | Photosynthesis | | | | | | 31/77 | |
| | | Sulfur metabolism | | | 20/42 | | | | |
| | Carbohydrate metabolism | Amino sugar and nucleotide sugar metabolism | | | | | 44/133 | | |
| | | Glyoxylate and dicarboxylate metabolism | | | 31/78 | | | | |
| | Biosynthesis of other secondary metabolites | Flavonoid biosynthesis | 10/25 | | | | | | |
| | | Anthocyanin biosynthesis | 2/2 | | | | | | |
| | | Stilbenoid, diarylheptanoid and gingerol biosynthesis | 4/9 | | | | | | |
| | | Tropane, piperidine and pyridine alkaloid biosynthesis | | | | | | | 17/35 |
| | Amino acid metabolism | Valine, leucine and isoleucine biosynthesis | | | 11/21 | | | | |
| | | Arginine and proline metabolism | 15/54 | | | | | | |
| **Genetic Information Processing** | Translation | Ribosome | | | | | | | 168/361 |
| | Replication and repair | Homologous recombination | | | | | 22/64 | | |
| **Environmental Information Processing** | Membrane transport | ABC transporters | | | 14/32 | | | | |

**Table C.7:** GO terms enriched specifically by MutSub DEGs in GABA mutants after submergence. Red/blue indicate up-/down-regulated genes, respectively. The GO terms are in the same order as in Fig 3.33.

| GO term | Ontology | DEGs ratio: No. of DEGs divided by total genes | | | | | |
|---|---|---|---|---|---|---|---|
| | | *gad1** | *gad1KO* | *gad2-1* | *gad1245* | *gad2OE* | *pop2-8* |
| GO:0009751 response to salicylic acid | BP | | 32/169 | 14/169 | 40/169 | 42/169 | 43/169 |
| GO:0071396 cellular response to lipid | BP | | 70/540 | | 70/540 | 85/540 | 85/540 |
| GO:1901701 cellular response to oxygen-containing compound | BP | | 90/741 | | 96/741 | 112/741 | 113/741 |
| GO:0071398 cellular response to fatty acid | BP | | 25/107 | | 28/107 | 30/107 | 28/107 |
| GO:2000022 regulation of jasmonic acid mediated signaling pathway | BP | | 16/41 | | 17/41 | 19/41 | 15/41 |
| GO:0009867 jasmonic acid mediated signaling pathway | BP | | 25/98 | | 26/98 | 29/98 | 26/98 |
| GO:0071395 cellular response to jasmonic acid stimulus | BP | | 25/103 | | 27/103 | 30/103 | 27/103 |
| GO:0000302 response to reactive oxygen species | BP | | 32/159 | | 38/159 | 36/159 | 43/159 |
| GO:0031347 regulation of defense response | BP | | 40/273 | | 53/273 | 53/273 | 52/273 |
| GO:0071949 FAD binding | MF | | 19/80 | | 24/80 | 24/80 | 26/80 |
| GO:0042430 indole-containing compound metabolic process | BP | 9/79 | 20/79 | | 33/79 | 26/79 | 31/79 |
| **GO:0010150 leaf senescence** | BP | 15/143 | 39/143 | 12/143 | 37/143 | 40/143 | 40/143 |
| GO:0016054 organic acid catabolic process | BP | 16/167 | 36/167 | 17/167 | 41/167 | 40/167 | 42/167 |
| GO:0046395 carboxylic acid catabolic process | BP | 15/154 | 32/154 | 14/154 | 36/154 | 37/154 | 39/154 |
| GO:0043436 oxoacid metabolic process | BP | 45/1179 | 116/1179 | 57/1179 | 168/1179 | 161/1179 | 168/1179 |
| GO:0019752 carboxylic acid metabolic process | BP | 38/1049 | | 45/1049 | 141/1049 | 140/1049 | 144/1049 |
| GO:0042435 indole-containing compound biosynthetic process | BP | | | | 24/55 | 19/55 | 22/55 |
| GO:0009072 aromatic amino acid family metabolic process | BP | | | | 30/84 | 24/84 | 23/84 |
| GO:1901605 alpha-amino acid metabolic process | BP | | | | 58/298 | 57/298 | 55/298 |
| GO:0004674 protein serine/threonine kinase activity | MF | | | | 107/896 | 115/896 | 162/896 |
| GO:0016773 phosphotransferase activity, alcohol group as acceptor | MF | | | | | 148/1303 | 198/1303 |
| GO:0008194 UDP-glycosyltransferase activity | MF | 18/289 | | 20/289 | 42/289 | | 49/289 |
| GO:0015996 chlorophyll catabolic process | BP | 6/20 | 8/20 | 5/20 | | | |
| GO:0006787 porphyrin-containing compound catabolic process | BP | 6/25 | | | | | |
| GO:0033015 tetrapyrrole catabolic process | BP | 6/25 | | | | | |
| GO:0046527 glucosyltransferase activity | MF | | 29/180 | | 32/180 | | |
| GO:0000976 transcription regulatory region sequence-specific DNA binding | MF | | 99/1010 | 41/1010 | | | |
| GO:0001067 regulatory region nucleic acid binding | MF | | 99/1010 | 41/1010 | | | |
| **GO:1900055 regulation of leaf senescence** | BP | 7/46 | 13/46 | | | | |
| GO:1990837 sequence-specific double-stranded DNA binding | MF | | 100/1035 | 41/1035 | | | |
| GO:0003978 UDP-glucose 4-epimerase activity | MF | | 6/8 | | | | |
| GO:0043565 sequence-specific DNA binding | MF | | 122/1301 | | | | |
| GO:0050373 UDP-arabinose 4-epimerase activity | MF | | 5/5 | | | | |
| GO:0046379 extracellular polysaccharide metabolic process | BP | | 5/5 | | | | |
| GO:0045230 capsule organization | BP | | 5/5 | | | | |
| GO:0045227 capsule polysaccharide biosynthetic process | BP | | 5/5 | | | | |
| GO:0033358 UDP-L-arabinose biosynthetic process | BP | | 5/5 | | | | |
| GO:0045226 extracellular polysaccharide biosynthetic process | BP | | 5/5 | | | | |
| **GO:1900057 positive regulation of leaf senescence** | BP | 6/18 | 11/18 | | 8/18 | 10/18 | 9/18 |
| GO:0042537 benzene-containing compound metabolic process | BP | | 18/78 | | 20/78 | 21/78 | |

Continuation of Table C.7

| GO term | Ontology | DEGs ratio: No. of DEGs divided by total genes | | | | | |
|---|---|---|---|---|---|---|---|
| | | *gad1** | *gad1KO* | *gad2-1* | *gad1245* | *gad2OE* | *pop2-8* |
| GO:0032870 cellular response to hormone stimulus | BP | | 102/999 | | | 120/999 | |
| GO:0071310 cellular response to organic substance | BP | | 115/1182 | | 126/1182 | 138/1182 | |
| GO:0009627 systemic acquired resistance | BP | | | | 24/84 | 19/84 | 22/84 |
| GO:0016053 organic acid biosynthetic process | BP | | | | 85/577 | 75/577 | |
| GO:0009073 aromatic amino acid family biosynthetic process | BP | | | | 18/57 | | |
| GO:0016143 S-glycoside metabolic process | BP | | | | 28/119 | | |
| GO:0019760 glucosinolate metabolic process | BP | | | | 28/119 | | |
| GO:0008652 cellular amino acid biosynthetic process | BP | | | | 40/233 | | |
| GO:0009684 indoleacetic acid biosynthetic process | BP | | | | 8/12 | | |
| GO:0015297 antiporter activity | MF | | | | 34/205 | | |
| GO:0002213 defense response to insect | BP | | | | 11/29 | | |
| GO:0016844 strictosidine synthase activity | MF | | | | 8/15 | | |
| GO:0009074 aromatic amino acid family catabolic process | BP | | 8/21 | | 10/21 | | |
| GO:0009683 indoleacetic acid metabolic process | BP | | | | 8/13 | | |
| GO:0009063 cellular amino acid catabolic process | BP | 9/89 | | | 21/89 | 20/89 | |
| GO:0009308 amine metabolic process | BP | | | | 27/134 | | |
| GO:0010112 regulation of systemic acquired resistance | BP | | | | 10/23 | | |
| GO:0000162 tryptophan biosynthetic process | BP | | | | 11/27 | 10/27 | 11/27 |
| GO:0046219 indolalkylamine biosynthetic process | BP | | | | 11/27 | 10/27 | 11/27 |
| GO:1901657 glycosyl compound metabolic process | BP | | | | 35/202 | | |
| GO:0009309 amine biosynthetic process | BP | | | | 15/50 | 14/50 | |
| GO:0042401 cellular biogenic amine biosynthetic process | BP | | | | 15/50 | 14/50 | |
| GO:0046394 carboxylic acid biosynthetic process | BP | | | | 81/542 | 74/542 | |
| GO:0015291 secondary active transmembrane transporter activity | MF | | 39/313 | | 47/313 | 53/313 | |
| GO:0097237 cellular response to toxic substance | BP | | | | 36/198 | 36/198 | |
| GO:1901607 alpha-amino acid biosynthetic process | BP | | | | 35/191 | 34/191 | |
| GO:0044106 cellular amine metabolic process | BP | | | | 23/81 | 20/81 | |
| GO:1901606 alpha-amino acid catabolic process | BP | | 15/68 | | 20/68 | 19/68 | |
| GO:0006576 cellular biogenic amine metabolic process | BP | | | | 21/70 | 19/70 | |
| GO:0032787 monocarboxylic acid metabolic process | BP | | 58/538 | | 76/538 | 75/538 | 80/538 |
| GO:0014070 response to organic cyclic compound | BP | | 41/316 | 18/316 | 52/316 | 54/316 | 57/316 |
| GO:0072329 monocarboxylic acid catabolic process | BP | | 16/65 | | 17/65 | 18/65 | 19/65 |
| GO:0004364 glutathione transferase activity | MF | | | | 17/64 | 20/64 | 19/64 |
| GO:0050660 flavin adenine dinucleotide binding | MF | | 26/169 | | 36/169 | 35/169 | 41/169 |
| GO:0006568 tryptophan metabolic process | BP | | | | 16/37 | 14/37 | 14/37 |
| GO:0006586 indolalkylamine metabolic process | BP | | | | 16/37 | 14/37 | 14/37 |
| GO:0006468 protein phosphorylation | BP | | | | | | 185/1277 |
| GO:0016301 kinase activity | MF | | | | | | 212/1514 |
| GO:0016310 phosphorylation | BP | | | | | | 226/1750 |
| GO:0006796 phosphate-containing compound metabolic process | BP | | | | | | 295/2517 |
| GO:0030554 adenyl nucleotide binding | MF | | | | | | 302/2625 |
| GO:0032559 adenyl ribonucleotide binding | MF | | | | | | 302/2614 |
| GO:0042542 response to hydrogen peroxide | BP | | 17/69 | | 17/69 | 18/69 | 21/69 |

Continuation of Table C.7

| GO term | Ontology | DEGs ratio: No. of DEGs divided by total genes | | | | | |
|---|---|---|---|---|---|---|---|
| | | *gad1** | *gad1KO* | *gad2-1* | *gad1245* | *gad2OE* | *pop2-8* |
| GO:0009738 abscisic acid-activated signaling pathway | BP | | 38/262 | | | 50/262 | 49/262 |
| GO:0071215 cellular response to abscisic acid stimulus | BP | | 41/293 | | | 52/293 | 53/293 |
| GO:0097306 cellular response to alcohol | BP | | 41/293 | | | 52/293 | 53/293 |
| GO:0002237 response to molecule of bacterial origin | BP | | | | | 14/43 | 15/43 |
| GO:0006749 glutathione metabolic process | BP | | | | 19/85 | 22/85 | |
| GO:0036293 response to decreased oxygen levels | BP | 22/269 | 96/269 | 27/269 | 83/269 | 88/269 | 87/269 |
| GO:0071456 cellular response to hypoxia | BP | 19/239 | 91/239 | 27/239 | 80/239 | 84/239 | 83/239 |
| GO:0036294 cellular response to decreased oxygen levels | BP | 20/241 | 92/241 | 27/241 | 80/241 | 84/241 | 83/241 |
| GO:0071453 cellular response to oxygen levels | BP | 20/241 | 92/241 | 27/241 | 80/241 | 84/241 | 83/241 |
| GO:0042742 defense response to bacterium | BP | | 71/457 | | 85/457 | 90/457 | 110/457 |
| GO:0009651 response to salt stress | BP | | 88/470 | 28/470 | 79/470 | 95/470 | 97/470 |
| GO:0009737 response to abscisic acid | BP | 27/603 | 107/603 | 34/603 | 100/603 | 119/603 | 129/603 |
| GO:0097305 response to alcohol | BP | 27/610 | 107/610 | 34/610 | 100/610 | 120/610 | 130/610 |
| GO:0010200 response to chitin | BP | | 50/138 | 21/138 | 50/138 | 45/138 | 57/138 |
| GO:0010243 response to organonitrogen compound | BP | | 60/261 | 25/261 | 66/261 | 60/261 | 75/261 |
| GO:0033993 response to lipid | BP | 41/966 | 152/966 | 52/966 | 159/966 | 179/966 | 185/966 |
| GO:0009753 response to jasmonic acid | BP | 15/196 | 50/196 | 24/196 | 64/196 | 66/196 | 59/196 |
| GO:0070542 response to fatty acid | BP | 15/200 | 50/200 | 24/200 | 65/200 | 66/200 | 60/200 |
| GO:0009507 chloroplast | CC | | 107/2449 | | | 164/2449 | 387/2449 |
| GO:0003729 mRNA binding | MF | | | | | | 200/1030 |
| GO:0003723 RNA binding | MF | | | | | | 298/1929 |
| GO:0005840 ribosome | CC | | | | | | 120/528 |
| GO:0005976 polysaccharide metabolic process | BP | 17/494 | 52/494 | 15/494 | 66/494 | 51/494 | 87/494 |
| GO:0045229 external encapsulating structure organization | BP | 15/582 | 56/582 | 22/582 | 72/582 | 60/582 | 101/582 |
| GO:0009733 response to auxin | BP | 13/415 | 26/415 | 20/415 | 50/415 | 50/415 | 65/415 |
| GO:0009734 auxin-activated signaling pathway | BP | 11/224 | 21/224 | 17/224 | 42/224 | 41/224 | 48/224 |
| GO:0071365 cellular response to auxin stimulus | BP | 11/241 | 21/241 | 17/241 | 43/241 | 43/241 | 52/241 |
| GO:0045490 pectin catabolic process | BP | | 13/100 | 7/100 | 14/100 | | |
| GO:0046128 purine ribonucleoside metabolic process | BP | | 8/38 | | | | |
| GO:0019187 beta-1,4-mannosyltransferase activity | MF | | 7/27 | | | | |
| GO:0051753 mannan synthase activity | MF | | 7/27 | | | | |
| GO:0019253 reductive pentose-phosphate cycle | BP | | 6/21 | | | | |
| GO:0019685 photosynthesis, dark reaction | BP | | 6/21 | | | | |
| GO:0009250 glucan biosynthetic process | BP | | 14/139 | | | | |
| GO:0042278 purine nucleoside metabolic process | BP | | 8/41 | | | | |
| GO:0016052 carbohydrate catabolic process | BP | 9/298 | 26/298 | 11/298 | | | |
| GO:0051273 beta-glucan metabolic process | BP | | 14/107 | | 15/107 | | |
| GO:0009163 nucleoside biosynthetic process | BP | | 8/26 | | | | |
| GO:0042455 ribonucleoside biosynthetic process | BP | | 8/26 | | | | |
| GO:0042451 purine nucleoside biosynthetic process | BP | | 8/25 | | | | |
| GO:0046129 purine ribonucleoside biosynthetic process | BP | | 8/25 | | | | |
| GO:0010148 transpiration | BP | | | 3/6 | | | |
| GO:0034756 regulation of iron ion transport | BP | 3/8 | | | | | |

Continuation of Table C.7

| GO term | Ontology | DEGs ratio: No. of DEGs divided by total genes | | | | | |
|---|---|---|---|---|---|---|---|
| | | *gad1** | *gad1KO* | *gad2-1* | *gad1245* | *gad2OE* | *pop2-8* |
| GO:0006833 water transport | BP | | | 5/39 | 10/39 | | 14/39 |
| GO:0042044 fluid transport | BP | | | 5/39 | 10/39 | | 14/39 |
| GO:0032870 cellular response to hormone stimulus | BP | | | 29/999 | 80/999 | 77/999 | |
| GO:0071310 cellular response to organic substance | BP | | | 32/1182 | 84/1182 | | |
| GO:0009926 auxin polar transport | BP | | | | 15/95 | 19/95 | 23/95 |
| GO:0009832 plant-type cell wall biogenesis | BP | | | | 22/185 | | 35/185 |
| GO:0045489 pectin biosynthetic process | BP | | | | 12/59 | | |
| GO:0009416 response to light stimulus | BP | | | | 64/746 | | 98/746 |
| GO:0009639 response to red or far red light | BP | | | | 28/231 | | |
| GO:0009664 plant-type cell wall organization | BP | | 14/153 | | 23/153 | | |
| GO:0016837 carbon-oxygen lyase activity, acting on polysaccharides | MF | 4/34 | 8/34 | 5/34 | 9/34 | 9/34 | |
| GO:0030570 pectate lyase activity | MF | 4/27 | 8/27 | 5/27 | 9/27 | 9/27 | |
| GO:0010393 galacturonan metabolic process | BP | 7/171 | 21/171 | 8/171 | 27/171 | 23/171 | |
| GO:0045488 pectin metabolic process | BP | 7/170 | 21/170 | 8/170 | 27/170 | 23/170 | |
| GO:0000272 polysaccharide catabolic process | BP | 8/189 | 21/189 | | 25/189 | | |
| GO:0000271 polysaccharide biosynthetic process | BP | | 22/239 | | 29/239 | | 43/239 |
| GO:0016758 transferase activity, transferring hexosyl groups | MF | 10/366 | 28/366 | | 37/366 | | |
| GO:0030243 cellulose metabolic process | BP | | 13/94 | | 15/94 | | |
| GO:0034637 cellular carbohydrate biosynthetic process | BP | | 22/240 | | 26/240 | | |
| GO:0042254 ribosome biogenesis | BP | | | | | | 97/430 |
| GO:0015934 large ribosomal subunit | CC | | | | | | 56/195 |
| GO:0022613 ribonucleoprotein complex biogenesis | BP | | | | | | 103/535 |
| GO:0022625 cytosolic large ribosomal subunit | CC | | | | | | 45/147 |
| GO:0009658 chloroplast organization | BP | | | | | 30/239 | 54/239 |
| GO:0042651 thylakoid membrane | CC | | 27/466 | | | 49/466 | 79/466 |
| GO:0034660 ncRNA metabolic process | BP | | | | | | 79/536 |
| GO:0006778 porphyrin-containing compound metabolic process | BP | | | | | | 25/106 |
| GO:0016556 mRNA modification | BP | | | | | | 15/45 |
| GO:0033013 tetrapyrrole metabolic process | BP | | | | | | 25/107 |
| GO:0015994 chlorophyll metabolic process | BP | | | | | | 24/90 |
| GO:0034470 ncRNA processing | BP | | | | | | 71/450 |
| GO:0008168 methyltransferase activity | MF | | | | | | 64/395 |
| GO:1901659 glycosyl compound biosynthetic process | BP | | | | | | 21/74 |
| GO:0006779 porphyrin-containing compound biosynthetic process | BP | | | | | | 22/75 |
| GO:0033014 tetrapyrrole biosynthetic process | BP | | | | | | 23/78 |
| GO:0006261 DNA-dependent DNA replication | BP | | | | | | 35/148 |
| GO:0042255 ribosome assembly | BP | | | | | | 27/98 |
| GO:0006271 DNA strand elongation involved in DNA replication | BP | | | | | | 11/16 |
| GO:0022616 DNA strand elongation | BP | | | | | | 11/16 |
| GO:0015995 chlorophyll biosynthetic process | BP | | | | | | 22/65 |
| GO:0031969 chloroplast membrane | CC | | | | | | 56/294 |
| GO:0042170 plastid membrane | CC | | | | | | 57/302 |
| GO:0006260 DNA replication | BP | | | | | | 42/195 |

Continuation of Table C.7

| GO term | Ontology | DEGs ratio: No. of DEGs divided by total genes | | | | | |
|---|---|---|---|---|---|---|---|
| | | *gad1** | *gad1KO* | *gad2-1* | *gad1245* | *gad2OE* | *pop2-8* |
| GO:0043603 cellular amide metabolic process | BP | | | | | | 145/1068 |
| GO:0042788 polysomal ribosome | CC | | | | | | 30/98 |
| GO:0019843 rRNA binding | MF | | | | | | 38/144 |
| GO:0043604 amide biosynthetic process | BP | | | | | | 135/916 |
| GO:0016072 rRNA metabolic process | BP | | | | | | 59/299 |
| GO:0006364 rRNA processing | BP | | | | | | 59/294 |
| GO:0015935 small ribosomal subunit | CC | | | | | | 38/150 |
| GO:0005730 nucleolus | CC | | | | | | 88/537 |
| GO:0006518 peptide metabolic process | BP | | | | | | 136/950 |
| GO:0009451 RNA modification | BP | | | | | | 69/315 |
| GO:1901566 organonitrogen compound biosynthetic process | BP | | | | | | 240/1790 |
| GO:0042273 ribosomal large subunit biogenesis | BP | | | | | | 35/114 |
| GO:0006412 translation | BP | | | | | | 130/842 |
| GO:0009657 plastid organization | BP | | | | | | 64/310 |
| GO:0022627 cytosolic small ribosomal subunit | CC | | | | | | 34/113 |
| GO:0043043 peptide biosynthetic process | BP | | | | | | 130/847 |
| GO:0009505 plant-type cell wall | CC | | 28/237 | | 29/237 | 38/237 | 56/237 |
| GO:0046658 anchored component of plasma membrane | CC | | 20/173 | | 24/173 | 32/173 | 44/173 |
| GO:0005911 cell-cell junction | CC | | 51/967 | | 62/967 | 79/967 | 162/967 |
| GO:0009526 plastid envelope | CC | | 45/736 | | | 62/736 | 137/736 |
| GO:0009941 chloroplast envelope | CC | | 45/717 | | | 62/717 | 135/717 |
| GO:0009534 chloroplast thylakoid | CC | | 35/540 | | | 60/540 | 98/540 |
| GO:0009535 chloroplast thylakoid membrane | CC | | 27/445 | | | 48/445 | 75/445 |
| GO:0055035 plastid thylakoid membrane | CC | | 27/446 | | | 48/446 | 75/446 |
| GO:0009914 hormone transport | BP | | | | 21/119 | 25/119 | 31/119 |
| GO:0060918 auxin transport | BP | | | | 21/116 | 25/116 | 30/116 |
| GO:0016051 carbohydrate biosynthetic process | BP | | 36/376 | | 37/376 | | 64/376 |
| GO:0044264 cellular polysaccharide metabolic process | BP | 11/325 | 31/325 | | 43/325 | | 59/325 |
| GO:0006073 cellular glucan metabolic process | BP | 9/249 | 27/249 | | 34/249 | | 46/249 |
| GO:0044042 glucan metabolic process | BP | 9/255 | 27/255 | | 34/255 | | 46/255 |

**Table C.8:** Shared or uniquely enriched mutation-specific pathways among GABA mutants after submergence.

| Class | Sub Class | Description | DEGs ratio: No. of DEGs divided by total genes | | | | | |
|---|---|---|---|---|---|---|---|---|
| | | | *gad1** | *gad1KO* | *gad2-1* | *gad1245* | *gad2OE* | *pop2-8* |
| **Metabolism** | Amino acid metabolism | Valine, leucine and isoleucine degradation | 8/52 | 13/52 | 11/52 | 15/52 | 14/52 | 20/52 |
| | Lipid metabolism | Fatty acid degradation | 5/47 | 11/47 | 7/47 | 16/47 | 19/47 | 19/47 |
| | | alpha-Linolenic acid metabolism | 4/43 | 12/43 | 9/43 | 16/43 | 20/43 | 17/43 |
| | Metabolism of other amino acids | beta-Alanine metabolism | 7/47 | 9/47 | 7/47 | 11/47 | 18/47 | 18/47 |
| | Metabolism of terpenoids and polyketides | Zeatin biosynthesis | 5/32 | 8/32 | 5/32 | 9/32 | 11/32 | 14/32 |
| **Environmental Information Processing** | Signal transduction | Plant hormone signal transduction | 18/289 | 46/289 | 18/289 | 64/289 | 64/289 | 75/289 |
| **Metabolism** | Amino acid metabolism | Glycine, serine and threonine metabolism | 6/70 | 13/70 | | 18/70 | 19/70 | 25/70 |
| | | Cysteine and methionine metabolism | | 21/124 | 8/124 | 28/124 | 26/124 | 34/124 |
| | | Lysine degradation | 3/31 | | | 8/31 | | |
| | | Arginine and proline metabolism | 5/54 | | 6/54 | 16/54 | 15/54 | 19/54 |
| | | Tyrosine metabolism | | | | 12/41 | 11/41 | 15/41 |
| | | Phenylalanine metabolism | | | | 9/33 | | 12/33 |
| | | Tryptophan metabolism | 5/64 | 12/64 | | 25/64 | 21/64 | 22/64 |
| | | Phenylalanine, tyrosine and tryptophan biosynthesis | | | | 21/56 | 16/56 | 21/56 |
| | Biosynthesis of other secondary metabolites | Indole alkaloid biosynthesis | | 2/4 | | 3/4 | 3/4 | 3/4 |
| | | Phenylpropanoid biosynthesis | | 21/128 | | 27/128 | 33/128 | |
| | | Isoquinoline alkaloid biosynthesis | | | | 6/22 | | 9/22 |
| | | Glucosinolate biosynthesis | | | | 8/26 | | 16/26 |
| | | Biosynthesis of various plant secondary metabolites | | 12/64 | | | 17/64 | 22/64 |
| | Carbohydrate metabolism | Pentose and glucuronate interconversions | 6/107 | 17/107 | 7/107 | | | |
| | | Ascorbate and aldarate metabolism | | | 6/63 | 13/63 | | |
| | | Starch and sucrose metabolism | | 30/171 | | 28/171 | 32/171 | 46/171 |
| | Energy metabolism | Photosynthesis - antenna proteins | | | | | 7/22 | 10/22 |
| | | Nitrogen metabolism | | 9/43 | | | 11/43 | |
| | Lipid metabolism | Glycerolipid metabolism | | 12/66 | | 15/66 | 19/66 | 21/66 |
| | Metabolism of cofactors and vitamins | Pantothenate and CoA biosynthesis | 3/34 | | | | 10/34 | 14/34 |
| | | Porphyrin metabolism | 4/53 | | | | | 24/53 |
| | Metabolism of other amino acids | Cyanoamino acid metabolism | | 14/70 | 6/70 | 15/70 | 17/70 | 24/70 |
| | | Glutathione metabolism | | | | 25/103 | 27/103 | 31/103 |
| | Metabolism of terpenoids and polyketides | Limonene and pinene degradation | | | | 4/6 | 4/6 | 4/6 |

Continuation of Table C.8

| Class | Sub Class | Description | DEGs ratio: No. of DEGs divided by total genes | | | | | |
|---|---|---|---|---|---|---|---|---|
| | | | *gad1** | *gad1KO* | *gad2-1* | *gad1245* | *gad2OE* | *pop2-8* |
| **Environmental Information Processing** | Signal transduction | MAPK signaling pathway - plant | | 28/139 | | 28/139 | 28/139 | |
| **Metabolism** | Amino acid metabolism | Lysine biosynthesis | | | | | | 7/15 |
| | | Histidine metabolism | | | | | | 8/19 |
| | Biosynthesis of other secondary metabolites | Caffeine metabolism | | | | | 2/3 | |
| | | Anthocyanin biosynthesis | | | | | 2/2 | |
| | Carbohydrate metabolism | Galactose metabolism | 5/57 | | | | | |
| | | Glyoxylate and dicarboxylate metabolism | | 13/78 | | | | |
| | | Propanoate metabolism | | | 5/41 | | | |
| | Energy metabolism | Carbon fixation in photosynthetic organisms | | 11/69 | | | | |
| | Lipid metabolism | Glycerophospholipid metabolism | | 15/99 | | | | |
| | | Linoleic acid metabolism | | | 2/9 | | | |
| | | Sphingolipid metabolism | | | | | 8/29 | |
| | Metabolism of terpenoids and polyketides | Diterpenoid biosynthesis | | | | 6/21 | | |
| | | Carotenoid biosynthesis | | 6/29 | | | | |
| **Organismal Systems** | Environmental adaptation | Plant-pathogen interaction | | | | 34/204 | | |
| | | Circadian rhythm - plant | | 7/39 | | | | |
| **Genetic Information Processing** | Replication and repair | DNA replication | | | | | | 22/48 |
| | | Base excision repair | | | | | | 14/42 |
| | Translation | Ribosome | | | | | | 98/361 |

# APPENDIX D

# SUPPLEMENTARY DATA FOR CHAPTER 4

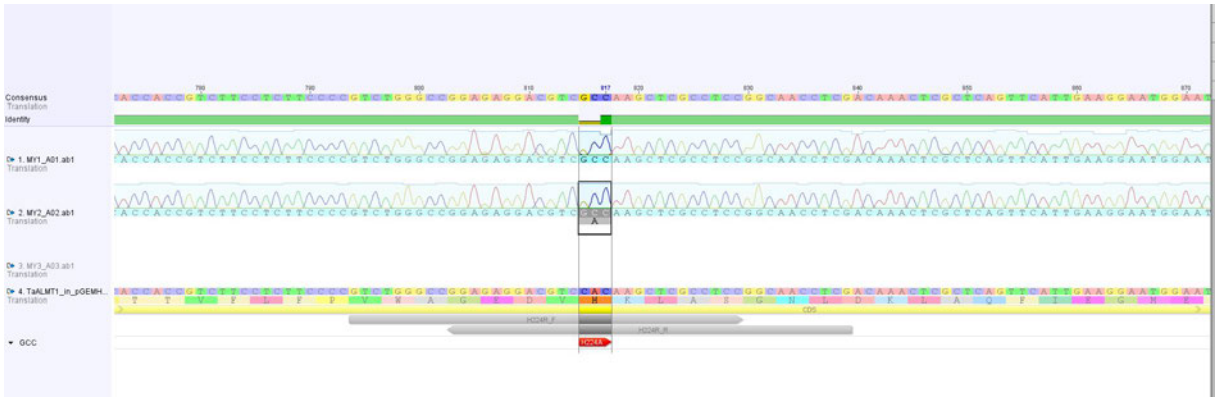

**(a)** Histidine (H) to alanine (A) mutation of *TaALMT1*

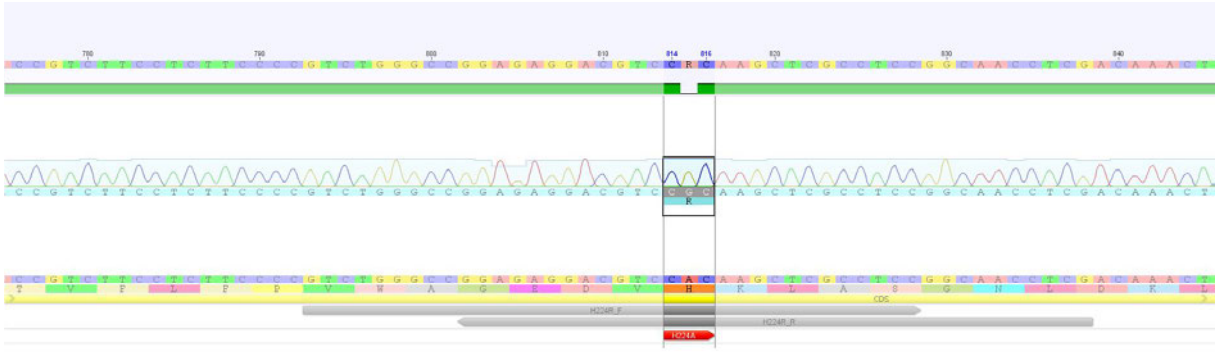

**(b)** Histidine (H) to arginine (R) mutation of *TaALMT1*

**Figure D.1:** Conformation of mutation in $TaALMT1^{H224A}$ and $TaALMT1^{H224R}$. (a): the Histindine to Alanine (H224A) mutation. (b): the Histidine to Arginine (H224R) mutation.

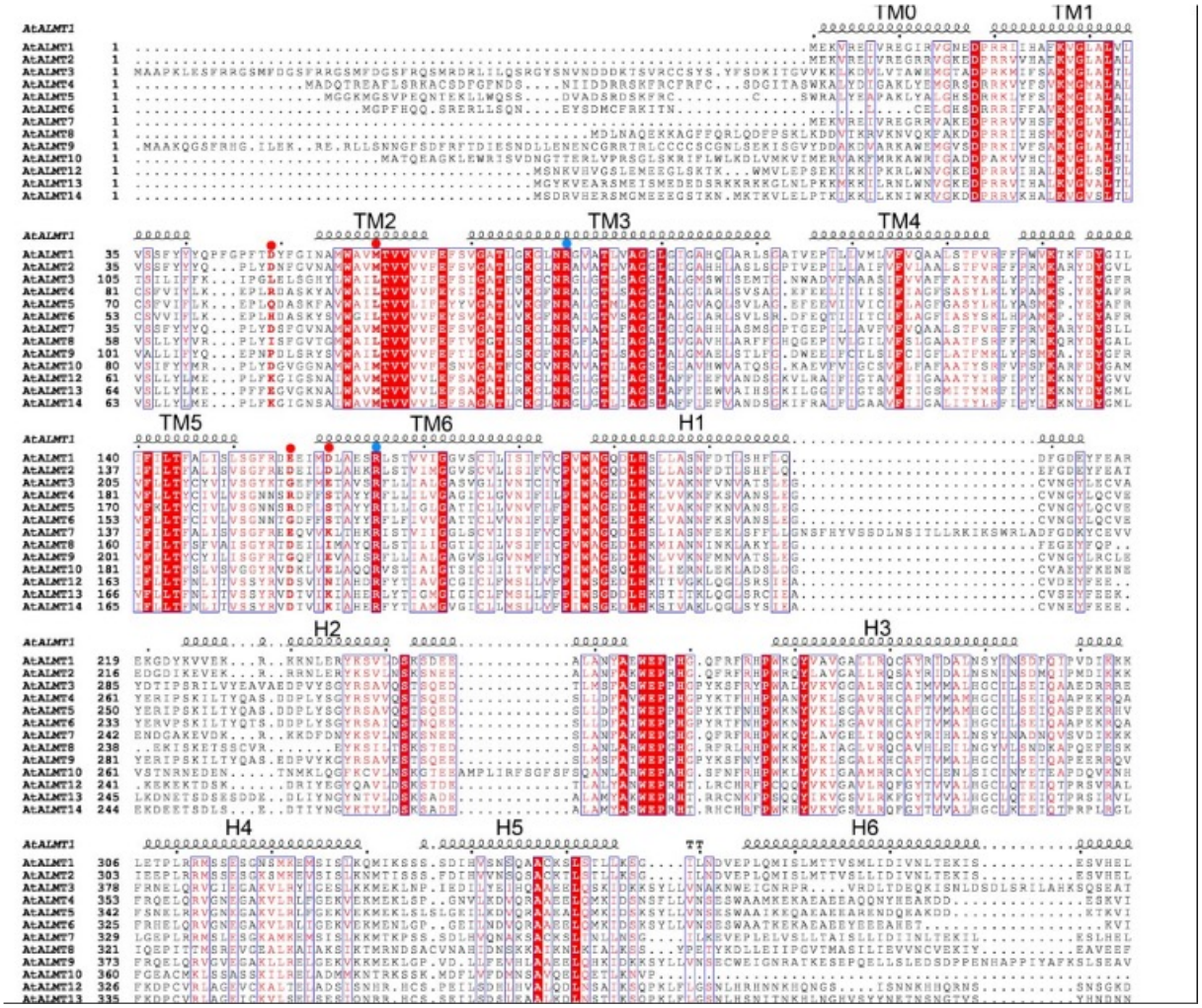


**Figure D.2:** Alignment of Arabidopsis AtALMT proteins. Supplementary figure of Wang et al. (2021a). The GABA-binding motif in Wheat TaALMT1 and Arabidopsis AtALMT1 are both in the sixth transmembrane domain (TMD) TM6 and H1 of the cytosolic domain (CTD).

# Bibliography

M. Abbas, S. Berckhan, D. J. Rooney, D. J. Gibbs, J. V. Conde, C. S. Correia, G. W. Bassel, N. M. de la Rosa, J. León, D. Alabadí, M. A. Blázquez, and M. J. Holdsworth. Oxygen sensing coordinates photomorphogenesis to facilitate seedling survival. *Current Biology*, 25(11):1483–1488, 2015.

R. Ahlfors, S. Lång, K. Overmyer, P. Jaspers, M. Brosché, A. Tauriainen, H. Kollist, H. Tuominen, E. Belles-Boix, M. Piippo, D. Inzé, E. T. Palva, and J. Kangasjärvi. Arabidopsis RADICAL-INDUCED CELL DEATH1 belongs to the WWE protein–protein interaction domain protein family and modulates abscisic acid, ethylene, and methyl jasmonate responses. *The Plant Cell*, 16(7):1925–1937, 2004.

N. Akçay, M. Bor, T. Karabudak, F. Özdemir, and İ. Türkan. Contribution of gamma amino butyric acid (GABA) to salt stress responses of nicotiana sylvestris CMSII mutant and wild type plants. *Journal of Plant Physiology*, 169(5):452–458, 2012.

N. Al-Quraan and H. Al-Omari. GABA accumulation and oxidative damage responses to salt, osmotic and $H_2O_2$ treatments in two lentil (*Lens culinaris* Medik) accessions. *Plant Biosystems - An International Journal Dealing with all Aspects of Plant Biology*, 151(1):148–157, 2017.

W. Allan, C. Peiris, A. Bown, and B. Shelp. Gamma-hydroxybutyrate accumulates in green tea and soybean sprouts in response to oxygen deficiency. *Canadian Journal of Plant Science*, 83(4):951–953, 2003.

W. L. Allan, J. P. Simpson, S. M. Clark, and B. J. Shelp. $\gamma$-hydroxybutyrate accumulation in arabidopsis and tobacco plants is a general response to abiotic stress: putative regulation by redox balance and glyoxylate reductase isoforms. *Journal of Experimental Botany*, 59(9):2555–2564, 2008.

W. L. Allan, K. E. Breitkreuz, J. C. Waller, J. P. Simpson, G. J. Hoover, A. Rochon, D. J. Wolyn, D. Rentsch, W. A. Snedden, and B. J. Shelp. Detoxification of succinate semialdehyde in arabidopsis glyoxylate reductase and NAD kinase mutants subjected to submergence stress. *Botany*, 90(1):51–61, 2012.

D. K. Allen and J. D. Young. Tracing metabolic flux through time and space with isotope labeling experiments. *Current Opinion in Biotechnology*, 64:92–100, 2020.

J. B. Alpuerto, R. M. F. Hussain, and T. Fukao. The key regulator of submergence tolerance, *SUB1A*, promotes photosynthetic and metabolic recovery from submergence damage in rice leaves. *Plant, Cell & Environment*, 39(3):672–684, 2015.

I. Amin, S. Rasool, M. A. Mir, W. Wani, K. Z. Masoodi, and P. Ahmad. Ion homeostasis for salinity tolerance in plants: a molecular approach. *Physiologia Plantarum*, 171(4): 578–594, 2020.

A. D. Angeli, J. Zhang, S. Meyer, and E. Martinoia. AtALMT9 is a malate-activated vacuolar chloride channel required for stomatal opening in Arabidopsis. *Nature Communications*, 4(1):1–10, 2013.

M. Ansari, , S. Hasan, S. U. Jalil, and and. Leaf senescence and GABA shunt. *Bioinformation*, 10(12):734–736, 2014.

M. P. Apse, G. S. Aharon, W. A. Snedden, and E. Blumwald. Salt tolerance conferred by overexpression of a vacuolar $Na^+/H^+$ antiport in *Arabidopsis*. *Science*, 285(5431): 1256–1258, 1999.

N. W. Arnell, S. Brown, S. N. Gosling, P. Gottschalk, J. Hinkel, C. Huntingford, B. Lloyd-Hughes, J. A. Lowe, R. J. Nicholls, T. J. Osborn, T. M. Osborne, G. A. Rose, P. Smith, T. R. Wheeler, and P. Zelazowski. The impacts of climate change across the globe: A multi-sectoral assessment. *Climatic Change*, 134(3):457–474, 2016.

B. Arsova, U. Hoja, M. Wimmelbacher, E. Greiner, Ş. Üstün, M. Melzer, K. Petersen, W. Lein, and F. Börnke. Plastidial thioredoxin z interacts with two fructokinase-like proteins in a thiol-dependent manner: Evidence for an essential role in chloroplast development in *Arabidopsis* and *Nicotiana benthamiana*. *The Plant Cell*, 22(5):1498–1515, 2010.

K. B. Axelsen and M. G. Palmgren. Inventory of the superfamily of P-type ion pumps in Arabidopsis. *Plant Physiology*, 126(2):696–706, 2001.

J. Bailey-Serres and L. Voesenek. Flooding stress: acclimations and genetic diversity. *Annual Review of Plant Biology*, 59:313–339, 2008.

J. Bailey-Serres and L. A. Voesenek. Life in the balance: a signaling network controlling survival of flooding. *Current opinion in plant biology*, 13(5):489–494, 2010.

J. Bailey-Serres, T. Fukao, D. J. Gibbs, M. J. Holdsworth, S. C. Lee, F. Licausi, P. Perata, L. A. Voesenek, and J. T. van Dongen. Making sense of low oxygen sensing. *Trends in Plant Science*, 17(3):129–138, 2012.

D. Balfagón, A. Gómez-Cadenas, J. L. Rambla, A. Granell, C. de Ollas, D. C. Bassham, R. Mittler, and S. I. Zandalinas. $\gamma$-aminobutyric acid plays a key role in plant acclimation to a combination of high light and heat stress. *Plant Physiology*, 188(4):2026–2038, 2022.

C. Balzergue, T. Dartevelle, C. Godon, E. Laugier, C. Meisrimler, J.-M. Teulon, A. Creff, M. Bissler, C. Brouchoud, A. Hagège, J. Müller, S. Chiarenza, H. Javot, N. Becuwe-Linka, P. David, B. Péret, E. Delannoy, M.-C. Thibaud, J. Armengaud, S. Abel, J.-L. Pellequer, L. Nussaume, and T. Desnos. Low phosphate activates STOP1-ALMT1 to rapidly inhibit root cell elongation. *Nature Communications*, 8(1):1–16, 2017.

V. Banti, F. Mafessoni, E. Loreti, A. Alpi, and P. Perata. The heat-inducible transcription factor *HsfA2* enhances anoxia tolerance in Arabidopsis. *Plant Physiology*, 152(3): 1471–1483, 2010.

H. Bao, X. Chen, S. Lv, P. Jiang, J. Feng, P. Fan, L. Nie, and Y. Li. Virus-induced gene silencing reveals control of reactive oxygen species accumulation and salt tolerance in tomato by $\gamma$-aminobutyric acid metabolic pathway. *Plant, cell & environment*, 38(3): 600–613, 2015.

J. M. Barbosa, N. K. Singh, J. H. Cherry, and R. D. Locy. Nitrate uptake and utilization is modulated by exogenous $\gamma$-aminobutyric acid in *Arabidopsis thaliana* seedlings. *Plant Physiology and Biochemistry*, 48(6):443–450, 2010.

J. Barceló and C. Poschenrieder. Fast root growth responses, root exudates, and internal detoxification as clues to the mechanisms of aluminium toxicity and resistance: a review. *Environmental and Experimental Botany*, 48(1):75–92, 2002.

A. Batushansky, M. Kirma, N. Grillich, P. A. Pham, D. Rentsch, G. Galili, A. R. Fernie, and A. Fait. The transporter GAT1 plays an important role in GABA-mediated carbon-nitrogen interactions in *Arabidopsis*. *Frontiers in Plant Science*, 6, 2015.

S. Baud, M.-N. Vaultier, and C. Rochat. Structure and expression profile of the sucrose synthase multigene family in *Arabidopsis*. *Journal of Experimental Botany*, 55(396): 397–409, 2004.

Z. G. Beamer, P. Routray, W.-G. Choi, M. K. Spangler, A. Lokdarshi, and D. M. Roberts. Aquaporin family lactic acid channel NIP2;1 promotes plant survival under low oxygen stress in *Arabidopsis*. *Plant Physiology*, 187(4):2262–2278, 2021.

N. Beuve, N. Rispail, P. Lainé, J.-B. Cliquet, A. Ourry, and E. Le Deunff. Putative role of $\gamma$-aminobutyric acid (GABA) as a long-distance signal in up-regulation of nitrate uptake in *Brassica napus* L. *Plant, Cell & Environment*, 27(8):1035–1046, 2004.

Y. Biniaz, A. Tahmasebi, A. Afsharifar, A. Tahmasebi, and P. Poczai. Meta-analysis of common and differential transcriptomic responses to biotic and abiotic stresses in *Arabidopsis thaliana*. *Plants*, 11(4):502, 2022.

M. S. Biswas, H. Fukaki, I. C. Mori, K. Nakahara, and J. Mano. Reactive oxygen species and reactive carbonyl species constitute a feed-forward loop in auxin signaling for lateral root formation. *The Plant Journal*, 100(3):536–548, 2019.

F. Bloom and L. Iversen. Localizing 3H-GABA in nerve terminals of rat cerebral cortex by electron microscopic autoradiography. *Nature*, 229(5287):628–630, 1971.

A. M. Bolger, M. Lohse, and B. Usadel. Trimmomatic: a flexible trimmer for Illumina sequence data. *Bioinformatics*, 30(15):2114–2120, 2014.

O. Borsani, J. Zhu, P. E. Verslues, R. Sunkar, and J.-K. Zhu. Endogenous siRNAs derived from a pair of natural cis-antisense transcripts regulate salt tolerance in *Arabidopsis*. *Cell*, 123(7):1279–1291, 2005.

N. Bouché and H. Fromm. GABA in plants: just a metabolite? *Trends in plant science*, 9 (3):110–115, 2004.

N. Bouché, A. Fait, D. Bouchez, S. G. Møller, and H. Fromm. Mitochondrial succinic-semialdehyde dehydrogenase of the $\gamma$-aminobutyrate shunt is required to restrict levels of reactive oxygen intermediates in plants. *Proceedings of the National Academy of Sciences*, 100(11):6843–6848, 2003.

N. Bouché, A. Fait, M. Zik, and H. Fromm. The root-specific glutamate decarboxylase (GAD1) is essential for sustaining GABA levels in *Arabidopsis*. *Plant Molecular Biology*, 55(3):315–325, 2004.

A. W. Bown, K. B. MacGregor, and B. J. Shelp. Gamma-aminobutyrate: defense against invertebrate pests? *Trends in Plant Science*, 11(9):424–427, 2006.

C. Branco-Price, K. A. Kaiser, C. J. Jang, C. K. Larive, and J. Bailey-Serres. Selective mRNA translation coordinates energetic and metabolic adjustments to cellular oxygen deprivation and reoxygenation in *Arabidopsis thaliana*. *The Plant Journal*, 56(5):743–755, 2008.

K. E. Breitkreuz, W. L. Allan, O. R. Van Cauwenberghe, C. Jakobs, D. Talibi, B. André, and B. J. Shelp. A novel $\gamma$-hydroxybutyrate dehydrogenase identification and expression of an *Arabidopsis* cDNA and potential role under oxygen deficiency. *Journal of Biological Chemistry*, 278(42):41552–41556, 2003.

V. Buchanan-Wollaston, T. Page, E. Harrison, E. Breeze, P. O. Lim, H. G. Nam, J.-F. Lin, S.-H. Wu, J. Swidzinski, K. Ishizaki, and C. J. Leaver. Comparative transcriptome

analysis reveals significant differences in gene expression and signalling pathways between developmental and dark/starvation-induced senescence in Arabidopsis. *The Plant Journal*, 42(4):567–585, 2005.

W. F. Campos, K. Dressano, P. H. Ceciliato, J. C. Guerrero-Abad, A. L. Silva, C. S. Fiori, A. M. do Canto, T. Bergonci, L. A. Claus, M. C. Silva-Filho, and D. S. Moura. *Arabidopsis thaliana* rapid alkalinization factor 1-mediated root growth inhibition is dependent on calmodulin-like protein 38. *Journal of Biological Chemistry*, 293(6): 2159–2171, 2018.

J. Cao, Y. Liang, T. Yan, X. Wang, H. Zhou, C. Chen, Y. Zhang, B. Zhang, S. Zhang, J. Liao, S. Cheng, J. Chu, X. Huang, D. Xu, J. Li, X. W. Deng, and F. Lin. The photomorphogenic repressors BBX28 and BBX29 integrate light and brassinosteroid signaling to inhibit seedling development in Arabidopsis. *The Plant Cell*, 34(6):2266–2285, 2022.

P. Carillo. GABA Shunt in Durum Wheat. *Frontiers in Plant Science*, 9, 2018.

M. Carlson. *GO.db: A set of annotation maps describing the entire Gene Ontology*, 2021.

F. Ö. Çekiç. Exogenous GABA stimulates endogenous GABA and phenolic acid contents in tomato plants under salt stress. *Celal Bayar University Journal of Science*, 14(1): 61–64, 2018.

C. Chaffei, K. Pageau, A. Suzuki, H. Gouia, M. H. Ghorbel, and C. Masclaux-Daubresse. Cadmium toxicity induced changes in nitrogen management in lycopersicon esculentum leading to a metabolic safeguard through an amino acid storage strategy. *Plant and cell physiology*, 45(11):1681–1693, 2004.

R. Chang, C. J. H. Jang, C. Branco-Price, P. Nghiem, and J. Bailey-Serres. Transient MPK6 activation in response to oxygen deprivation and reoxygenation is mediated by mitochondria and aids seedling survival in *Arabidopsis*. *Plant Molecular Biology*, 78(1): 109–122, 2011.

M. H. Che-Othman, R. P. Jacoby, A. H. Millar, and N. L. Taylor. Wheat mitochondrial respiration shifts from the tricarboxylic acid cycle to the GABA shunt under salt stress. *New Phytologist*, 225(3):1166–1180, 2020.

F. Chen, X. Shi, L. Chen, M. Dai, Z. Zhou, Y. Shen, J. Li, G. Li, N. Wei, and X. W. Deng. Phosphorylation of FAR-RED ELONGATED HYPOCOTYL1 is a key mechanism defining signaling dynamics of phytochrome a under red and far-red light in *Arabidopsis*. *The Plant Cell*, 24(5):1907–1920, 2012.

Y. Chen, A. T. Lun, and G. K. Smyth. From reads to genes to pathways: differential expression analysis of RNA-Seq experiments using Rsubread and the edgeR quasi-likelihood pipeline. *F1000Research*, 5, 2016.

S. M. Clark, R. D. Leo, P. K. Dhanoa, O. R. V. Cauwenberghe, R. T. Mullen, and B. J. Shelp. Biochemical characterization, mitochondrial localization, expression, and potential functions for an *Arabidopsis* $\gamma$-aminobutyrate transaminase that utilizes both pyruvate and glyoxylate. *Journal of Experimental Botany*, 60(6):1743–1757, 2009.

C. Coenen and T. L. Lomax. Auxin—cytokinin interactions in higher plants: old problems and new tools. *Trends in plant science*, 2(9):351–356, 1997.

S. J. Conn, B. Hocking, M. Dayod, B. Xu, A. Athman, S. Henderson, L. Aukett, V. Conn, M. K. Shearer, S. Fuentes, et al. Protocol: optimising hydroponic growth systems for nutritional and physiological analysis of arabidopsis thaliana and other plants. *Plant methods*, 9(1):1–11, 2013.

J. R. Conway, A. Lex, and N. Gehlenborg. UpSetR: an R package for the visualization of intersecting sets and their properties. *Bioinformatics*, 2017.

A. Costa, L. Luoni, C. A. Marrano, K. Hashimoto, P. Köster, S. Giacometti, M. I. D. Michelis, J. Kudla, and M. C. Bonza. $Ca^{2+}$-dependent phosphoregulation of the plasma membrane $Ca^{2+}$-ATPase ACA8 modulates stimulus-induced calcium signatures. *Journal of Experimental Botany*, 68(12):3215–3230, 2017.

S. de Bianchi, N. Betterle, R. Kouril, S. Cazzaniga, E. Boekema, R. Bassi, and L. Dall'Osto. *Arabidopsis* mutants deleted in the light-harvesting protein Lhcb4 have a disrupted photosystem II macrostructure and are defective in photoprotection. *The Plant Cell*, 23 (7):2659–2679, 2011.

R. de Marchi, M. Sorel, B. Mooney, I. Fudal, K. Goslin, K. Kwaśniewska, P. T. Ryan, M. Pfalz, J. Kroymann, S. Pollmann, A. Feechan, F. Wellmer, S. Rivas, and E. Graciet. The N-end rule pathway regulates pathogen responses in plants. *Scientific Reports*, 6 (1):1–15, 2016.

U. Deinlein, A. B. Stephan, T. Horie, W. Luo, G. Xu, and J. I. Schroeder. Plant salt-tolerance mechanisms. *Trends in plant science*, 19(6):371–379, 2014.

A. J. Delauney and D. P. S. Verma. Proline biosynthesis and osmoregulation in plants. *The plant journal*, 4(2):215–223, 1993.

E. Delhaize, P. R. Ryan, D. M. Hebb, Y. Yamamoto, T. Sasaki, and H. Matsumoto. Engineering high-level aluminum tolerance in barley with the *ALMT1* gene. *Proceedings of the National Academy of Sciences*, 101(42):15249–15254, 2004.

C. Dent, W. Stepka, and F. Steward. Detection of the free amino-acids of plant cells by partition chromatography. *Nature*, 160(4072):682–683, 1947.

H. Diab and A. Limami. Reconfiguration of N metabolism upon hypoxia stress and recovery: Roles of alanine aminotransferase (AlaAT) and glutamate dehydrogenase (GDH). *Plants*, 5(2):25, 2016.

Z. J. Ding, J. Y. Yan, X. Y. Xu, G. X. Li, and S. J. Zheng. WRKY46 functions as a transcriptional repressor of ALMT1, regulating aluminum-induced malate secretion in Arabidopsis. *The Plant Journal*, 76(5):825–835, 2013.

Z. J. Ding, J. Y. Yan, C. X. Li, G. X. Li, Y. R. Wu, and S. J. Zheng. Transcription factor WRKY46 modulates the development of Arabidopsis lateral roots in osmotic/salt stress conditions via regulation of ABA signaling and auxin homeostasis. *The Plant Journal*, 84(1):56–69, 2015.

A. Dobin, C. A. Davis, F. Schlesinger, J. Drenkow, C. Zaleski, S. Jha, P. Batut, M. Chaisson, and T. R. Gingeras. STAR: ultrafast universal RNA-seq aligner. *Bioinformatics*, 29(1): 15–21, 2012.

I. Dreyer, J. L. Gomez-Porras, D. M. Riaño-Pachón, R. Hedrich, and D. Geiger. Molecular evolution of slow and quick anion channels (SLACs and QUACs/ALMTs). *Frontiers in Plant Science*, 3:263, 2012.

Z. Duren, Y. Wang, J. Wang, X.-M. Zhao, L. Lv, X. Li, J. Liu, X.-G. Zhu, L. Chen, and Y. Wang. Hierarchical graphical model reveals HFR1 bridging circadian rhythm and flower development in *Arabidopsis thaliana*. *NPJ systems biology and applications*, 5(1): 1–11, 2019.

S. Durinck, P. T. Spellman, E. Birney, and W. Huber. Mapping identifiers for the integration of genomic datasets with the R/Bioconductor package biomart. *Nature protocols*, 4(8):1184, 2009.

C. Eisenach, U. Baetz, N. V. Huck, J. Zhang, A. D. Angeli, G. J. Beckers, and E. Martinoia. ABA-induced stomatal closure involves ALMT4, a phosphorylation-dependent vacuolar anion channel of Arabidopsis. *The Plant Cell*, 29(10):2552–2569, 2017.

T. Enomoto, M. Tokizawa, H. Ito, S. Iuchi, M. Kobayashi, Y. Y. Yamamoto, Y. Kobayashi, and H. Koyama. STOP1 regulates the expression of *HsfA2* and *GDH*s that are critical for low-oxygen tolerance in Arabidopsis. *Journal of experimental botany*, 70(12):3297–3311, 2019.

A. Fait, A. Yellin, and H. Fromm. GABA shunt deficiencies and accumulation of reactive oxygen intermediates: insight from *Arabidopsis* mutants. *FEBS letters*, 579(2):415–420, 2005.

X. Feng. GABA regulation of stomatal function in *Arabidopsis thaliana*. *PhD thesis, University of Adelaide*, 2021.

S. Ferreira, E. Moreira, I. Amorim, C. Santos, and P. Melo. *Arabidopsis thaliana* mutants devoid of chloroplast glutamine synthetase (GS2) have non-lethal phenotype under photorespiratory conditions. *Plant Physiology and Biochemistry*, 144:365–374, 2019.

S. Field, W. C. Conner, and D. M. Roberts. *Arabidopsis* CALMODULIN-LIKE 38 regulates hypoxia-induced autophagy of SUPPRESSOR OF GENE SILENCING 3 bodies. *Frontiers in Plant Science*, 12:1872, 2021.

J. Flexas, J. Bota, F. Loreto, G. Cornic, and T. Sharkey. Diffusive and metabolic limitations to photosynthesis under drought and salinity in C3 plants. *Plant biology*, 6(03):269–279, 2004.

J.-X. Fontaine, T. Tercé-Laforgue, P. Armengaud, G. Clément, J.-P. Renou, S. Pelletier, M. Catterou, M. Azzopardi, Y. Gibon, P. J. Lea, B. Hirel, and F. Dubois. Characterization of a NADH-dependent glutamate dehydrogenase mutant of *Arabidopsis* demonstrates the key role of this enzyme in root carbon and nitrogen metabolism. *The Plant Cell*, 24(10):4044–4065, 2012.

E. Foo, J. J. Ross, N. W. Davies, J. B. Reid, and J. L. Weller. A role for ethylene in the phytochrome-mediated control of vegetative development. *The Plant Journal*, 46(6): 911–921, 2006.

B. G. Forde and P. J. Lea. Glutamate in plants: metabolism, regulation, and signalling. *Journal of Experimental Botany*, 58(9):2339–2358, 2007.

S. R. Fuhs and T. Hunter. pHisphorylation: the emergence of histidine phosphorylation as a reversible regulatory modification. *Current Opinion in Cell Biology*, 45:8–16, 2017.

T. Fukao and J. Bailey-Serres. Plant responses to hypoxia - is survival a balancing act? *Trends in Plant Science*, 9(9):449–456, 2004.

T. Fukao, B. E. Barrera-Figueroa, P. Juntawong, and J. M. Peña-Castro. Submergence and waterlogging stress in plants: A review highlighting research opportunities and understudied aspects. *Frontiers in Plant Science*, 10:340, 2019.

D. Funck, B. Stadelhofer, and W. Koch. Ornithine-$\delta$-aminotransferase is essential for arginine catabolism but not for proline biosynthesis. *BMC Plant Biology*, 8(1):40, 2008.

G. Garg, K. Prachi, and S. Bhati. Aluminum-activated malate transporter protein (ALMT):"Prime GABA receptor" in plants under abiotic stress: A review. *Octa Journal of Biosciences*, 5(2), 2017.

R. Gentleman. *annotate: Annotation for microarrays*, 2021.

D. J. Gibbs, S. C. Lee, N. M. Isa, S. Gramuglia, T. Fukao, G. W. Bassel, C. S. Correia, F. Corbineau, F. L. Theodoulou, J. Bailey-Serres, and M. J. Holdsworth. Homeostatic response to hypoxia is regulated by the N-end rule pathway in plants. *Nature*, 479(7373): 415–418, 2011.

D. J. Gibbs, J. V. Conde, S. Berckhan, G. Prasad, G. M. Mendiondo, and M. J. Holdsworth. Group VII ethylene response factors coordinate oxygen and nitric oxide signal transduction and stress responses in plants. *Plant Physiology*, 169(1):23–31, 2015.

J. Gibbs and H. Greenway. Mechanisms of anoxia tolerance in plants. I. Growth, survival and anaerobic catabolism. *Functional Plant Biology*, 30(1):1–47, 2003.

M. Gilliham and M. Hrmova. Alluminating structure key to stress tolerance. *Cell Research*, 32(1):5–6, 2021.

M. Gilliham and S. D. Tyerman. Linking metabolism to membrane signaling: The GABA–malate connection. *Trends in Plant Science*, 21(4):295–301, 2016.

B. Giuntoli, S. C. Lee, F. Licausi, M. Kosmacz, T. Oosumi, J. T. van Dongen, J. Bailey-Serres, and P. Perata. A trihelix DNA binding protein counterbalances hypoxia-responsive transcriptional activation in Arabidopsis. *PLOS Biology*, 12(9):e1001950, 2014.

W. González, J. Riedelsberger, S. E. Morales-Navarro, J. Caballero, J. H. Alzate-Morales, F. D. González-Nilo, and I. Dreyer. The pH sensor of the plant $k^+$-uptake channel KAT1 is built from a sensory cloud rather than from single key amino acids. *Biochemical Journal*, 442(1):57–63, 2012.

S. Gonzali, E. Loreti, C. Solfanelli, G. Novi, A. Alpi, and P. Perata. Identification of sugar-modulated genes and evidence for in vivo sugar sensing in *Arabidopsis*. *Journal of plant research*, 119(2):115–123, 2006.

B. D. Gruber, E. Delhaize, A. E. Richardson, U. Roessner, R. A. James, S. M. Howitt, and P. R. Ryan. Characterisation of HvALMT1 function in transgenic barley plants. *Functional Plant Biology*, 38(2):163, 2011.

T. Hachiya, J. Inaba, M. Wakazaki, M. Sato, K. Toyooka, A. Miyagi, M. Kawai-Yamada, D. Sugiura, T. Nakagawa, T. Kiba, A. Gojon, and H. Sakakibara. Excessive ammonium assimilation by plastidic glutamine synthetase causes ammonium toxicity in *Arabidopsis thaliana*. *Nature Communications*, 12(1):1–10, 2021.

T.-h. Ham, S.-h. Chu, S.-J. Han, and S.-N. Ryu. $\gamma$-aminobutyric acid metabolism in plant under environment stressses. *Korean Journal of Crop Science*, 57(2):144–150, 2012.

C. Hanfrey, S. Sommer, M. J. Mayer, D. Burtin, and A. J. Michael. *Arabidopsis* polyamine biosynthesis: absence of ornithine decarboxylase and the mechanism of arginine decarboxylase activity. *The Plant Journal*, 27(6):551–560, 2001.

S. Hartman, Z. Liu, H. van Veen, J. Vicente, E. Reinen, S. Martopawiro, H. Zhang, N. van Dongen, F. Bosman, G. W. Bassel, E. J. W. Visser, J. Bailey-Serres, F. L. Theodoulou, K. H. Hebelstrup, D. J. Gibbs, M. J. Holdsworth, R. Sasidharan, and L. A. C. J. Voesenek. Ethylene-mediated nitric oxide depletion pre-adapts plants to hypoxia stress. *Nature Communications*, 10(1):1–9, 2019.

H. Hediji, W. Djebali, C. Cabasson, M. Maucourt, P. Baldet, A. Bertrand, L. B. Zoghlami, C. Deborde, A. Moing, R. Brouquisse, et al. Effects of long-term cadmium exposure on growth and metabolomic profile of tomato plants. *Ecotoxicology and environmental safety*, 73(8):1965–1974, 2010.

F. Hijaz and N. Killiny. Exogenous GABA is quickly metabolized to succinic acid and fed into the plant TCA cycle. *Plant Signaling & Behavior*, 14(3):e1573096, 2019.

F. Hijaz, Y. Nehela, and N. Killiny. Application of gamma-aminobutyric acid increased the level of phytohormones in *Citrus sinensis*. *Planta*, 248(4):909–918, 2018.

B. Hirel and P. J. Lea. The biochemistry, molecular biology, and genetic manipulation of primary ammonia assimilation. In *Advances in Photosynthesis and Respiration*, pages 71–92. Springer, 2002.

M. Hodges. Enzyme redundancy and the importance of 2-oxoglutarate in plant ammonium assimilation. *Journal of Experimental Botany*, 53(370):905–916, 2002.

G. J. Hoover, O. R. Van Cauwenberghe, K. E. Breitkreuz, S. M. Clark, A. R. Merrill, and B. J. Shelp. Characteristics of an *Arabidopsis* glyoxylate reductase: general biochemical properties and substrate specificity for the recombinant protein, and developmental expression and implications for glyoxylate and succinic semialdehyde metabolism in planta. *Botany*, 85(9):883–895, 2007.

H. Hõrak, M. Sierla, K. Tõldsepp, C. Wang, Y.-S. Wang, M. Nuhkat, E. Valk, P. Pechter, E. Merilo, J. Salojärvi, K. Overmyer, M. Loog, M. Brosché, J. I. Schroeder, J. Kangasjärvi, and H. Kollist. A dominant mutation in the HT1 kinase uncovers roles of MAP kinases and GHR1 in $CO_2$-induced stomatal closure. *The Plant Cell*, 28(10):2493–2509, 2016.

Z.-h. HOU, G.-h. LIU, L.-x. HOU, L.-x. WANG, and L. Xin. Regulatory function of polyamine oxidase-generated hydrogen peroxide in ethylene-induced stomatal closure in *Arabidopsis thaliana*. *Journal of Integrative Agriculture*, 12(2):251–262, 2013.

Y. Y. Hsiao, R. C. Van, S. H. Hung, H. H. Lin, and R. L. Pan. Roles of histidine residues in plant vacuolar $H^+$-pyrophosphatase. *Biochimica et Biophysica Acta (BBA) - Bioenergetics*, 1608(2-3):190–199, 2004.

X. Hu, Z. Xu, W. Xu, J. Li, N. Zhao, and Y. Zhou. Application of $\gamma$-aminobutyric acid demonstrates a protective role of polyamine and GABA metabolism in muskmelon seedlings under $Ca(NO_3)_2$ stress. *Plant Physiology and Biochemistry*, 92:1–10, 2015.

C. Huang, Q. B. Yu, X. B. Yuan, Z. R. Li, J. Wang, L. S. Ye, L. Xu, and Z.-N. Yang. Rubisco accumulation is important for the greening of the *fln2-4* mutant in *Arabidopsis*. *Plant Science*, 236:185–194, 2015.

S. Huang, T. D. Colmer, and A. H. Millar. Does anoxia tolerance involve altering the energy currency towards PPi? *Trends in plant science*, 13(5):221–227, 2008.

K. ichiro Shimazaki, M. Doi, S. M. Assmann, and T. Kinoshita. Light regulation of stomatal movement. *Annual Review of Plant Biology*, 58(1):219–247, 2007.

A. U. Igamberdiev and A. T. Eprintsev. Organic acids: The pools of fixed carbon involved in redox regulation and energy balance in higher plants. *Frontiers in Plant Science*, 7: 1042, 2016.

A. U. Igamberdiev, C. Stasolla, and R. D. Hill. Low oxygen stress, nonsymbiotic hemoglobins, NO, and programmed cell death. In *Low-Oxygen Stress in Plants*, pages 41–58. Springer, 2014.

M. Ikeda, N. Mitsuda, T. Ishizuka, M. Satoh, and M. Ohme-Takagi. The CIB1 transcription factor regulates light-and heat-inducible cell elongation via a two-step HLH/bHLH system. *Journal of Experimental Botany*, 72(5):1795–1808, 2021.

K. P. Ismond, R. Dolferus, M. D. Pauw, E. S. Dennis, and A. G. Good. Enhanced low oxygen survival in Arabidopsis through increased metabolic flux in the fermentative pathway. *Plant Physiology*, 132(3):1292–1302, 2003.

S. Iuchi, H. Koyama, A. Iuchi, Y. Kobayashi, S. Kitabayashi, Y. Kobayashi, T. Ikka, T. Hirayama, K. Shinozaki, and M. Kobayashi. Zinc finger protein STOP1 is critical for proton tolerance in Arabidopsis and coregulates a key gene in aluminum tolerance. *Proceedings of the National Academy of Sciences*, 104(23):9900–9905, 2007.

S. U. Jalil, I. Ahmad, and M. I. Ansari. Functional loss of GABA transaminase (GABA-T) expressed early leaf senescence under various stress conditions in *Arabidopsis thaliana*. *Current Plant Biology*, 9-10:11–22, 2017.

S. Jansson. A guide to the *Lhc* genes and their relatives in *Arabidopsis*. *Trends in Plant Science*, 4(6):236–240, 1999.

J. Jaślan and A. De Angeli. Heterologous expression reveals that GABA does not directly inhibit the vacuolar anion channel *At*ALMT9. *Plant Physiology*, 189(2):469–472, 2022.

X. Jin, T. Liu, J. Xu, Z. Gao, and X. Hu. Exogenous GABA enhances muskmelon tolerance to salinity-alkalinity stress by regulating redox balance and chlorophyll biosynthesis. *BMC Plant Biology*, 19(1):1–15, 2019.

M. M. Julkowska, K. Klei, L. Fokkens, M. A. Haring, M. E. Schranz, and C. Testerink. Natural variation in rosette size under salt stress conditions corresponds to developmental differences between arabidopsis accessions and allelic variation in the *LRR-KISS* gene. *Journal of Experimental Botany*, 67(8):2127–2138, 2016.

M. S. Kalhor, S. Aliniaeifard, M. Seif, E. J. Asayesh, F. Bernard, B. Hassani, and T. Li. Enhanced salt tolerance and photosynthetic performance: Implication of $\gamma$-amino butyric acid application in salt-exposed lettuce (*Lactuca sativa* L.) plants. *Plant Physiology and Biochemistry*, 130:157–172, 2018.

T. Katori, A. Ikeda, S. Iuchi, M. Kobayashi, K. Shinozaki, K. Maehashi, Y. Sakata, S. Tanaka, and T. Taji. Dissecting the genetic control of natural variation in salt tolerance of *Arabidopsis thaliana* accessions. *Journal of Experimental Botany*, 61(4): 1125–1138, 2010.

F. Kellermeier, P. Armengaud, T. J. Seditas, J. Danku, D. E. Salt, and A. Amtmann. Analysis of the root system architecture of *Arabidopsis* provides a quantitative readout of crosstalk between nutritional signals. *The Plant Cell*, 26(4):1480–1496, 2014.

H. S. Kim, W. Park, H. S. Lee, J. H. Shin, and S. J. Ahn. Subcellular journey of rare cold inducible 2 protein in plant under stressful condition. *Frontiers in Plant Science*, 11: 610251, 2021.

J. H. Kim, N. H. Nguyen, C. Y. Jeong, N. T. Nguyen, S.-W. Hong, and H. Lee. Loss of the r2r3 MYB, AtMyb73, causes hyper-induction of the SOS1 and SOS3 genes in response to high salinity in arabidopsis. *Journal of Plant Physiology*, 170(16):1461–1465, 2013.

H.-H. Kirch, D. Bartels, Y. Wei, P. S. Schnable, and A. J. Wood. The ALDH gene superfamily of *Arabidopsis*. *Trends in Plant Science*, 9(8):371–377, 2004.

M. Klecker, P. Gasch, H. Peisker, P. Dörmann, H. Schlicke, B. Grimm, and A. Mustroph. A shoot-specific hypoxic response of Arabidopsis sheds light on the role of the phosphate-responsive transcription factor PHOSPHATE STARVATION RESPONSE1. *Plant Physiology*, 165(2):774–790, 2014.

Y. Kobayashi, V. Lakshmanan, Y. Kobayashi, M. Asai, S. Iuchi, M. Kobayashi, H. P. Bais, and H. Koyama. Overexpression of *AtALMT1* in the *Arabidopsis thaliana* ecotype

columbia results in enhanced Al-activated malate excretion and beneficial bacterium recruitment. *Plant Signaling & Behavior*, 8(9):e25565, 2013.

Y. Kobayashi, Y. Ohyama, Y. Kobayashi, H. Ito, S. Iuchi, M. Fujita, C.-R. Zhao, T. Tanveer, M. Ganesan, M. Kobayashi, et al. STOP2 activates transcription of several genes for Al-and low pH-tolerance that are regulated by STOP1 in *Arabidopsis*. *Molecular Plant*, 7(2):311–322, 2014.

L. V. Kochian. Cellular mechanisms of aluminum toxicity and resistance in plants. *Annual review of plant biology*, 46(1):237–260, 1995.

R. Kolde. pheatmap: Pretty Heatmaps. *R package version 1.0. 12*, 2019.

J. Köster and S. Rahmann. Snakemake – a scalable bioinformatics workflow engine. *Bioinformatics*, 28(19):2520–2522, 2012.

P. Köster, L. Wallrad, K. H. Edel, M. Faisal, A. A. Alatar, and J. Kudla. The battle of two ions: $Ca^{2+}$ signalling against $Na^{+}$ stress. *Plant Biology*, 21(S1):39–48, 2018.

H. Kovács, D. Aleksza, A. I. Baba, A. Hajdu, A. M. Király, L. Zsigmond, S. Z. Tóth, L. Kozma-Bognár, and L. Szabados. Light control of salt-induced proline accumulation is mediated by ELONGATED HYPOCOTYL 5 in *Arabidopsis*. *Frontiers in Plant Science*, 10:1584, 2019.

J. Krasensky and C. Jonak. Drought, salt, and temperature stress-induced metabolic rearrangements and regulatory networks. *Journal of Experimental Botany*, 63(4):1593–1608, 2012.

T. Kretzschmar, M. A. F. Pelayo, K. R. Trijatmiko, L. F. M. Gabunada, R. Alam, R. Jimenez, M. S. Mendioro, I. H. Slamet-Loedin, N. Sreenivasulu, J. Bailey-Serres, A. M. Ismail, D. J. Mackill, and E. M. Septiningsih. A trehalose-6-phosphate phosphatase enhances anaerobic germination tolerance in rice. *Nature Plants*, 1(9):1–5, 2015.

O. Kürsteiner, I. Dupuis, and C. Kuhlemeier. The *Pyruvate decarboxylase1* gene of Arabidopsis is required during anoxia but not other environmental stresses. *Plant Physiology*, 132(2):968–978, 2003.

J. M. Kwak, I. C. Mori, Z.-M. Pei, N. Leonhardt, M. A. Torres, J. L. Dangl, R. E. Bloom, S. Bodde, J. D. Jones, and J. I. Schroeder. NADPH oxidase *AtrbohD* and *AtrbohF* genes function in ROS-dependent ABA signaling in Arabidopsis. *The EMBO journal*, 22(11):2623–2633, 2003.

M. Lancien and M. R. Roberts. Regulation of *Arabidopsis thaliana* 14-3-3 gene expression by $\gamma$-aminobutyric acid. *Plant, cell & environment*, 29(7):1430–1436, 2006.

D. S. Latchman. Transcription factors: an overview. *The international journal of biochemistry & cell biology*, 29(12):1305–1312, 1997.

J. S. Lee, S. Wang, S. Sritubtim, J.-G. Chen, and B. E. Ellis. Arabidopsis mitogen-activated protein kinase MPK12 interacts with the MAPK phosphatase IBR5 and regulates auxin signaling. *The Plant Journal*, 57(6):975–985, 2009.

T. A. Lee and J. Bailey-Serres. Integrative analysis from the epigenome to translatome uncovers patterns of dominant nuclear regulation during transient stress. *The Plant Cell*, 31(11):2573–2595, 2019.

T. A. Lee and J. Bailey-Serres. Conserved and nuanced hierarchy of gene regulatory response to hypoxia. *New Phytologist*, 229(1):71–78, 2020.

J. Lehmann, M. E. Jørgensen, S. Fratz, H. M. Müller, J. Kusch, S. Scherzer, C. Navarro-Retamal, D. Mayer, J. Böhm, K. R. Konrad, U. Terpitz, I. Dreyer, T. D. Mueller, M. Sauer, R. Hedrich, D. Geiger, and T. Maierhofer. Acidosis-induced activation of anion channel SLAH3 in the flooding-related stress response of *Arabidopsis*. *Current Biology*, 31(16):3575–3585, 2021.

D. Leister. Photosynthesis: Complex flexibilities. *Nature Plants*, 2(9):1–2, 2016.

J. León, M. C. Castillo, and B. Gayubas. The hypoxia-reoxygenation stress in plants. *Journal of Experimental Botany*, 72(16):5841–5856, 2020.

M. Li, S. Guo, X. Yang, Q. Meng, and X. Wei. Exogenous gamma-aminobutyric acid increases salt tolerance of wheat by improving photosynthesis and enhancing activities of antioxidant enzymes. *Biologia plantarum*, 60(1):123–131, 2016a.

S. Li and M. Hong. Protonation, tautomerization, and rotameric structure of histidine: A comprehensive study by magic-angle-spinning solid-state NMR. *Journal of the American Chemical Society*, 133(5):1534–1544, 2011.

Y. Li, B. Liu, Y. Peng, C. Liu, X. Zhang, Z. Zhang, W. Liang, F. Ma, and C. Li. Exogenous GABA alleviates alkaline stress in *Malus hupehensis* by regulating the accumulation of organic acids. *Scientia Horticulturae*, 261:108982, 2020.

Z. Li, Y. Peng, and B. Huang. Physiological effects of $\gamma$-aminobutyric acid application on improving heat and drought tolerance in creeping bentgrass. *Journal of the American Society for Horticultural Science*, 141(1):76–84, 2016b.

J. Liao, X. Wu, Z. Xing, Q. Li, Y. Duan, W. Fang, and X. Zhu. $\gamma$-aminobutyric acid (GABA) accumulation in tea (*Camellia sinensis* L.) through the GABA shunt and polyamine degradation pathways under anoxia. *Journal of Agricultural and Food Chemistry*, 65 (14):3013–3018, 2017.

S.-M. Liao, Q.-S. Du, J.-Z. Meng, Z.-W. Pang, and R.-B. Huang. The multiple roles of histidine in protein interactions. *Chemistry Central Journal*, 7(1):1–12, 2013a.

Y. Liao, G. K. Smyth, and W. Shi. featureCounts: an efficient general purpose program for assigning sequence reads to genomic features. *Bioinformatics*, 30(7):923–930, 2013b.

F. Licausi, M. Kosmacz, D. A. Weits, B. Giuntoli, F. M. Giorgi, L. A. C. J. Voesenek, P. Perata, and J. T. van Dongen. Oxygen sensing in plants is mediated by an N-end rule pathway for protein destabilization. *Nature*, 479(7373):419–422, 2011.

A. Ligaba, L. Maron, J. Shaff, L. Kochian, and M. Piñeros. Maize ZmALMT2 is a root anion transporter that mediates constitutive root malate efflux. *Plant, Cell & Environment*, 35(7):1185–1200, 2012.

A. Ligaba, I. Dreyer, A. Margaryan, D. J. Schneider, L. Kochian, and M. Piñeros. Functional, structural and phylogenetic analysis of domains underlying the al sensitivity of the aluminum-activated malate/anion transporter, TaALMT1. *The Plant Journal*, 76 (5):766–780, 2013.

J. F. Lin and S. H. Wu. Molecular events in senescing *Arabidopsis* leaves. *The Plant Journal*, 39(4):612–628, 2004.

Q. Lin, J. Yang, Q. Wang, H. Zhu, Z. Chen, Y. Dao, and K. Wang. Overexpression of the trehalose-6-phosphate phosphatase family gene *AtTPPF* improves the drought tolerance of *Arabidopsis thaliana*. *BMC Plant Biology*, 19(1):1–15, 2019.

C. Lindermayr and J. Durner. Interplay of reactive oxygen species and nitric oxide: nitric oxide coordinates reactive oxygen species homeostasis. *Plant Physiology*, 167(4): 1209–1210, 2015.

C. Liu, L. Zhao, and G. Yu. The dominant glutamic acid metabolic flux to produce $\gamma$-amino butyric acid over proline in *Nicotiana tabacum* leaves under water stress relates to its significant role in antioxidant activity. *Journal of Integrative Plant Biology*, 53(8): 608–618, 2011.

D. Liu, J. Zhan, Z. Luo, N. Zeng, W. Zhang, H. Zhang, and L. Li. Quantitative proteomics and relative enzymatic activities reveal different mechanisms in two peanut cultivars (*Arachis hypogaea* L.) under waterlogging conditions. *Frontiers in Plant Science*, 12: 716114, 2021.

F. Liu, T. VanToai, L. P. Moy, G. Bock, L. D. Linford, and J. Quackenbush. Global transcription profiling reveals comprehensive insights into hypoxic response in Arabidopsis. *Plant Physiology*, 137(3):1115–1129, 2005.

G. Lobet, L. Pagès, and X. Draye. A novel image-analysis toolbox enabling quantitative analysis of root system architecture. *Plant Physiology*, 157(1):29–39, 2011.

Y. Long, S. D. Tyerman, and M. Gilliham. Cytosolic GABA inhibits anion transport by wheat ALMT1. *New Phytologist*, 225(2):671–678, 2019.

E. Loreti, A. Poggi, G. Novi, A. Alpi, and P. Perata. A genome-wide analysis of the effects of sucrose on gene expression in Arabidopsis seedlings under anoxia. *Plant Physiology*, 137(3):1130–1138, 2005.

E. Loreti, H. van Veen, and P. Perata. Plant responses to flooding stress. *Current Opinion in Plant Biology*, 33:64–71, 2016.

G. Lü, Y. Liang, X. Wu, J. Li, W. Ma, Y. Zhang, and H. Gao. Molecular cloning and functional characterization of mitochondrial malate dehydrogenase (mMDH) is involved in exogenous GABA increasing root hypoxia tolerance in muskmelon plants. *Scientia Horticulturae*, 258:108741, 2019.

S. X. Lu, S. M. Knowles, C. Andronis, M. S. Ong, and E. M. Tobin. CIRCADIAN CLOCK ASSOCIATED1 and LATE ELONGATED HYPOCOTYL function synergistically in the circadian clock of Arabidopsis. *Plant physiology*, 150(2):834–843, 2009.

F. Ludewig, A. Hüser, H. Fromm, L. Beauclair, and N. Bouché. Mutants of GABA transaminase (POP2) suppress the severe phenotype of *succinic semialdehyde dehydrogenase* (*ssadh*) mutants in Arabidopsis. *PLOS ONE*, 3(10):e3383, 2008.

K. Luu, N. Rajagopalan, J. C. Ching, M. C. Loewen, and M. E. Loewen. The malate-activated ALMT12 anion channel in the grass *Brachypodium distachyon* is co-activated by $Ca^{2+}$/calmodulin. *Journal of Biological Chemistry*, 294(15):6142–6156, 2019.

Q. Ma, Z. Xia, Z. Cai, L. Li, Y. Cheng, J. Liu, and H. Nian. *GmWRKY16* enhances drought and salt tolerance through an ABA-mediated pathway in *Arabidopsis thaliana*. *Frontiers in Plant Science*, 9:1979, 2019.

Y. Ma, P. Wang, Z. Chen, Z. Gu, and R. Yang. GABA enhances physio-biochemical metabolism and antioxidant capacity of germinated hulless barley under NaCl stress. *Journal of Plant Physiology*, 231:192–201, 2018.

H. Maaroufi-Dguimi, M. Debouba, L. Gaufichon, G. Clément, H. Gouia, A. Hajjaji, and A. Suzuki. An Arabidopsis mutant disrupted in *ASN2* encoding asparagine synthetase 2 exhibits low salt stress tolerance. *Plant Physiology and Biochemistry*, 49(6):623–628, 2011.

S. Maiale, D. H. Sánchez, A. Guirado, A. Vidal, and O. A. Ruiz. Spermine accumulation under salt stress. *Journal of Plant Physiology*, 161(1):35–42, 2004.

I. T. Major, Y. Yoshida, M. L. Campos, G. Kapali, X.-F. Xin, K. Sugimoto, D. O. Ferreira, S. Y. He, and G. A. Howe. Regulation of growth-defense balance by the JASMONATE ZIM-DOMAIN (JAZ)-MYC transcriptional module. *New Phytologist*, 215(4):1533–1547, 2017.

N. Meguro, H. Tsuji, Y. Suzuki, N. Tsutsumi, A. Hirai, and M. Nakazono. Analysis of expression of genes for mitochondrial aldehyde dehydrogenase in maize during submergence and following re-aeration. *Breeding Science*, 56(4):365–370, 2006.

D. W. Mekonnen, U.-I. Flügge, and F. Ludewig. Gamma-aminobutyric acid depletion affects stomata closure and drought tolerance of *Arabidopsis thaliana*. *Plant Science*, 245:25–34, 2016.

B. Menand, K. Yi, S. Jouannic, L. Hoffmann, E. Ryan, P. Linstead, D. G. Schaefer, and L. Dolan. An ancient mechanism controls the development of cells with a rooting function in land plants. *Science*, 316(5830):1477–1480, 2007.

X. Meng, L. Li, R. Narsai, I. D. Clercq, J. Whelan, and O. Berkowitz. Mitochondrial signalling is critical for acclimation and adaptation to flooding in *Arabidopsis thaliana*. *The Plant Journal*, 103(1):227–247, 2020.

S. Meyer, A. D. Angeli, A. R. Fernie, and E. Martinoia. Intra- and extra-cellular excretion of carboxylates. *Trends in Plant Science*, 15(1):40–47, 2010a.

S. Meyer, P. Mumm, D. Imes, A. Endler, B. Weder, K. A. Al-Rasheid, D. Geiger, I. Marten, E. Martinoia, and R. Hedrich. *At*ALMT12 represents an R-type anion channel required for stomatal movement in Arabidopsis guard cells. *The Plant Journal*, 63(6):1054–1062, 2010b.

S. Meyer, J. Scholz-Starke, A. D. Angeli, P. Kovermann, B. Burla, F. Gambale, and E. Martinoia. Malate transport by the vacuolar AtALMT6 channel in guard cells is subject to multiple regulation. *The Plant Journal*, 67(2):247–257, 2011.

S. Michaeli and H. Fromm. Closing the loop on the GABA shunt in plants: are GABA metabolism and signaling entwined? *Frontiers in Plant Science*, 6:419, 2015.

S. Michaeli, A. Fait, K. Lagor, A. Nunes-Nesi, N. Grillich, A. Yellin, D. Bar, M. Khan, A. R. Fernie, F. J. Turano, and H. Fromm. A mitochondrial GABA permease connects the GABA shunt and the TCA cycle, and is essential for normal carbon metabolism. *The Plant Journal*, 67(3):485–498, 2011.

A. Misra, T. D. McKnight, and K. K. Mandadi. Bromodomain proteins GTE9 and GTE11 are essential for specific BT2-mediated sugar and ABA responses in *Arabidopsis thaliana*. *Plant Molecular Biology*, 96(4-5):393–402, 2018.

M. Mithran, E. Paparelli, G. Novi, P. Perata, and E. Loreti. Analysis of the role of the pyruvate decarboxylase gene family in *Arabidopsis thaliana* under low-oxygen conditions. *Plant Biology*, 16(1):28–34, 2014.

Y. Miyashita and A. G. Good. Contribution of the GABA shunt to hypoxia-induced alanine accumulation in roots of *Arabidopsis thaliana*. *Plant and Cell Physiology*, 49(1): 92–102, 2008.

M. Moison, A. Marmagne, S. Dinant, F. Soulay, M. Azzopardi, J. Lothier, S. Citerne, H. Morin, N. Legay, F. Chardon, J.-C. Avice, M. Reisdorf-Cren, and C. Masclaux-Daubresse. Three cytosolic glutamine synthetase isoforms localized in different-order veins act together for N remobilization and seed filling in Arabidopsis. *Journal of Experimental Botany*, 69(18):4379–4393, 2018.

L. Mommer and E. J. W. Visser. Underwater photosynthesis in flooded terrestrial plants: A matter of leaf plasticity. *Annals of Botany*, 96(4):581–589, 2005.

H. Motoda, T. Sasaki, Y. Kano, P. R. Ryan, E. Delhaize, H. Matsumoto, and Y. Yamamoto. The membrane topology of ALMT1, an aluminum-activated malate transport protein in wheat (*Triticum aestivum*). *Plant Signaling & Behavior*, 2(6):467–472, 2007.

S. Munemasa, F. Hauser, J. Park, R. Waadt, B. Brandt, and J. I. Schroeder. Mechanisms of abscisic acid-mediated control of stomatal aperture. *Current Opinion in Plant Biology*, 28:154–162, 2015.

R. Munns and A. Termaat. Whole-plant responses to salinity. *Functional Plant Biology*, 13(1):143–160, 1986.

R. Munns and M. Tester. Mechanisms of salinity tolerance. *Annual Review of Plant Biology*, 59(1):651–681, 2008.

R. Munns, R. A. James, and A. Läuchli. Approaches to increasing the salt tolerance of wheat and other cereals. *Journal of experimental botany*, 57(5):1025–1043, 2006.

A. Mustroph, M. E. Zanetti, C. J. H. Jang, H. E. Holtan, P. P. Repetti, D. W. Galbraith, T. Girke, and J. Bailey-Serres. Profiling translatomes of discrete cell populations resolves altered cellular priorities during hypoxia in *Arabidopsis*. *Proceedings of the National Academy of Sciences*, 106(44):18843–18848, 2009.

A. Mustroph, S. C. Lee, T. Oosumi, M. E. Zanetti, H. Yang, K. Ma, A. Yaghoubi-Masihi, T. Fukao, and J. Bailey-Serres. Cross-kingdom comparison of transcriptomic adjustments to low-oxygen stress highlights conserved and plant-specific responses. *Plant Physiology*, 152(3):1484–1500, 2010.

C. Nunes, L. E. O'Hara, L. F. Primavesi, T. L. Delatte, H. Schluepmann, G. W. Somsen, A. B. Silva, P. S. Fevereiro, A. Wingler, and M. J. Paul. The trehalose 6-phosphate/SnRK1 signaling pathway primes growth recovery following relief of sink limitation. *Plant Physiology*, 162(3):1720–1732, 2013.

C. Papdi, I. Pérez-Salamó, M. P. Joseph, B. Giuntoli, L. Bögre, C. Koncz, and L. Szabados. The low oxygen, oxidative and osmotic stress responses synergistically act through the ethylene response factor VII genes *RAP*2.12, *RAP*2.2 and *RAP*2.3. *The Plant Journal*, 82(5):772–784, 2015.

J. Passioura. Water transport in and to roots. *Annual Review of Plant Physiology and Plant Molecular Biology*, 39(1):245–265, 1988.

J. Patel, M. Ariyaratne, S. Ahmed, L. Ge, V. Phuntumart, A. Kalinoski, and P. F. Morris. Dual functioning of plant arginases provides a third route for putrescine synthesis. *Plant Science*, 262:62–73, 2017.

M. J. Paul, L. F. Primavesi, D. Jhurreea, and Y. Zhang. Trehalose metabolism and signaling. *Annual Review of Plant Biology*, 59(1):417–441, 2008.

Z. Peleg and E. Blumwald. Hormone balance and abiotic stress tolerance in crop plants. *Current Opinion in Plant Biology*, 14(3):290–295, 2011.

B. Péret, B. D. Rybel, I. Casimiro, E. Benková, R. Swarup, L. Laplaze, T. Beeckman, and M. J. Bennett. Arabidopsis lateral root development: an emerging story. *Trends in Plant Science*, 14(7):399–408, 2009.

J. J. Petricka, C. M. Winter, and P. N. Benfey. Control of arabidopsis root development. *Annual review of plant biology*, 63:563–590, 2012.

J. Pfalz, K. Liere, A. Kandlbinder, K.-J. Dietz, and R. Oelmüller. pTAC2, -6, and -12 are components of the transcriptionally active plastid chromosome that are required for plastid gene expression. *The Plant Cell*, 18(1):176–197, 2005.

A. Piechatzek. Exploring the role of GABA in stomatal $CO_2$ responses and carbon metabolism. *PhD thesis, submitted*, 2022.

M. Pietrzykowska, M. Suorsa, D. A. Semchonok, M. Tikkanen, E. J. Boekema, E.-M. Aro, and S. Jansson. The light-harvesting chlorophyll *a/b* binding proteins lhcb1 and lhcb2 play complementary roles during state transitions in *Arabidopsis*. *The Plant Cell*, 26(9): 3646–3660, 2014.

M. A. Piñeros, G. M. A. Cançado, L. G. Maron, S. M. Lyi, M. Menossi, and L. V. Kochian. Not all ALMT1-type transporters mediate aluminum-activated organic acid responses:

the case of *ZmALMT1* - an anion-selective transporter. *The Plant Journal*, 53(2): 352–367, 2007.

M. A. Piñeros, G. M. Cançado, and L. V. Kochian. Novel properties of the wheat aluminum tolerance organic acid transporter (TaALMT1) revealed by electrophysiological characterization in *Xenopus* oocytes: functional and structural implications. *Plant Physiology*, 147(4):2131–2146, 2008.

K. Podlešáková, L. Ugena, L. Spíchal, K. Doležal, and N. De Diego. Phytohormones and polyamines regulate plant stress responses by altering GABA pathway. *New biotechnology*, 48:53–65, 2019.

C. Pucciariello and P. Perata. New insights into reactive oxygen species and nitric oxide signalling under low oxygen in plants. *Plant, Cell & Environment*, 40(4):473–482, 2016.

C. Pucciariello, S. Parlanti, V. Banti, G. Novi, and P. Perata. Reactive oxygen species-driven transcription in Arabidopsis under oxygen deprivation. *Plant Physiology*, 159(1): 184–196, 2012.

J. Qiu, S. W. Henderson, M. Tester, S. J. Roy, and M. Gilliham. SLAH1, a homologue of the slow type anion channel SLAC1, modulates shoot $Cl^-$ accumulation and salt tolerance in *Arabidopsis thaliana*. *Journal of experimental botany*, 67(15):4495–4505, 2016.

G. M. Rae, K. David, and M. Wood. The dormancy marker *DRM1/ARP* associated with dormancy but a broader role *in planta*. *Developmental Biology Journal*, 2013, 2013.

G. M. Rae, V. N. Uversky, K. David, and M. Wood. Drm1 and drm2 expression regulation: potential role of splice variants in response to stress and environmental factors in arabidopsis. *Molecular genetics and genomics*, 289(3):317–332, 2014.

S. A. Ramesh, S. D. Tyerman, B. Xu, J. Bose, S. Kaur, V. Conn, P. Domingos, S. Ullah, S. Wege, S. Shabala, J. A. Feijó, P. R. Ryan, and M. Gilliham. GABA signalling modulates plant growth by directly regulating the activity of plant-specific anion transporters. *Nature Communications*, 6(1):1–10, 2015.

S. A. Ramesh, M. Kamran, W. Sullivan, L. Chirkova, M. Okamoto, F. Degryse, M. McLaughlin, M. Gilliham, and S. D. Tyerman. Aluminum-activated malate transporters can facilitate GABA transport. *The Plant Cell*, 30(5):1147–1164, 2018.

R. Ramos-Ruiz, F. Martinez, and G. Knauf-Beiter. The effects of GABA in plants. *Cogent Food & Agriculture*, 5(1):1670553, 2019.

A. S. Reddy, G. S. Ali, H. Celesnik, and I. S. Day. Coping with stresses: roles of calcium- and calcium/calmodulin-regulated gene expression. *The Plant Cell*, 23(6):2010–2032, 2011.

H. Renault, V. Roussel, A. El Amrani, M. Arzel, D. Renault, A. Bouchereau, and C. Deleu. The *Arabidopsis pop2-1* mutant reveals the involvement of GABA transaminase in salt stress tolerance. *BMC plant biology*, 10(1):1–16, 2010.

H. Renault, A. E. Amrani, R. Palanivelu, E. P. Updegraff, A. Yu, J.-P. Renou, D. Preuss, A. Bouchereau, and C. Deleu. GABA accumulation causes cell elongation defects and a decrease in expression of genes encoding secreted and cell wall-related proteins in *Arabidopsis thaliana*. *Plant and Cell Physiology*, 52(5):894–908, 2011.

S. M. Rich, O. Pedersen, M. Ludwig, and T. D. Colmer. Shoot atmospheric contact is of little importance to aeration of deeper portions of the wetland plant *Meionectes brownii*; submerged organs mainly acquire $O_2$ from the water column or produce it endogenously in underwater photosynthesis. *Plant, cell & environment*, 36(1):213–223, 2013.

J. K. Roberts, J. Callis, D. Wemmer, V. Walbot, and O. Jardetzky. Mechanisms of cytoplasmic pH regulation in hypoxic maize root tips and its role in survival under hypoxia. *Proceedings of the National Academy of Sciences*, 81(11):3379–3383, 1984.

N. H. Roosens, T. T. Thu, H. M. Iskandar, and M. Jacobs. Isolation of the ornithine-$\delta$-aminotransferase cDNA and effect of salt stress on its expression in *Arabidopsis thaliana*. *Plant Physiol*, 117(1):263–71, 1998.

J. B. Rossel, P. B. Walter, L. Hendrickson, W. S. Chow, A. Poole, P. M. Mullineaux, and B. J. Pogson. A mutation affecting *ASCORBATE PEROXIDASE 2* gene expression reveals a link between responses to high light and drought tolerance. *Plant, Cell & Environment*, 29(2):269–281, 2006.

F. R. Rossi, A. Gárriz, M. Marina, and F. L. Pieckenstain. Modulation of polyamine metabolism in *Arabidopsis thaliana* by salicylic acid. *Physiologia Plantarum*, 173(3): 843–855, 2021.

O. Rötzschke, J. M. Lau, M. Hofstätter, K. Falk, and J. L. Strominger. A pH-sensitive histidine residue as control element for ligand release from HLA-DR molecules. *Proceedings of the National Academy of Sciences*, 99(26):16946–16950, 2002.

G. H. M. Sagor, S. Zhang, S. Kojima, S. Simm, T. Berberich, and T. Kusano. Reducing cytoplasmic polyamine oxidase activity in *Arabidopsis* increases salt and drought tolerance by reducing reactive oxygen species production and increasing defense gene expression. *Frontiers in Plant Science*, 7:214, 2016.

M. Salehin, B. Li, M. Tang, E. Katz, L. Song, J. R. Ecker, D. J. Kliebenstein, and M. Estelle. Auxin-sensitive Aux/IAA proteins mediate drought tolerance in Arabidopsis by regulating glucosinolate levels. *Nature communications*, 10(1):1–9, 2019.

A. Salvatierra, P. Pimentel, R. Almada, and P. Hinrichsen. Exogenous GABA application transiently improves the tolerance to root hypoxia on a sensitive genotype of *Prunus* rootstock. *Environmental and Experimental Botany*, 125:52–66, 2016.

T. Sasaki, Y. Yamamoto, B. Ezaki, M. Katsuhara, S. J. Ahn, P. R. Ryan, E. Delhaize, and H. Matsumoto. A wheat gene encoding an aluminum-activated malate transporter. *The Plant Journal*, 37(5):645–653, 2004.

R. Sasidharan, C. Chinnappa, M. Staal, J. T. M. Elzenga, R. Yokoyama, K. Nishitani, L. A. Voesenek, and R. Pierik. Light quality-mediated petiole elongation in Arabidopsis during shade avoidance involves cell wall modification by xyloglucan endotransglucosylase/hydrolases. *Plant Physiology*, 154(2):978–990, 2010.

R. Sasidharan, J. Bailey-Serres, M. Ashikari, B. J. Atwell, T. D. Colmer, K. Fagerstedt, T. Fukao, P. Geigenberger, K. H. Hebelstrup, R. D. Hill, et al. Community recommendations on terminology and procedures used in flooding and low oxygen stress research. *New Phytologist*, 214(4):1403–1407, 2017.

T. Sato, S. Maekawa, M. Konishi, N. Yoshioka, Y. Sasaki, H. Maeda, T. Ishida, Y. Kato, J. Yamaguchi, and S. Yanagisawa. Direct transcriptional activation of *BT* genes by NLP transcription factors is a key component of the nitrate response in Arabidopsis. *Biochemical and Biophysical Research Communications*, 483(1):380–386, 2017.

H. Schluepmann and M. Paul. Trehalose metabolites in Arabidopsis—elusive, active and central. *The Arabidopsis book/American Society of Plant Biologists*, 7, 2009.

R. R. Schmidt, M. Fulda, M. V. Paul, M. Anders, F. Plum, D. A. Weits, M. Kosmacz, T. R. Larson, I. A. Graham, G. T. S. Beemster, F. Licausi, P. Geigenberger, J. H. Schippers, and J. T. van Dongen. Low-oxygen response is triggered by an ATP-dependent shift in oleoyl-CoA in *Arabidopsis*. *Proceedings of the National Academy of Sciences*, 115(51): E12101–E12110, 2018.

F. Schröder, J. Lisso, P. Lange, and C. Müssig. The extracellular EXO protein mediates cell expansion in Arabidopsis leaves. *BMC plant biology*, 9(1):1–12, 2009.

F. Schröder, J. Lisso, and C. Müssig. EXORDIUM-LIKE1 promotes growth during low carbon availability in Arabidopsis. *Plant Physiology*, 156(3):1620–1630, 2011.

H. S. Seifi, K. Curvers, D. Vleesschauwer, I. Delaere, A. Aziz, and M. Höfte. Concurrent overactivation of the cytosolic glutamine synthetase and the GABA shunt in the ABA-

deficient sitiens mutant of tomato leads to resistance against *Botrytis cinerea*. *New Phytologist*, 199(2):490–504, 2013.

S. Shabala, L. Shabala, J. Barcelo, and C. Poschenrieder. Membrane transporters mediating root signalling and adaptive responses to oxygen deprivation and soil flooding. *Plant, Cell & Environment*, 37(10):2216–2233, 2014.

M. Sharma and D. Bhatt. The circadian clock and defence signalling in plants. *Molecular Plant Pathology*, 16(2):210–218, 2014.

T. Sharma, I. Dreyer, L. Kochian, and M. A. Piñeros. The ALMT family of organic acid transporters in plants and their involvement in detoxification and nutrient security. *Frontiers in Plant Science*, 7:1488, 2016.

B. J. Shelp and A. Zarei. Subcellular compartmentation of 4-aminobutyrate (GABA) metabolism in arabidopsis: An update. *Plant Signaling & Behavior*, 12(5):e1322244, 2017.

B. J. Shelp, G. G. Bozzo, C. P. Trobacher, G. Chiu, and V. S. Bajwa. Strategies and tools for studying the metabolism and function of $\gamma$-aminobutyrate in plants. I. Pathway structure. *Botany*, 90(8):651–668, 2012.

B. J. Shelp, A. W. Bown, and A. Zarei. 4-aminobutyrate (GABA): a metabolite and signal with practical significance. *Botany*, 95(11):1015–1032, 2017.

B. J. Shelp, M. S. Aghdam, and E. J. Flaherty. $\gamma$-aminobutyrate (GABA) regulated plant defense: Mechanisms and opportunities. *Plants*, 10(9):1939, 2021.

S. Q. Shi, Z. Shi, Z. P. Jiang, L. wang Qi, X. M. Sun, C. xiu Li, J. F. Liu, W. F. Xiao, and S. G. Zhang. Effects of exogenous GABA on gene expression of *Caragana intermedia* roots under NaCl stress: regulatory roles for $H_2O_2$ and ethylene production. *Plant, Cell & Environment*, 33(2):149–162, 2010.

V. Shukla, L. Lombardi, S. Iacopino, A. Pencik, O. Novak, P. Perata, B. Giuntoli, and F. Licausi. Endogenous hypoxia in lateral root primordia controls root architecture by antagonizing auxin signaling in *Arabidopsis*. *Molecular Plant*, 12(4):538–551, 2019.

J. P. Simpson, R. Di Leo, P. K. Dhanoa, W. L. Allan, A. Makhmoudova, S. M. Clark, G. J. Hoover, R. T. Mullen, and B. J. Shelp. Identification and characterization of a plastid-localized *Arabidopsis* glyoxylate reductase isoform: comparison with a cytosolic isoform and implications for cellular redox homeostasis and aldehyde detoxification. *Journal of experimental botany*, 59(9):2545–2554, 2008.

W. A. Snedden, T. Arazi, H. Fromm, and B. J. Shelp. Calcium/calmodulin activation of soybean glutamate decarboxylase. *Plant Physiology*, 108(2):543–549, 1995.

W. A. Snedden, N. Koutsia, G. Baum, and H. Fromm. Activation of a recombinant petunia glutamate decarboxylase by calcium/calmodulin or by a monoclonal antibody which recognizes the calmodulin binding domain. *Journal of Biological Chemistry*, 271(8): 4148–4153, 1996.

H. Song, X. Xu, H. Wang, H. Wang, and Y. Tao. Exogenous $\gamma$-aminobutyric acid alleviates oxidative damage caused by aluminium and proton stresses on barley seedlings. *Journal of the Science of Food and Agriculture*, 90(9):1410–1416, 2010.

N. Su, Q. Wu, J. Chen, L. Shabala, A. Mithöfer, H. Wang, M. Qu, M. Yu, J. Cui, and S. Shabala. GABA operates upstream of $H^+$-ATPase and improves salinity tolerance in Arabidopsis by enabling cytosolic $K^+$ retention and $Na^+$ exclusion. *Journal of experimental botany*, 70(21):6349–6361, 2019.

G. Székely, E. Abrahám, A. Cséplo, G. Rigó, L. Zsigmond, J. Csiszár, F. Ayaydin, N. Strizhov, J. Jásik, E. Schmelzer, C. Koncz, and L. Szabados. Duplicated *P5CS* genes of Arabidopsis play distinct roles in stress regulation and developmental control of proline biosynthesis. *The Plant Journal*, 53(1):11–28, 2008.

M. D. Tagnon and K. O. Simeon. Aldehyde dehydrogenases may modulate signaling by lipid peroxidation-derived bioactive aldehydes. *Plant Signaling & Behavior*, 12(11): e1387707, 2017.

E. Taleisnik, A. A. Rodríguez, D. Bustos, L. Erdei, L. Ortega, and M. E. Senn. Leaf expansion in grasses under salt stress. *Journal of Plant Physiology*, 166(11):1123–1140, 2009.

B. G. Tamang and T. Fukao. Plant adaptation to multiple stresses during submergence and following desubmergence. *International journal of molecular sciences*, 16(12): 30164–30180, 2015.

X. Tan, H. Xu, S. Khan, M. A. Equiza, S. H. Lee, M. Vaziriyeganeh, and J. J. Zwiazek. Plant water transport and aquaporins in oxygen-deprived environments. *Journal of Plant Physiology*, 227:20–30, 2018.

H. Tang, H. Bi, B. Liu, S. Lou, Y. Song, S. Tong, N. Chen, Y. Jiang, J. Liu, and H. Liu. WRKY33 interacts with WRKY12 protein to up-regulate RAP2.2 during submergence induced hypoxia response in *Arabidopsis thaliana*. *New Phytologist*, 229(1):106–125, 2020.

N. L. Taylor, K. A. Howell, J. L. Heazlewood, T. Y. W. Tan, R. Narsai, S. Huang, J. Whelan, and A. H. Millar. Analysis of the rice mitochondrial carrier family reveals anaerobic accumulation of a basic amino acid carrier involved in arginine metabolism during seed germination. *Plant Physiology*, 154(2):691–704, 2010.

D. Tenenbaum and B. P. Maintainer. *KEGGREST: Client-side REST access to the Kyoto Encyclopedia of Genes and Genomes (KEGG)*, 2021.

Q. Tian, X. Zhang, S. Ramesh, M. Gilliham, S. D. Tyerman, and W.-H. Zhang. Ethylene negatively regulates aluminium-induced malate efflux from wheat roots and tobacco cells transformed with TaALMT1. *Journal of Experimental Botany*, 65(9):2415–2426, 2014.

X. L. Tian, X. L. Wu, Y. Li, and S. Q. Zhang. The effect of gamma-aminobutyric acid in superoxide dismutase, peroxidase and catalase activity response to salt stress in maize seedling. *Shi yan sheng wu xue bao*, 38(1):75–79, 2005.

K. Tõldsepp, J. Zhang, Y. Takahashi, Y. Sindarovska, H. Hõrak, P. H. Ceciliato, K. Koolmeister, Y.-S. Wang, L. Vaahtera, L. Jakobson, C.-Y. Yeh, J. Park, M. Brosche, H. Kollist, and J. I. Schroeder. Mitogen-activated protein kinases MPK4 and MPK12 are key components mediating $CO_2$-induced stomatal movements. *The Plant Journal*, 96(5):1018–1035, 2018.

S. Törnroth-Horsefield, Y. Wang, K. Hedfalk, U. Johanson, M. Karlsson, E. Tajkhorshid, R. Neutze, and P. Kjellbom. Structural mechanism of plant aquaporin gating. *Nature*, 439(7077):688–694, 2006.

K.-J. Tsai, C.-Y. Lin, C.-Y. Ting, and M.-C. Shih. Ethylene-regulated glutamate dehydrogenase fine-tunes metabolism during anoxia-reoxygenation. *Plant Physiology*, 172(3): 1548–1562, 2016.

H. Tsuji, N. Meguro, Y. Suzuki, N. Tsutsumi, A. Hirai, and M. Nakazono. Induction of mitochondrial aldehyde dehydrogenase by submergence facilitates oxidation of acetaldehyde during re-aeration in rice. *FEBS Letters*, 546(2-3):369–373, 2003.

S. D. Tyerman, R. Munns, W. Fricke, B. Arsova, B. J. Barkla, J. Bose, H. Bramley, C. Byrt, Z. Chen, T. D. Colmer, T. Cuin, D. A. Day, K. J. Foster, M. Gilliham, S. W. Henderson, T. Horie, C. L. D. Jenkins, B. N. Kaiser, M. Katsuhara, D. Plett, S. J. Miklavcic, S. J. Roy, F. Rubio, S. Shabala, M. Shelden, K. Soole, N. L. Taylor, M. Tester, M. Watt, S. Wege, L. H. Wegner, and Z. Wen. Energy costs of salinity tolerance in crop plants. *New Phytologist*, 221(1):25–29, 2019.

K. Urano, Y. Yoshiba, T. Nanjo, T. Ito, K. Yamaguchi-Shinozaki, and K. Shinozaki. Arabidopsis stress-inducible gene for arginine decarboxylase AtADC2 is required for accumulation of putrescine in salt tolerance. *Biochemical and Biophysical Research Communications*, 313(2):369–375, 2004.

K. Urano, T. Hobo, and K. Shinozaki. *Arabidopsis ADC* genes involved in polyamine biosynthesis are essential for seed development. *FEBS Letters*, 579(6):1557–1564, 2005.

J. T. van Dongen and F. Licausi. Oxygen sensing and signaling. *Annual Review of Plant Biology*, 66(1):345–367, 2015.

I. Ventura, L. Brunello, S. Iacopino, M. C. Valeri, G. Novi, T. Dornbusch, P. Perata, and E. Loreti. Arabidopsis phenotyping reveals the importance of alcohol dehydrogenase and pyruvate decarboxylase for aerobic plant growth. *Scientific Reports*, 10(1):1–14, 2020.

L. A. Voesenek and J. Bailey-Serres. Flood adaptive traits and processes: an overview. *New Phytologist*, 206(1):57–73, 2015.

C. Wang, L. Fan, H. Gao, X. Wu, J. Li, G. Lv, and B. Gong. Polyamine biosynthesis and degradation are modulated by exogenous gamma-aminobutyric acid in root-zone hypoxia-stressed melon roots. *Plant Physiology and Biochemistry*, 82:17–26, 2014.

F. Wang, Z.-H. Chen, X. Liu, T. D. Colmer, L. Shabala, A. Salih, M. Zhou, and S. Shabala. Revealing the roles of GORK channels and NADPH oxidase in acclimation to hypoxia in Arabidopsis. *Journal of Experimental Botany*, 68(12):3191–3204, 2017.

J. Wang, X. Yu, Z. J. Ding, X. Zhang, Y. Luo, X. Xu, Y. Xie, X. Li, T. Yuan, S. J. Zheng, W. Yang, and J. Guo. Structural basis of ALMT1-mediated aluminum resistance in *Arabidopsis*. *Cell Research*, 32(1):89–98, 2021a.

Q. Wang, L. Wang, U. Chandrasekaran, X. Luo, C. Zheng, and K. Shu. ABA biosynthesis and signaling cascades under hypoxia stress. *Frontiers in Plant Science*, 12, 2021b.

T. Wang, T. Tohge, A. Ivakov, B. Mueller-Roeber, A. R. Fernie, M. Mutwil, J. H. Schippers, and S. Persson. Salt-related MYB1 coordinates abscisic acid biosynthesis and signaling during salt stress in Arabidopsis. *Plant Physiology*, 169(2):1027–1041, 2015.

D. A. Weits, A. B. Kunkowska, N. C. W. Kamps, K. M. S. Portz, N. K. Packbier, Z. N. Venza, C. Gaillochet, J. U. Lohmann, O. Pedersen, J. T. van Dongen, and F. Licausi. An apical hypoxic niche sets the pace of shoot meristem activity. *Nature*, 569(7758): 714–717, 2019.

A. Winkel, T. D. Colmer, A. M. Ismail, and O. Pedersen. Internal aeration of paddy field rice (*Oryza sativa*) during complete submergence–importance of light and floodwater $O_2$. *New Phytologist*, 197(4):1193–1203, 2013.

M. Wrzaczek, M. Brosché, J. Salojärvi, S. Kangasjärvi, N. Idänheimo, S. Mersmann, S. Robatzek, S. Karpiński, B. Karpińska, and J. Kangasjärvi. Transcriptional regulation of the CRK/DUF26 group of Receptor-like protein kinases by ozone and plant hormones in Arabidopsis. *BMC Plant Biology*, 10(1):1–19, 2010.

Q. Wu, N. Su, X. Huang, J. Cui, L. Shabala, M. Zhou, M. Yu, and S. Shabala. Hypoxia-induced increase in gaba content is essential for restoration of membrane potential and preventing ros-induced disturbance to ion homeostasis. *Plant Communications*, 2(3): 100188, 2021.

X. Wu, Q. Jia, S. Ji, B. Gong, J. Li, G. Lü, and H. Gao. Gamma-aminobutyric acid (GABA) alleviates salt damage in tomato by modulating $Na^+$ uptake, the *GAD* gene, amino acid synthesis and reactive oxygen species metabolism. *BMC Plant Biology*, 20 (1):1–21, 2020.

L. Xiang, L. Hu, W. Xu, A. Zhen, L. Zhang, and X. Hu. Exogenous $\gamma$-aminobutyric acid improves the structure and function of photosystem II in muskmelon seedlings exposed to salinity-alkalinity stress. *PLOS ONE*, 11(10):e0164847, 2016.

J. Xiao, H. Cheng, X. Li, J. Xiao, C. Xu, and S. Wang. Rice WRKY13 regulates cross talk between abiotic and biotic stress signalling pathways by selective binding to different cis-elements. *Plant Physiology*, 163(4):1868–1882, 2013.

T. Xie, J. Ji, W. Chen, J. Yue, C. Du, J. Sun, L. Chen, Z. Jiang, and S. Shi. $\gamma$-aminobutyric acid is closely associated with accumulation of flavonoids. *Plant signaling & behavior*, 14(7):1604015, 2019.

S. G. Xing, Y. B. Jun, Z. W. Hau, and L. Y. Liang. Higher accumulation of $\gamma$-aminobutyric acid induced by salt stress through stimulating the activity of diamine oxidases in glycine max (l.) merr. roots. *Plant Physiology and Biochemistry*, 45(8):560–566, 2007.

B. Xu, Y. Long, X. Feng, X. Zhu, N. Sai, L. Chirkova, A. Betts, J. Herrmann, E. J. Edwards, M. Okamoto, et al. GABA signalling modulates stomatal opening to enhance plant water use efficiency and drought resilience. *Nature communications*, 12(1):1–13, 2021.

D. Xu. COP1 and BBXs-HY5-mediated light signal transduction in plants. *New Phytologist*, 228(6):1748–1753, 2019.

Y.-H. Xu, R. Liu, L. Yan, Z.-Q. Liu, S.-C. Jiang, Y.-Y. Shen, X.-F. Wang, and D.-P. Zhang. Light-harvesting chlorophyll *a/b*-binding proteins are required for stomatal response to abscisic acid in *Arabidopsis*. *Journal of Experimental Botany*, 63(3):1095–1106, 2011.

E. Yakir, D. Hilman, Y. Harir, and R. M. Green. Regulation of output from the plant circadian clock. *FEBS Journal*, 274(2):335–345, 2006.

M. Yamada, X. Han, and P. N. Benfey. Root meristem growth factor 1 controls root meristem size through reactive oxygen species signaling. *bioRxiv*, page 244947, 2018.

K. Yamaguchi, Y. Takahashi, T. Berberich, A. Imai, A. Miyazaki, T. Takahashi, A. Michael, and T. Kusano. The polyamine spermine protects against high salt stress in *Arabidopsis thaliana*. *FEBS letters*, 580(30):6783–6788, 2006.

M. Yamaguchi, T. Sasaki, M. Sivaguru, Y. Yamamoto, H. Osawa, S. J. Ahn, and H. Matsumoto. Evidence for the plasma membrane localization of Al-activated malate transporter (ALMT1). *Plant and Cell Physiology*, 46(5):812–816, 2005.

D.-L. Yang, Z. Shi, Y. Bao, J. Yan, Z. Yang, H. Yu, Y. Li, M. Gou, S. Wang, B. Zou, D. Xu, Z. Ma, J. Kim, and J. Hua. Calcium pumps and interacting BON1 protein modulate calcium signature, stomatal closure, and plant immunity. *Plant Physiology*, 175(1):424–437, 2017.

R. Yang, Q. Guo, and Z. Gu. Gaba shunt and polyamine degradation pathway on $\gamma$-aminobutyric acid accumulation in germinating fava bean (*Vicia faba* L.) under hypoxia. *Food chemistry*, 136(1):152–159, 2013.

R. Yang, L. Feng, S. Wang, N. Yu, and Z. Gu. Accumulation of $\gamma$-aminobutyric acid in soybean by hypoxia germination and freeze-thawing incubation. *Journal of the Science of Food and Agriculture*, 96(6):2090–2096, 2015.

E. Yeung, H. van Veen, D. Vashisht, A. L. S. Paiva, M. Hummel, T. Rankenberg, B. Steffens, A. Steffen-Heins, M. Sauter, M. de Vries, R. C. Schuurink, J. Bazin, J. Bailey-Serres, L. A. C. J. Voesenek, and R. Sasidharan. A stress recovery signaling network for enhanced flooding tolerance in *Arabidopsis thaliana*. *Proceedings of the National Academy of Sciences*, 115(26):E6085–E6094, 2018.

Y. Yoshitake, S. Nakamura, D. Shinozaki, M. Izumi, K. Yoshimoto, H. Ohta, and M. Shimojima. RCB-mediated chlorophagy caused by oversupply of nitrogen suppresses phosphate-starvation stress in plants. *Plant Physiology*, 185(2):318–330, 2021.

Q. Yu, H. Tian, K. Yue, J. Liu, B. Zhang, X. Li, and Z. Ding. A P-loop NTPase regulates quiescent center cell division and distal stem cell identity through the regulation of ROS homeostasis in *Arabidopsis* root. *PLOS Genetics*, 12(9):e1006175, 2016.

L. B. Yuan, L. Chen, N. Zhai, Y. Zhou, S. S. Zhao, L. L. Shi, S. Xiao, L. J. Yu, and L. J. Xie. The anaerobic product ethanol promotes autophagy-dependent submergence tolerance in *Arabidopsis*. *International Journal of Molecular Sciences*, 21(19):7361, 2020.

A. Zarei, C. P. Trobacher, and B. J. Shelp. Arabidopsis aldehyde dehydrogenase 10 family members confer salt tolerance through putrescine-derived 4-aminobutyrate (GABA) production. *Scientific reports*, 6:35115, 2016.

A. Zarei, G. Z. Chiu, G. Yu, C. P. Trobacher, and B. J. Shelp. Salinity-regulated expression of genes involved in GABA metabolism and signaling. *Botany*, 95(6):621–627, 2017.

V. Žárskỳ. Signal transduction: GABA receptor found in plants. *Nature plants*, 1(8):1–2, 2015.

F. Zeng, D. Konnerup, L. Shabala, M. Zhou, T. D. Colmer, G. Zhang, and S. Shabala. Linking oxygen availability with membrane potential maintenance and $K^+$ retention of barley roots: implications for waterlogging stress tolerance. *Plant, Cell & Environment*, 37(10):2325–2338, 2014.

J. Zeng, Z. Dong, H. Wu, Z. Tian, and Z. Zhao. Redox regulation of plant stem cell fate. *The EMBO journal*, 36(19):2844–2855, 2017.

K. Zhang, Y. Duan, Y. Cao, Y. Chen, Z. Zou, F. Li, Q. Shen, X. Yang, Y. Ma, W. Fang, and X. Zhu. *CsCuAOs* and *CsAMADH1* are required for putrescine-derived $\gamma$-aminobutyric acid accumulation in tea. *Foods*, 11(9):1356, 2022.

W. H. Zhang, P. R. Ryan, T. Sasaki, Y. Yamamoto, W. Sullivan, and S. D. Tyerman. Characterization of the TaALMT1 protein as an $Al^{3+}$-activated anion channel in transformed tobacco (*Nicotiana tabacum* L.) cells. *Plant and Cell Physiology*, 49(9):1316–1330, 2008.

M. Zik, T. Arazi, W. A. Snedden, and H. Fromm. Two isoforms of glutamate decarboxylase in Arabidopsis are regulated by calcium/calmodulin and differ in organ distribution. *Plant molecular biology*, 37(6):967–975, 1998.